

Optimized IVT mRNA workflows
with automated electrophoresis and LC/MS

From Start to Finish:

Agilent CQA Analysis Solutions for IVT mRNA-based Biotherapeutics

Application Compendium



Table of Contents

Introduction	
Importance of critical quality attribute (CQA) assessment in IVT mRNA biotherapeutic development	4
Automated electrophoresis systems	7
Bio liquid chromatography (Bio LC) solutions	9
Component: DNA starting material	11
Plasmid Analysis	
Plasmid Analysis Using the Agilent Fragment Analyzer Systems	12
Detection and Analysis of Restriction-Digested Plasmid Fragments	20
Component: IVT mRNA drug substance	26
mRNA intactness	
High-Sensitivity IVT mRNA Analysis Using the Agilent Fragment Analyzer Systems	27
Assessment of Long IVT mRNA Fragments with the Agilent Fragment Analyzer Systems	34
Best Practices for Analysis of In Vitro Transcribed (IVT) mRNA Using the Agilent Fragment Analyzer Systems	40
Best Practices for Analysis of IVT mRNA Using the Agilent Fragment Analyzer Systems - Sizing, Resolution, and Purity	51
Benefits of Quality Control in the IVT RNA Workflow Using the Agilent 5200 Fragment Analyzer System	60
Quality Control in IVT RNA Workflow Using Agilent TapeStation Systems	66
5' capping efficiency	
Rapid Analysis of mRNA 5' Capping with High Resolution LC/MS	72
Determining mRNA Capping with HILIC-MS on a Low-Adsorption Flow Path	82
3' poly(A) tail length	
Analysis of mRNA Poly-A Sequence Variants by High Resolution LC/MS	90
Analyzing Poly(A) Tails of In Vitro Transcribed RNA with the Agilent Fragment Analyzer System	102
Product related impurities: aggregate quantification	
Aggregate Analysis of mRNA Using the Agilent Infinity II Bio LC System and Bio-SEC Columns	109

Final: IVT mRNA drug product	116
Lipid identity and content	
Analysis of Lipid Nanoparticle Composition	117
Analysis of Lipid Nanoparticle Components Using Agilent 6545XT AdvancedBio LC/Q-TOF	125
LC/MS Analysis of Lipid Composition in an mRNA LNP Formulation: A Stability Study	131
RNA concentration and RNA encapsulation efficiency	
Determination of mRNA Encapsulation Efficiency with the Agilent 1290 Infinity II Bio LC System	139
RNA size and integrity	
Benefits of Quality Control in the IVT RNA Workflow Using the Agilent 5200 Fragment Analyzer System (see page 60)	
Quality Assurance in In Vitro Transcribed (IVT) RNA Vaccine Development Using Agilent Automated Electrophoresis Instruments	145
SEC-MALS for mRNA Characterization with the Agilent 1260 Infinity II Multi-Angle Light Scattering Detector	157
Product related impurities: aggregate quantification	
Aggregate Analysis of mRNA Using the Agilent Infinity II Bio LC System and Bio-SEC Columns (see page 109)	

Importance of critical quality attribute (CQA) assessment in IVT mRNA biotherapeutic development

In vitro transcribed (IVT) mRNA has emerged in recent years as an innovative biotherapeutic platform with potential applications ranging from vaccines for infectious diseases, gene editing, protein replacement, and cancer therapies. Development of an IVT mRNA therapeutic begins with synthesizing a DNA template, often a linearized plasmid DNA. This template, often a linearized plasmid, is then transcribed in vitro to produce mRNA. During the transcription process, a 5' cap and poly(A) tail are added to the mRNA to protect from degradation and facilitate translation into protein. The resulting IVT mRNA, referred to as the drug substance (DS), undergoes purification and is subsequently formulated into a delivery system, such as a lipid nanoparticle (LNP), to create the final drug product (DP). The LNPs not only protect the IVT mRNA from degradation in vivo but also enhance cellular uptake and translation efficiency. Given the complex and unique characteristics of these molecules—from the DNA template to the final drug product—quality assessment at various stages of the workflow is essential for the successful development of IVT mRNA biotherapeutics.

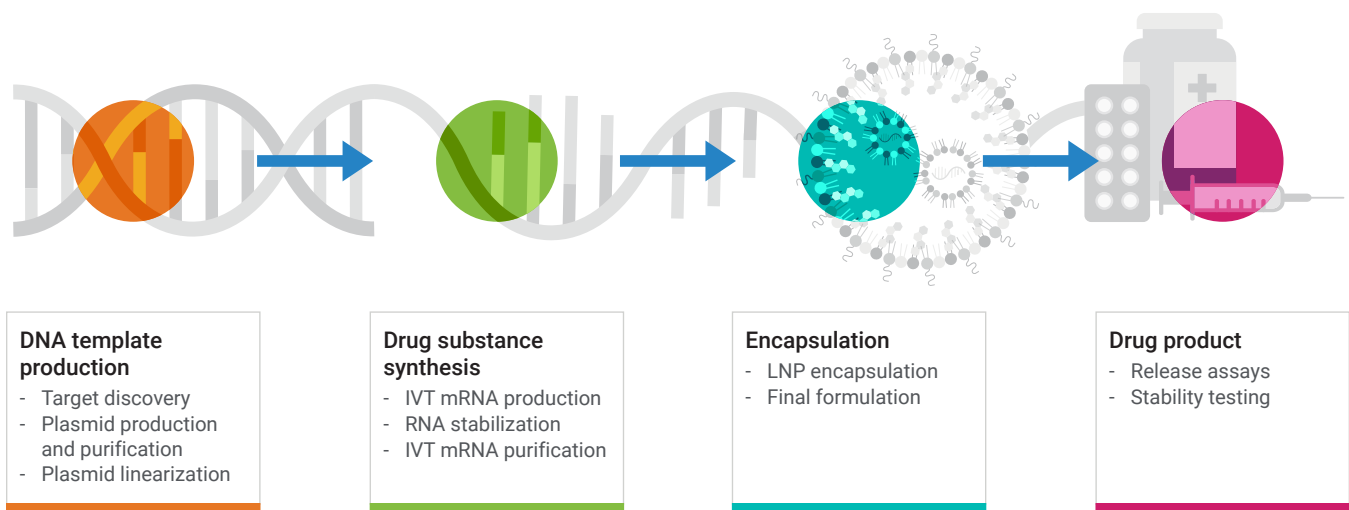


Figure 1. Generic IVT mRNA biotherapeutics development workflow.

As the field continues to evolve, ensuring the safety, efficacy, and consistency of biotherapeutics remains imperative. As such, different regulatory agencies have gathered guidance for the analytical procedures used in determining mRNA vaccine quality. For example, the US Pharmacopeia (USP) has compiled a list of guidelines for characterization and release testing of mRNA-based vaccines which includes several critical quality attributes (CQAs), such as identity, content, purity, potency, and safety. This systematic approach helps identify, analyze, and control these quality-affecting attributes, establishing a foundation for dependable documentation and standards to advance the growing IVT mRNA field.

Table 1A. Selected CQAs for mRNA drug substance.

Quality	Attribute	Method
Identity	mRNA sequence identity confirmation	High throughput sequencing (HTS)
		Sanger sequencing
		Reverse Transcriptase - PCR (RT-PCR)
Content	RNA concentration	Quantitative PCR (qPCR)
		Digital PCR (dPCR)
		Ultraviolet Spectroscopy (UV)
Integrity	mRNA intactness	Capillary electrophoresis*
		Capillary gel electrophoresis (CGE)*
		Agarose gel electrophoresis
Purity	5' capping efficiency	Reverse-phase liquid chromatography mass spectroscopy (RP-LC-MS/MS)* Ion pair reversed-phase high-performance liquid chromatography (IP-RP-HPLC)
	3' poly(A) tail length	Ion pair reversed-phase high-performance liquid chromatography (IP-RP-HPLC)
	Product related impurities - dsRNA	Immunoblot
		Enzyme-linked immunosorbent assay (ELISA)
	Product related impurities - aggregate quantitation	Size exclusion-high-performance liquid chromatography (SEC-HPLC)*
	Product related impurities - percentage of fragment mRNA	Reversed-phase HPLC (RP-HPLC)*
	Process related impurities - residual DNA template	Quantitative PCR (qPCR)
	Process related impurities - residual T7 RNA polymerase content	Enzyme-linked immunosorbent assay (ELISA)
	mRNA purity	Ion pair reversed-phase high-performance liquid chromatography (IP-RP-HPLC)
	Process related impurities - quantitation of free/non-incorporated nucleosides	Reverse-phase liquid chromatography mass spectroscopy (RP-LC-MS/MS)
Process related impurities - residual NTP and capping agent	Anion exchange high-performance liquid chromatography (AEX-HPLC)	

* Donated methods

Table 1B. Selected CQAs for mRNA drug product.

Quality	Attribute	Method
Identity	RNA identification	Sanger sequencing
		Reverse Transcriptase - PCR (RT-PCR)
	Identity of lipids	Reversed-phase high-performance liquid chromatography with charged aerosol detector (RP-HPLC-CAD) or evaporative light scattering detector (RP-HPLC-ELSD)
Content	RNA concentration/RNA encapsulation efficiency	Fluorescence-based assay
	Lipid content	Reversed-phase high-performance liquid chromatography with charged aerosol detector (RP-HPLC-CAD) or evaporative light scattering detector (RP-HPLC-ELSD)
Integrity	LNP size and polydispersity	Dynamic light scattering (DLS)
	RNA size and integrity	Capillary gel electrophoresis (CGE)*
Purity	Product related impurities - aggregate quantitation	Size exclusion-high-performance liquid chromatography (SEC-HPLC)*
	Product related impurities - percentage of fragment mRNA	Ion pair reversed-phase high-performance liquid chromatography (IP-RP-HPLC)*

* Donated methods

Note: Adapted from "Analytical Procedures for mRNA Vaccine Quality," draft guidelines: 3rd edition. www.usp.org ©The United States Pharmacopeial Convention, 2024

Agilent Technologies is committed to accelerating the advancement of science by providing complete, integrated solutions for various industries ranging from pharma and biopharma, chemical and energy, food, environmental and forensics sciences, and diagnostic and research labs. Many of the key CQAs and other quality control steps throughout the IVT mRNA biotherapeutic workflow can be addressed by Agilent solutions, including the automated electrophoresis and LC/MS systems.

Automated electrophoresis systems

The workflow for creating IVT mRNA biotherapeutics requires assessment of the DNA and IVT mRNA at many steps to ensure a high-quality and consistent product. The Agilent automated electrophoresis portfolio includes the Agilent Fragment Analyzer and Agilent TapeStation systems, both of which are used for analysis of nucleic acids. The Fragment Analyzer uses parallel capillary electrophoresis for high resolution separations of DNA and RNA and can be used at several steps of the IVT mRNA biotherapeutic workflow. The TapeStation offers quick analysis of DNA and RNA and has been used for at-line QC checks during vaccine development.

The Fragment Analyzer systems are designed to work with a wide range of analysis kits, including standard and high sensitivity RNA kits with optimized methods for IVT mRNA. The RNA kits provide high resolution for reliable and robust sizing and integrity analysis of IVT mRNA for CQA assessment of both the drug substance and drug product. In addition, the systems can be used for quality assessment of supercoiled and linearized DNA templates with the Plasmid DNA kit and the length of the poly(A) tail with the Small RNA kit.

The Agilent automated electrophoresis systems can be easily integrated into IVT mRNA biotherapeutic workflows. These solutions help deliver confidence in sample quality assessments during critical vaccine research, development, and production steps.



Figure 2. Agilent Fragment Analyzer system (left) and Agilent TapeStation system with Agilent ScreenTape technology (right).

Bio liquid chromatography (Bio LC) solutions

The Agilent InfinityLab Bio LC solutions play a pivotal role in assessing critical quality attributes (CQAs) throughout the IVT mRNA biotherapeutic workflow. These systems complement automated electrophoresis technologies by offering deeper insights into the molecular characteristics of mRNA and related biomolecules, ensuring the safety, efficacy, and consistency of final drug products.

The InfinityLab Bio LC portfolio provides versatile, high-performance liquid chromatography systems designed for the precise separation and analysis of complex biomolecules such as mAbs, mRNA, oligonucleotides, and their impurities. These adaptable systems integrate seamlessly into various stages of biopharmaceutical development, from early research to large-scale production. With advanced options such as biocompatible flow paths, online monitoring and high-pressure capabilities, Bio LC solutions from Agilent maintain the integrity and quality of sensitive biomolecules under a broad range of conditions.

The portfolio includes both biocompatible and bio-inert systems. Biocompatible systems, featuring iron-free flow paths, are ideal for applications where minimizing metal interactions is critical, such as mRNA and oligonucleotide analysis. Bio-inert systems, with completely metal-free flow paths, are tailored for the analysis of highly sensitive biomolecules, ensuring no risk of contamination even under challenging conditions.

In addition to core LC capabilities, InfinityLab Bio LC systems can be coupled with mass spectrometry (MS) for enhanced molecular characterization and impurity profiling. This combination provides detailed analyses of mRNA structure, modifications, and degradation products, supporting robust CQA monitoring throughout the development process. By integrating LC and MS technologies, Agilent Bio LC solutions offer a comprehensive analytical platform that upholds the rigorous standards required for mRNA biotherapeutic development.

Together, Agilent Bio LC solutions and MS options deliver a complete, integrated approach to quality assessment, ensuring that mRNA therapies meet stringent regulatory requirements and achieve the highest levels of performance and safety.



Figure 3. Agilent 1290 Infinity III Bio LC system, with optional evaporative light scattering detector (ELSD), and Agilent 6545XT Advance Bio LC/Q-TOF system (left); Agilent 1260 Infinity II Bio LC system with multi-angle light scattering detector (MALS) (right).

This compendium features a collection of application notes and technical overviews showcasing the Agilent Fragment Analyzer and TapeStation systems, InfinityLab Bio LC solutions, and 6545 XT Advance Bio LC/Q-TOF system within the IVT mRNA biotherapeutics workflow. The papers show how these instruments can be used to reliably assess CQA and includes applications for DNA starting material, drug substance, and drug product analysis. The detailed descriptions highlight the benefits of these analytical technologies, providing trustworthy data insights for objective decision-making.



Component: DNA starting material

Plasmid analysis

Plasmid Analysis Using the Agilent Fragment Analyzer Systems

Introductions

Plasmids are small, circular DNA molecules commonly found in bacteria that replicate autonomously¹. In the molecular biology laboratory, plasmids are ideally suited for experimental protocols employing cloning, a process in which a piece of DNA is inserted into the linearized plasmid, which is then circularized and introduced into host bacteria. The plasmid replicates with the bacteria, generating multiple copies of the plasmid and the sequence of interest independent of the bacterial chromosomal DNA. These artificially constructed plasmids can be used to help study DNA sequences or genes. Downstream applications using plasmids include genetic engineering and CRISPR technologies, gene therapy, pharmaceutical development, and recombinant DNA technologies².

Plasmids can appear in several conformations, including supercoiled, linear, and open-circular. To help ensure robust experimental results, it is important to begin with high-quality DNA. One of the methods to ensure the quality of plasmids for downstream use is analysis with gel electrophoresis. Each conformation will run differently through a gel. Supercoiled plasmid is the native conformation, composed of an intact double helix that is over- or under-wound. This compact supercoiled plasmid will migrate fastest through a gel matrix. This form is most critical to determining the quality of a plasmid, and so a common analysis is to determine the percentage of the plasmid that is of the supercoiled form. The linear plasmid has been cut at both strands in the same place and is in the relaxed or non-coiled state. It migrates slower than the supercoiled form on a gel. The nicked open-circular form of a plasmid is cut on only one of the two DNA strands, allowing for the formation to relax slightly and causing it to migrate the slowest of the plasmid formations on a gel.

The Agilent Fragment Analyzer system is an automated capillary electrophoresis instrument that can be used for quality control of a range of samples, including plasmids. With the Agilent Plasmid DNA kit, the Fragment Analyzer utilizes an optimized method that allows for accurate detection and sizing of supercoiled plasmids. The Plasmid DNA kit may also be used to detect plasmids in the linear form. When accurate sizing of linearized plasmids is necessary, the qualitative DNA kits for the Fragment Analyzer, such as the Agilent dsDNA 930 Reagent kit, are also available. An advantage of the qualitative DNA kits for the Fragment Analyzer is that the samples are prepared and injected separately from the markers, making it possible to analyze the same sample plate with multiple kits when needed. Due to the shape and large, irregular size of nicked open-circular plasmids, this form cannot be detected with the Plasmid DNA kit.

This technical overview examines the analytical specifications of the Plasmid DNA kit, highlighting the sizing and concentration range of the kit. In addition, several supercoiled plasmids are digested with restriction enzymes to produce the linear form to compare the sizing of the supercoiled DNA using the Plasmid DNA kit to the linear form with the dsDNA 930 kit.

Experimental

Plasmid information

Supercoiled plasmids of various sizes were obtained from GenScript and Origene and analyzed on an Agilent 5200 Fragment Analyzer system (p/n M5310AA) equipped with an Agilent FA 12-Capillary Array Short, 33 cm (p/n A2300-1250-3355). The plasmids were diluted to 0.5 ng/μL with 1x TE and prepared according to the Agilent DNF-940 Plasmid DNA Kit (p/n DNF-940-K0500) manual³. The plasmids used are summarized in Table 1.

Serial dilutions

The capabilities of the Plasmid DNA kit were examined through a series of serial dilutions to cover the concentration range of the kit. Each plasmid was diluted to 1 ng/μL with 1x TE, followed by two-fold dilutions down to 0.125 ng/μL. Multiple replicates of each dilution were analyzed with the Plasmid DNA kit.

Plasmid digests

One microgram of the 4.6 kb plasmid was digested with 1 μL *ScaI* (Thermo Fisher Scientific, p/n ER0431) following manufacturer's instructions. 1 μg of the 5.4, 6.2, and 7.6 kb plasmids were digested with 1 μL *BamHI-HF* (New England BioLabs, p/n R3136) following manufacturer's instructions. Aliquots of the supercoiled and the linearized plasmids were diluted to 0.5 ng/μL with 1x TE and analyzed on the Fragment Analyzer with both the Plasmid DNA kit and the Agilent dsDNA 930 Reagent kit (75-20000 bp) (p/n DNF-930)⁴.

Table 1. Plasmid sample information.

Plasmid ID	Plasmid Name	Company	p/n	Size (bp)
3.1 kb	pUC57 plasmid with 409 bp insert	GenScript	NA - custom synthesis	3,119
4.5 kb	pGuide-EF1a-GFP	Origene	GE100044	4,564
5.4 kb	pRS shRNA Vector	Origene	TR20003	5,430
6.2 kb	PCMVMIR MicroRNA Expression Vector	Origene	PCMVMIR	6,219
7.6 kb	pGFP-V-RS shRNA Vector	Origene	TR30007	7,584
8.5 kb	pRFP-CB-shLenti shRNA Vector	Origene	TR30032	8,491
10 kb	pCas-Scramble-EF1a-GFP	Origene	GET100021	10,469

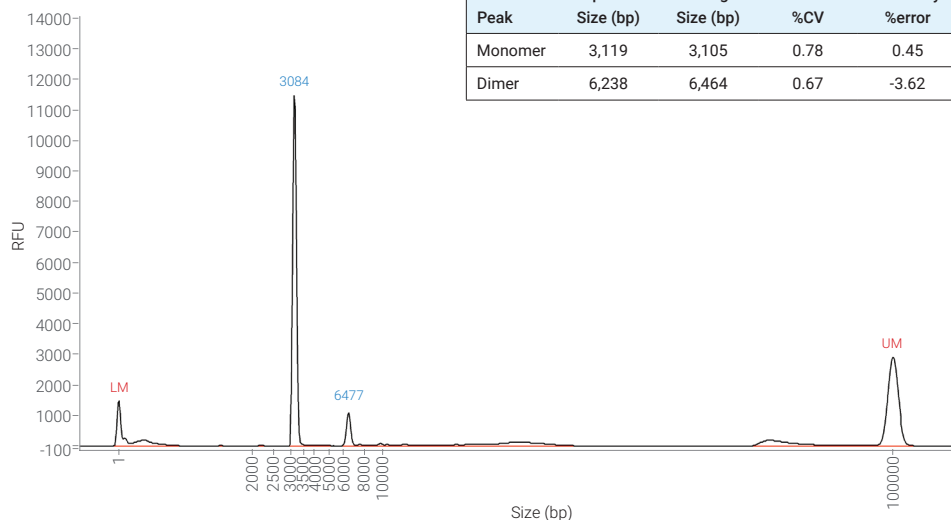
Results and discussion

Plasmid analysis

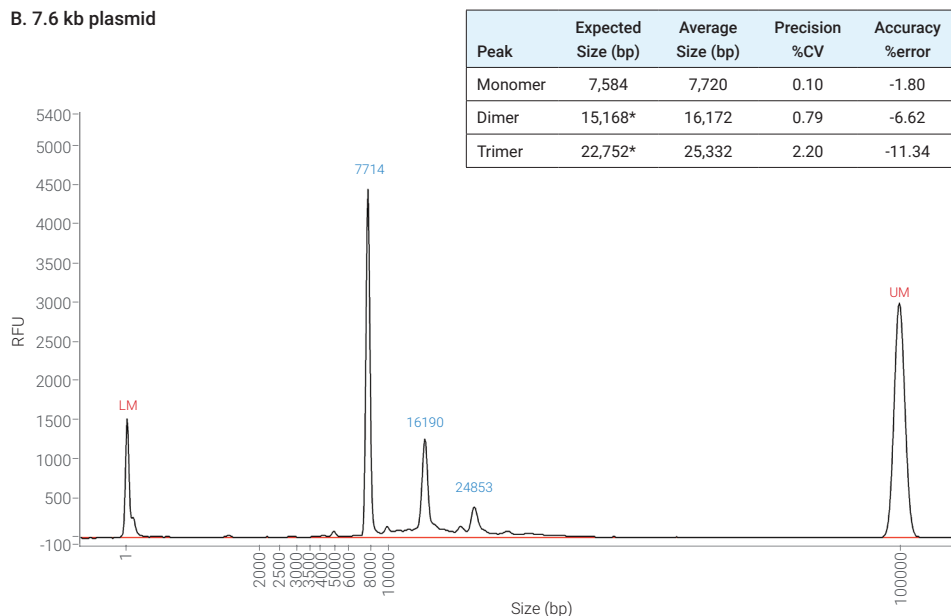
The Plasmid DNA kit was designed for the analysis of supercoiled plasmid DNA. The sizing ladder developed for the Plasmid DNA kit is comprised of supercoiled plasmids, allowing for accurate quality assessment and precise sizing of samples between 2,000 and 10,000 bp. Linear plasmids can also be analyzed for quality assessment (but not for sizing) using the kit. Relative concentration can be achieved for both forms of plasmids.

To demonstrate the capabilities of the Plasmid DNA kit, commercially available plasmids of various sizes ranging from 3 to 10 kb (Table 1) were analyzed on the Fragment Analyzer. The primary purpose of plasmid analysis is to confirm the size of the supercoiled plasmid and to examine the purity of the plasmid. Figure 1A shows a 3.1 kb plasmid, with most of the sample observed as a single sharp peak at 3,084 bp and a shorter fragment to the right of the fragment at 6,477 bp. The size of the main fragment is consistent with the size expected for the supercoiled plasmid, while the secondary fragment is likely a dimer concatemer. Concatemers occur when multiple copies of the monomeric plasmid link together as a result of homologous recombination during bacterial replication². The size of the second peak in this example is approximately double that of the monomer peak, confirming that it is a dimer concatemer. The electropherogram gives a visual representation of the purity of the sample while the data analysis software provides data such as the percent total of the peak, to further aid in determining the purity of a sample. In this example, the 3.1 kb peak represents 90.5% of the total sample.

A. 3.1 kb plasmid



B. 7.6 kb plasmid



C. 10 kb plasmid

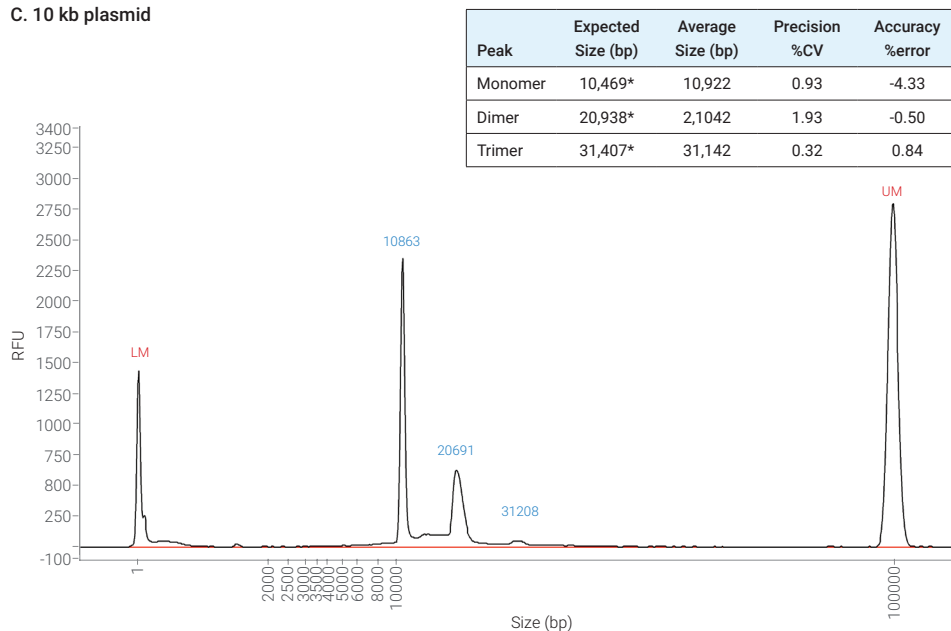


Figure 1. Supercoiled plasmids analyzed on the Agilent Fragment Analyzer system with the Agilent Plasmid DNA kit. A) A 3.1 kb plasmid with a single monomer concatemer. B) A 7.6 kb plasmid with dimer and trimer concatemers. C) A 10 kb plasmid with dimer and trimer concatemers. Inset tables indicate the size of the expected plasmid and the theoretical sizes of the concatemers, as well as the average size of each peak as reported by the Fragment Analyzer (n=4). *outside of kit specifications

In another example, a 7.6 kb plasmid displayed 3 sharp peaks at 7,714, 16,190, and 24,853 bp (Figure 1B). These sizes are consistent with the presence of the monomer form of the supercoiled plasmid, as well as dimer and trimer concatemers. Similarly, the 10 kb plasmid also displayed two sharp peaks at 10,863 and 20,691 bp, as well as a small smear at 31,208 bp (Figure 1C). While the larger sized peaks in both the 7.6 and 10 kb plasmids are consistent with the presence of dimer and trimer concatemers, it is important to note that these larger fragments are outside of the sizing range of the kit, and the reported sizes may be less accurate. Thus, to examine the sizing accuracy of the Plasmid DNA kit, only the first peak, or monomer, of each of the plasmids was further analyzed. The sizing reported by the Fragment Analyzer was consistent with the expected size of the supercoiled plasmid, with a high accuracy and less than 4.4% error for each plasmid. Additionally, an R^2 of 0.9995 indicated an excellent correlation between the expected plasmid size and that reported by the Fragment Analyzer (Figure 2).

Instrument comparison

The sizing accuracy of the Plasmid DNA kit was compared across two Fragment Analyzer instruments. Seven plasmids were analyzed in duplicate on each instrument, and the average size of the primary plasmid peak (excluding any concatemers) was compared across instruments. The sizing was consistent between each instrument. Each of the plasmids displayed a high accuracy, with less than 4.6% error across both instruments, well within the kit specifications of 10%. In addition, each instrument displayed a %CV of less than 2.7% for each fragment, indicating excellent sizing precision between runs (Figure 3).

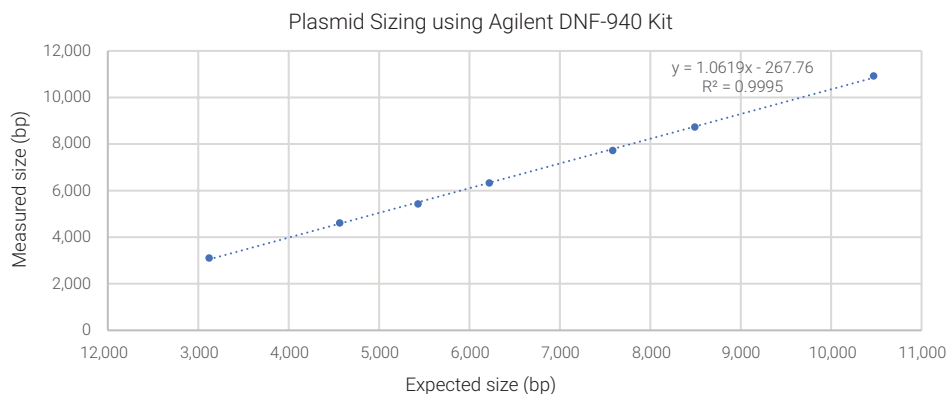
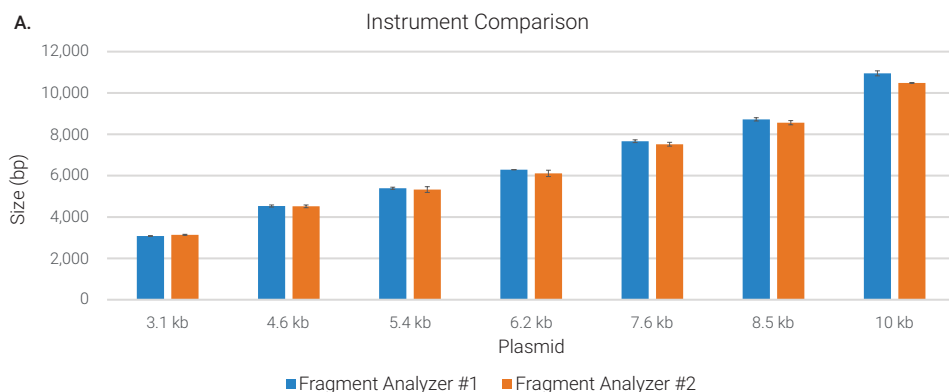


Figure 2. A selection of supercoiled plasmids ranging in size from 3.1 to 10 kb at a concentration of 0.5 ng/μL were analyzed on the Agilent Plasmid DNA kit with the Agilent Fragment Analyzer system. The average size of the primary plasmid peak reported by the Fragment Analyzer was compared to the known size of the plasmid. The measured size correlated well with the expected size of the supercoiled plasmid (n=4).



Plasmid ID	Average Size (bp)		Precision %CV		Accuracy %error	
	Fragment Analyzer #1	Fragment Analyzer #2	Fragment Analyzer #1	Fragment Analyzer #2	Fragment Analyzer #1	Fragment Analyzer #2
3.1 kb	3,084	3,137	0.00	0.81	1.12	-0.58
4.6 kb	4,536	4,518	1.12	1.46	0.61	1.02
5.4 kb	5,394	5,331	0.93	2.63	0.67	1.82
6.2 kb	6,287	6,110	0.00	2.52	-1.09	1.75
7.6 kb	7,667	7,520	0.88	1.21	-1.09	0.85
8.5 kb	8,723	8,562	0.90	1.16	-2.73	-0.83
10 kb	10,949	10,482	1.11	0.18	-4.58	-0.12

Figure 3. Various supercoiled plasmids ranging in size from 3.1 to 10 kb at a concentration of 1 ng/μL were analyzed on the Agilent Plasmid DNA kit using two Agilent 5200 Fragment Analyzer instruments. A) The reported size of each plasmid was consistent between instruments. Error bars indicate standard deviation. B) The size, %CV, and %error for each plasmid are shown (n=2 per instrument).

Concentration range of the Plasmid DNA kit

A two-fold serial dilution of each plasmid was performed to investigate the impact of concentration on sizing.

The plasmids were diluted from 1 to 0.125 ng/μL and analyzed on the Fragment Analyzer system with the Plasmid DNA kit. Shown in Figure 4 are overlays of the resulting electropherograms. The primary plasmid peak and any concatemers were visualized across the entire concentration range, highlighting the sensitivity of the Fragment Analyzer to detect samples and impurities at even low concentrations. Furthermore, the size of the primary peak for each of the seven plasmids tested remained consistent throughout the dilution series (Figure 4C).

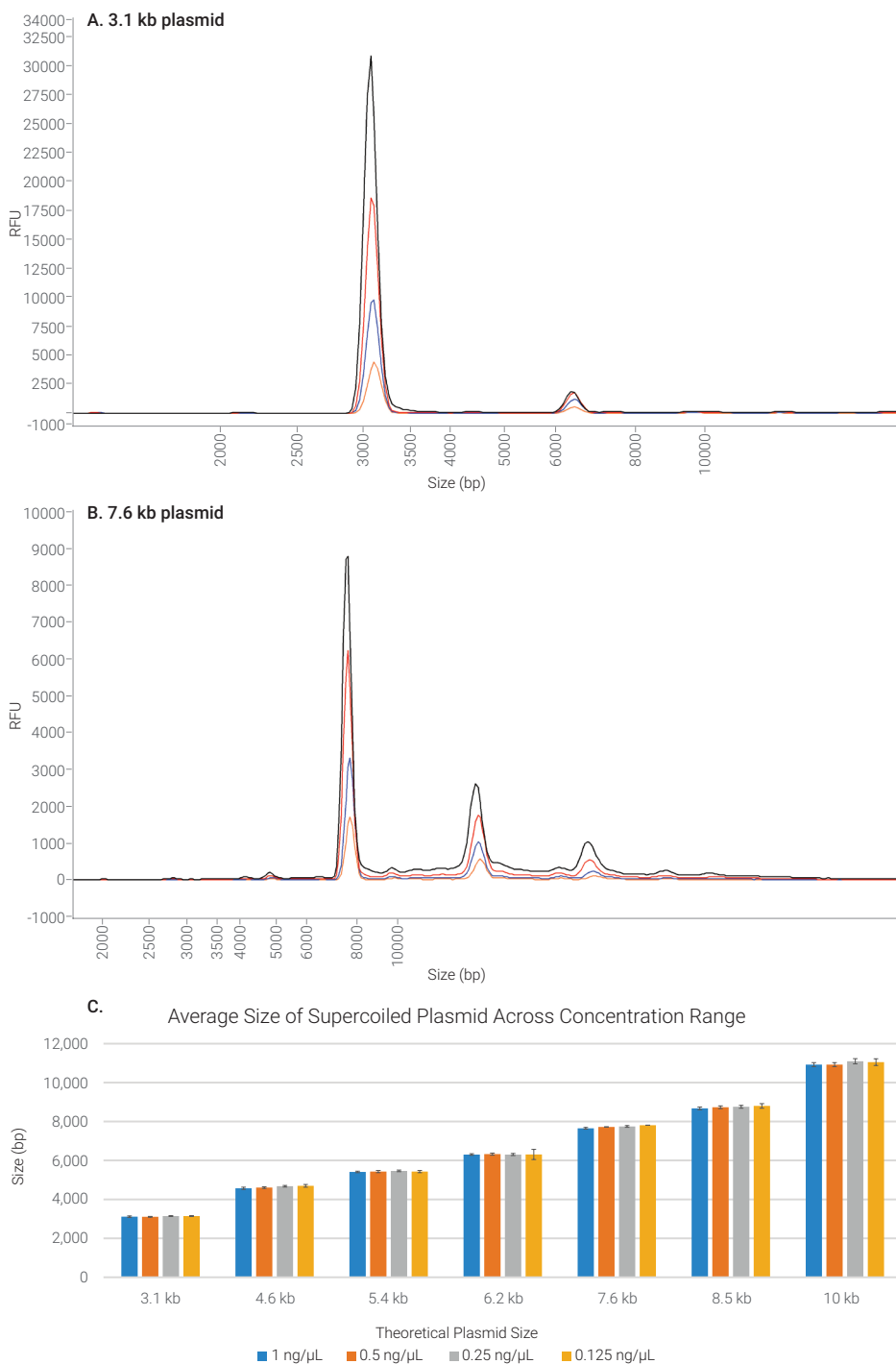


Figure 4. Serial dilutions of each plasmid from 1 to 0.125 ng/μL were analyzed with the Agilent Plasmid DNA kit on the Agilent Fragment Analyzer. Electropherograms are zoomed-in to highlight the main plasmid and any impurities. Shown are examples of A) a 3.1 kb plasmid with a single, small concatemer, and B) a 7.6 kb plasmid with two prominent concatemers. All peaks were observed in each sample across all concentrations tested. C) The size of the primary peak of each plasmid was compared across all concentrations. The average size of the fragment remained consistent across each concentration. n=4 replicates per concentration.

Comparison of supercoiled and linear plasmid sizing

As previously mentioned, the Plasmid DNA kit can be utilized for the analysis of supercoiled and linear DNA, with accurate sizing of only the supercoiled form.

Linearized plasmids can be detected and examined for purity using the Plasmid DNA kit. For accurate sizing, linearized plasmids can be analyzed on the Fragment Analyzer using a range of qualitative DNA kits, each with different sizing ranges ideal for analysis of DNA fragments from 35 to 20,000 bp.

To demonstrate the abilities of the Fragment Analyzer to accurately size plasmid DNA, the supercoiled plasmids were analyzed using the Plasmid DNA kit, and then linearized through single restriction digest. The linearized plasmid was then analyzed using the dsDNA 930 Reagent kit. Shown in Figure 5 are examples of the 4.6 kb supercoiled and linear plasmids analyzed on their respective kits. Figure 5A is an overlay of a 4.6 kb supercoiled (black) and linearized (red) plasmid analyzed on the Plasmid DNA kit. While the supercoiled form displays the expected plasmid size of approximately 4.6 kb, the size of the digested linear plasmid is not accurate (Figure 5A). In contrast, the linearized plasmid analyzed with a qualitative DNA kit reports a size of approximately 4.6 kb, and a 0.2% error indicative of high accuracy (n=4) (Figure 5B). The supercoiled plasmid can be detected but does not size accurately on the qualitative DNA kits (data not shown).

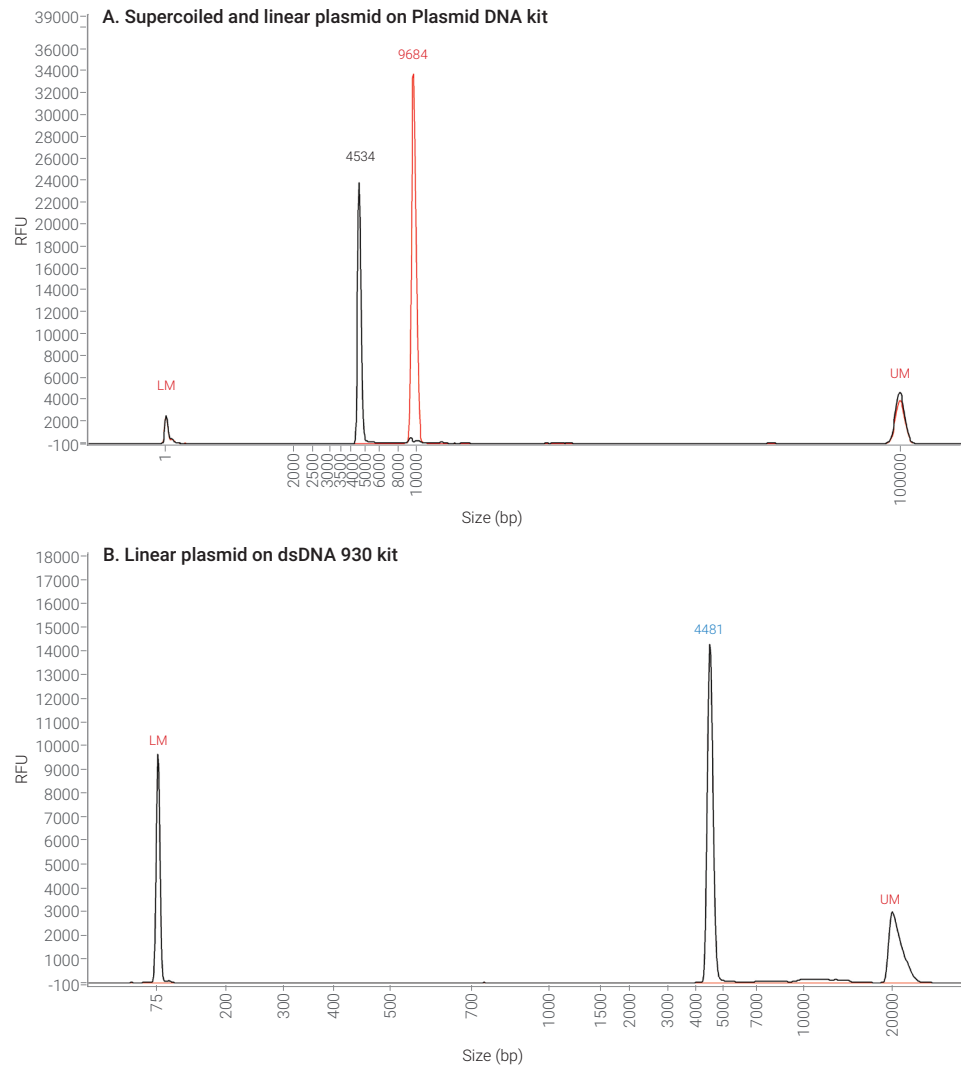


Figure 5. A 4.6 kb plasmid was analyzed on the Agilent Fragment Analyzer. A) The supercoiled form (black trace) can be accurately sized on the Agilent Plasmid DNA kit, while the linearized form (red trace) can be detected, but not sized. B) The digested form of the plasmid can be accurately sized using a qualitative DNA kit, the Agilent dsDNA 930 Reagent kit.

To provide further evidence that the extra peaks evident in some of the plasmids are concatemers, the 5.4, 6.2, and 7.2 plasmids were linearized using a single restriction digest. The enzyme successfully digested each of the concatemers, resulting in a single peak in the linear form of the plasmid. The linear plasmids were sized with the dsDNA 930 Reagent kit and were consistent with the size of the monomer peak of the supercoiled plasmid. Figure 6 shows the supercoiled (A) and linear (B) forms of the 5.4 kb plasmid.

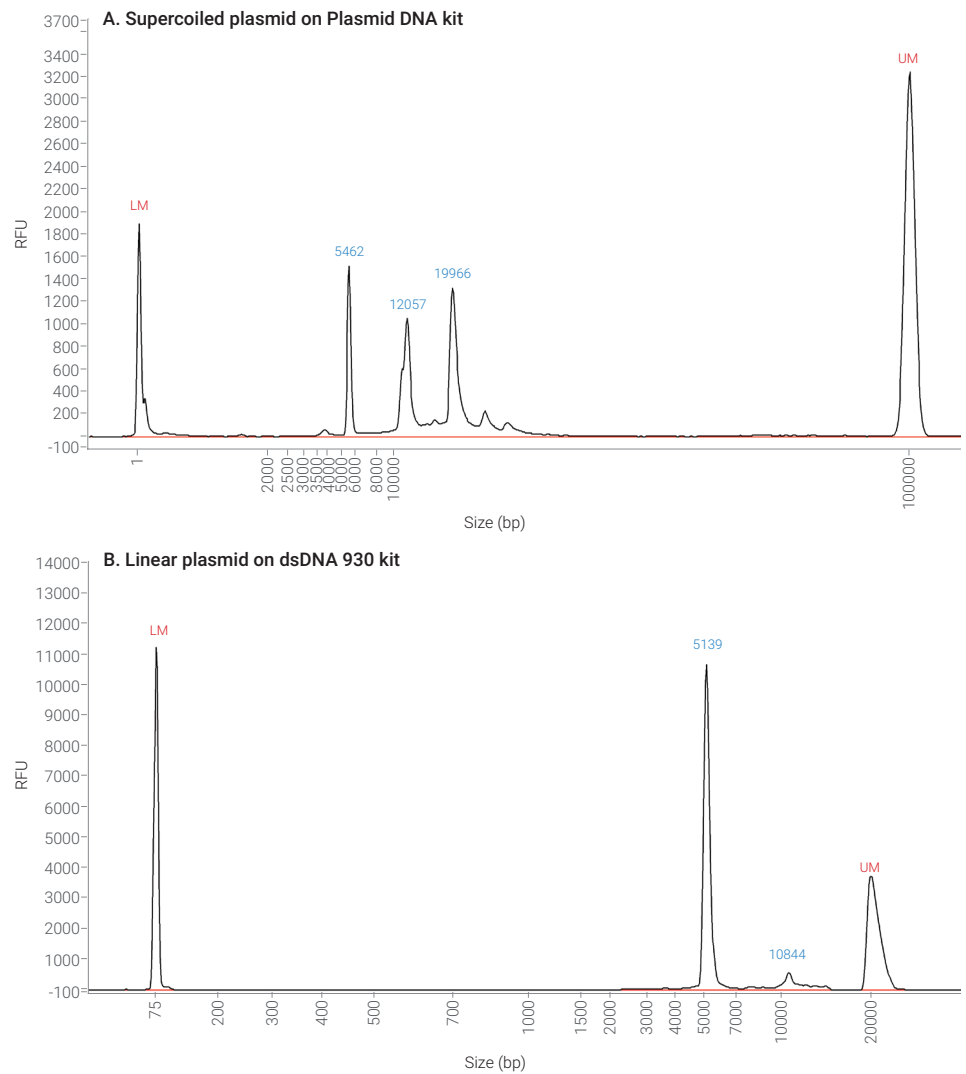


Figure 6. A 5.4 kb plasmid was analyzed on the Agilent Fragment Analyzer. A) The supercoiled form of the plasmid on the Agilent Plasmid DNA kit shows monomer, dimer, and trimer concatemers. B) The plasmid was digested with *Bam*HI and the linear form analyzed on the Agilent dsDNA 930 kit.

Conclusion

Automated electrophoresis with the Agilent Fragment Analyzer instrument along with the Agilent Plasmid DNA kit provides a quick and easy solution to analyze plasmids. The Plasmid DNA kit enables accurate sizing of supercoiled plasmid DNA up to 10 kb over a broad concentration range. While the Plasmid DNA kit is optimized for supercoiled DNA, detection of linearized plasmids is also possible with the kit. Accurate sizing of the linear plasmid can be achieved with the Agilent qualitative kits for the Fragment Analyzer systems.

References

1. National Human Genome Research Institute. Plasmid <https://www.genome.gov/genetics-glossary/Plasmid> (accessed Jul 29, 2021).
2. Lara, A. R.; Ramírez, O. T.; Wunderlich, M. Plasmid DNA Production for Therapeutic Applications. *Methods Mol. Biol.* **2012**, *824*, 271–303.
3. Agilent DNF-940 Plasmid DNA Quick Guide for Fragment Analyzer Systems, *Agilent Technologies kit quick guide*, publication number SD-AT000126, **2020**.
4. Agilent DNF-930 Reagent Kit (75 – 20000 bp) Quick Guide for Fragment Analyzer Systems, *Agilent Technologies kit quick guide*, publication number SD-AT000124, **2020**.

www.agilent.com

For Research Use Only. Not for use in diagnostic procedures.
PR7000-8248

This information is subject to change without notice.

© Agilent Technologies, Inc. 2021
Published in the USA, November 1, 2021
5994-4241EN

Detection and Analysis of Restriction-Digested Plasmid Fragments

Authors

Chava Pocerlich, Jolita Uthe,
and Kyle Luttgahm,
Agilent Technologies, Inc.

Abstract

Molecular biology research, including synthetic biology, agrobiolgy, and systems biology applications often use cloning vectors in their workflows. Quality control analysis of the cloning vector containing the DNA insert of interest is an essential initial step ensuring downstream success. The DNA insert and cloning vector are typically evaluated by restriction digestion and separated by manual gel electrophoresis. An alternative to manual gel electrophoresis is the Agilent ZAG DNA Analyzer system (ZAG system), which was specifically designed for efficient and accurate automated fragment analysis. The ZAG system is ideal for high-throughput fragment analysis with user-specified flagging criteria to easily identify the presence of the DNA insert, eliminating manual analysis errors. To demonstrate the efficiency and accuracy of DNA insert assessment in cloning vectors, the ZAG system was utilized to identify the presence or absence of an insert in two different plasmids. The ZAG system provided essential quality control analysis of the DNA insert with accurate sizing and automated detection.

Introduction

Plasmids or vectors are utilized as a means of transportation for delivering and manipulating foreign DNA inside a host cell. The uses and applications of plasmids continue to expand into all areas of scientific research and are continuously undergoing advancements. Industries that routinely make use of plasmid-based research span from molecular biology, synthetic biology, and agrobiotechnology to medicine, including a wide range of applications such as biofuels and fine chemical production, biosensors, bioremediation, and biomedical therapies¹.

Analysis and validation of DNA plasmids to confirm that they contain the sequence of interest are vital quality control steps that can provide insight into the production process. Fragment analysis will determine if the plasmid was properly constructed by detecting the presence or absence of the insert. A truncated insert or an insert that is longer than expected may suggest an issue in the cloning process. Quality assessment of the plasmid and insert can provide vital insight into the workflow, saving time by pointing the user towards the probable issue.

Screening large sample sets of plasmids is an extremely time-consuming and labor-intensive process typically involving manual agarose gel electrophoresis. This application note demonstrates high-throughput analysis of restriction digested plasmids with the ZAG DNA Analyzer system. Two commercially available plasmids, Cebpb (NM_009883) mouse tagged ORF clone (ORF clone) and pCMV6-Entry tagged cloning vector (cloning vector) were subjected to double restriction digestion and analyzed for the presence or absence of the insert.

Experimental

Plasmid samples

Cebpb (NM_009883) mouse tagged ORF clone (Origene, p/n MR227563) and pCMV6-entry tagged cloning vector (Origene, p/n PS100001) were diluted to 200 ng/μL. The plasmids were double digested with FastDigest SfaI (Thermo Fisher Scientific, p/n FD2094) and MluI (Thermo Fisher Scientific, p/n FD0564) restriction enzymes, according to the manufacturer's instructions.

Fragment size analysis

The digested samples were diluted with 1x TE to approximately 1 ng/μL and aliquoted to a 96-well plate for analysis with the Agilent ZAG 130 dsDNA kit (75-20000 bp) (ZAG 130 kit) (p/n ZAG-130-5000) on the Agilent ZAG DNA Analyzer system (p/n M5320AA). For comparison, the same samples were analyzed on the Agilent 5200 and 5300 Fragment Analyzer systems (p/n M5310AA and M5311AA, respectively) using the dsDNA 930 Reagent kit (75-20000 bp) (p/n DNF-930).

Results and Discussion

Analysis with the ZAG DNA Analyzer system

Many applications utilizing cloning plasmids require a quality control checkpoint to ensure that the plasmids have the proper DNA inserts. Conventionally, plasmids with the insert of interest are linearized by digestion and screened by gel electrophoresis. Typical agarose gel electrophoresis requires significant monitoring and manual data annotation using external software analysis of the gel image. An alternative to traditional gel electrophoresis workflows is the ZAG system. High-throughput needs are met by analyzing 96 samples simultaneously, in as little as 30 minutes. The ZAG system has the added advantage of the Agilent ProSize data analysis software (ProSize software), which provides automatic sizing and flag analysis with optional Boolean operators for simplified identification of the presence of a fragment², eliminating additional manual annotations required by traditional gel electrophoresis protocols. In addition, the ZAG system provides reproducible separation of DNA fragments with a 3 bp resolution³ allowing for the detection of closely sized fragments. The ZAG system is an indispensable tool for high-throughput applications and ensures quick screening for desired DNA inserts in cloning plasmids with automatic software analysis.

To demonstrate the efficiency of the ZAG system for quality control of cloning plasmids, two plasmids with and without inserts were analyzed. The ORF clone contained a DNA insert while the cloning vector did not. Both plasmids underwent double restriction digestion and were directly analyzed on the ZAG system with the ZAG 130 kit. Restriction enzymes cut the circular plasmid at specific cloning sites separating the plasmid from the DNA insert. In general, analysis by electrophoresis separates the insert from the plasmid displaying two bands if the insert was present in the plasmid. Those plasmids not containing an insert produce a single fragment representing the empty plasmid backbone. Analysis with the ZAG system of the double-digested ORF clone showed the insert fragment at 838 bp and the plasmid backbone at 4,598 bp, while the cloning vector resulted in a single fragment at 4,544 bp representing the plasmid backbone. ProSize software displays the results as both an electropherogram and a digital gel image allowing for easy visualization of the insert (Figure 1). The results matched the expected number of fragments from each plasmid.

Analysis of the double-digested plasmids also provides quality control information on the DNA insert. The complete and correct DNA insert needs to be introduced into the plasmid to ensure successful downstream outcomes. A quick assessment of the size of the insert will give insight as to whether the correct and complete insert has been included into the plasmid. A truncated or longer than expected insert will alert the investigator to the fact that there is a problem in the cloning process.

Comparison of the expected insert size of 888 bp and reported size of 838 bp demonstrated a very close concordance. The ZAG system reported very high accuracy with less than 7.5% error and high precision with $\leq 1.3\%$ CV for both the insert and plasmid backbone (Table 1). Analysis by the ZAG system of the DNA insert and plasmid backbone provided very accurate and precise sizing and confirmed that the correct insert was present.

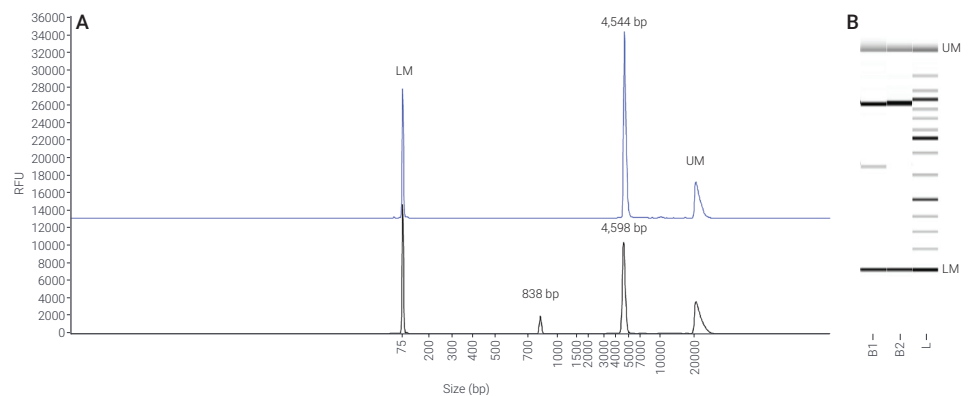


Figure 1. Overlay of restriction digested plasmids with a DNA insert (B1, black) and without (B2, blue) analyzed on the Agilent ZAG DNA Analyzer system with the ZAG 130 dsDNA kit (75-20000 bp). (A) Electropherogram; (B) Corresponding digital gel image. LM = lower marker; UM = upper marker; L = ladder.

Table 1. Sizing accuracy and precision of the restriction digested plasmid fragments using the Agilent ZAG DNA Analyzer system and ZAG 130 dsDNA kit (75-20000 bp).

Fragment Sizing with the ZAG DNA Analyzer System				
Sample	Expected Size (bp)	Average Size (bp, n=423)	Accuracy (%Error)	Precision (%CV)
Cebpb (NM_009883)	Insert - 888	838	5.6%	-0.8%
Mouse Tagged ORF Clone	Plasmid - 4,912	4,598	-6.4%	1.0%
pCMV6-Entry Tagged Cloning Vector	Plasmid - 4,912	4,544	-7.5%	1.3%

Analysis with the 5200 and 5300 Fragment Analyzer system

The ZAG system and associated analysis kits were developed for fast, high-throughput fragment analysis while providing highly accurate sizing results. The 5200 and 5300 Fragment Analyzer systems are also capable of fragment analysis, utilizing the same technology as the ZAG system. Typically, the Fragment Analyzer systems are utilized with their quantitative kits, providing quality assessment, concentration, and sizing of nucleic acid samples. However, the Fragment Analyzer also has qualitative kits that provide fragment analysis and sizing analogous to the ZAG system. Researchers requiring high-throughput DNA fragment analysis utilize a ZAG system, while laboratories with low-to-high throughput requirements that require the flexibility of both DNA and RNA analysis prefer a Fragment Analyzer system.

To demonstrate the congruity of fragment analysis between the ZAG and Fragment Analyzer systems, the digested plasmids were also analyzed with the 5200 and 5300 Fragment Analyzer systems and the dsDNA 930 Reagent kit (75-20000 bp).

The 5200 Fragment Analyzer system analyzes 12 samples at a time, while the 5300 Fragment Analyzer system is analogous to the ZAG system in that they are both capable of simultaneous analysis of 96 samples. The ZAG 130 dsDNA kit and Fragment Analyzer dsDNA 930 Reagent kit have the same analytical specifications, allowing for seamless comparison between instruments (Table 2). The wide concentration range offered by both kits often eliminates a dilution step and enables direct processing of samples with unknown concentrations, saving time in the workflow.

The plasmid and insert sizes from both the 5200 and 5300 Fragment Analyzer systems were similar to the fragment sizes reported by the ZAG system and varied by $\leq 1.5\%$ (Figure 2). Accuracy and precision with both the 5200 and 5300 Fragment Analyzer systems were likewise similar to the ZAG system with accuracy $\leq 6.8\%$ error and precision $\leq 1.3\%$ CV. The results demonstrated an excellent concordance between the ZAG and the 5200 and 5300 Fragment Analyzer systems.

Table 2. Comparison of the analytical specifications of the Agilent ZAG 130 dsDNA kit and the Fragment Analyzer dsDNA 930 Reagent kit.

Analytical Specifications	ZAG System 130 dsDNA Kit	5200/5300 Fragment Analyzer System dsDNA 930 Reagent Kit
Size Range	75 to 20,000 bp	75 to 20,000 bp
Sizing Accuracy	10%	10%
Sizing Precision	2%	2%
Concentration Range	0.5 to 50 ng/ μ L	0.5 to 50 ng/ μ L

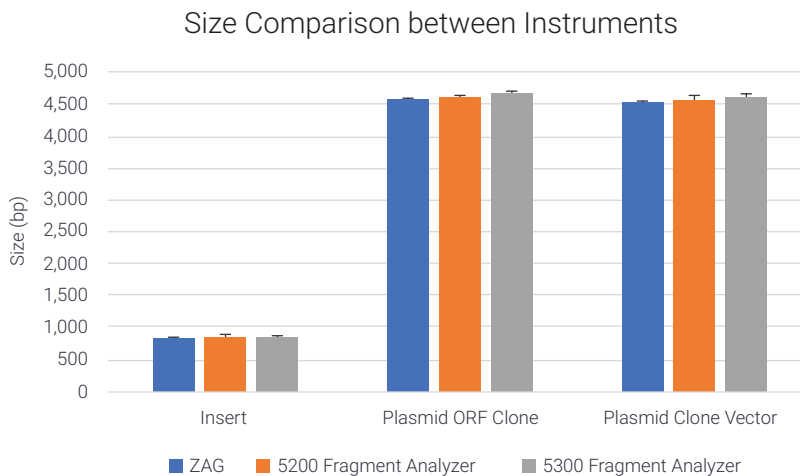


Figure 2. Plasmid and DNA insert sizing comparison between the Agilent ZAG DNA Analyzer system and the Agilent 5200 and 5300 Fragment Analyzer systems.

Flag Analysis by ProSize data analysis software

Automated processing of the large data sets and generation of digital reports allows researchers to save time and avoid errors from tedious manual data processing, especially in high-throughput, fast-pace research environments. Processing of large data sets is supported by the Flag Analysis option in the ProSize software. Flag Analysis allows the user to specify criteria to be met within the data. The numerical range for parameters of interest (i.e., sample size, or concentration, or peak height) can be defined by several

Boolean operators such as AND, OR, AND NOT, and NOR. Boolean operators are essential in defining the precise fragment search results, especially in complex scenarios where fast and accurate detection of many different DNA fragments or their combinations is required. The binary outcome where 0 = false and 1 = true specifies if the flag criteria were met.

In this study, presence or absence of the insert fragment in the digested plasmids was reported by utilizing Flag Analysis, where the binary designation of the true/false result offered a quick evaluation

of the entire 96-well sample plate. The flag criteria were set with the Boolean operators AND, AND NOT to screen for the DNA insert of a known size (Figure 3). The flag analysis data can be exported in a .CSV format to an excel spreadsheet for processing.

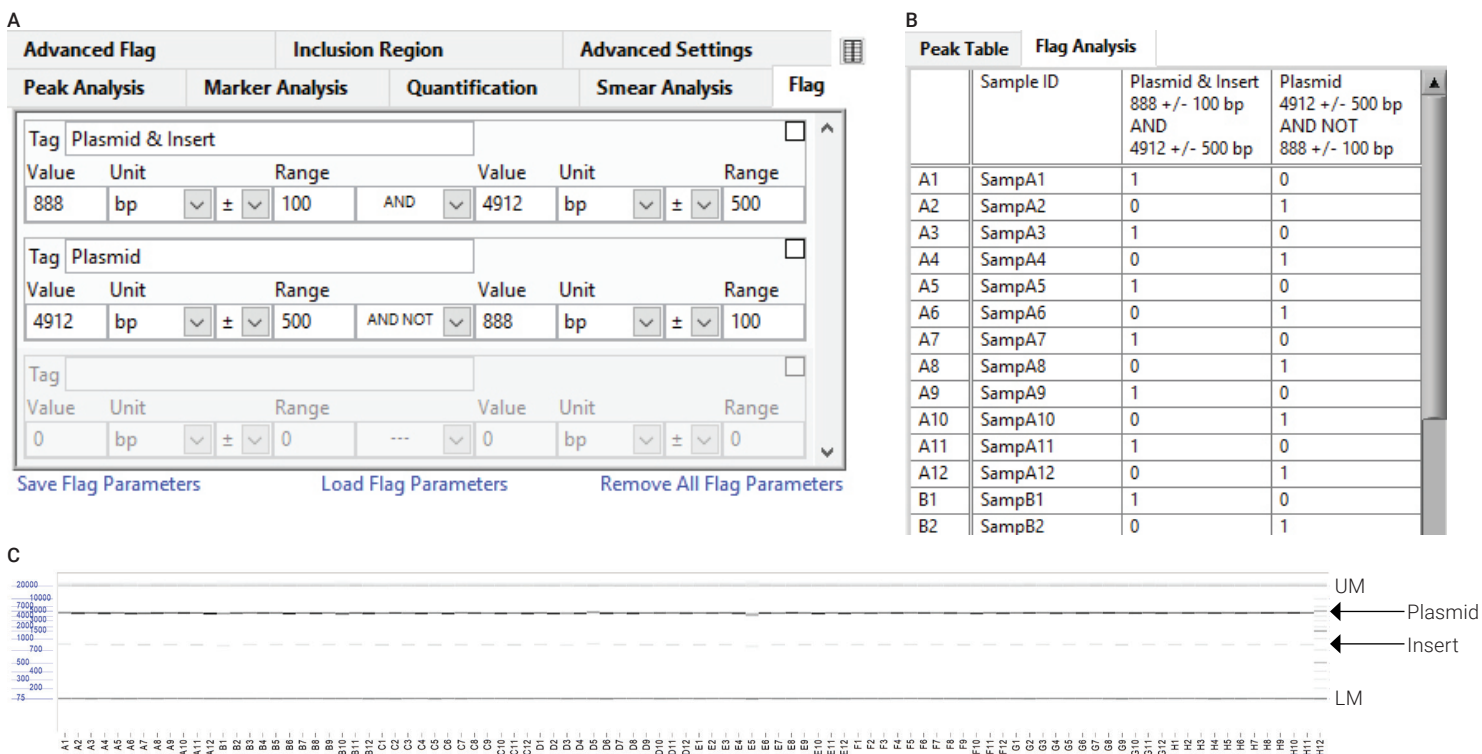


Figure 3. Flag Analysis with the Agilent ProSize data analysis software: (A) table for setting the Flag Analysis criteria using Boolean operators; (B) Flag Analysis results table; (C) digital gel image of the entire 96-well plate. Wells on the plate receive a 1=true or 0=false conveying if they met the criteria of two fragments within the designated size ranges.

Conclusion

Plasmid constructs are commonly used across industries for a multitude of molecular biology applications that are involved in the production of DNA fragments, RNA fragments, proteins, and enzymes. Quality analysis of the plasmid and the DNA insert of interest is a necessary first step to ensure downstream success. Analysis of two plasmids, the Cebpb (NM_009883) mouse tagged ORF clone and pCMV6-entry tagged cloning vector, with the Agilent ZAG DNA Analyzer system identified the presence of a DNA insert in the Cebpb (NM_009883) mouse tagged ORF clone but not in the pCMV6-Entry tagged cloning vector. Analysis with the ZAG system verified the expected results from the plasmid constructs. The ZAG and Fragment Analyzer systems both provided accurate sizing of the plasmid and DNA insert. Sizing of the DNA insert offered essential quality information confirming the insert was not altered during the cloning process.

References

1. Nora, L. C.; Westmann, C. A.; Martins-Santana, L.; de Fátima Alves, L.; Monteiro, L.; Guazzaroni, M.; Silva-Rocha, R. The Art of Vector Engineering: Towards the Construction of Next-Generation Genetic Tools. *Microb. Biotech.* **2019**, *12*(1), 125–147.
2. Genotyping with Agilent ZAG DNA Analyzer System. *Agilent Technologies application note*, publication number 5994-1186EN, **2019**.
3. Highly Resolved Separation of DNA Fragments on the Agilent 5200 Fragment Analyzer system. *Agilent Technologies application note*, publication number 5994-0517EN, **2019**.

www.agilent.com/genomics/zag

For Research Use Only. Not for use in diagnostic procedures.
PR7000-7626

This information is subject to change without notice.

© Agilent Technologies, Inc. 2020
Printed in the USA, December 15, 2020
5994-2919EN



Component: IVT mRNA drug substance

mRNA intactness, 5' capping efficiency, and 3' poly(A) tail length

High-Sensitivity IVT mRNA Analysis Using the Agilent Fragment Analyzer Systems

Introduction

Recently, quality analysis of in vitro transcribed (IVT) mRNA has become an essential part of biotherapeutic workflows, such as vaccine development. The Agilent Fragment Analyzer systems offer a variety of RNA analysis kits to aid in the assessment of some of the key critical quality attributes (CQAs) assessed throughout these workflows, including size, integrity, and purity of the IVT mRNA. Among the RNA kits for the Fragment Analyzer is the Agilent High-Sensitivity (HS) RNA kit (15 nt) (part number DNF-472). New methods for assessment of IVT mRNA on the Fragment Analyzer systems have been developed for the HS RNA kit, expanding the options beyond the original methods for total RNA and ribo-depleted RNA.¹ Total RNA and IVT mRNA each have unique analysis requirements and different profiles necessitating distinct methods for each. Electrophoresis of IVT mRNA depicts the sample as a single sharp peak, with any impurities or degradation flanking the peak. In its use as a biotherapeutic, CQAs including purity and sizing of the main peak are evaluated. Due to differences in RNA sample profiles, analysis requirements, and concentration ranges, new HS RNA methods were developed to specifically focus on the growing demands for IVT mRNA therapeutics.

The new methods available for the HS RNA kit provide optimized injection and separation conditions for IVT mRNA samples. The optimized conditions can accommodate samples up to 9,000 nt over a broad concentration range, while still using the same HS RNA kit and reagents (methods A and B).² The analytical specifications for the expanded HS RNA kit for IVT mRNA analysis methods, in addition to total RNA and ribo-depleted RNA, are summarized in Table 1. The HS IVT mRNA low-concentration method (method A) is for samples of low concentration, with an input range of 500 to 2,500 pg/ μ L. The HS IVT mRNA mid-concentration method (method B) is for mid-range concentration samples from 2,500 to 10,000 pg/ μ L, bridging the gap between the standard sensitivity Agilent RNA kit (15 nt) (part number DNF-471) and the HS RNA kit method A range. Both methods are used for analysis of smaller IVT mRNAs from 200 to 6,000 nt. Additional extended methods are available for the sizing of long IVT mRNAs from 500 to 9,000 nt for both the low- and mid-concentration ranges (methods AE and BE, respectively). These methods use a longer separation time and an alternative ladder for analysis. In addition to the extended sizing range, these methods offer high resolution of closely sized fragments throughout the sizing range of the kit. This technical overview details the different methods available for the analysis of IVT RNA using the HS RNA kit on the Fragment Analyzer.

Experimental

Reference IVT RNA samples (GenScript Biotech special order for 1,808, 4,305, and 9,000 nt) were prepared in nuclease-free water at 10 ng/μL, and concentration was confirmed with a NanoDrop spectrophotometer. Further dilutions were prepared to fit the concentration ranges of the different methods (Table 1). Multiple replicates of all samples were assessed using the HS RNA kit on the Agilent 5200 and 5300 Fragment Analyzer systems equipped with 12, 48, and 96 short capillary arrays. The method was chosen to fit the sizing and concentration ranges of the kits. The 1,808 and 4,305 nt samples used methods A and B, while all three samples were analyzed with the extended methods AE and BE. Samples of lower concentrations from 15 to 2,500 pg/μL used the longer injection in method A, and concentrations from 2,500 to 10,000 pg/μL used the shorter injection time in method B. For methods A and B, used the Agilent HS RNA Ladder (part number DNF-386-U015) was heat denatured at 70 °C for 2 minutes and diluted to 2 ng/μL with nuclease-free water before running, according to the quick guide.² The extended methods AE and BE used an alternative RNA marker from Lonza (part number 50575) in place of the Agilent HS RNA Ladder. The Lonza RNA marker was diluted to 25 ng/μL and concentration was confirmed with the Nanodrop. Then, it was heat denatured at 70 °C for 2 minutes and diluted to 2 ng/μL with nuclease-free water before addition to the plate.

Results and discussion

IVT mRNA analysis with the Fragment Analyzer systems and HS RNA kit

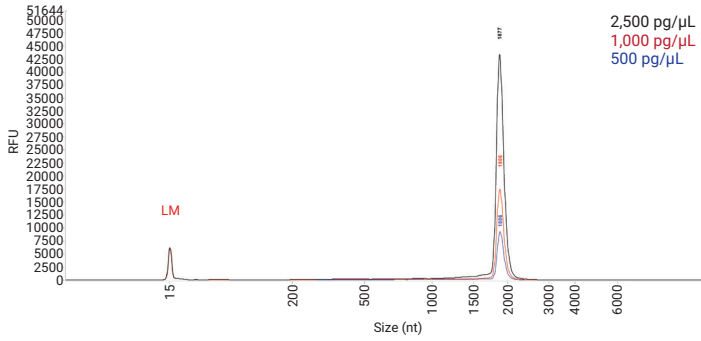
The HS RNA kit for the Fragment Analyzer has a sizing range of 200 to 6,000 nt. Several methods can be used with the kit to enable assessment of IVT mRNA samples across a broad concentration range. Following separation, the samples are automatically analyzed and can be visualized as both a digital gel image and a detailed electropherogram. To demonstrate the capabilities of the HS RNA kit and the IVT mRNA methods A and B, reference samples of 1,808 and 4,305 nt were analyzed at different concentrations, covering the ranges of both methods. Method A is used for low input concentration ranges from 500 to 2,500 pg/μL, while method B is for mid-range concentrations from 2,500 to 10,000 pg/μL. The electropherogram overlays in Figure 1 highlight the similar sizing achieved across the concentration ranges of both methods A and B.

Results of the average size of each IVT mRNA sample across the concentration ranges of both methods A and B display an excellent linear trendline and Y-equation with slopes below 0.01. A slope of 0 indicates no change in sizing over the concentration range. The slope of the 1,808 nt IVT mRNA was 0.0092, while the slope of the 4,305 nt sample was close to 0, at 0.0012, indicating excellent cohesion between the low- and mid-concentration ranges of the two methods (Figure 1E). This data demonstrates that the IVT mRNA methods A and B for the HS RNA kit both give similar sizing data for IVT mRNA samples across a broad concentration range, enabling researchers to achieve reliable data for a variety of samples with a single kit.

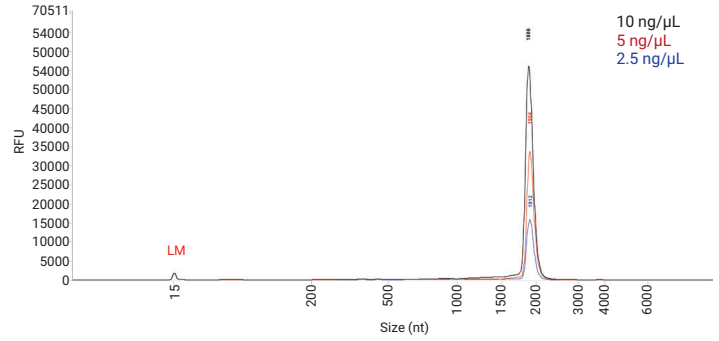
Table 1. Analytical specifications of the Agilent HS RNA kit (15 nt) and associated methods used for analysis of total RNA, ribo-depleted RNA, and IVT mRNA with the Agilent Fragment Analyzer systems.

Reagent Kit	HS RNA kit (15 nt) (p/n DNF-472)					
Application	Total RNA	Ribo-depleted RNA	IVT mRNA			
Method	DNA-472T33 - HS Total RNA 15 nt	DNF-472M33 - HS mRNA 15 nt	DNF-472A33 - HS IVT mRNA Low Concentration (method A)	DNF-472AE33 - HS IVT mRNA Extended Low Concentration (method AE)	DNF-472B33 - HS IVT mRNA Mid Concentration (method B)	DNF-472BE33 - HS IVT mRNA Extended Mid Concentration (method BE)
Size Range	200–6,000 nt	200–6,000 nt	200–6,000 nt	500–9,000 nt	200–6,000 nt	500–9,000 nt
Concentration Range	50–5,000 pg/μL	500–5,000 pg/μL	500–2,500 pg/μL	500–2,500 pg/μL	2,500–10,000 pg/μL	2,500–10,000 pg/μL
Sensitivity	15 pg/μL	250 pg/μL	15 pg/μL	15 pg/μL	NA	NA
Injection time	150 s	200 s	150 s	150 s	50 s	50 s
Separation Time	40 min	40 min	45 min	90 min	45 min	90 min
Sizing Accuracy (% Error)	20%	20%	15%	15%	15%	15%
Sizing Precision (% CV)	20%	20%	< 10%	< 10%	< 5%	< 5%
Qualitative Range	50–5,000 pg/μL	500–5,000 pg/μL	NA	NA	NA	NA
Quantification Accuracy (% Error)	30%	30%	NA	NA	NA	NA
Quantification Precision (%CV)	20%	20%	NA	NA	NA	NA

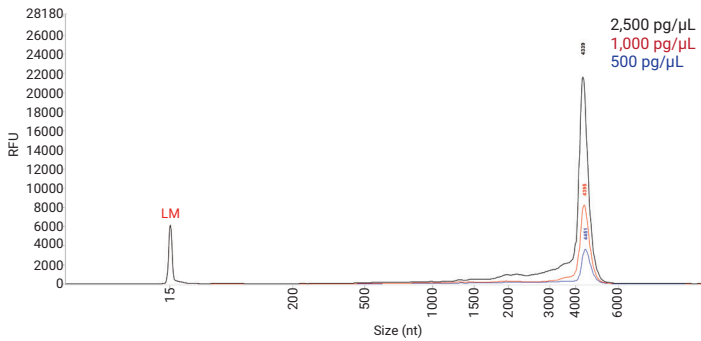
A) 1,808 nt IVT mRNA, method A



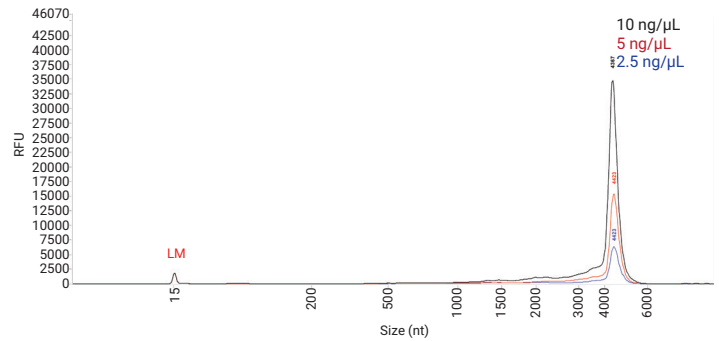
B) 1,808 nt IVT mRNA, method B



C) 4,305 nt IVT mRNA, method A



D) 4,305 nt IVT mRNA, method B



E) Consistent IVT mRNA sizing across IVT mRNA methods A and B

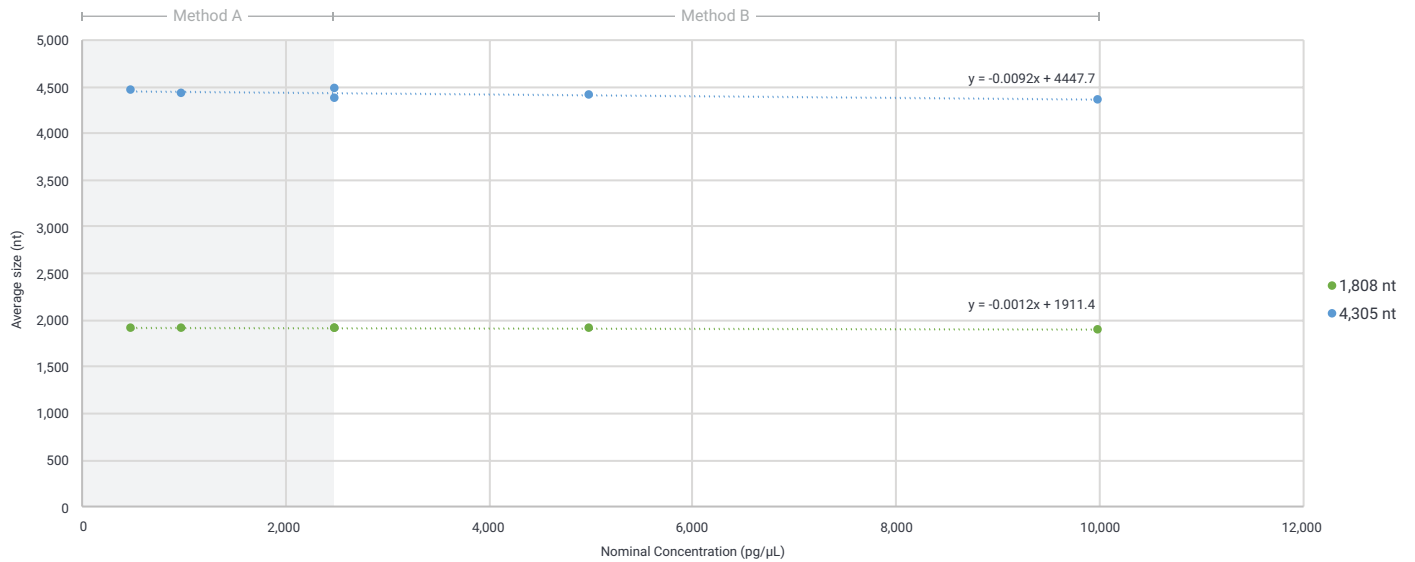


Figure 1. Reference IVT mRNA samples were analyzed on the Agilent Fragment Analyzer systems using the Agilent HS RNA kit with the optimized IVT mRNA methods. Overlay electropherograms of 1,808 nt IVT mRNA with A) method A ($n = 14$) and B) method B ($n = 20$ to 25), and the 4,305 nt IVT mRNA with C) method A ($n = 22$) and D) method B ($n = 30$ to 36). E) Analysis of the average size of each sample across the concentration ranges of both methods. Each sample concentration was run in multiple replicates on the 5200 and 5300 Fragment Analyzer systems.

Sizing accuracy

To evaluate the sizing accuracy of the methods, different concentrations of the reference samples were analyzed in multiple replicates and compared to their known sizes. Figure 2 summarizes the sizing accuracy of each sample. For the low-concentration method A, the 1,808 and 4,305 nt samples displayed an average accuracy of 5.6% error or less. Comparable results were achieved with the mid-concentration method B, with all samples showing an accuracy of 6.1% error or less. Samples run with both methods A and B were well below the sizing accuracy for IVT mRNA with the HS RNA kit of $\pm 15\%$ error. Importantly, the longer injection time of method B did not affect the sizing accuracy of the IVT mRNA samples compared to the shorter injection time of method A. Across the concentration range of both samples, the sizing accuracy was well within the specifications of the IVT mRNA methods for the HS RNA kit.

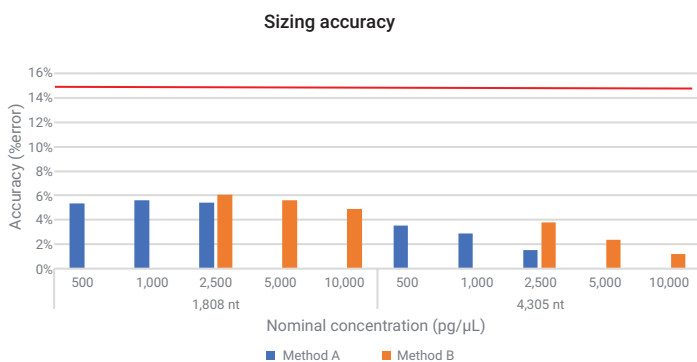


Figure 2. Sizing accuracy of the 1,808 and 4,305 nt IVT mRNA samples at different input concentrations analyzed on the Agilent Fragment Analyzer systems using the Agilent HS RNA kit with methods A and B. All samples were below the kit specification of 15% (red line). Each sample concentration was run in multiple replicates on the 5200 and 5300 Fragment Analyzer systems. ($n = 14$ to 36 replicates per method, size, and concentration.)

Sizing precision

The HS RNA kit quick guide for IVT mRNA² states that the sizing precision for the low-concentration method A is 10% CV, while the mid-range concentration method B is 5% CV. To demonstrate this, two reference samples were assessed at different concentrations covering the ranges of the methods. As shown in Figure 3, the average precision of each sample was less than 3.2% CV for either method, which is well below the kit specifications, with method B displaying slightly lower values than method A. The slight difference may be due to the longer injection time that was used for method A to detect lower concentrations. This is evidenced by the difference in the 2,500 pg/μL sample, which was analyzed with both methods. For example, the sizing precision of the 1,808 nt sample at 2,500 pg/μL was 1.85% CV with method A, and 0.77% CV with method B. Overall, both methods showed excellent precision at all concentrations, with method B displaying slightly lower values.

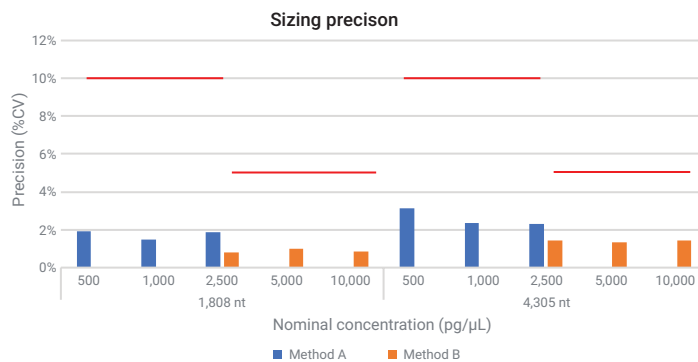


Figure 3. Sizing precision of the 1,808 and 4,305 nt IVT mRNA samples analyzed on the Agilent Fragment Analyzer systems using the Agilent HS RNA kit with IVT mRNA methods A and B. All sample sizes and concentrations were below the kit specification of 10% CV for method A and 5% CV for method B (red lines). Each sample concentration was run in multiple replicates on the 5200 and 5300 Fragment Analyzer systems. ($n = 14$ to 36 replicates per method, size, and concentration.)

Sensitivity and purity assessment

A CQA for IVT mRNA is the percent purity of the IVT mRNA fragment. This can be assessed using the Agilent ProSize data analysis software smear analysis function to identify the percentage of the sample that is composed of the main peak compared to any impurities or degradation. For this analysis, it is necessary to load the sample at a concentration that is high enough for detection of even small amounts of impurities while staying under the recommended RFU value of less than 60,000 to avoid overloading the system.

The HS IVT mRNA low-concentration method A is for samples of low concentration, with an input range of 500 to 2,500 pg/μL to allow for impurity detection. The sensitivity of the method allows for a limit of detection down to 15 pg/μL with consistent sizing, as shown in Figure 4. However, when the total sample concentration is below 500 pg/μL, small impurity peaks may not be detected, impacting percent purity analysis.

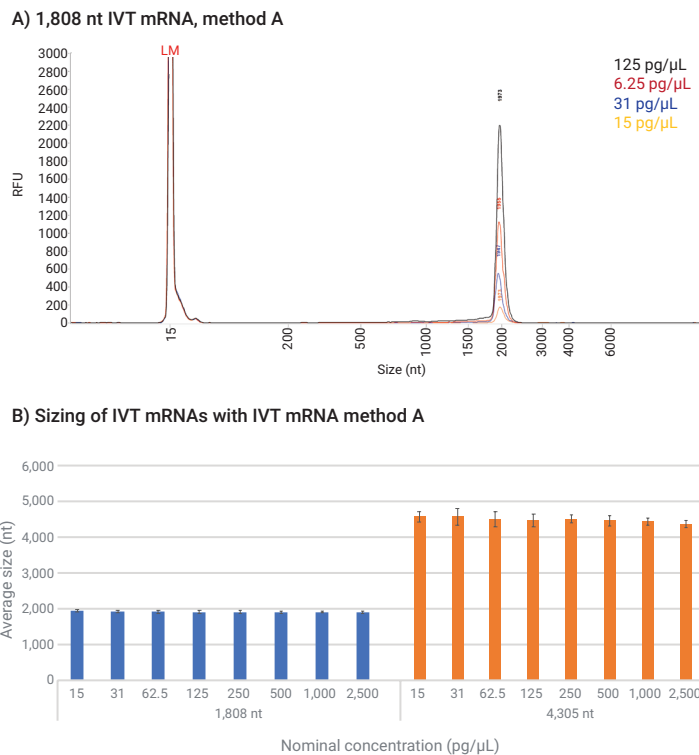


Figure 4. Sensitivity of the Agilent Fragment Analyzer for assessment of IVT mRNA using the Agilent HS RNA kit and the low-concentration method A. A) Electropherogram overlay of 1,808 nt sample, from 15 to 125 pg/μL. B) Average size of the IVT mRNA samples across the concentration range of 15 to 2,500 pg/μL. (n = 14 to 48 replicates per method, size, and concentration.)

As shown in Figure 5, the percent purity is more variable at the lower end of the sensitivity range of the kit, indicated by the %CV values at about 10% or greater for the 1,800 sample at 15 pg/μL and the 4,305 sample at 15 and 30 pg/μL. Within the concentration range of the kit, 500 to 2,500 pg/μL, the %CV of the purity assessment is below 4% for each sample size, highlighting the excellent integrity assessment that can be achieved with the Fragment Analyzer.

For reliable assessment of the impurities within a sample, it is recommended that the method is run with a concentration that gives a peak height of greater than 15,000 RFU, but no more than 60,000 RFU, for the main fragment. However, since all IVT mRNA samples have different sequences, compositions, and modifications that can affect purity, it is important to assess each sample individually and may be necessary to optimize the method or concentration to fit the needs of specific samples.

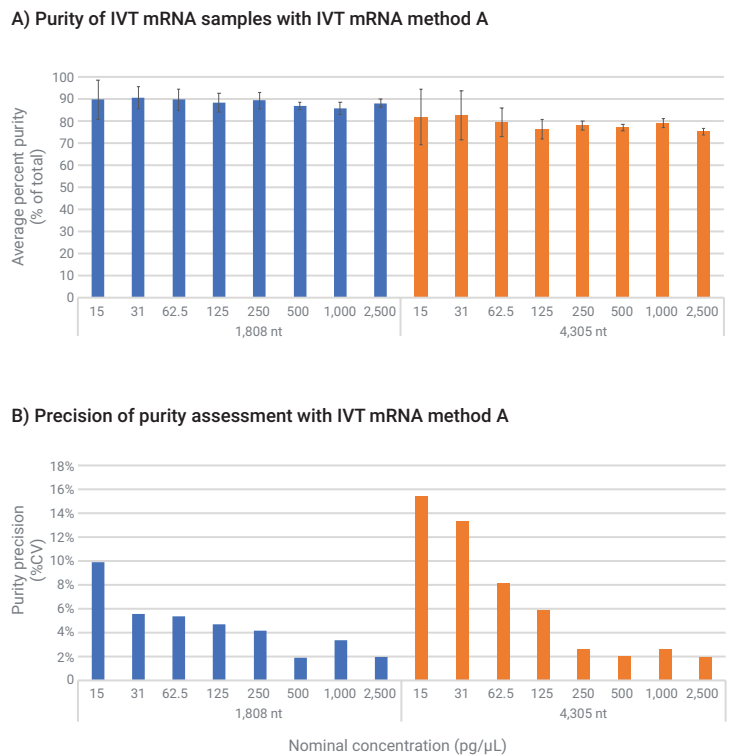


Figure 5. Purity of IVT mRNA samples at different concentrations assessed on the Agilent Fragment Analyzer using the Agilent HS RNA kit and the IVT mRNA low-concentration method A. A) Percent purity. B) Precision of the purity analysis. (n = 14 to 52 replicates per concentration.)

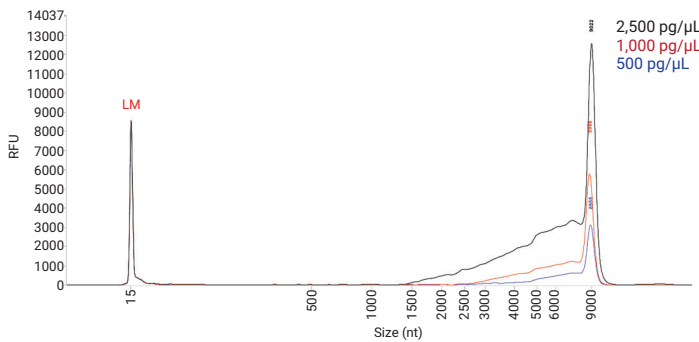
Extended method sizing accuracy and precision

Extended methods AE and BE, for IVT mRNA samples with an expected size larger than 6,000 nt, have been developed, covering the same concentration ranges as methods A and B. These methods use a longer separation time and use an alternative ladder for sizing of samples from 500 through 9,000 nt. In addition, methods AE and BE can provide higher separation resolution of closely sized fragments. To highlight the larger sizing range of these methods, as well as to demonstrate the capabilities of the extended methods for smaller sizes, the 1,808, 4,305, and a 9,000 nt IVT mRNA reference samples were analyzed on the HS RNA kit using the extended methods AE and BE. An overlay of the 9,000 nt IVT mRNA sample is shown in Figure 6A and 6B. Like methods A and B, all samples displayed excellent sizing analysis, with consistent sizing across the entire concentration range for both methods AE and BE, as demonstrated with slopes close to zero (Figure 6C).

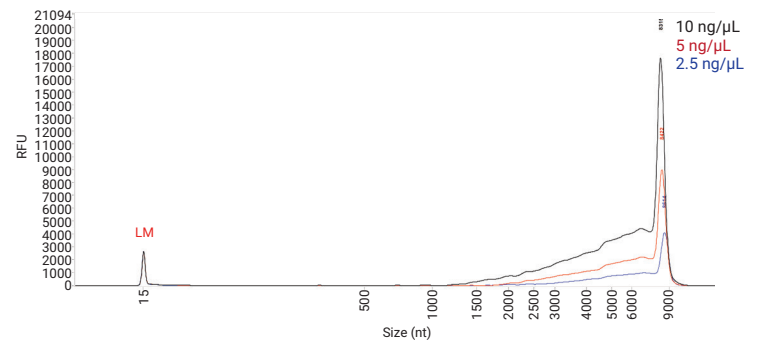
Sizing accuracy evaluation of the 1,808, 4,205, and 9,000 nt samples with the extended low-concentration method AE were below 6.2% error. Comparable sizing accuracy results were achieved with the extended mid-concentration method BE, with all samples showing a percent error of less than 7.5% (Figure 7A). The extended separation methods gave similar sizing accuracy to the normal methods. In addition, all samples showed excellent sizing precision, with the samples at each concentration having a %CV of less than 6.6% with the longer injection time of method AE, and less than 2.4% for method BE that has the shorter injection time (Figure 7B).

All samples were well within the kit specification for sizing accuracy and precision using each of the IVT mRNA methods for the HS RNA kit, with method BE displaying slightly better precision. Together, these results highlight the capabilities of the HS RNA kit to analyze IVT mRNAs over a broad range, from 200 to 9,000 nt in length and 500 to 10,000 pg/μL in concentration.

A) 9,000 nt IVT mRNA, method AE



B) 9,000 nt IVT mRNA, method BE



C) Consistent IVT mRNA sizing across IVT mRNA methods AE and BE

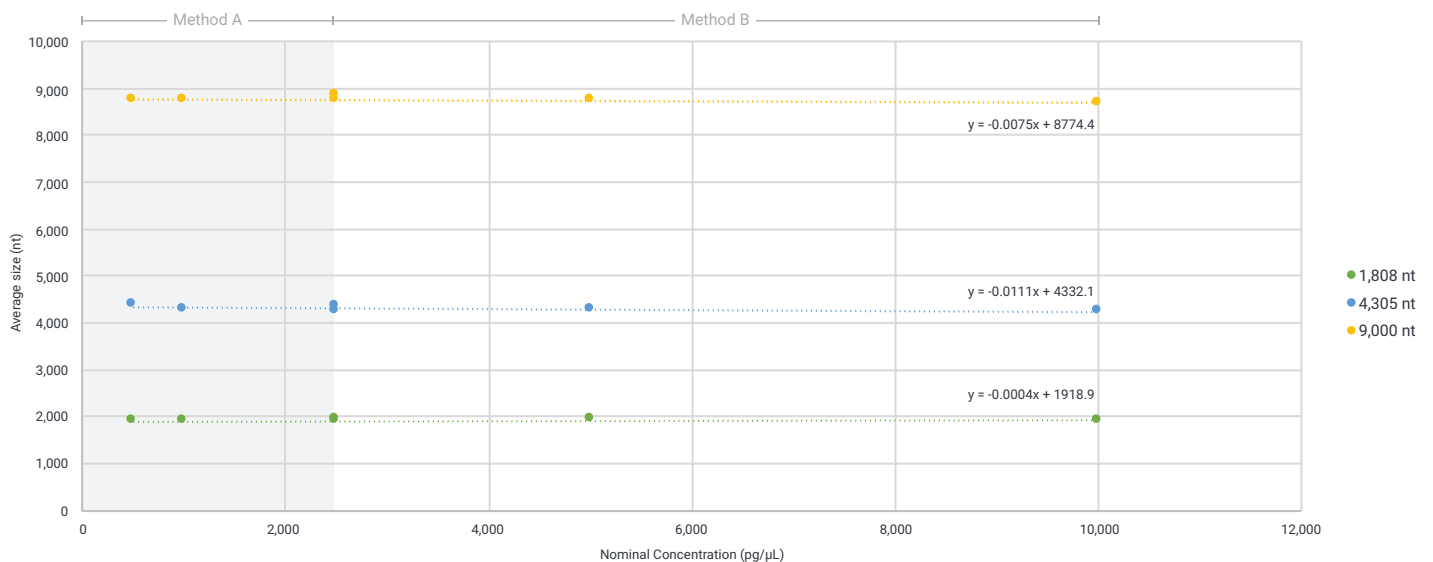
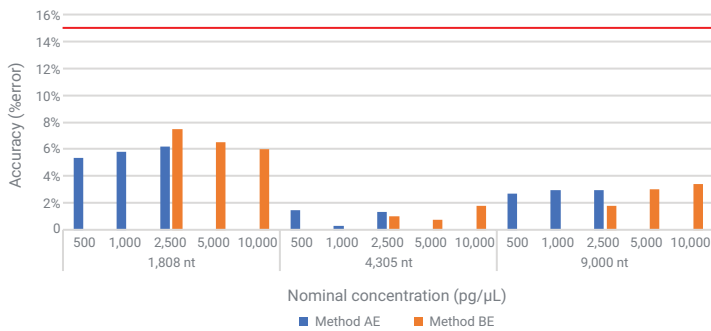


Figure 6. 1,808, 4,305, and 9,000 nt IVT mRNA samples were analyzed on the Agilent Fragment Analyzer systems using the Agilent HS RNA kit with the extended methods AE and BE. Overlay electropherogram of the 9,000 nt sample assessed with A) method AE and B) method BE. C) Sizing analysis across the range of both methods AE and BE. ($n = 10$ to 34 replicates per size and method.)

A) Sizing accuracy of extended IVT mRNA methods AE and BE



B) Sizing precision of extended IVT mRNA methods AE and BE

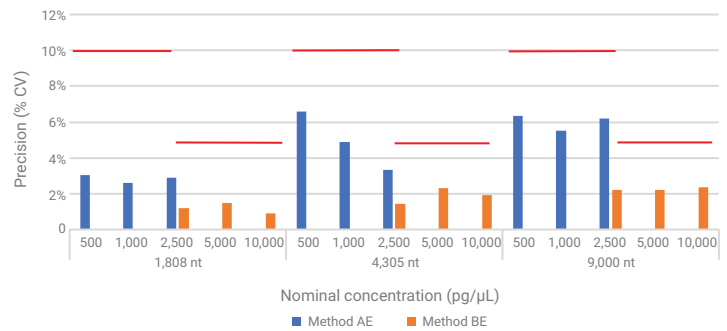


Figure 7. The A) average sizing accuracy and B) sizing precision of three IVT mRNA samples at different concentrations were assessed on the Agilent Fragment Analyzer system using the Agilent HS RNA kit with the extended methods AE and BE. Each sample concentration was run in multiple replicates on the 5200 and 5300 Fragment Analyzer systems. ($n = 10$ to 34 replicates per size and method.)

Conclusion

The Agilent HS RNA kit for the Agilent Fragment Analyzer systems is used for IVT mRNA analysis of samples from 200 to 9,000 nt. Several methods were developed to separate the large sizing range while also incorporating an expansive concentration range. Methods A and B are for analysis of 200 to 6,000 nt IVT mRNA, covering a low-range concentration of 500 to 2,500 pg/μL with method A, and a mid-range concentration of 2,500 to 10,000 pg/μL with method B. Additionally, the kit offers extended methods for analysis of longer samples up to 9,000 nt (methods AE and BE) while encompassing the same concentration ranges. Together, the new methods encompass broad sizing and concentration ranges suitable for sizing, integrity, and purity analysis of a wide variety of IVT mRNA samples with a single kit using the Agilent Fragment Analyzer systems.

References

1. Agilent DNF-472 (15 nt) HS RNA Kit - Total RNA and ribo-depleted RNA. *Agilent Technologies quick guide*, publication number SD-AT000132, **2024**
2. Agilent DNF-472 (15 nt) HS RNA Kit - IVT mRNA. *Agilent Technologies quick guide*, publication number D0117260, **2024**

www.agilent.com/genomics/fragment-analyzer

For Research Use Only. Not for use in diagnostic procedures.
PR7001-3033

This information is subject to change without notice.

© Agilent Technologies, Inc. 2024
Published in the USA, September 1, 2024
5994-7644EN

Assessment of Long IVT mRNA Fragments with the Agilent Fragment Analyzer Systems

Authors

Denise Warzak, Chava Pocerlich,
and Kit-Sum Wong
Agilent Technologies, Inc.

Abstract

The use of *in vitro* transcription (IVT) mRNA is becoming widespread in research areas such as ribozyme and aptamer synthesis, mRNA synthesis, RNA interference, and antisense RNA techniques. Longer RNA transcripts greater than 3,000 nt are needed for gene structure and functional studies. Reliable sizing, quantification, and quality assessment of IVT mRNA greater than 6,000 nt was obtained using the Agilent 5200 Fragment Analyzer system with the Agilent RNA kit (15 nt) and an extended RNA method.

Introduction

The synthesis of IVT mRNA results in many different types of RNA including viral RNA, mRNA, aptamer, dsRNA, CRISPR gRNA, riboprobe, and miRNA with endless application possibilities. Conventionally synthesized RNA fragments are less than 100 nt in length, but research in gene structure and functional studies requires RNA longer than 3,000 nt. In addition, RNA is prone to degradation due to factors including structure, light, heat, and RNases. The ability to detect low amounts of RNA degradation is important to the success of diverse RNA applications. The parallel capillary electrophoresis instrumentation portfolio from Agilent Technologies provides sensitive and reliable solutions for assessing varied lengths of RNA constructs¹. The Fragment Analyzer system with the RNA kit (15 nt) provides reliable sizing and quality assessment of short and long IVT RNA.

Experimental

The experiments in this study were performed with a 5200 Fragment Analyzer system and can be replicated with comparable results on Agilent 5300 and 5400 Fragment Analyzer systems.

Separation method of RNA transcripts

IVT mRNA was produced using the RiboMAX Large Scale RNA Production System (Promega, #P1300). RNA transcripts 9,000 and 10,000 nt in length were diluted in nuclease-free water. The diluted transcripts were separated on the Agilent 5200 Fragment Analyzer system with the Agilent RNA kit (15 nt) (p/n DNF-471) with the following modifications.

The Agilent RNA Ladder (p/n DNF-382-U020) was replaced with the Lonza RNA marker 500, 1,000, 1,500, 2,000, 2,500, 3,000, 4,000, 5,000, 6,000, and 9,000 nt (Lonza, #50575) (long RNA Ladder). The stock of long RNA Ladder was diluted in nuclease-free water to 96 ng/ μ L, and the concentration confirmed with the Qubit 4.0 using the RNA HS assay kit (Thermo Fisher Sci., #Q32852). The long RNA Ladder was added to the Agilent RNA Diluent Marker (15 nt) (p/n DNF-369-0004) at the same ratio as described in the RNA kit protocol (2 μ L ladder to 22 μ L RNA Diluent Marker).

The standard separation method (8 kV for 45 minutes) for the RNA kit (15 nt) was manually altered in the Agilent 5200 Fragment Analyzer software (extended RNA method) for fragments greater than 6,000 nt to improve the resolution of high molecular weight fragments. The extended RNA method has a lower separation voltage (4 kV) and longer separation time (90 minutes) providing better separation of impurities from fragments greater than 6,000 nt (Table 1).

The extended RNA method with the long RNA Ladder was employed for all subsequent runs described within this Application Note.

Degradation series

A 100 μ L sample of the 9,000 nt IVT mRNA (100 ng/ μ L) was heat denatured in a thermocycler at 70 °C. 12 μ L aliquots were collected every two minutes, for 16 minutes, from the PCR tube and placed on ice until further analysis. The degradation series was then analyzed according to the separation method previously described.

Capped versus uncapped

A 1,800 nt IVT mRNA was transcribed using the RiboMAX kit (Promega, #P1711) with and without 5' capping and separated with the described extended RNA method.

Table 1. The Agilent RNA kit (15 nt) standard and extended method protocol for the Agilent 5200 Fragment Analyzer system.

	Agilent RNA Kit (15 nt)	
	Sample Injection	Separation Method
Standard Method	5 kV, 4 seconds	8 kV, 45 minutes
Extended Method	5 kV, 4 seconds	4 kV, 90 minutes

Results and discussion

Comparison of the normal and extended RNA method

As IVT mRNA transcripts become longer, sizing ladders need to be extended and analysis methods re-evaluated to provide the best possible results. The 5200 Fragment Analyzer system with the RNA kit (15 nt) provides accurate sizing up to 6,000 nt for IVT RNA. To accommodate accurate sizing of longer IVT mRNA, a ladder with appropriate length fragments is required. The Lonza RNA marker (long RNA Ladder) is suitable for sizing IVT mRNA above 6,000 nt due to the additional number of fragments: 500, 1,000, 1,500, 2,000, 2,500, 3,000, 4,000, 5,000, 6,000, and 9,000 nt and was used in place of the Agilent RNA Ladder (15 nt). Longer fragments require extended separation time, which aids in achieving the best resolution possible. The RNA kit (15 nt) separation method was manually adapted in the 5200 Fragment Analyzer system software (extended RNA method) to facilitate separation of IVT mRNA longer than 6,000 nt and provide better resolution of impurities from the peak of interest.

The long RNA Ladder was diluted to 96 ng/ μ L and separated on the 5200 Fragment Analyzer system with the RNA kit (15 nt) standard method and the extended RNA method (Figure 1). Both methods provided similar separation pattern of all 10 ladder fragments. The long RNA Ladder separated with the extended method displayed enhanced resolution

compared to the standard method as seen by the increased spacing between the ladder peaks and the increased sharpness of the 9,000 nt peak. The enhanced resolution achieved with the extended method aids in the detection of minor degradation, contamination, or sizing differences from incomplete transcription.

Sizing with the long RNA Ladder was

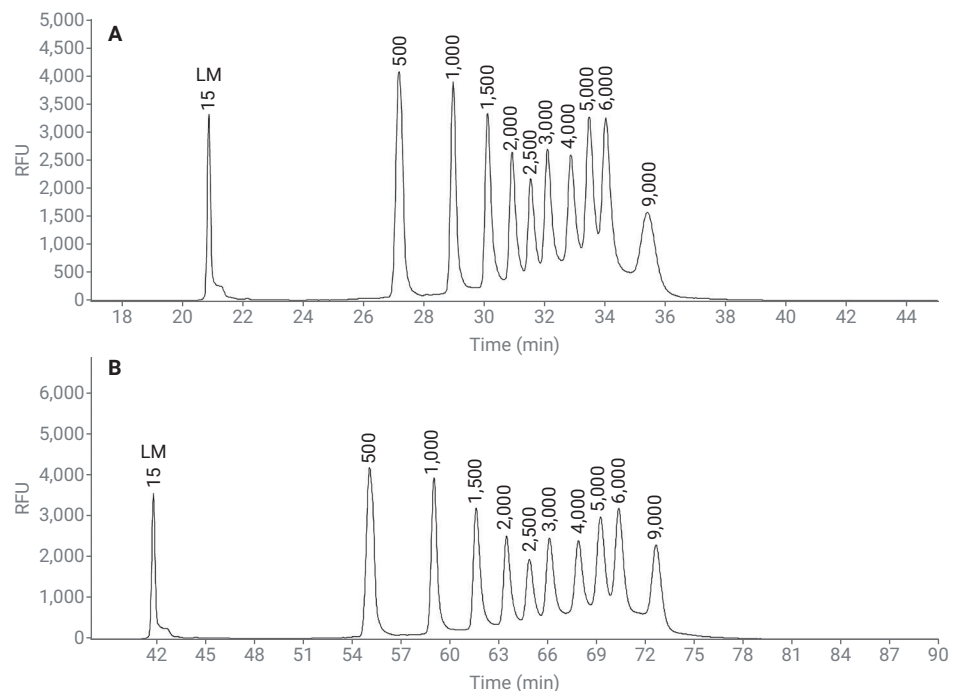


Figure 1. The long RNA Ladder separated on the Agilent 5200 Fragment Analyzer system with the Agilent RNA kit (15 nt) (A) normal method (8 kV, 45 minutes) (B) extended RNA method (4 kV, 90 minutes). LM = lower marker.

assessed with the 9,000 and 10,000 nt IVT mRNA transcripts. The RNA kit (15 nt) provides reliable quantitation for a single RNA fragment with a concentration range from 1 to 100 ng/μL. To reflect this, a dilution series of each sample over the entire concentration range of the kit (100, 50, 10 and 1 ng/μL) was assessed on the 5200 Fragment Analyzer system with the RNA kit (15 nt) standard RNA method (Figure 2) and the extended RNA method (Figure 3). Both methods reported precise sizing as indicated by the low percent coefficient of variance (% CV) throughout the dilution series (Table 2). In addition, a low percent error throughout the dilution series for both samples and with both methods indicated accurate sizing. The extended RNA method reported a lower average percent error (-0.7 %) over the entire concentration range compared to the standard RNA method (8.4 %) for the 9,000 nt sample. The 10,000 nt IVT mRNA average percent sizing error was similar between the two separation methods. The extended RNA method is recommended when extremely accurate sizing or high resolution is needed for determining the presence of degradation or sizing differences from incomplete transcription in IVT mRNA samples longer than 6,000 nt.

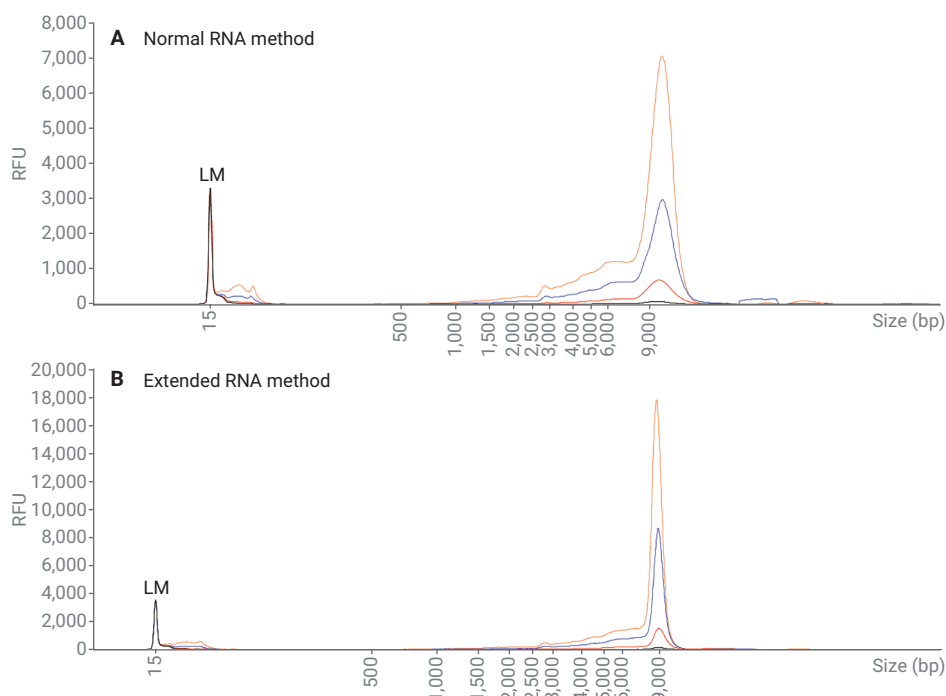


Figure 2. Overlay of the 9,000 nt IVT mRNA fragments over a dilution series of 100, 50, 10, 1 ng/μL separated on the Agilent 5200 Fragment Analyzer system with the Agilent RNA kit (15 nt) using the long RNA Ladder and (A) the normal RNA method (B) the extended RNA method. LM = lower marker.

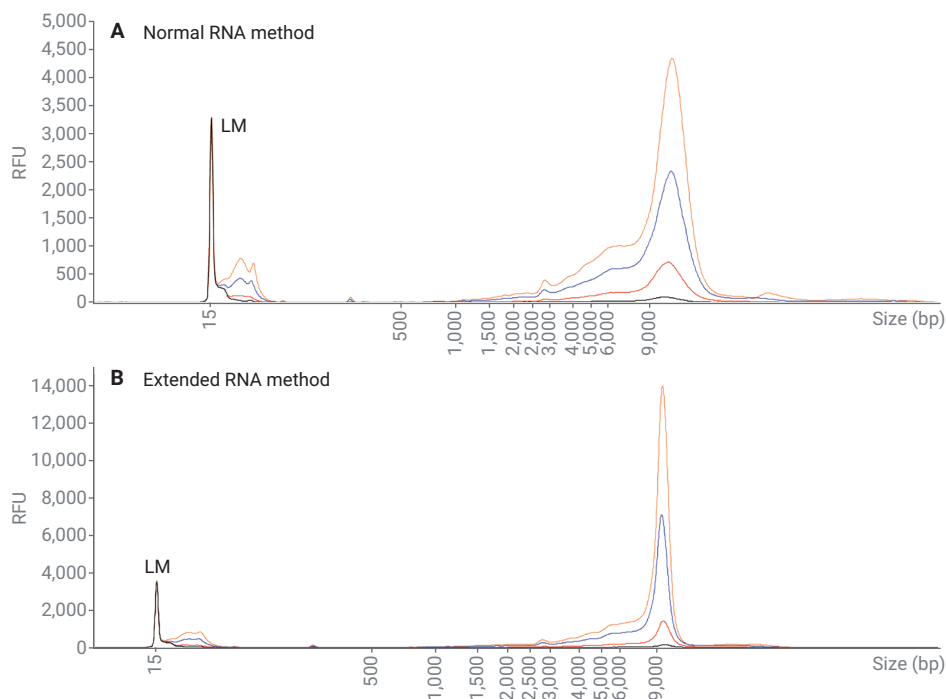


Figure 3. Overlay of the 10,000 nt IVT mRNA fragments over a dilution series of 100, 50, 10, 1 ng/μL separated on the Agilent 5200 Fragment Analyzer system with the Agilent RNA kit (15 nt) using the long RNA Ladder and (A) the normal RNA method (B) the extended RNA method. LM = lower marker.

Degradation series

The smear analysis feature in the Agilent ProSize data analysis software can be used to determine the percent of degradation from the DNA template, and the percent of IVT mRNA. The 9,000 nt IVT mRNA was degraded at 70 °C for 0 to 16 minutes. Every two minutes an aliquot was taken and placed on ice. The degradation series was separated on the 5200 Fragment Analyzer system with the RNA kit (15 nt) using the extended RNA method and long RNA Ladder (Figure 4). The electropherogram and gel image displayed a decrease in the expected peak height with increased degradation time. Smear analysis was performed to determine the percent of degradation (smear range 75 to 7,500 nt) and the percent of the peak of interest (smear range 7,500 to 11,000 nt). The percent concentration was recorded for each smear range and compared between time points. As expected, the percent degradation increased with incubation time, in correlation with a decreased percent of the peak of interest as the sample degraded (Table 3). A narrow smear analysis range of the peak of interest can help to identify varying sizing from incomplete transcription. The smear analysis feature offers a simple approach for assessing sample quality.

Table 2. IVT RNA analyzed on the Agilent 5200 Fragment Analyzer system with the Agilent RNA kit (15 nt) and separated with both the normal RNA method and the extended RNA method (A) 9,000 nt sample (B) 10,000 nt sample. *n=3.

Concentration (ng/μL)	Sizing Throughout Dilution Series					
	Theoretical Size 8,989 nt					
	Normal RNA Method			Extended RNA Method		
	Average* (nt)	% CV	% Error	Average* (nt)	% CV	% Error
100	9,910	1.6 %	10.2 %	8,705	0.9 %	-3.2 %
50	9,862	0.8 %	9.7 %	9,051	2.3 %	0.7 %
10	9,718	0.6 %	8.1 %	8,977	0.4 %	-0.1 %
1	9,491	0.4 %	5.6 %	8,971	0.7 %	-0.2 %
1 to 100	9,745	0.8 %	8.4 %	8,926	0.8 %	-0.7 %

Concentration (ng/μL)	Sizing Throughout Dilution Series					
	Theoretical Size 10,003 nt					
	Normal RNA Method			Extended RNA Method		
	Average* (nt)	% CV	% Error	Average* (nt)	% CV	% Error
100	10,736	0.2 %	7.3 %	9,453	1.3 %	-5.5 %
50	10,676	0.3 %	6.7 %	9,501	1.1 %	-5.0 %
10	10,496	0.4 %	4.9 %	9,597	0.8 %	-4.1 %
1	10,197	0.8 %	1.9 %	9,620	0.2 %	-3.8 %
1 to 100	10,526	0.4 %	5.2 %	9,543	0.5 %	-4.6 %

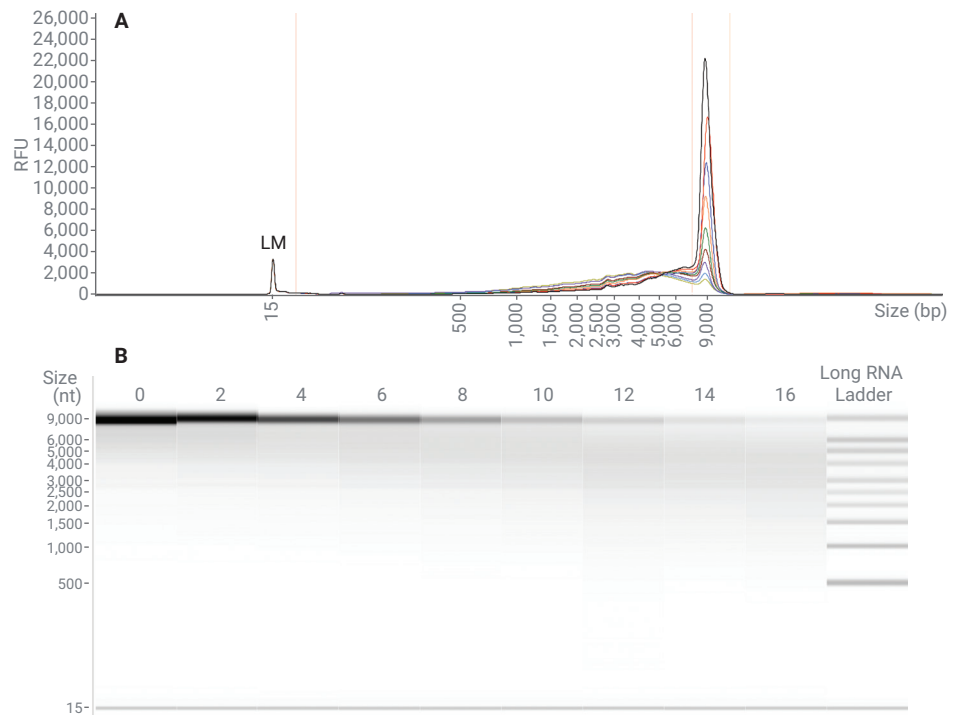


Figure 4. 9,000 nt IVT mRNA analyzed on the Agilent 5200 Fragment Analyzer system with the Agilent RNA kit (15 nt) using the long RNA Ladder and extended RNA method over a degradation series at 70 °C from 0 to 16 minutes. (A) Electropherogram overlay of degradation series. (B) Gel image of degradation. LM = lower marker.

Capped versus uncapped

A common modification made to IVT mRNA transcript is the addition of a 7-methylguanylate cap at the 5' end. A 5' cap stabilizes the RNA transcript, prevents degradation, and assists in binding during translation. Capped and uncapped 1,800 nt IVT mRNA were analyzed on the 5200 Fragment Analyzer system with the RNA kit (15 nt) using the extended RNA method and long RNA Ladder (Figure 5). The extended RNA method was used to provide the best resolution possible. An average size of 1,810 nt was observed for both the capped and uncapped RNA transcripts. RNA capping did not influence the sizing or general profile of the transcript.

Conclusion

The Agilent 5200 Fragment Analyzer system offers reliable quality control analysis essential to IVT mRNA workflows. Accurate sizing of IVT mRNA greater than 6,000 nt was achieved with the Agilent RNA kit (15 nt) using a long RNA Ladder with both the normal and extended RNA method. The extended RNA method offers the option of exceptional sizing to confirm complete transcription and the ability to distinguish minute amounts of degradation. The ProSize Smear Analysis tab in the Agilent ProSize data analysis software enables the simultaneous detection of the percent of the peak of interest and the percent of degradation. This feature aids the user in quickly identifying a quality sample. In addition, the 5200 Fragment Analyzer and the RNA kit (15 nt) provided accurate sizing with the addition of a 7-methylguanylate cap at the 5' end of the RNA transcript.

Reference

www.agilent.com

For Research Use Only. Not for use in diagnostic procedures.

This information is subject to change without notice.

Table 3. Smear analysis of the percent concentration for two regions of the 9,000 nt IVT mRNA throughout the degradation series separated on the Agilent 5200 Fragment Analyzer system with the Agilent RNA kit (15 nt) using the extended RNA method and the long RNA Ladder. *n=2.

Smear Analysis of Degradation Series 9,000 nt IVT RNA		
70 °C Incubation Time (minutes)	Percent of Degradation (75 to 7,500 nt)*	Percent of Peak of Interest (7,500 to 11,000 nt)*
0	36.8 %	62.7 %
2	44.6 %	54.9 %
4	52.3 %	46.7 %
6	60.8 %	36.5 %
8	70.0 %	28.1 %
10	77.3 %	20.9 %
12	85.3 %	13.4 %
14	87.7 %	10.4 %
16	90.5 %	7.5 %

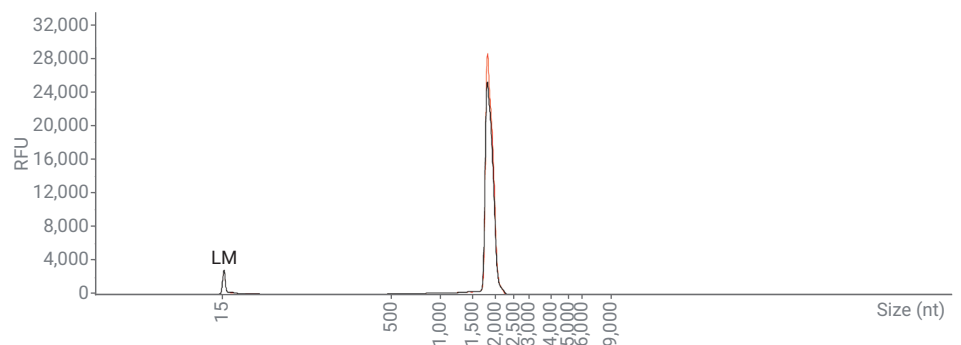


Figure 5. Overlay of the 1,800 nt IVT mRNA fragments capped (red) and uncapped (black) separated on the Agilent 5200 Fragment Analyzer system with the Agilent RNA kit (15 nt) using the extended RNA method and the long RNA Ladder. LM= lower marker

1. Warzak, D.; Pocerlich, C.; Wong, K-S. Benefits of Quality Control in the IVT RNA Workflow Using the Agilent 5200 Fragment Analyzer System, *Agilent Technologies Application Note*, publication number 5994-0512EN, **2018**.

Best Practices for Analysis of In Vitro Transcribed (IVT) mRNA Using the Agilent Fragment Analyzer systems

Introduction

The recent success of in vitro transcription (IVT) mRNA as an emergent platform has brought to the forefront the need for reliable and robust quality control (QC) analysis throughout the workflow. Within the IVT workflow for mRNA vaccine production there are many opportunities for QC that help in the development of a consistent product. The Agilent Fragment Analyzer systems can be utilized for several QC steps at different checkpoints in the mRNA vaccine development workflow.¹ QC steps that can be performed using the Fragment Analyzer include determining the quality and size of the linearized plasmid, size and purity of the IVT mRNA^{2,3}, length of the poly(A) tail⁴, and purity of the final mRNA vaccine product¹.

IVT mRNA yield and quality can be affected by a multitude of factors, including temperature, incubation time, sequence, secondary structure, and mRNA size. This technical overview discusses best handling practices for IVT mRNA and analysis with the Fragment Analyzer systems, including sample handling and quantification tips. Also, we provide guidance for determining the appropriate methods of analysis of IVT mRNA samples and options for optimizing the QC process for different mRNA transcripts.

Experimental

Aliquots of Lambda DNA (Thermo Fisher Scientific, part number SD0021) were PCR amplified using Phusion DNA polymerase to generate templates of sizes ranging from approximately 200 to 6,000 base pairs (bp), shown in Table 1. Following amplification, each PCR reaction was purified using the NucleoSpin Gel and PCR Clean-up kit (Takara Bio, part number 740609.50) and quantified using the Qubit fluorometer (Thermo Fisher Scientific).

The purified PCR products were then used as DNA templates for in vitro transcription. One µg of each template was used to prepare an IVT mRNA sample using the T7 RiboMAX Express Large Scale mRNA Production System (Promega, part number P1320). The IVT mRNA fragments were purified using the mRNA Clean & Concentrator-5 kit (Zymo Research, part number R1013). The final samples were quantified using the NanoDrop One spectrophotometer (Thermo Fisher Scientific), and the size and purity were assessed using the Agilent 5200 and 5300 Fragment Analyzer systems with the Agilent RNA kit (15 nt) (part number DNF-471).⁵

Table 1. List of IVT mRNA samples used in this study and their sequence size.

Reaction Number	Sequence Size (nt)
1	212
2	410
3	493
4	894
5	996
6	1,902
7	2,055
8	3,900
9	4,053
10	5,979

Results and discussion

Mixing

RNA is easily degraded by improper sample handling, such as overmixing and unsuitable storage conditions. To provide guidance on the most efficient method for mixing IVT mRNA with the Agilent RNA Diluent Marker for analysis with the Fragment Analyzer systems, various mixing methods were explored. First, a 2,055 nt sample was prepared in a master mix, mixed by pipetting, then aliquoted onto the sample plate (wells 1 to 5). The same sample was loaded directly onto the plate with the diluent marker and analyzed immediately after heat denaturation with no mixing (wells 6 to 10).

As shown in the digital gel images in Figure 1, the master mixed samples display uniform bands, while the samples that were not mixed show a large variation in peak intensity. This variation will affect the peak height, reported concentration, and percent total calculations from the Fragment Analyzer analysis. This data provides evidence that proper mixing of IVT mRNA samples is necessary for reliable sample analysis.

The Agilent RNA kit (15 nt) for the Fragment Analyzer lists various methods that are acceptable for mixing total RNA samples with the RNA Diluent Marker. To ensure that each of these methods were acceptable for use with IVT mRNA, 996 and 2,055 nt IVT mRNA samples were prepared with the different mixing methods.

In method A, a master mix was prepared by vortexing enough sample and RNA Diluent Marker for aliquoting into five wells. In method B, 22 µL of diluent marker and 2 µL of sample were added to five individual wells of a PCR plate and mixed using a plate vortex (VWR, part number 102093-352) set at 2,000 rpm for two minutes. In method C, the samples and diluent marker were also added to five individual wells but were mixed five times using a pipette set to 20 µL.

The prepared sample plates were heat denatured at 70 °C for 2 minutes, snap cooled at 4 °C, and analyzed on the Fragment Analyzer with the RNA analysis method. The size, concentration, percent total, and peak heights for each sample (2,055 nt shown in Figure 2; 996 nt not shown) did not significantly change between the mixing methods. Importantly, the mixing method did not elicit any degradation or size shifting of the sample. Together, these data indicate that mixing of IVT mRNA samples with the RNA Diluent Marker is crucial for reliable analysis of IVT mRNA, and that any mixing method will provide similar results.

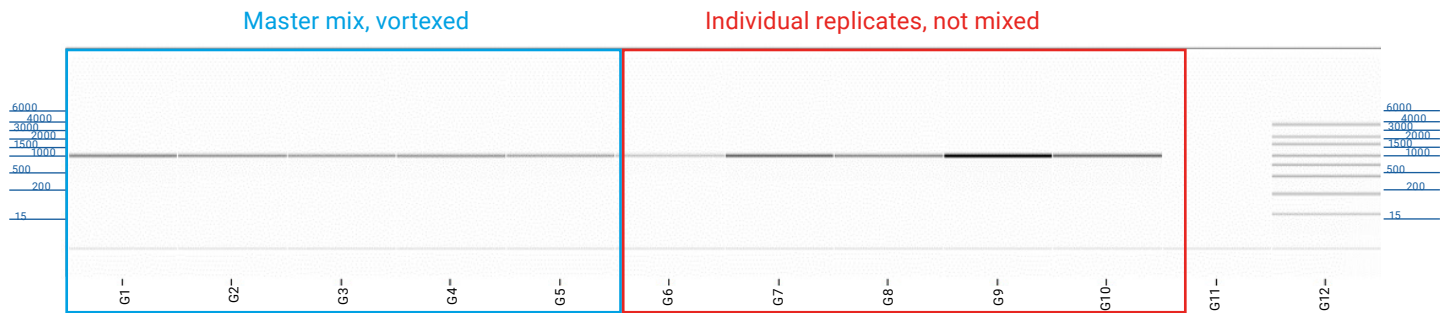


Figure 1. Digital gel image of an IVT mRNA sample on the Agilent 5200 Fragment Analyzer system prepared as a master mix and vortexed (wells 1 to 5, blue outline) compared to samples prepared individually and not mixed (wells 6 to 10, red outline). Samples that were not mixed show clear differences in peak intensity, compared to the uniform bands of the mixed samples (n = 5 samples per method).

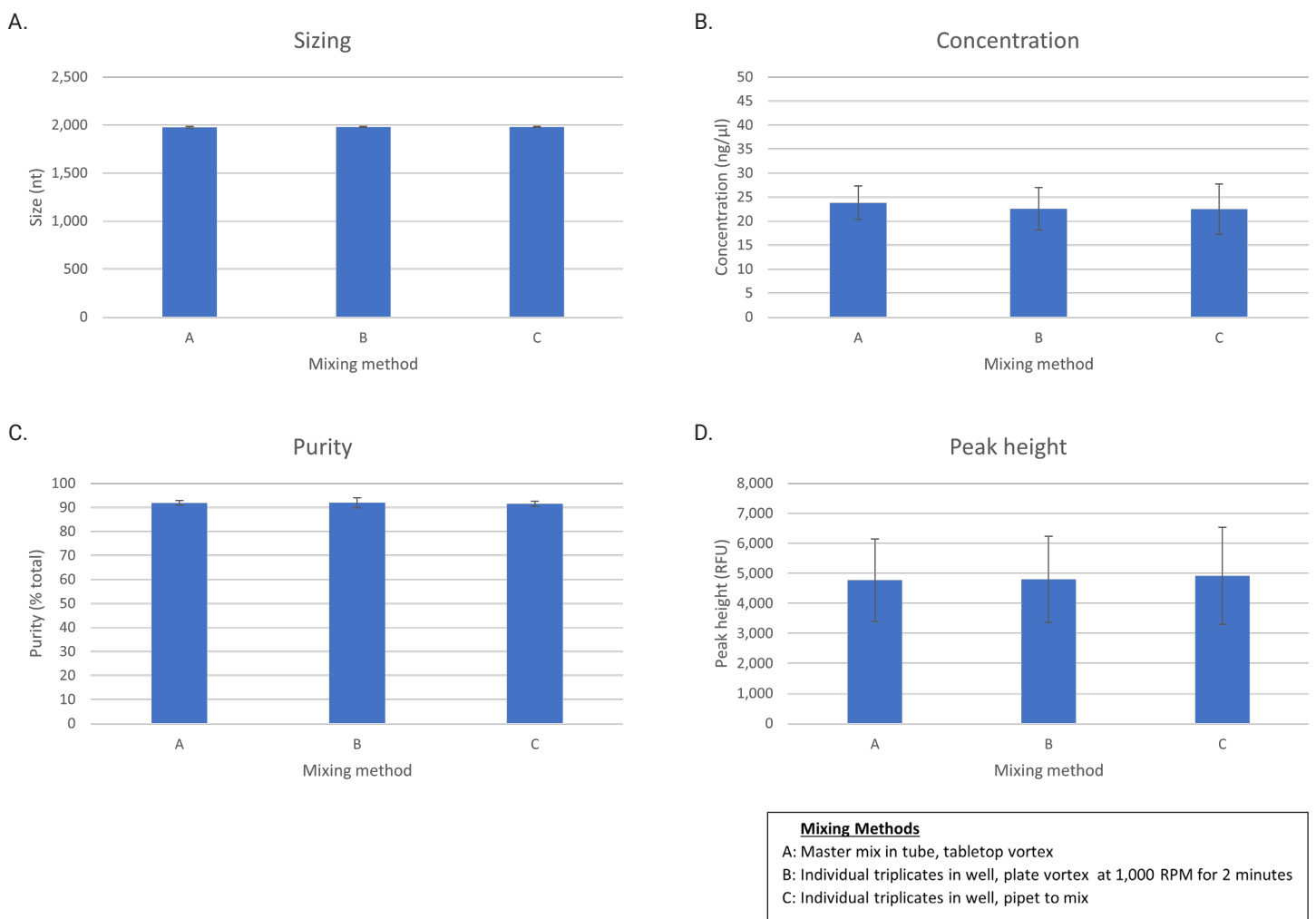
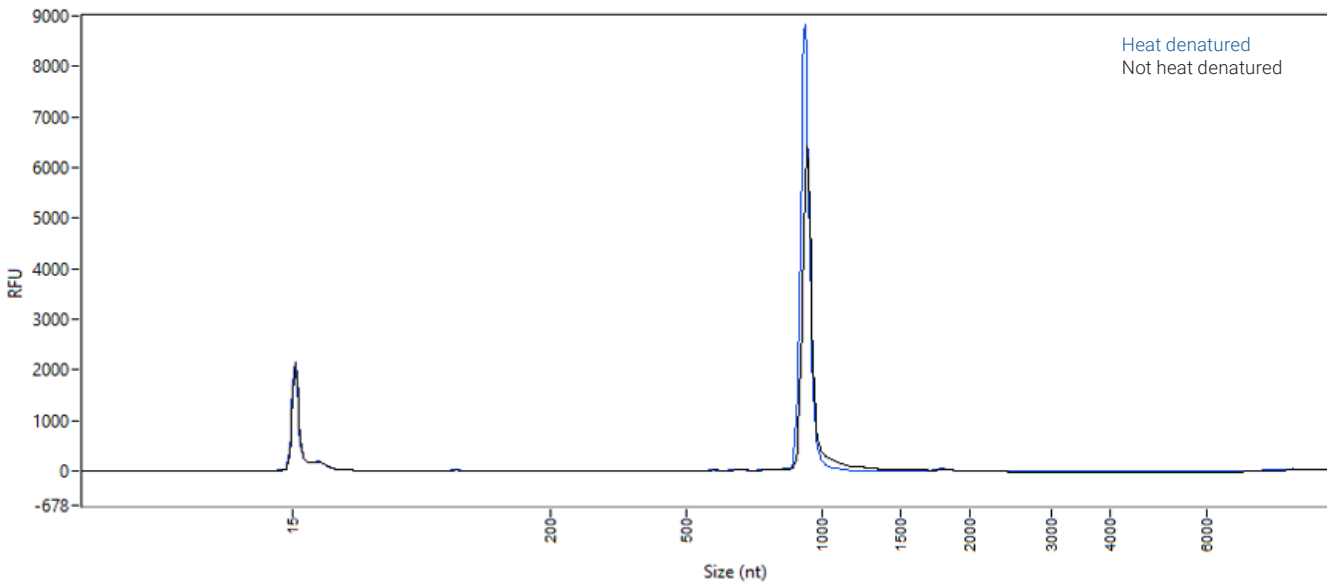


Figure 2. Comparison of different methods of mixing a 2,055 nt IVT mRNA sample with the Agilent RNA Diluent Marker for analysis with the RNA kit on a 5200 Fragment Analyzer system. The A) sample size, B) concentration, C) purity total, and D) peak height was not significantly changed with the different mixing methods (n = 5).

A.



B.

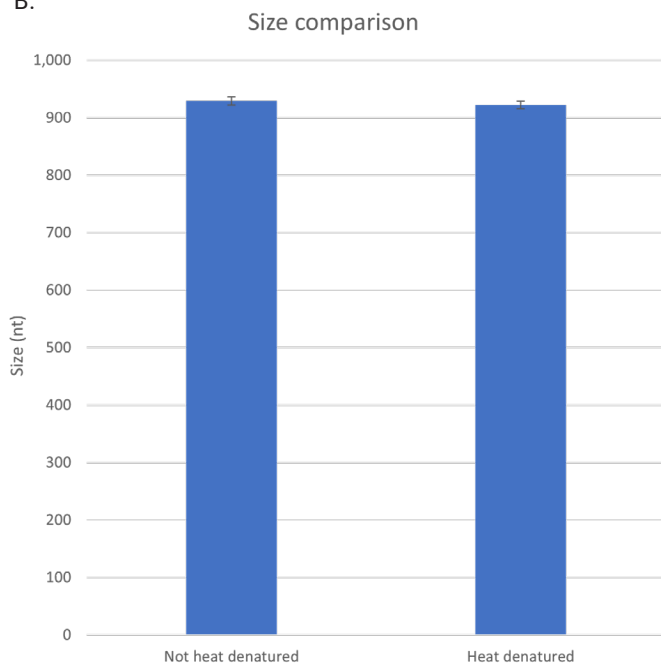


Figure 3. Effect of heat denaturation of IVT mRNA samples analyzed on the Agilent 5300 Fragment Analyzer system. A) Representative electropherogram overlay and B) average fragment size ($n = 46$) of a 996 nt IVT mRNA sample with and without heat denaturation. Error bars represent standard deviation.

Heat denaturing

Denaturation is a common method in RNA protocols to eliminate secondary structures present in the RNA. This can be done by applying heat to the samples or mixing them with a chemical denaturant. Analysis of samples with the Fragment Analyzer requires samples to be mixed with the RNA Diluent Marker, which contains 50% formamide, a common storage solvent that protects RNA from degradation by RNases and provides some level of denaturation. Thus, we examined if heat denaturation is also necessary for IVT mRNA analysis with the Fragment Analyzer.

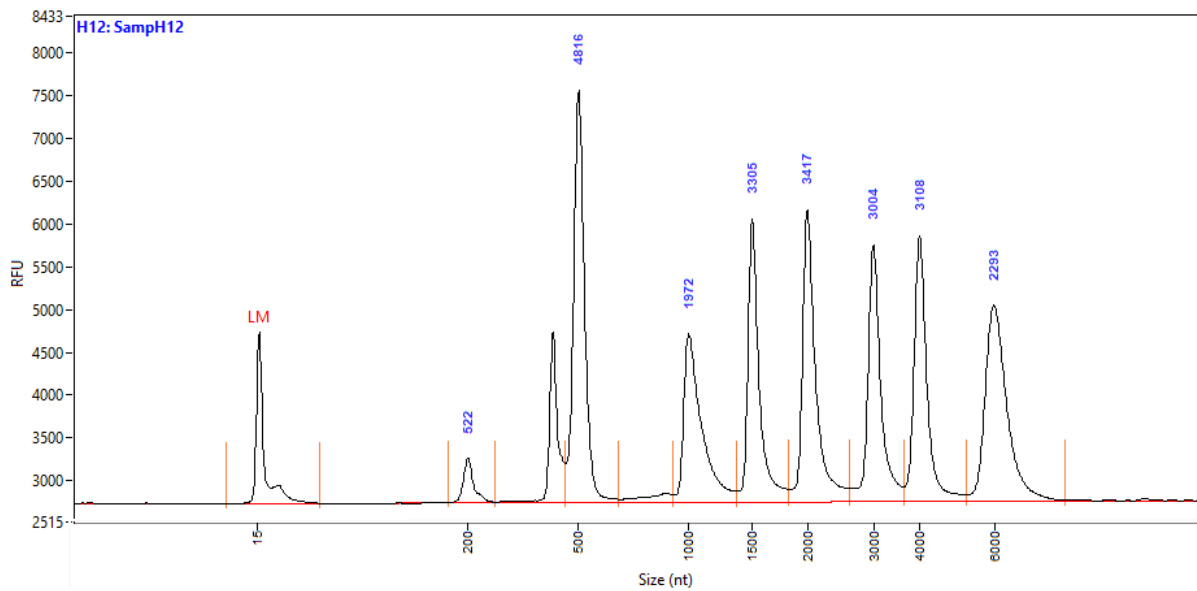
IVT mRNA samples of various sizes and the Agilent RNA Ladder were mixed with the RNA Diluent Marker and analyzed on the Fragment Analyzer before and after heat denaturation at 70 °C for 2 minutes, then snap cooled to 4 °C.

A comparison of the samples before and after heat denaturation indicates that heat denaturation results in a sharper peak. This change in sample distribution may impact peak heights and thus could influence the reported purity of the sample. For example, Figure 3A is an overlay of a 996 nt IVT mRNA sample before and after heat denaturation. In this example, heat denaturation of the sample increased the sharpness of the peak but did not significantly affect the reported percent purity. However, the size of the IVT mRNA sample remains consistent with and without heat denaturation (Figure 3B).

Heat denaturation is required for the RNA Ladder. As shown in Figure 4, heat denaturation of the ladder results in sharper peaks of uniform heights and eliminates secondary structures, such as the split peak seen at 500 nt when the

ladder is not heat denatured. Depending on the sample, heat denaturation may or may not be required before analysis with the Fragment Analyzer system. If a secondary structure is seen, the sample can be heat denatured and reanalyzed for best results.

A. Not heat denatured



B. Heat denatured

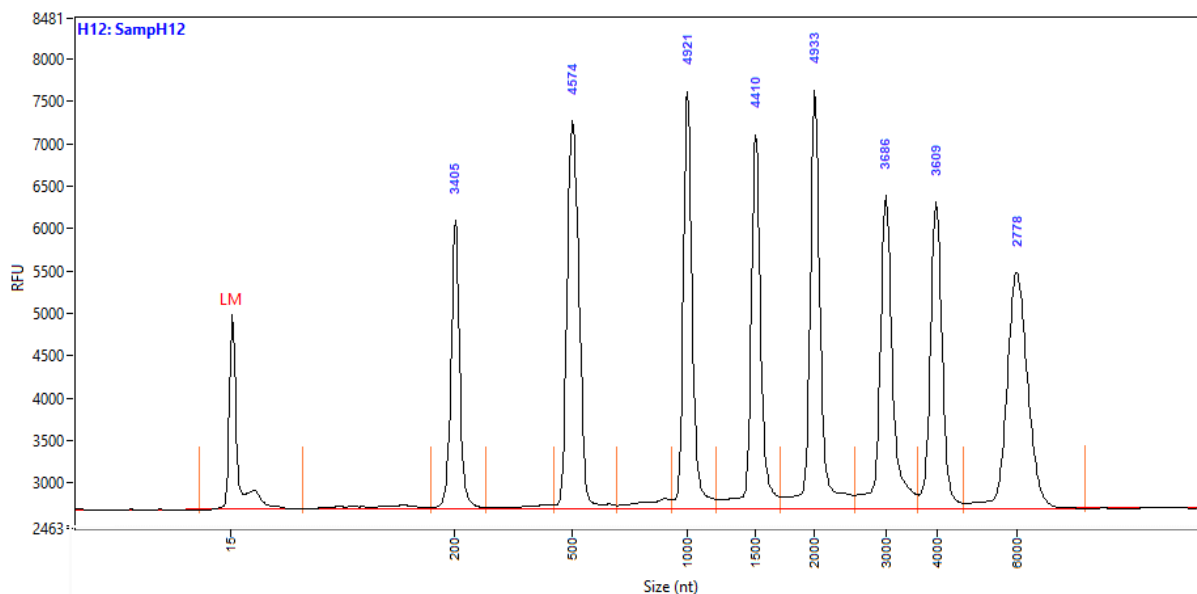


Figure 4. Heat denaturation of the Agilent RNA Ladder is required for accurate sizing analysis with the Agilent 5200 Fragment Analyzer system, as indicated in the electropherogram image of the ladder A) without and B) with heat denaturation. Heat denaturation eliminates secondary structure and results in sharper, more consistent peak heights throughout the size range of the ladder.

Stability

The Fragment Analyzer system can hold up to three 96-well sample plates and can be programmed to run multiple sample rows consecutively. To ensure that IVT mRNA remains stable at room temperature over time, replicates of a 2,055 nt sample were prepared (n = 5) and analyzed with the RNA kit (15 nt) over 10 subsequent runs, with

approximately one hour elapsing between the start of each run. No significant change in sample appearance, size, or percent purity was observed over this time (Figure 5). The IVT mRNA samples analyzed were stable at room temperature for 10 hours, providing sufficient time to analyze many rows of samples on the Fragment Analyzer without having to worry about degradation.

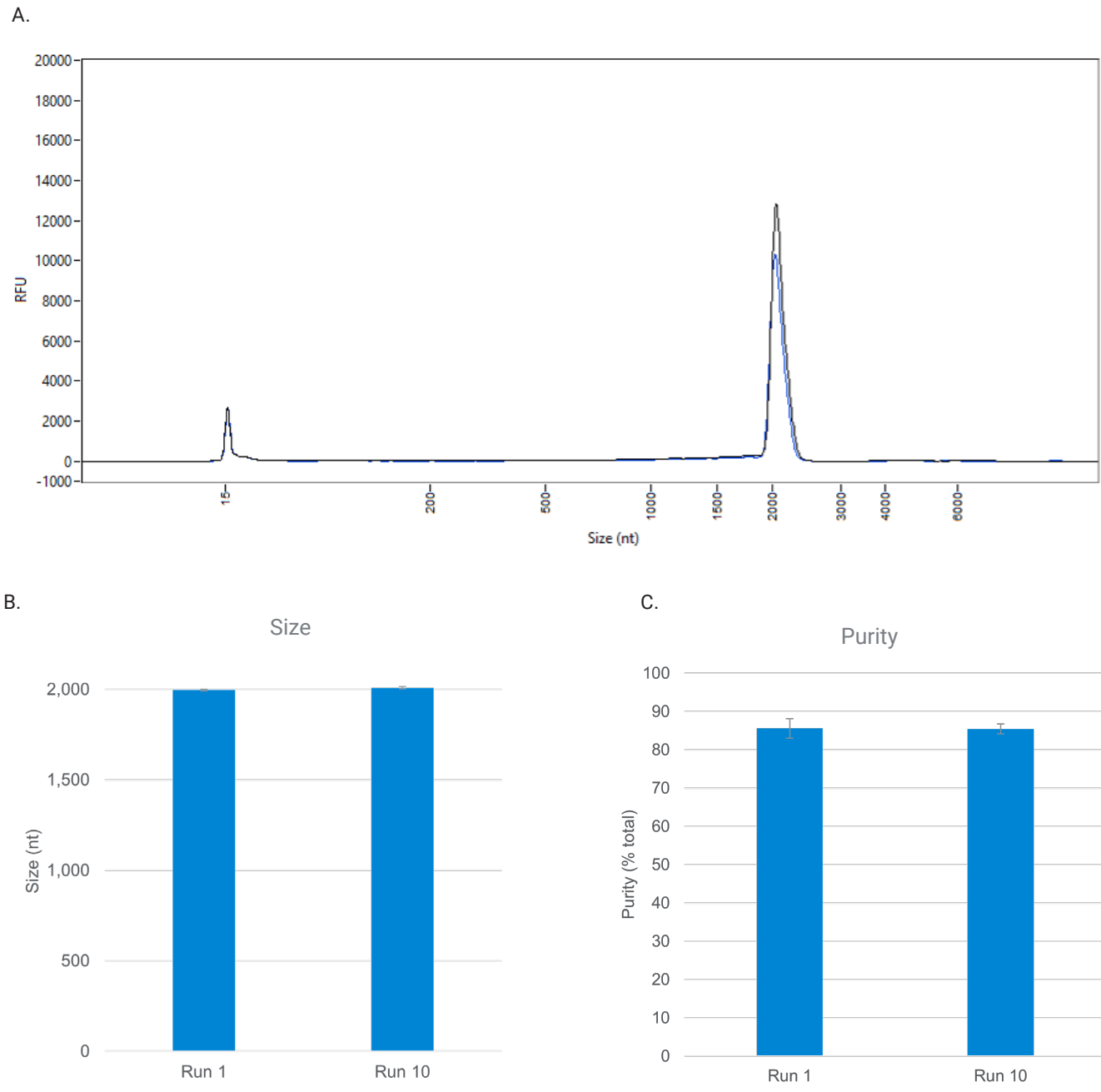


Figure 5. IVT mRNA samples prepared for analysis on an Agilent 5200 Fragment Analyzer system remained stable at room temperature for approximately 10 hours. A representative 2,055 nt IVT mRNA sample was analyzed over 10 subsequent runs, with no significant change in A) sample distribution, B) size, or C) purity, which was assessed using the percent total with a smear range from 1,800 to 2,400 nt.

Instrument reproducibility

To investigate the reproducibility of IVT mRNA analysis, triplicate replicates of IVT mRNA samples of sizes 212, 894, and 1,902 nt were each analyzed across four Agilent Fragment Analyzer systems simultaneously. The average reported size of each fragment is shown in Figure 6, and

is consistent between all instruments with a %CV of less than 0.5% for each sample. Also, the size percent error was excellent, with less than 8% error for the 212 nt sample, less than 3% error for the 894 nt sample, and less than 1.5% error for the 1,902 nt sample.

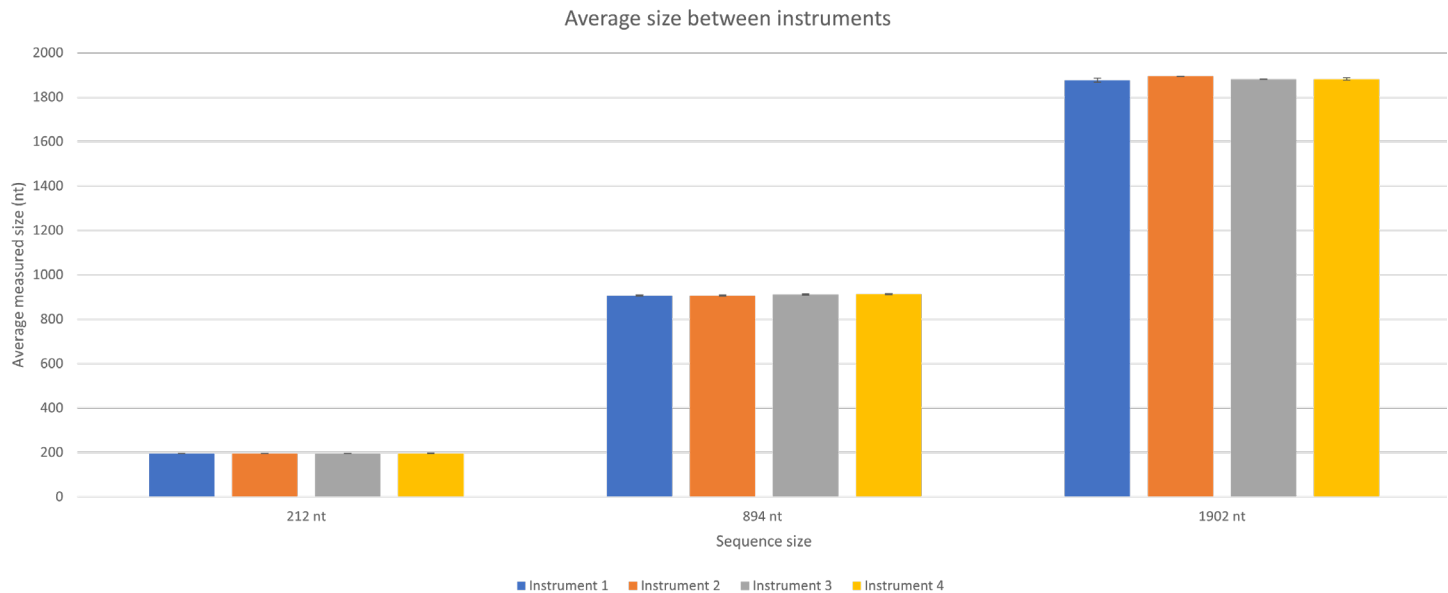


Figure 6. Three IVT mRNA samples of varying sizes were evaluated in triplicate across four Agilent 5200 Fragment Analyzer systems to demonstrate the ability of the instruments to provide reproducible analysis data. The average size of each fragment remained consistent across all instruments tested. Error bars show standard deviation.

IVT mRNA quantification

The RNA kit for the Fragment Analyzer recommends that samples are loaded within a specific concentration range that is necessary for appropriate analysis of the sample. To ensure that samples fit this range, it is important to accurately quantify the sample. Common techniques for quantification of total RNA include either UV-Vis spectrometry or fluorescent methods. However, fluorescent systems such as the Agilent Fragment Analyzer and the Qubit fluorometer (Thermo Fisher Scientific) utilize an intercalating dye that may not bind to IVT mRNA with appropriate affinity to allow for accurate quantification of these samples. To provide guidance for the most accurate quantification of IVT mRNA, UV-Vis and fluorescent methods were compared. Several IVT mRNA samples of varying sizes were quantified with UV-Vis spectrometry using a NanoDrop One spectrophotometer (Thermo Fisher Scientific) and diluted with nuclease-free water to 60, 30, and 15 ng/ μ L to fit the range of the Fragment Analyzer. The concentration of each sample dilution was confirmed with the NanoDrop. These samples were then evaluated with the Fragment Analyzer and the Qubit for

comparison. While the concentration of the samples decreased with the serial dilution as expected, the reported concentration from both the Fragment Analyzer and the Qubit did not correlate with the expected concentration from the NanoDrop. For example, shown in Figure 7 is the reported concentration of a 996 nt sample using the NanoDrop, Qubit, and Fragment Analyzer. Results were consistent among many samples that ranged in size from approximately 100 to 4,000 nt. For each fragment, the measured concentrations from the Qubit and Fragment Analyzer were reproducible and consistent with each other, but were lower than the expected concentration reported by the NanoDrop. Thus, for the most accurate quantification of IVT mRNA, and to determine the concentration at which to load samples onto the Fragment Analyzer, it is recommended to use UV-Vis methods. Also, for the most reliable size and purity analysis with the Fragment Analyzer, it is recommended to optimize the input concentration used. If comparing multiple replicates, the best practice would be to ensure that all samples are at the same concentration before loading them onto the instrument.

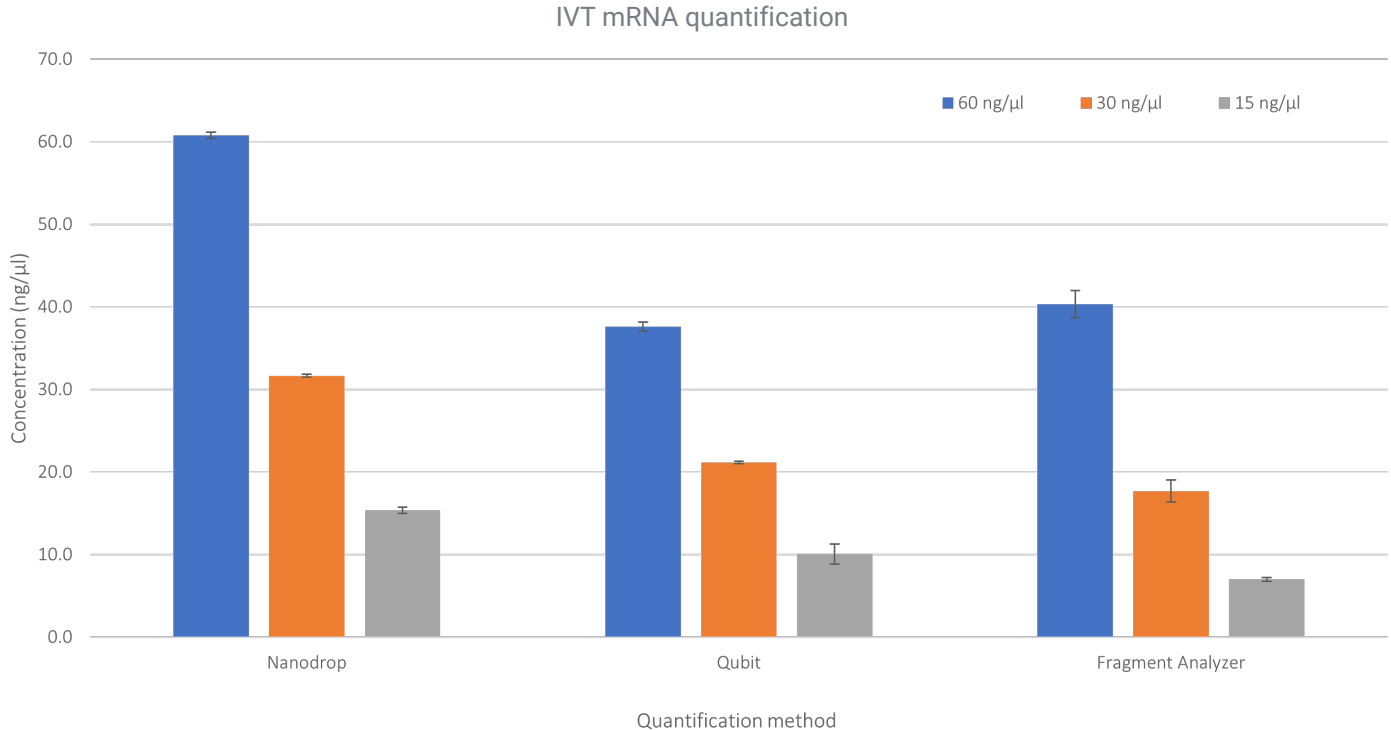


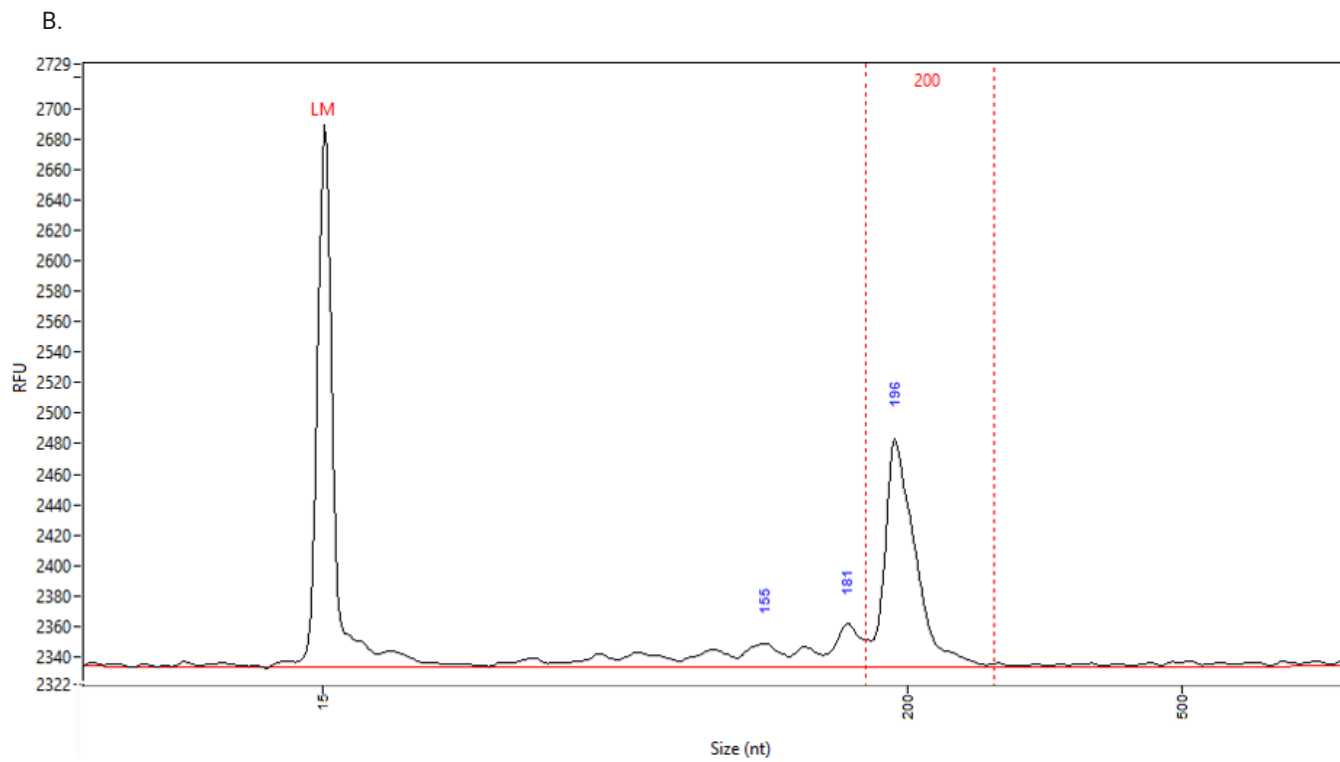
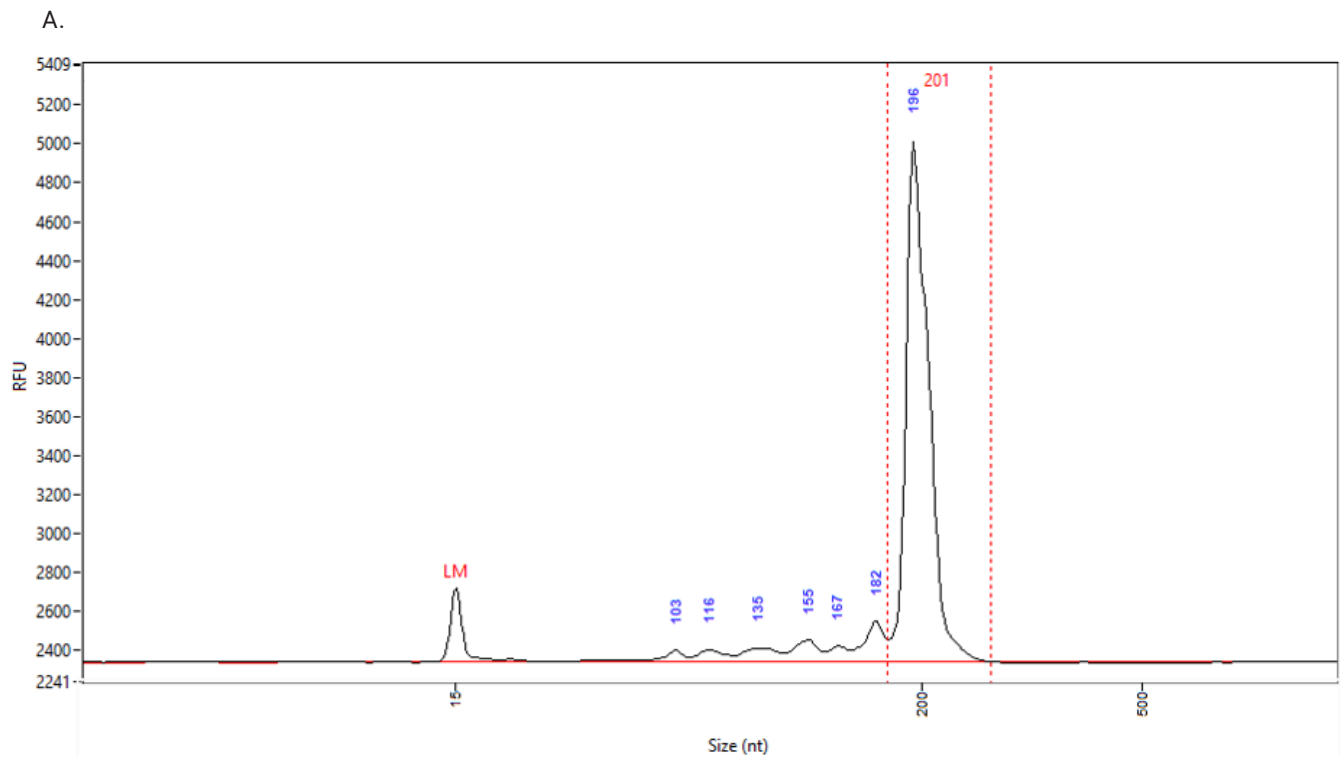
Figure 7. Reported concentration of a 996 nt IVT mRNA sample using the NanoDrop, Qubit, and Agilent 5200 Fragment Analyzer system.

Concentration range

The RNA kit (15 nt) for the Fragment Analyzer system was designed for analysis of total RNA smears covering a large concentration range, which has been further refined for IVT mRNA fragments. Since IVT mRNA fragments are seen as sharp peaks, the same concentration range does not apply. The same sample concentration will give larger peak heights, and, if too high, may cause cross-talk in the surrounding wells. The fragment peak height should be optimized for accurate analysis. The maximum peak height recommendation is approximately 24,000 RFU to avoid cross-talk. If samples show a higher peak height, they should be diluted with nuclease-free water and the analysis run repeated.

In addition, one of the primary goals of IVT mRNA analysis with the Fragment Analyzer is to examine the sample for percent purity. Thus, the sample must be run at a high enough concentration to allow for the reliable detection of any small impurities present in the sample. If the concentration tested is too low, these impurity peaks may be too small to be successfully integrated in the electropherogram, and the reported percent purity will be overexaggerated. Within the Agilent ProSize data analysis software, the minimum peak height can be adjusted to ensure that all peaks are successfully integrated, thus allowing for better analysis of sample purity.

As an example, shown in Figure 8 is a 212 nt IVT mRNA sample that was analyzed at various concentrations. At the highest concentration, 100 ng/μL, the main fragment is displayed as a large peak at approximately 200 nt, with many smaller impurity peaks to the left (Figure 8A). As the sample concentration decreases, the number of impurity peaks that are automatically integrated into the analysis decreases, as indicated by the peaks with a number above them. The smaller peaks without a number are not being integrated into the analysis as the signal-to-noise-ratio is too low, and the peaks could be considered noise (Figure 8B). At the lower end of the concentration range, 3 ng/μL, the main peak height is decreased, and the small impurity peaks are not visualized (Figure 8C). It should be noted that IVT mRNA fragments can run differently based on the sequence and composition of the sample, and what works well for one transcript will not necessarily work for all. Thus, it is best practice to optimize the input concentration for each type of sample to be analyzed. As a guideline, it is recommended to start sample analysis within the recommended range of 1 to 100 ng/μL^{2,5} and optimize the sample concentration to fit the guidelines stated here.



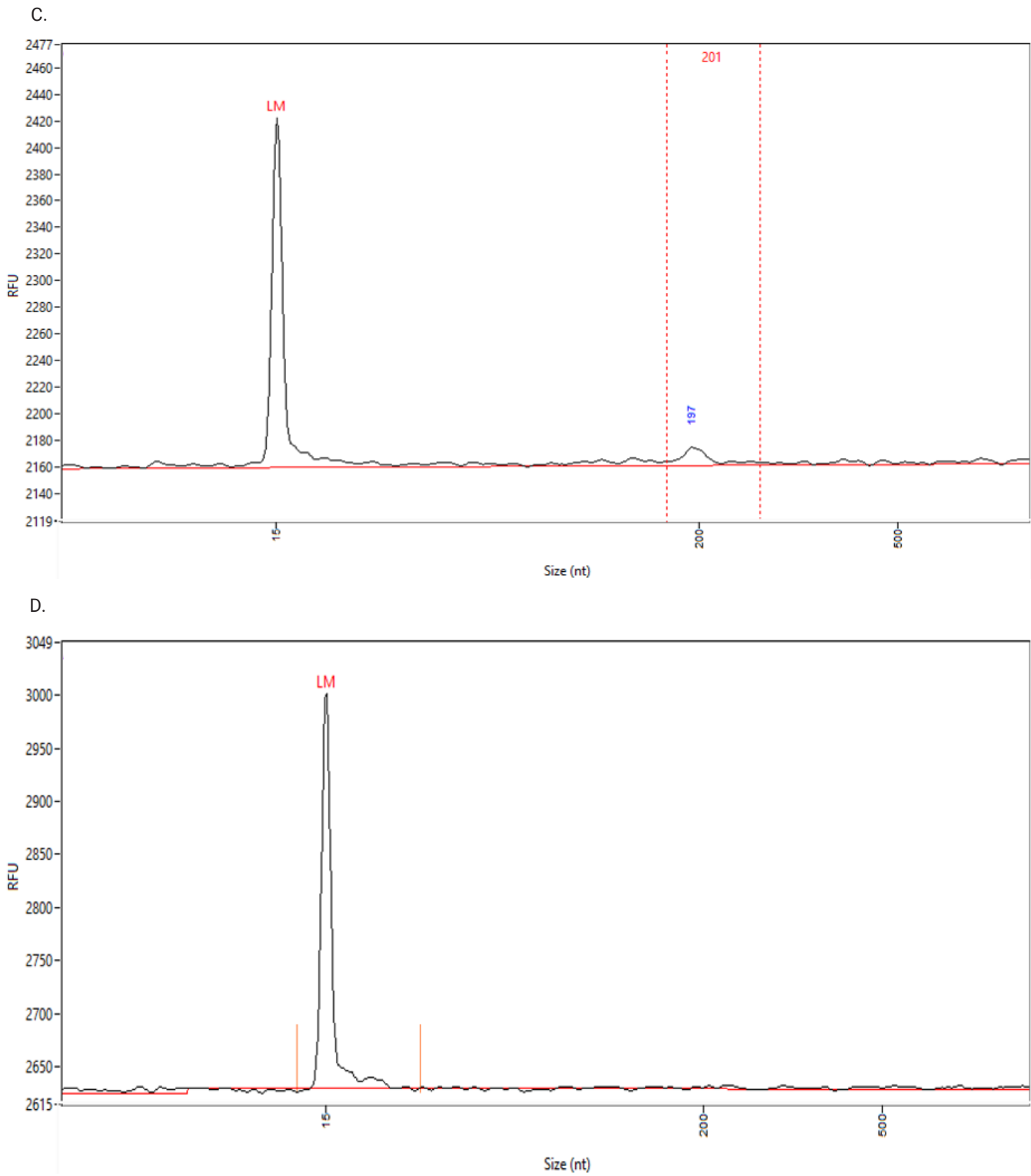


Figure 8. Serial dilution of a 212 nt IVT mRNA fragment analyzed on an Agilent 5200 Fragment Analyzer system. Shown are electropherogram images of the sample at concentrations of A) 100, B) 12.5, and C) 1.56 ng/ μ L. D) A sample well with diluent marker only, used as a negative control.

Conclusion

The Agilent RNA kit (15 nt) for the Agilent Fragment Analyzer systems can be utilized in many steps of the IVT mRNA vaccine development workflow for size and purity assessment. IVT mRNA fragments may behave differently in automated electrophoresis due to factors such as size, sequence, and composition. Thus, this technical overview highlights sample handling techniques and guidelines that should be utilized for accurate and reliable IVT mRNA analysis with the Fragment Analyzer.

References

1. Quality Assurance in In Vitro Transcribed (IVT) RNA Vaccine Development using Agilent Automated Electrophoresis Instruments. *Agilent Technologies white paper*, publication number 5994-4760EN, **2022**.
2. Benefits of Quality Control in the IVT RNA Workflow Using the Agilent 5200 Fragment Analyzer System. *Agilent Technologies application note*, publication number 5994-0512EN, **2019**.
3. Assessment of Long IVT mRNA Fragments with the Agilent 5200 Fragment Analyzer System. *Agilent Technologies application note*, publication number 5994-0878EN, **2019**.
4. Analyzing Poly(A) Tails of In Vitro Transcribed RNA with the Agilent Fragment Analyzer System. *Agilent Technologies application note*, publication number 5994-5325EN, **2022**.
5. Agilent DNF-471 RNA Kit (15 nt) Quick Guide for the Fragment Analyzer Systems. *Agilent Technologies quick guide*, publication number SD-AT000131, **2022**.

www.agilent.com/genomics/fragment-analyzer

For Research Use Only. Not for use in diagnostic procedures.
PR7001-0991

This information is subject to change without notice.

© Agilent Technologies, Inc. 2023
Published in the USA, May 17, 2023
5994-5927EN

Best Practices for Analysis of IVT mRNA using the Agilent Fragment Analyzer systems

Sizing, Resolution, and Purity

Introduction

Reliable and robust quality control (QC) analysis is essential throughout in vitro transcription (IVT) mRNA workflows, including vaccine development and therapeutics. Providing consistent QC minimizes risk during process development and production. Throughout the IVT mRNA vaccine workflow, there are many opportunities for QC to help aid in the development of a consistent product. The Agilent Fragment Analyzer systems can be utilized for several of these QC steps at different checkpoints in the mRNA vaccine development workflow (Figure 1)¹. QC steps that can be performed by the Fragment Analyzer include determining the quality and size of the linearized plasmid, size and purity of the IVT mRNA^{2,3}, length of the poly(A) tail⁴, and integrity of the final IVT mRNA vaccine product.

Best handling practices for analysis of IVT mRNA with the Fragment Analyzer systems have been described⁵. This technical overview examines the ability of the systems to accurately assess IVT mRNA sizing, resolution, and percent purity.

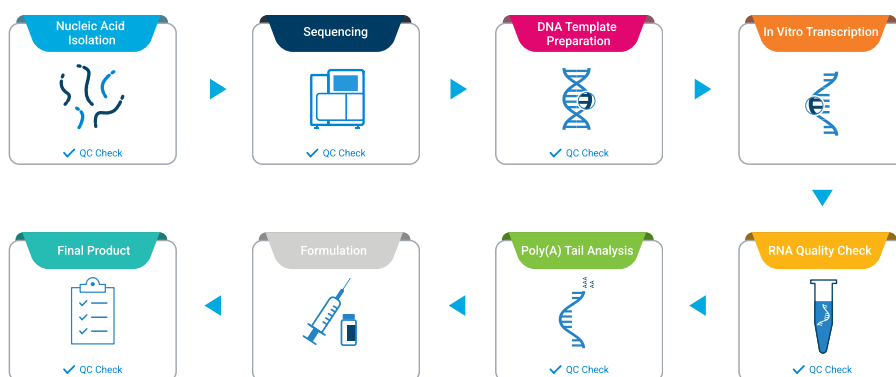


Figure 1. IVT RNA workflow with QC steps where the Agilent Fragment Analyzer systems can be used.

Experimental

Aliquots of Lambda DNA (Thermo p/n SD0021) were PCR amplified using Phusion DNA polymerase to generate templates of sizes ranging from approximately 200 to 6,000 bp (Table 1). Following amplification, each PCR reaction was purified using the NucleoSpin Gel and PCR Clean-up kit (Takara Bio p/n 740609.50) and quantified using Qubit.

The purified PCR products were then used as DNA templates for in vitro transcription. One microgram of each template was used to prepare an IVT mRNA sample using the T7 RiboMAX Express Large Scale RNA Production System (Promega p/n P1320). The IVT mRNA fragments were purified using the RNA Clean & Concentrator-5 kit (Zymo p/n R1013). The final samples were quantified using NanoDrop, and the size and purity were assessed using the Agilent Fragment Analyzer system with the Agilent RNA kit (15 nt) (p/n DNF-471)⁶.

Table 1. List of IVT mRNA samples used in this study and their sequence size

Reaction #	Sequence size (bp)
1	212
2	410
3	493
4	894
5	996
6	1,902
7	2,055
8	3,900
9	4,053
10	5,979

Sizing

To investigate the ability of the Fragment Analyzer to accurately size IVT mRNA, serial dilutions of several samples of various sizes from approximately 200 to 4,000 nt were prepared. Each dilution, from 15 to 60 ng/ μ l, was analyzed in triplicate using the RNA kit. Figure 2 shows a representative example of a 2,055 nt IVT mRNA, with each concentration overlaid to demonstrate consistent sizing across different concentrations. The average peak size of each of the different-sized samples at three different concentrations is shown in Figure 3. The reported size stayed consistent at each concentration tested, from 15 to 60 ng/ μ l.

The kit specification for IVT mRNA sizing accuracy is 10% and sizing precision 5 %CV. Here, 10 samples of varying sizes between 200 and 4,000 nt were tested at three different concentrations in triplicate. All samples displayed a sizing percent error of 10% or less, and a %CV of 1 or less across the dilution series (Figure 3). The percent error indicates good accuracy compared to the expected size across the sizing range of the kit. The low %CV is well below the kit specifications, indicating excellent precision between replicates for each size and concentration tested.

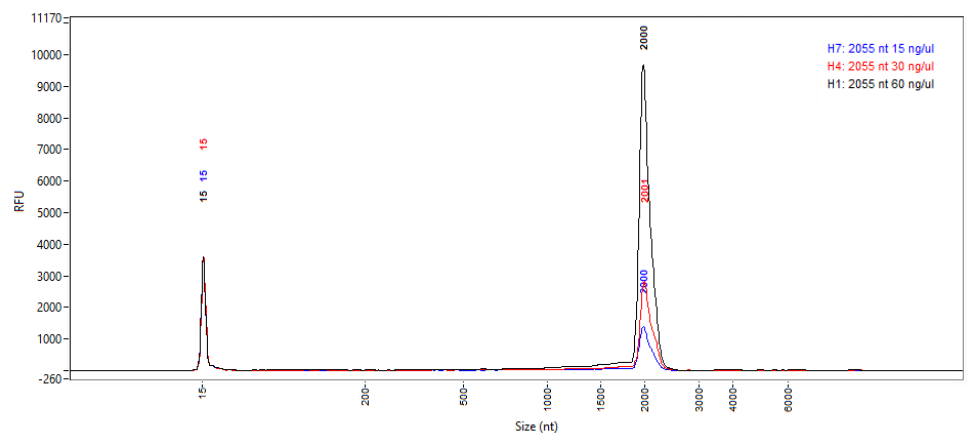


Figure 2. Representative electropherogram overlay of an IVT mRNA sample at 2,055 nt

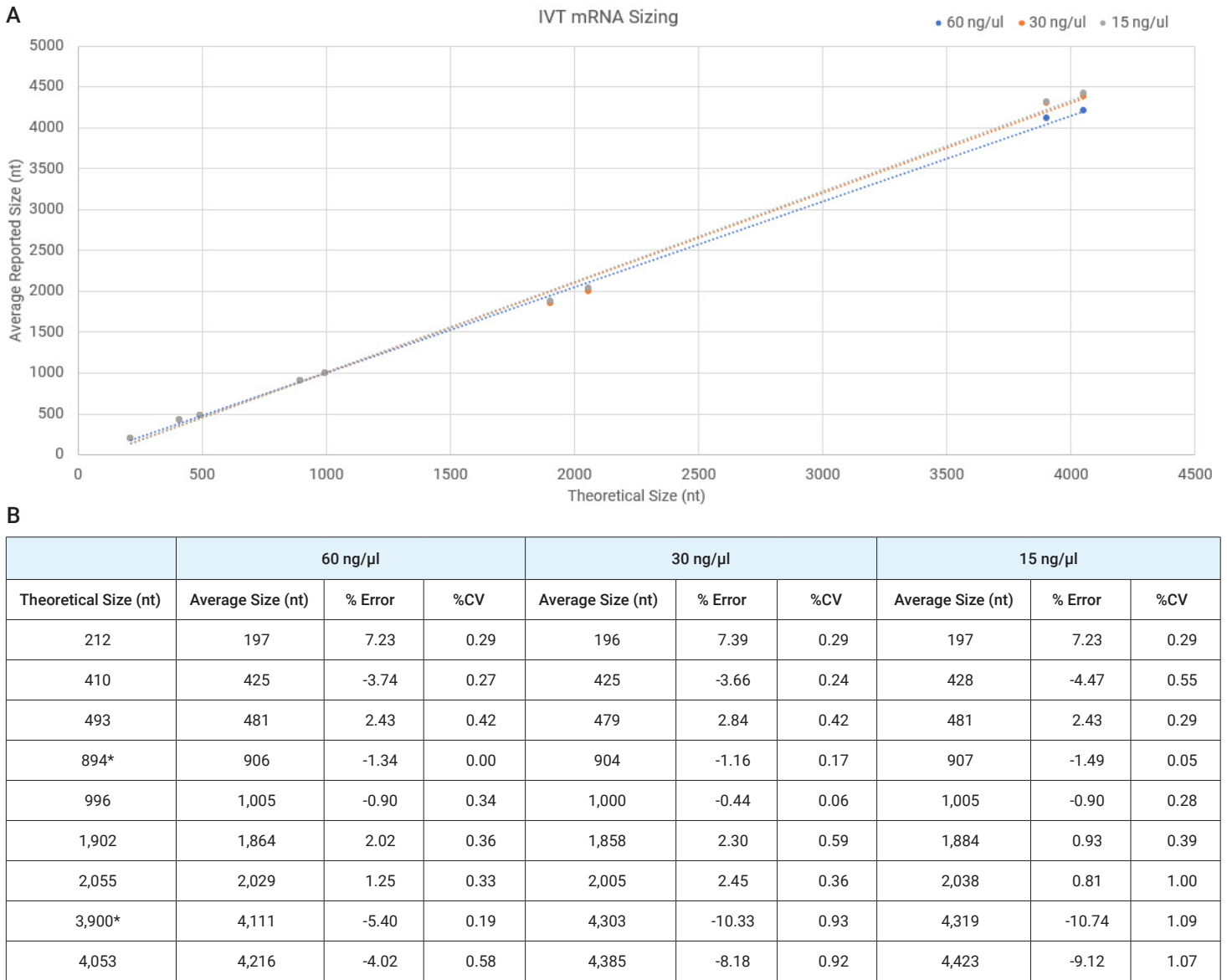


Figure 3. A) Average peak size of all IVT mRNA samples analyzed on the Agilent Fragment Analyzer system with the RNA kit. B) Table of each concentration tested. The % error and %CV at each concentration was well within the specifications of the kit. n = 3 replicates for each size and concentration tested (*n = 2).

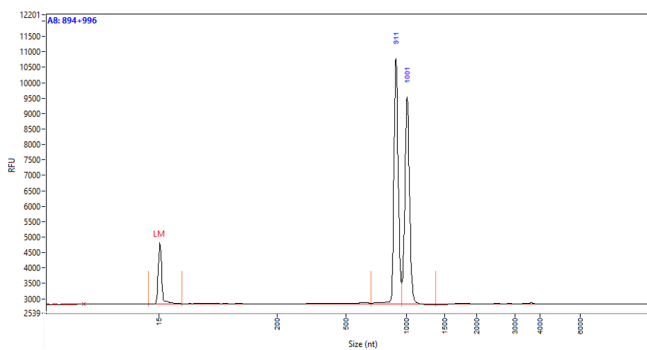
Resolution

Separation resolution with the Fragment Analyzer has been examined in previous studies to demonstrate the ability of the system to separate two DNA fragments close in size and define the differing degrees of separation that can be seen in electropherograms^{7,8}. In this study, IVT mRNA samples of different known sizes were analyzed both individually and mixed together to examine the resolution capabilities of the system for

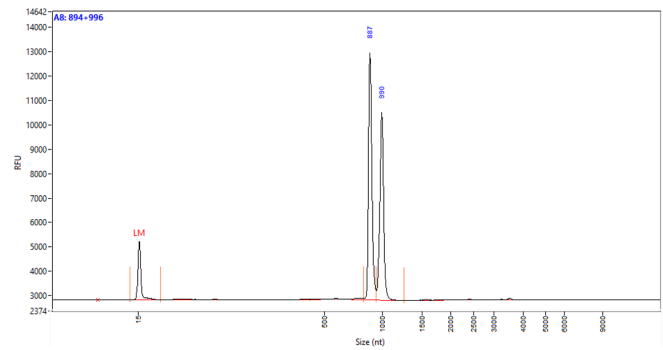
IVT mRNA. For example, an 894 and a 996 nt fragment, a size difference of 10.2%, showed complete baseline resolution (Figure 4A), with two distinct peaks being picked by the data analysis software algorithm. In a second example, 1,902 and 2,055 nt IVT mRNA (a 7.4% difference) samples showed limited resolution. Two peaks were detected in this size range but were not completely baseline resolved.

The Extended Method has been optimized for enhanced separation resolution of closely sized fragments^{3,6}. For example, while the 1,902 and 2,055 nt mix showed only limited resolution with the normal method (Figure 4C), the fragments were partially resolved with the extended method (Figure 4D).

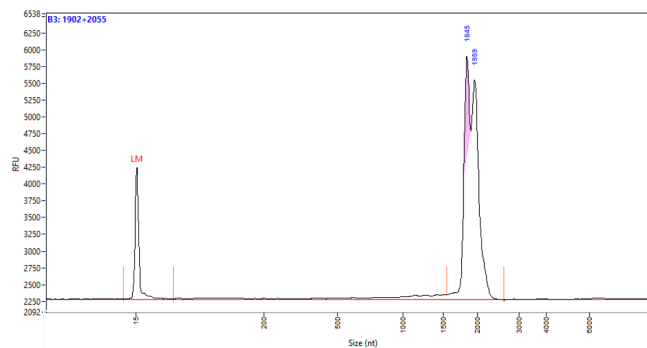
A. 894 nt + 996 nt mix. Regular method



B. 894 nt + 996 nt mix. Extended method



C. 1,902 nt + 2,055 nt mix. Regular method



D. 1,902 nt + 2,055 nt mix. Extended method

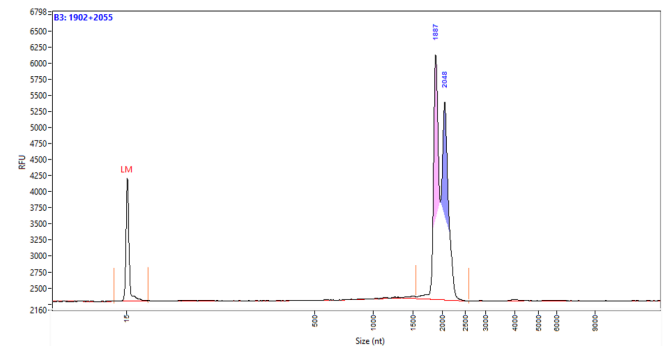
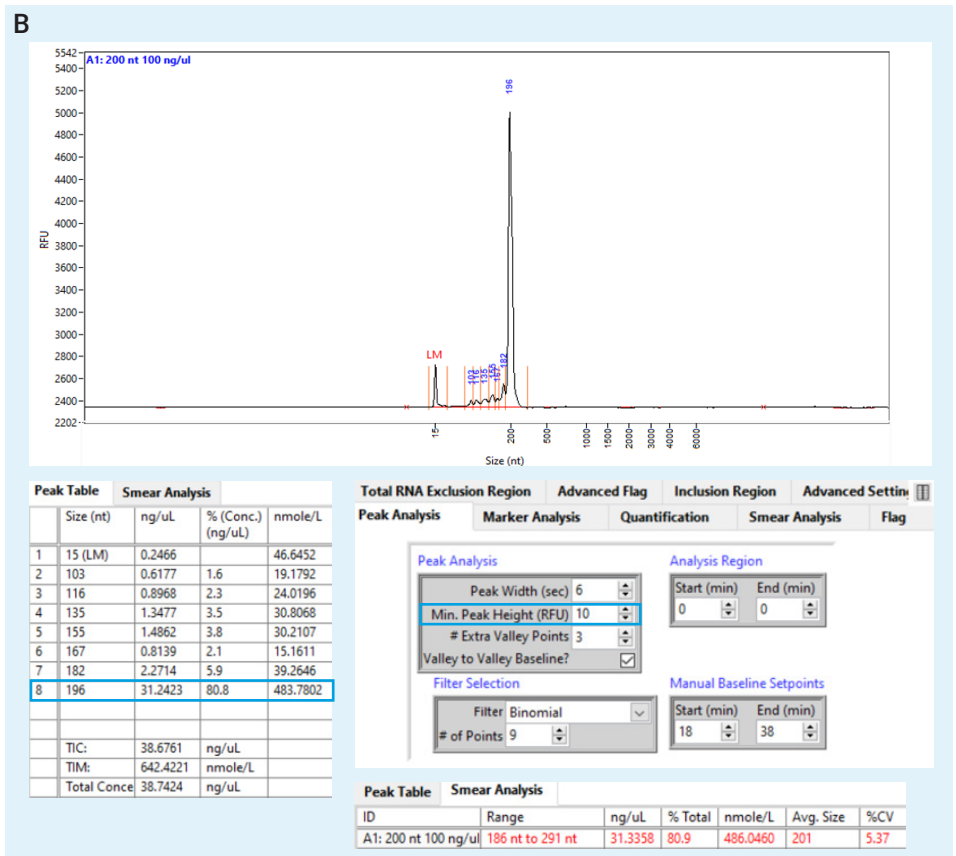
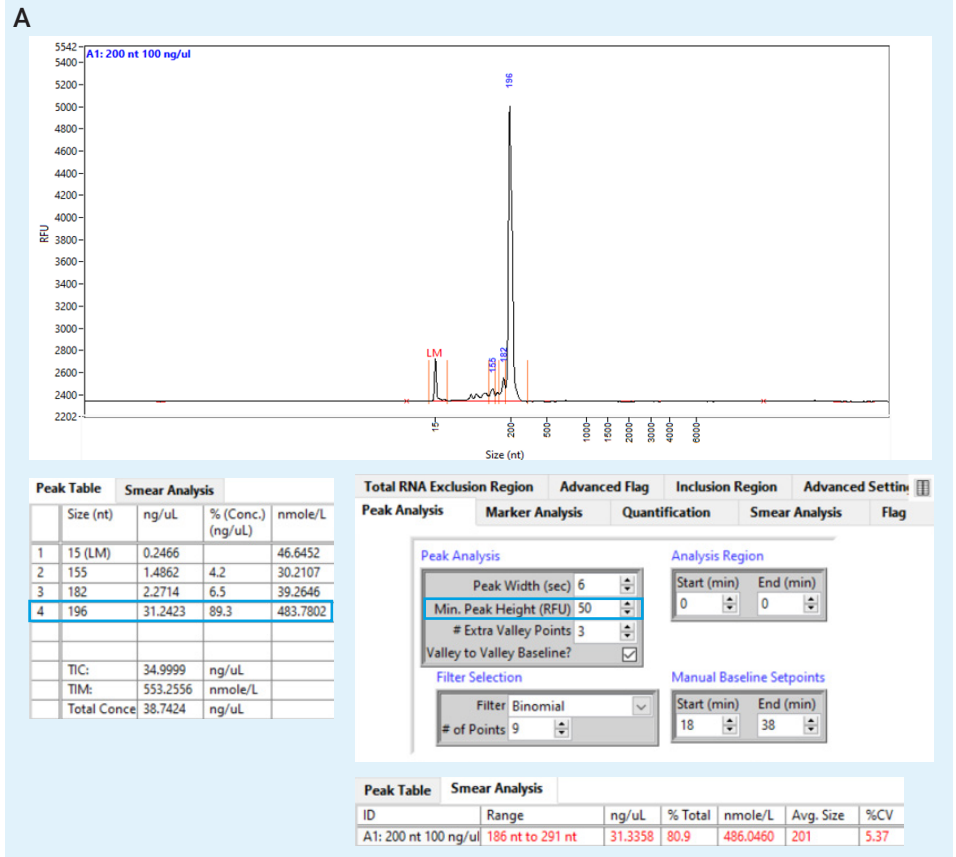


Figure 4. Resolution of the Agilent Fragment Analyzer system for IVT mRNA samples. Fragments of 894 and 996 nt were completely resolved with both A) the RNA method and B) the extended method. C) The 1,902 and 2,055 nt fragments displayed limited resolution with the regular method, but analysis with the D) extended method improved resolution of the fragments.

IVT mRNA integrity

An important aspect of IVT mRNA quality analysis is determining the integrity of the sample. To appropriately determine the percent purity of a sample, data analysis methods must be able to differentiate the main peak from any impurities or degradation. The Agilent ProSize data analysis software that is used with the Fragment Analyzer has methods that automatically detect sample peaks and report the size, concentration, and percent total of the integrated peaks. A user can also adjust settings such as the peak width and height to ensure that the entire sample is properly integrated, and to allow for the most accurate data calculations. For example, Figure 5A shows the electropherogram, Peak Table, and smear analysis table for an IVT mRNA sample that was automatically analyzed using the methods peak analysis settings, as shown. In the electropherogram, the sample is displayed as a single large peak at 196 nt, with several small peaks smearing to the left. However, the software only detects two of these peaks, at 155 and 182 nt. Changing the Minimum Peak Height from 50 to 10 RFU allows for more appropriate integration of the entire sample, with seven sample peaks being detected (Figure 4B). Further, with the standard method, the percent concentration (used to indicate the percent purity of the integrated sample peaks) of the 196 nt peak changed from 89.3 to 80.8%, giving a more accurate representation of the integrity of the sample.

The software also has a smear analysis function that can be utilized to determine the average size, concentration, and percent total of a user-defined region instead of a single peak. A smear analysis region can be set by defining a set base pair range and can be further adjusted using the mouse to grab and pull the dashed red lines, as shown in Figure 5C. In a smear analysis, the data calculations are based on the total area



under the curve of the sample line and above the red baseline, instead of only the integrated peaks. For example, as shown in Figure 5A-B, the concentration and percent total do not change, regardless of the number of peaks that are integrated.

The concentration of the sample may impact the percent purity calculations, as too high of a concentration can cause overloading, and too low may make the impurity peaks impossible to detect, and difficult to differentiate from background noise⁵. To demonstrate this, the percent total of the 212 nt IVT mRNA sample was analyzed across a serial dilution. The peaks in each sample were integrated as discussed, and the percent total averaged across three replicates for concentration. As shown in Figure 5D, the percent total at a sample concentration of 100 ng/μl is on average 78.6%. At concentrations of 6.25 to 50 ng/μl, the percent remains consistently at about 66%. Lower concentrations result in more variability in the percent, as the smaller impurity peaks are no longer detected. The optimal concentration range for analysis with the Fragment Analyzer is thus ~ 6 to 50 ng/μl with these samples. For the most accurate analysis of IVT mRNA on the Fragment Analyzer, it is recommended to optimize the input concentration for different sample types, and ensure all samples are loaded onto the instrument at the same concentration⁵.

The Fragment Analyzer was used to calculate the percent purity of a variety of IVT mRNA samples across the sizing range of the RNA kit. Each sample was analyzed across three individual capillaries in parallel at 50 ng/μl to demonstrate the reproducibility of the system (Figure 5E). At each size tested, the standard deviation of the purity was less than 1.2 and the %CV was less than 1.9%, indicating excellent precision between the replicates.

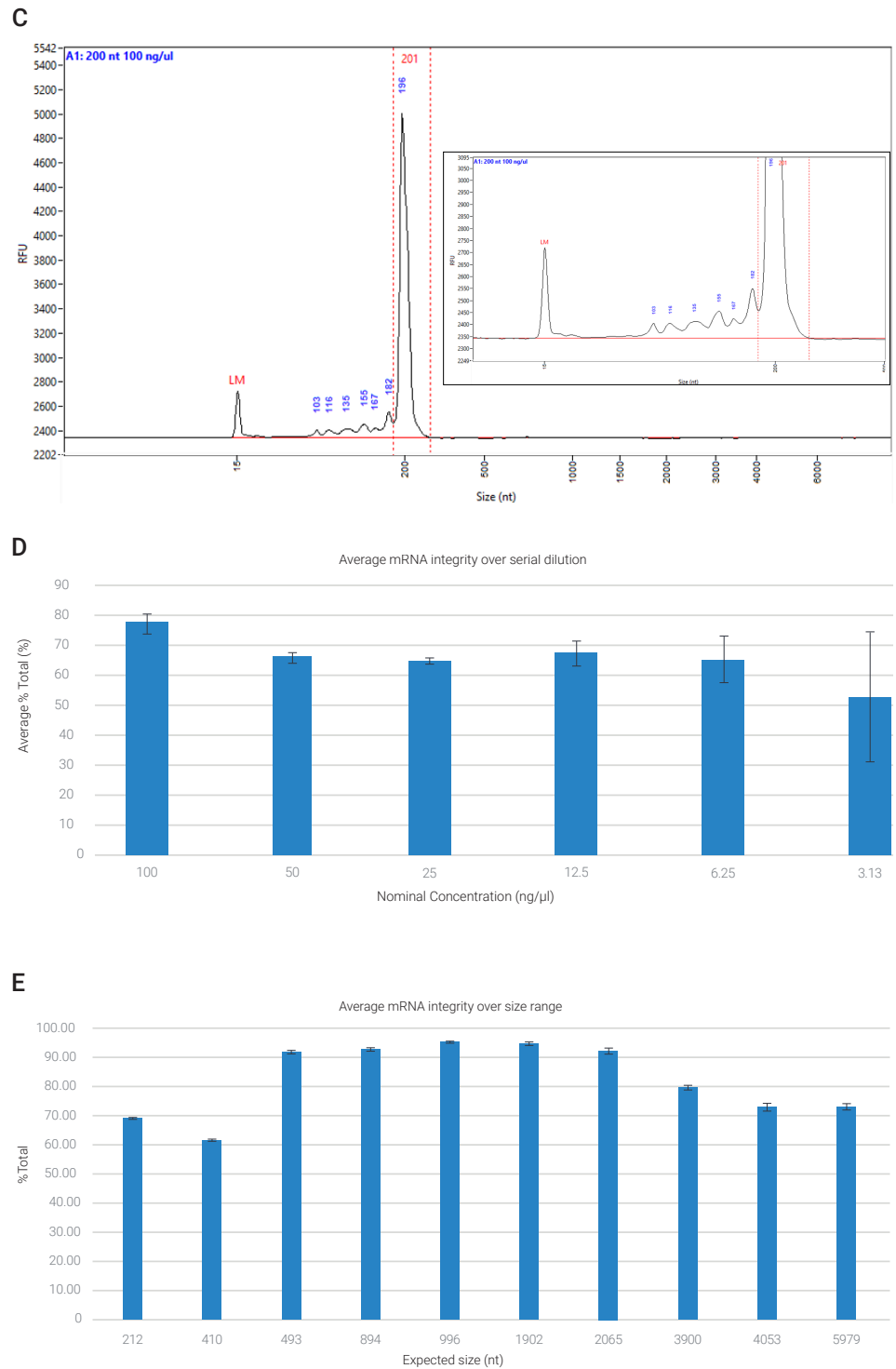


Figure 5. Best practices for integrating samples for purity analysis with the Agilent Fragment Analyzer system and Agilent ProSize data analysis software. An IVT RNA sample was analyzed with A) standard Peak Analysis settings, as shown, and B) with the minimum peak height decreased from 50 to 10 RFU. The resulting electropherograms, Peak Tables, and Smear Analysis Tables are shown. C) Smear analysis is performed by adjusting location of the red dashed lines. D) Purity across serial dilution of a 212 nt IVT mRNA. E) Average mRNA integrity of samples across the sizing range of the kit, with error bars representing standard deviation and indicating the high reproducibility at each size (n = 3).

Controlled mRNA integrity assessment

To examine the ability of the Fragment Analyzer to accurately assess mRNA integrity, a series of controlled experiments in which a smaller IVT mRNA sample was spiked into a larger sample at known concentrations was performed. The percent total of each fragment was calculated using smear analysis ranges specific to each fragment. In the example shown in Figure 6, a 1,902 nt IVT mRNA sample was kept at a constant concentration, and an 894 nt sample was added at varying amounts from 1.5 to 20% of the concentration. The smear ranges are shown in Figure 6A, with the first smear range encompassing the smaller impurity peak, and the second smear range encompassing the main fragment. The average percent total of each peak is shown in Figure 6B. It is important to note that the main fragment is not 100% pure, and that even at 0% spike-in, the purity of the sample is 87%. The percent total of the spiked-in fragment matches expectations from 1.5 to 20%. The percent total of the main fragment, indicative of the percent purity, decreases in direct correlation with the amount of smaller fragment spiked-in.

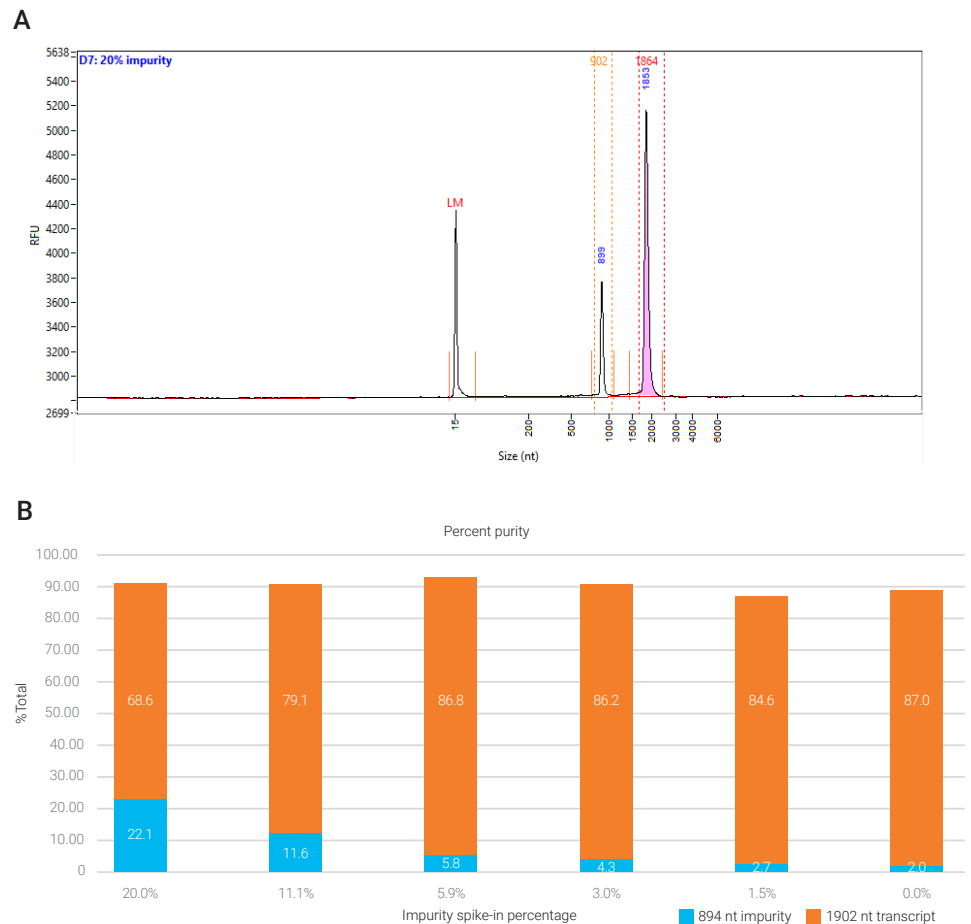


Figure 6. Controlled impurity experiments. An 894 nt IVT mRNA was intentionally added to a 1,902 nt sample at known concentrations, and analyzed on the Agilent Fragment Analyzer system. A) An example electropherogram of a 20% impurity spike-in is shown. B) The percent total of the 894 nt spiked-in impurity peak is shown in blue. The percent total of the 1,902 nt peak, indicative of the total integrity of the sample, is shown in orange.

Degradation series

To further investigate IVT mRNA integrity analysis on the Fragment Analyzer system, a 2,055 nt sample was intentionally heat degraded and analyzed at different time points. The electrophoretic profile of the sample as it is degraded is shown in Figure 7. The intact sample is displayed as a

single peak, with some slight peak broadening at the base. As the sample is degraded for longer amounts of time, the peak height decreases, and a smear to the left of the peak becomes more substantial. The smear analysis range for each sample was determined by adjusting the dashed lines in the

electropherograms to flank the main fragment, excluding the smear. The average percent total for each sample among the degradation is shown in Figure 7E. The percent purity recorded by the Fragment Analyzer directly correlated with the amount of time the samples underwent heat degradation.

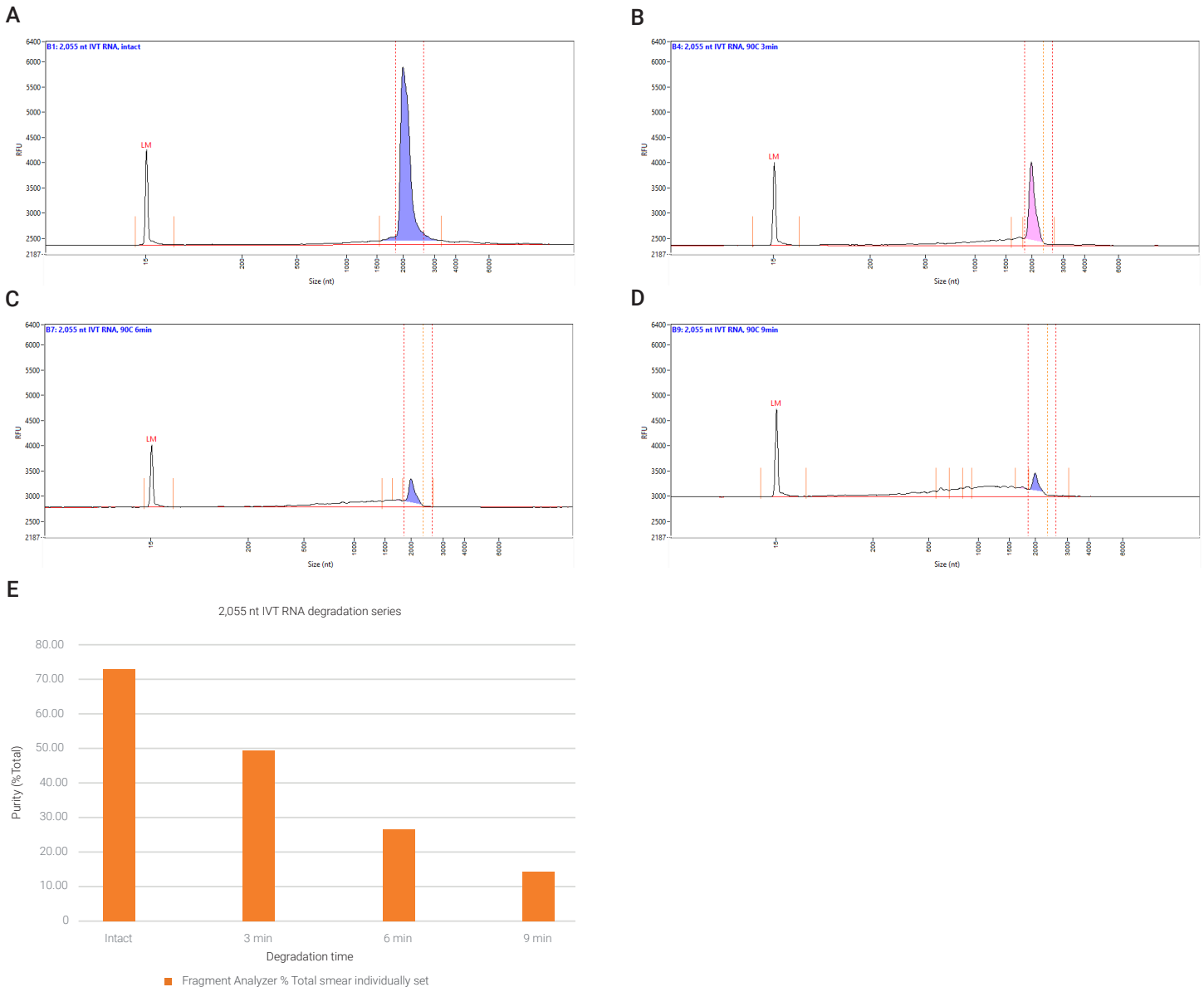


Figure 7. A 2,055 nt IVT mRNA sample was intentionally heat degraded and assessed for purity on the Agilent Fragment Analyzer system. Electropherogram images of the A) intact sample and after B) 3 minutes, C) 6 minutes, and D) 9 minutes of heat degradation demonstrate the decreasing peak heights of the sample as it is further degraded. E) The percent total of each peak decreased from an average of 73% purity for intact sample to 14% following 9 minutes of heat degradation.

Conclusion

The Agilent RNA kit (15 nt) for the Agilent Fragment Analyzer systems can be utilized in many steps of the IVT mRNA vaccine development workflow for size and integrity assessment. This technical overview highlights the accurate and precise sizing, high resolution, and reliable purity analysis that can be achieved with the Fragment Analyzer for IVT mRNA.

References

1. Quality Assurance in In Vitro Transcribed (IVT) RNA Vaccine Development using Agilent Automated Electrophoresis Instruments. *Agilent Technologies white paper*, publication number 5994-4760EN, **2022**.
2. Benefits of Quality Control in the IVT RNA Workflow Using the Agilent 5200 Fragment Analyzer System. *Agilent Technologies application note*, publication number 5994-0512EN, **2019**.
3. Assessment of Long IVT mRNA Fragments with the Agilent 5200 Fragment Analyzer System. *Agilent Technologies application note*, publication number 5994-0878EN, **2019**.
4. Analyzing Poly(A) Tails of In Vitro Transcribed RNA with the Agilent Fragment Analyzer System. *Agilent Technologies application note*, publication number 5994-5325EN, **2022**.
5. Best Practices for Analysis of In Vitro Transcription RNA Using the Agilent Fragment Analyzer systems. *Agilent Technologies application note*, publication number 5994-5927EN, **2023**.
6. Agilent DNF-471 RNA Kit (15 nt) Quick Guide for the Fragment Analyzer Systems. *Agilent Technologies quick guide*, publication number SD-AT000131, **2022**.
7. Highly Resolved Separation of DNA Fragments on the Agilent 5200 Fragment Analyzer System. *Agilent Technologies application note*, publication number 5994-0517, **2019**.
8. Separation Resolution Capabilities of the Agilent ZAG 135 and 110 dsDNA Kits and the Agilent Fragment Analyzer dsDNA 935 and 915 Reagent Kits. *Agilent Technologies application note*, publication number 5994-3638, **2021**.

www.agilent.com/genomics/vaccine-qc

For Research Use Only. Not for use in diagnostic procedures.

PR7001-1390

This information is subject to change without notice.

Benefits of Quality Control in the IVT RNA Workflow Using the Agilent 5200 Fragment Analyzer System

Authors

Denise Warzak,
Chava Pocerich, and
Kit-Sum Wong
Agilent Technologies, Inc.

Abstract

Quality control (QC) analysis is an essential part of the *in vitro* transcription (IVT) RNA workflow. Utilizing QC checkpoints at critical junctures in the IVT RNA process eliminates unsuitable samples, saves time and money, and maximizes resources. The Agilent 5200 Fragment Analyzer system provides sensitive and reliable quality control analysis of RNA with the Agilent RNA kit (15 nt) and Agilent HS RNA kit (15 nt). Analysis of DNA with various DNA kits. QC during IVT allows for detection of poor PCR amplification, poor transcription, DNA template contamination of RNA, degraded RNA, ensuring downstream applications are starting with high-quality RNA.

Introduction

The importance of quality control (QC) in laboratory processes is often overlooked but should be considered an essential part of every procedure. Parallel capillary electrophoresis solutions from Agilent provide the benefit of extremely sensitive, reliable, and high throughput QC for *in vitro* transcription (IVT) RNA applications. These solutions help to deliver a consistent and reproducible RNA product. RNA is prone to degradation due to temperature and ever-present RNases. Hence, there are two critical QC checkpoints in the IVT RNA workflow to ensure the production of quality RNA: after amplification and after transcription (Figure 1). The Agilent 5200 Fragment Analyzer system aids in determining if the PCR amplification, transcription, and product cleanup procedures were successful. Detection of degraded, contaminated, or otherwise unsuitable RNA allows researchers to rework or remove these samples early in the process. Analyzing IVT RNA starting material for downstream applications confirms it meets or exceeds quality requirements and ensures that the experiment is starting off in the right direction.

Experimental

The experiments in this study were performed with a 5200 Fragment Analyzer system and can be replicated with comparable results on Agilent 5300 and 5400 Fragment Analyzer systems.

PCR product was analyzed on the Agilent 5200 Fragment Analyzer system with the Agilent dsDNA 930 Reagent kit (75-20000 bp) (p/n DNF-930). Various lengths of IVT RNA were diluted with nuclease-free water and analyzed on the Agilent 5200 Fragment Analyzer system with the Agilent RNA kit (15 nt) (p/n DNF-471), with the separation time extended by 5 minutes. mRNA separated from ribosomal RNA was analyzed on the Agilent 5200 Fragment Analyzer system with the Agilent HS RNA kit (15 nt) (p/n DNF-472) and the HS mRNA 15 nt method.

RNA analysis kit selection

The Agilent RNA kit and Agilent HS RNA kit were designed for analysis of RNA fragments and smears ranging from 200 to 6,000 nt in size. The Agilent RNA kit is intended for a higher concentration of total RNA samples between 5 to 500 ng/μL RNA. In addition, the kit works well for RNA fragments such as IVT RNA or IVT mRNA between approximately 10 to 20 ng/μL up to 100 ng/μL. In contrast, the Agilent HS RNA kit is aimed at lower concentration total RNA and mRNA depleted ribosomal RNA samples between 50 and 5,000 pg/μL. Both kits provide reliable sizing and quantification of IVT RNA, including sgRNA.¹

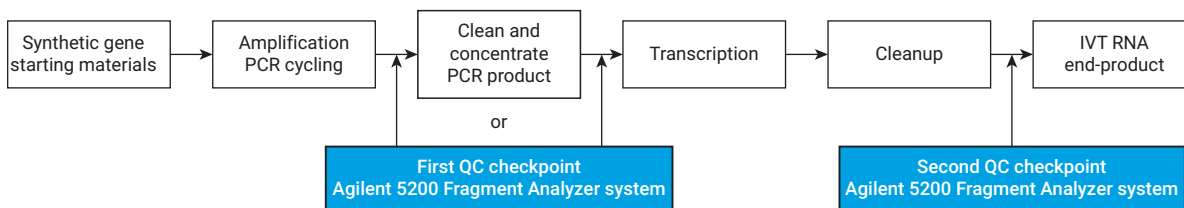


Figure 1. The Agilent 5200 Fragment Analyzer system provides dependable quality control analysis throughout the IVT process.

Sizing IVT RNA

The Agilent RNA kit is the recommended kit for analysis of IVT RNA and IVT mRNA due to the high concentration of a single fragment. Various concentrations (100, 50, 10, and 1 ng/ μ L) of 1,800 and 6,000 nt IVT RNA were analyzed on the Agilent 5200 Fragment Analyzer system with the Agilent RNA kit (Figure 2). The 1,800 and 6,000 nt RNA fragments had an average size of 1,836 and 6,503 nt, respectively, with low % CV and % error indicating consistent data analysis and accurate sizing throughout the dilution series (Table 1). Concentration measurements at 50 and 100 ng/ μ L for both the 1,800 and 6,000 nt RNA fragments reported excellent accuracy below 18 % error, within the specifications of the RNA kit.

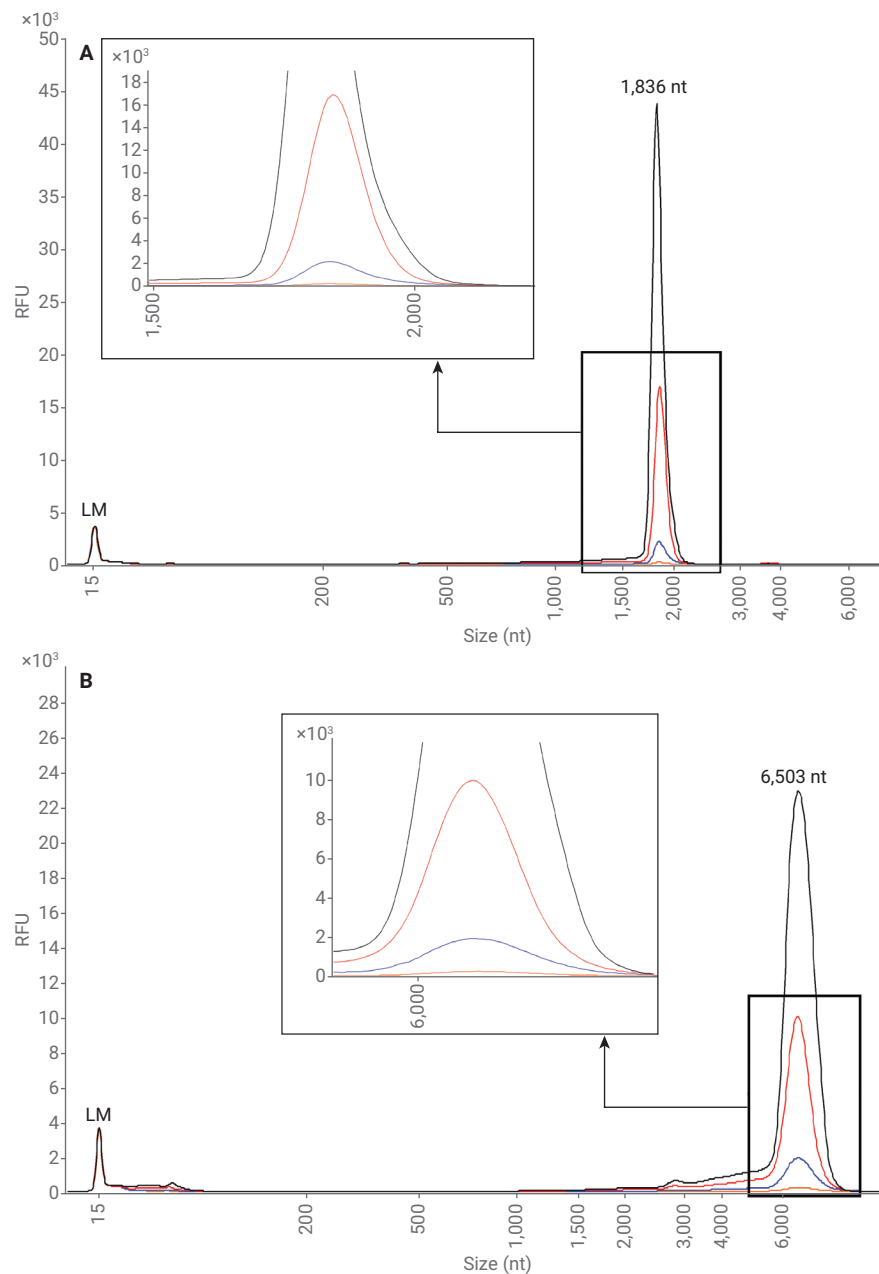


Figure 2. Overlay of the IVT RNA fragment analyzed on the Agilent 5200 Fragment Analyzer system with the Agilent RNA kit (15 nt) over a dilution series of 100, 50, 10, and 1 ng/ μ L. Run time was extended to 5 minutes. (A) 1,800 nt RNA fragment. (B) 6,000 nt RNA fragment. LM = lower marker.

Analysis of ribosomal depleted mRNA

mRNA pulled from ribosomal RNA was analyzed on the Agilent 5200 Fragment Analyzer system with the Agilent HS RNA kit – HS mRNA 15 nt. mthds file (Figure 3). The HS mRNA method file in the Agilent HS RNA kit was designed for analysis of ribosomal depleted mRNA. This method produces low concentration mRNA that separates as a smear. The HS mRNA method utilizes a longer sample injection time to accommodate the low concentration mRNA and is not recommended for highly concentrated synthetic mRNA or IVT mRNA. In addition, ProSize data analysis software automatically reports the percent of ribosomal RNA contamination in each sample with the HS mRNA method.

Quality control

There are several key challenges associated with IVT RNA workflows such as overall time, yield, RNA degradation, and incomplete enzyme reactions. Many IVT reactions take 2 to 3 hours to produce maximum RNA yields, with low yields leading to repeated IVT reactions. The Agilent 5200 Fragment Analyzer system offers reliable and sensitive quantification and sizing of nucleic acids to help optimize reaction conditions and determine input volumes needed for successful amplification and transcription yields.

Table 1. Sizing of 1,800 and 6,000 nt IVT RNA throughout a dilution series (100, 50, 10, and 1 ng/μL), *n=3.

Concentration (ng/μL)	Sizing throughout dilution series					
	1,800 nt Fragment ~Theoretical Size 1,800 nt			6,000 nt Fragment ~Theoretical Size 6,039 nt		
	Average* (nt)	%CV	% Error	Average* (nt)	%CV	% Error
100	1,819	0.5 %	1.1 %	6,503	0.4 %	7.7%
50	1,838	0.6 %	2.1 %	6,503	0.2 %	7.7%
10	1,838	0.1 %	2.1 %	6,503	0.4 %	7.7%
1	1,847	0.5 %	2.6 %	6,503	0.4 %	7.7%
Entire Range	1,836	0.7 %	2.0 %	6,503	0.3 %	7.7%

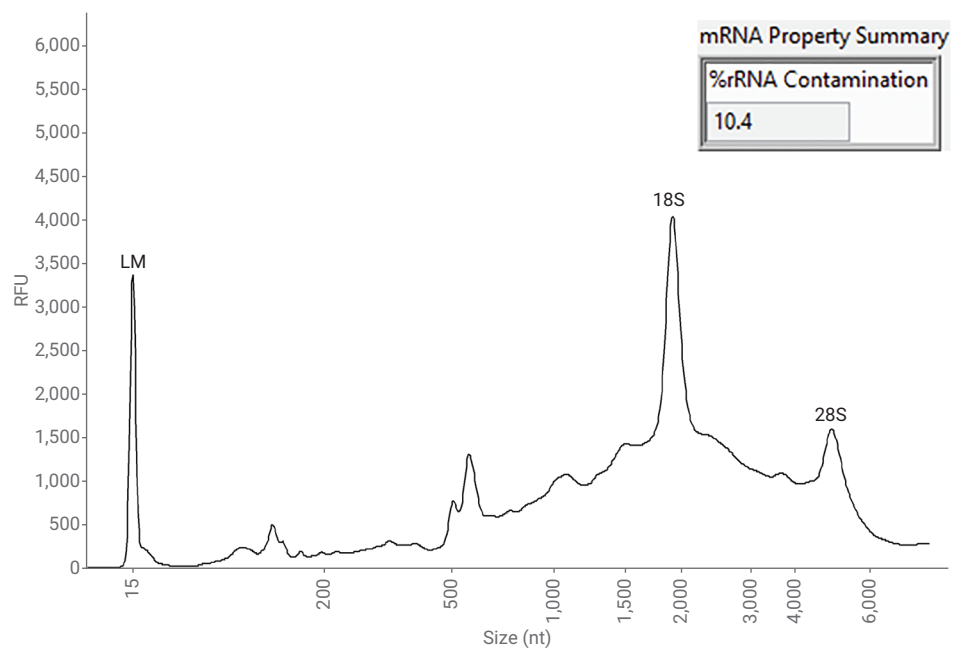


Figure 3. Ribosomal depleted rat kidney mRNA was analyzed on the Agilent 5200 Fragment Analyzer system with the Agilent HS RNA kit (15 nt) and the HS mRNA method. The mRNA still contained some 18S and 28S ribosomal RNA. LM = lower marker.

First QC checkpoint

The first quality control check for IVT is recommended after amplification and can be performed either before or after PCR clean-up. The Agilent 5200 Fragment Analyzer system provides essential information including the concentration of the PCR product, which is required for transcription and the size of the fragment, which reveals if the product of interest was amplified. In addition, the quality or purity of the amplification is assessed through visualization of the electropherogram. The purity of the amplification product will help the user to determine if further cleanup is necessary. Successful PCR reactions produce a single fragment, while a poor PCR reaction generates multiple unwanted peaks (Figure 4). Salt concentrations during PCR can reach 100 to 200 mM chloride levels, which may inhibit transcription. Noisy or spiky baselines seen on the electropherograms are indications of high salt levels. Salt levels over 50 mM are easily detected². PCR cleanup or dilution of samples – or both – can help eliminate high salt concentration concerns.

Second QC checkpoint

The second recommended QC checkpoint occurs after transcription. Cleanup of the transcription product involves the use of DNase to eliminate the DNA template, leaving a purified RNA product. The Agilent 5200 Fragment Analyzer system can detect the presence of a DNA template in RNA. The DNA template is distinguishable from RNA due to the size difference. In instances where DNase is not utilized, or the reaction is incomplete, the DNA template will be visible in the electropherogram.

For example purposes only, IVT RNA not treated with DNase was separated on the Agilent 5200 Fragment Analyzer system with the Agilent RNA kit (Figure 5). An expected single RNA product was seen at 1,831 nt along with a much larger DNA template. Running the separation an extra five minutes is recommended to ensure visualization of any possible DNA template. Successful transcription and cleanup will produce a single RNA peak, while problematic transcription results in several smaller unwanted peaks (Figure 6).

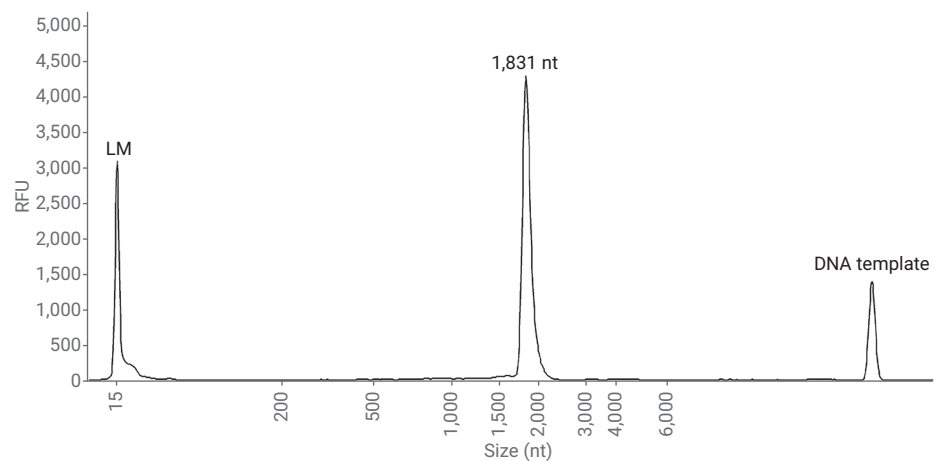


Figure 5. IVT RNA analyzed on the Agilent 5200 Fragment Analyzer system with the Agilent RNA kit (15 nt). The DNA template is detected when the sample is not treated with DNase. LM = lower marker.

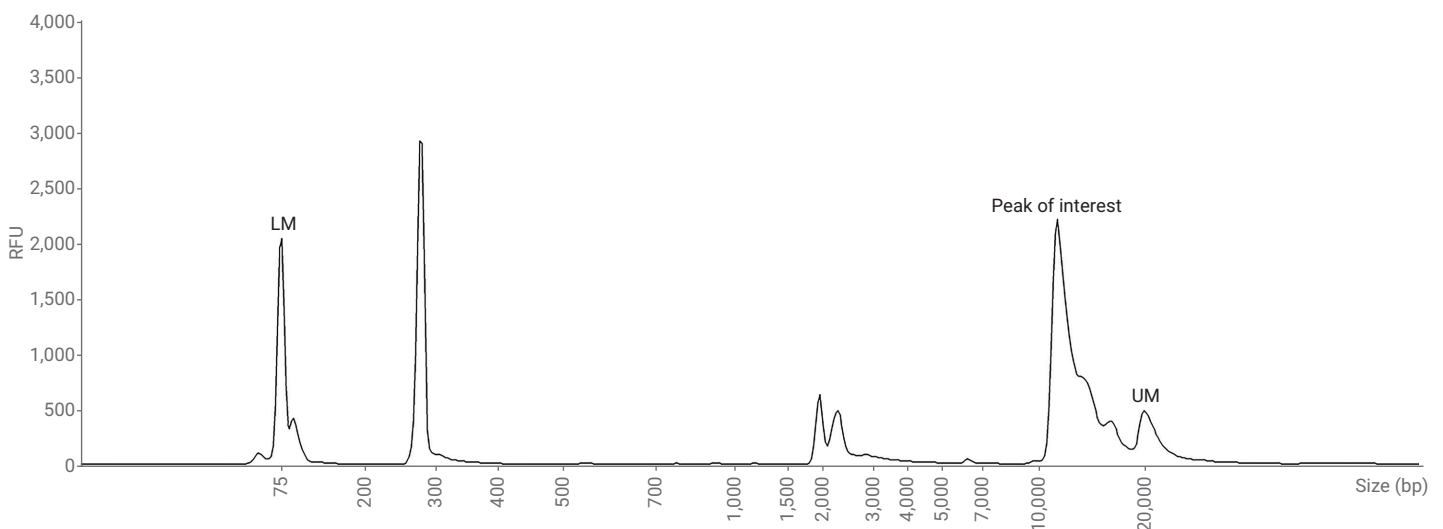


Figure 4. PCR product analyzed on the Agilent 5200 Fragment Analyzer system with the Agilent dsDNA 930 Reagent kit (75-20000 bp). Multiple unwanted peaks indicate a poor PCR reaction. LM = lower marker; UM = upper marker.

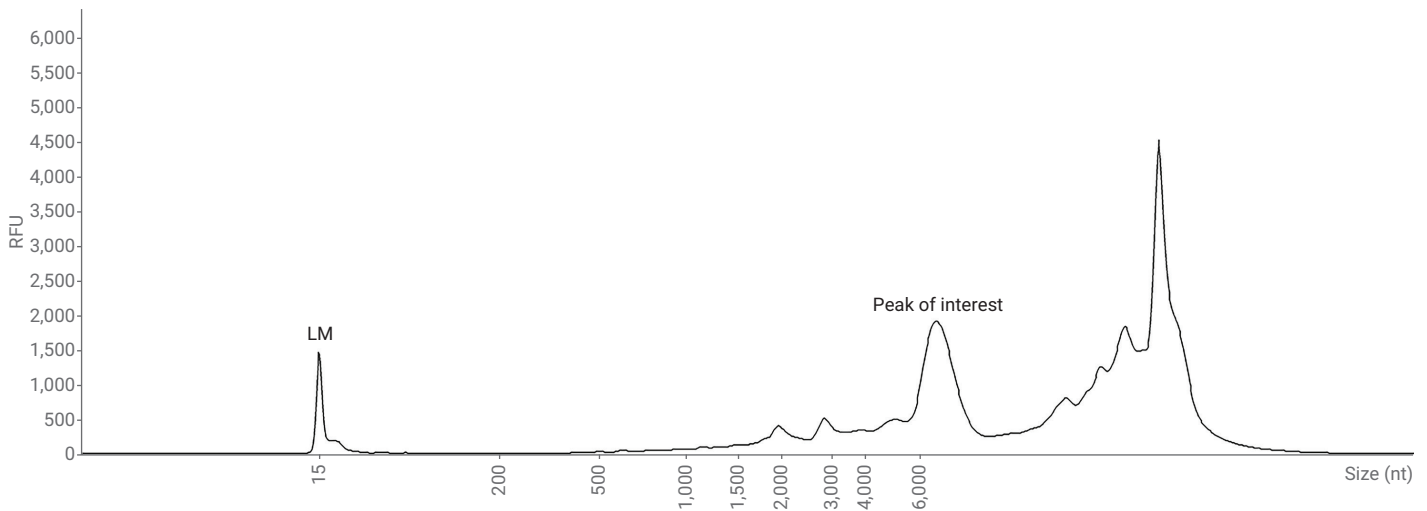


Figure 6. IVT RNA analyzed on the Agilent 5200 Fragment Analyzer system with the Agilent RNA kit (15 nt). Low-quality transcription results in multiple peaks. LM = lower marker.

Conclusions

Quality control analysis is an important part of IVT RNA workflow, which is utilized in multiple downstream applications. Beginning with quality RNA assists in starting the applications off in the right direction. QC after PCR ensures that the DNA of interest is amplified and free of contamination. The second quality control step ensures successful transcription of the RNA of interest and detects the presence of RNA degradation or DNA template contamination, or both. The Agilent 5200 Fragment Analyzer system provides sensitive and reliable quality control analysis of the IVT RNA workflow.

References

1. Luttgarm, K.; Pocerlich, C. Single-Guide RNA Quality Assessment by the Agilent 5200 Fragment Analyzer System, *Agilent Technologies Application Note*, publication number 5994-0523EN, **2017**.
2. Pocerlich, C.; Deist, B.; Pike, W.; Warzak, D. Best Sizing Practices with the Agilent 5200 Fragment Analyzer System. *Agilent Technologies Application Note*, publication number 5994-0585EN, **2018**.

www.agilent.com/genomics/vaccine-qc

For Research Use Only. Not for use in diagnostic procedures.
PR7001-1529

This information is subject to change without notice.

Quality Control in IVT RNA Workflow using Agilent TapeStation Systems

Introduction

Precise and accurate quality control (QC) analysis is a critical part of the in vitro transcription (IVT) RNA workflow. RNA produced by IVT can be used in a variety of applications including vaccines, gene therapies, cancer treatments, treatments for chronic infections, and therapies for autoimmune disorders. IVT RNA workflows (Figure 1) begin with the initial genetic starting material, which can include linearized DNA plasmids, PCR amplified DNA, or cDNA. After purification of the DNA template, the IVT reaction generates RNA, which is then purified to achieve the final product. QC of the DNA template and final RNA product is critical for IVT workflows.

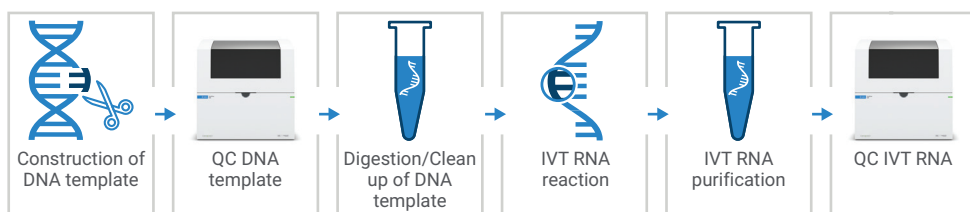


Figure 1. IVT RNA workflow with QC steps where the Agilent TapeStation systems can be used.

Accurate sizing and QC of the DNA assists in verifying amplification of the target DNA, verifies complete linearization of DNA plasmids, and confirms purity. Templates containing DNA from regions outside of the intended transcript interfere with transcription of the target RNA. Additionally, DNA templates with unexpected digestion can produce incomplete RNA products. Ensuring sizing and quality of the final IVT RNA product provides assurance that the IVT RNA is suitable for downstream use. Poor RNA transcription, or contamination and degradation of the final product, impairs the potential therapeutic application of the RNA. It is therefore essential to assess DNA transcripts and final IVT RNA for both size and purity.

The Agilent automated electrophoresis systems, including the TapeStation and Fragment Analyzer systems,¹ can be used for QC and size analysis during the IVT RNA workflow. This technical overview discusses the use of the TapeStation in IVT RNA workflows. The TapeStation system easily switches between DNA and RNA analysis, allowing for quick and reliable quality checks and sizing of DNA and IVT RNA products to help optimize the workflow and ensure a good final product for downstream applications.

Methods

The experiments in this study were performed using the Agilent 4200 TapeStation system (p/n G2991BA), and can be replicated on the Agilent 4150 TapeStation system (p/n G2992AA). DNA templates were prepared from PCR amplification of Lambda DNA with Phusion High-Fidelity DNA polymerase (Thermo Fisher Scientific p/n F530S) and standard protocols. The DNA templates were analyzed on the TapeStation instrument with the Agilent D5000 ScreenTape (p/n 5067-5588) and Agilent D5000 reagents (p/n 5067-5589).

Three IVT RNA samples were generated using Promega T7 RiboMAX Express (Promega p/n P1320). Sample 1, a single IVT control included with the T7 RiboMAX Express kit, yields two fragments with expected sizes of 1,065 nt and 2,346 nt in length. Samples 2 and 3, generated from PCR amplified DNA templates, yield RNA with the expected sizes of 2,055 nt and 4,053 nt, respectively. The IVT RNA was diluted with nuclease-free water, and analyzed on the TapeStation instrument with the Agilent RNA ScreenTape (p/n 5067-5576), Agilent RNA ScreenTape Sample Buffer (p/n 5067-5577), and Agilent RNA ScreenTape Ladder (p/n 5067-5578).

Results and discussion

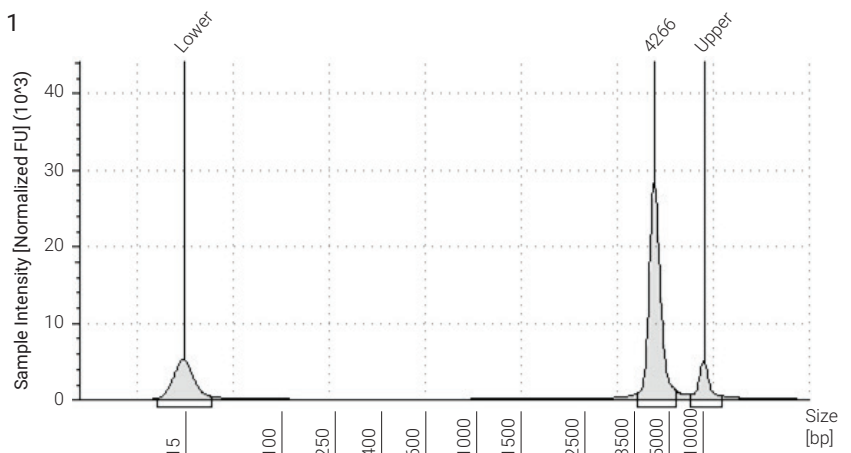
Assessment of DNA template

DNA templates were assessed for size and purity with the D5000 ScreenTape and reagents. Figure 2 shows the electropherograms of the DNA templates. Sample 1, the control provided in the T7 RiboMAX Express kit, has an estimated size of 4,200 bp. Samples 2 and 3 were generated from PCR amplification of Lambda DNA. Sample 2 has an expected size of 2,073 bp, and sample 3 has an expected size of 4,071 bp. Representative electropherograms from each sample are shown in Figure 2. In all cases, the electropherogram displays a single peak very close to the expected size. The samples were analyzed for both accuracy and precision. Sizing accuracy for each sample was determined by calculating percent error based on the expected size. The precision of each sample was measured by evaluating the percent coefficient of variation (CV). All samples displayed a low percent error (less than 10%) and CV (less than 1%) (Table 1). The single peak and low percent error of each sample indicates minimal off-target amplification. Precise and accurate QC of the DNA templates ensures the samples are ready to move to the next step in the IVT workflow.

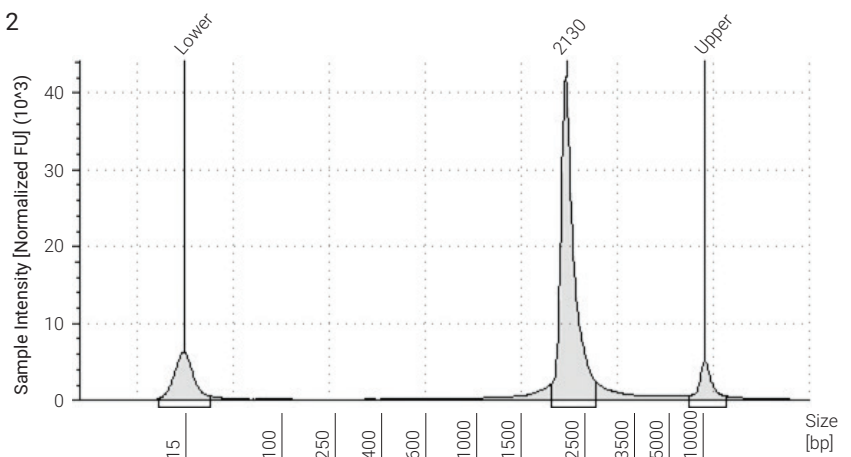
Table 1. Analysis of DNA templates using the Agilent D5000 ScreenTape assay. The expected size, measured size, percent error, standard deviation, and percent CV are shown. n=3 for each sample.

Sample ID	DNA Template Expected Size (bp)	Measured Size (bp)	% Error	Standard Deviation	%CV
1	4,200	4,275	1.79%	7.35	0.17%
2	2,073	2,133	2.91%	4.71	0.22%
3	4,071	4,423	8.63%	3.50	0.08%

A) Sample 1



B) Sample 2



C) Sample 3

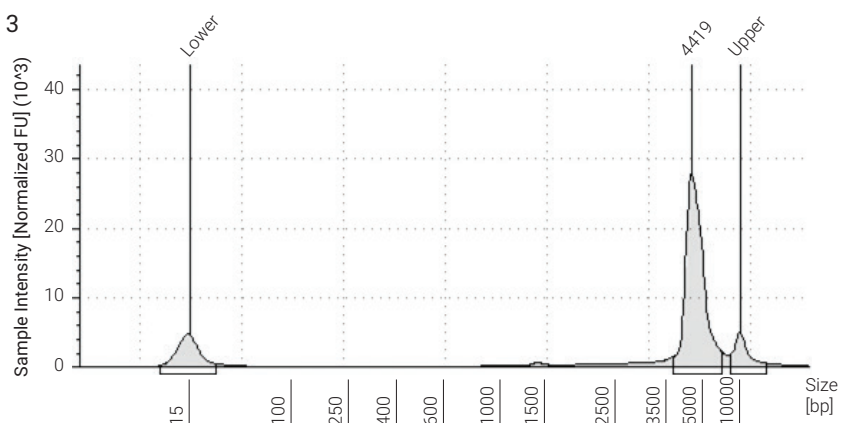
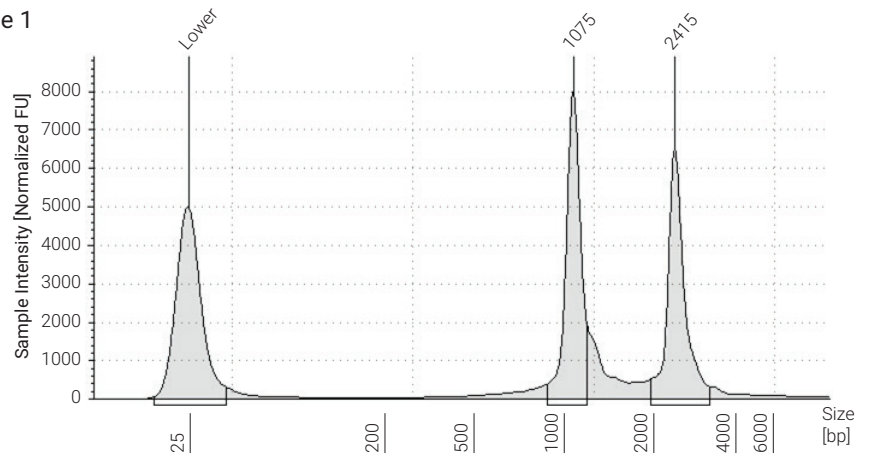


Figure 2. DNA templates of (A) sample 1, (B) sample 2, and (C) sample 3 were analyzed on the Agilent 4200 TapeStation system with the Agilent D5000 assay. Example electropherograms of the DNA templates analyzed at a concentration of approximately 40 ng/ μ L are shown.

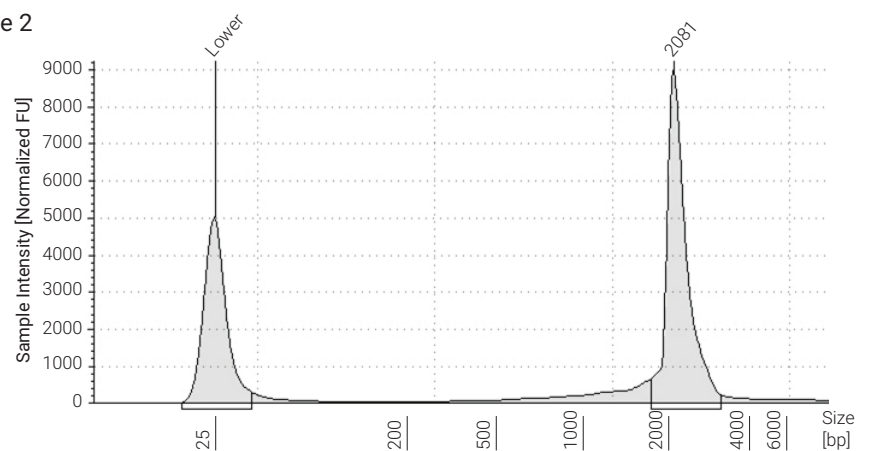
Assessment of IVT RNA

The DNA templates were used to generate three IVT RNA samples. Sample 1, the positive control, produces two fragments with expected sizes of 1,065 nt and 2,346 nt. Samples 2 and 3 were generated from PCR-amplified DNA templates, and have fragments with expected sizes of 2,055 nt and 4,053 nt, respectively. Each sample was analyzed for size and purity on the TapeStation system with the RNA ScreenTape assay. A representative electropherogram for each sample is shown in Figure 3. All samples contain clearly defined peaks, which correspond to the expected sizes of IVT RNA.

A) Sample 1



B) Sample 2



C) Sample 3

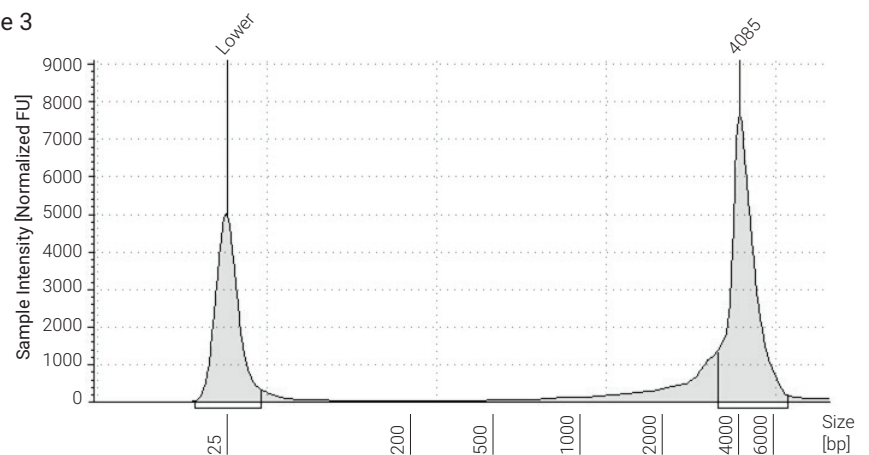


Figure 3. IVT RNA samples were analyzed on the Agilent 4200 TapeStation system with the Agilent RNA ScreenTape assay. Approximately 100 ng/ μ L of RNA for each sample was analyzed. The electropherogram from (A) sample 1 displays two peaks, as expected. The electropherograms from (B) sample 2 and (C) sample 3 each display the expected single peak.

For each sample, two concentrations of approximately 100 ng/μL and 50 ng/μL were analyzed for accuracy (percent error) and precision (%CV). In all cases, the samples displayed low percent error (less than 20%) and %CV (less than 5%), indicating the TapeStation instrument and RNA ScreenTape measurements for IVT RNA are accurate and precise (Table 2). The concentrations tested do not impact the sizing, as shown in the overlay of electropherograms for sample 1 (Figure 4).

Table 2. Accuracy and precision of IVT RNA samples. Approximately 100 ng/μL and 50 ng/μL of samples 1-3 were analyzed on the Agilent TapeStation system with the RNA ScreenTape assay. For all samples, n=3.

Sample	Theoretical Size (nt)	100 ng/μL			50 ng/μL		
		Average Measured Size (nt)	% Error	%CV	Average Measured Size (nt)	% Error	%CV
1	1,065	1,092	2.54%	2.09%	1,104	3.66%	2.12%
	2,346	2,466	5.12%	1.54%	2,502	6.65%	2.20%
2	2,055	2,123	3.31%	2.21%	2,154	4.82%	2.94%
3	4,053	4,085	0.79%	4.28%	4,392	8.36%	1.73%

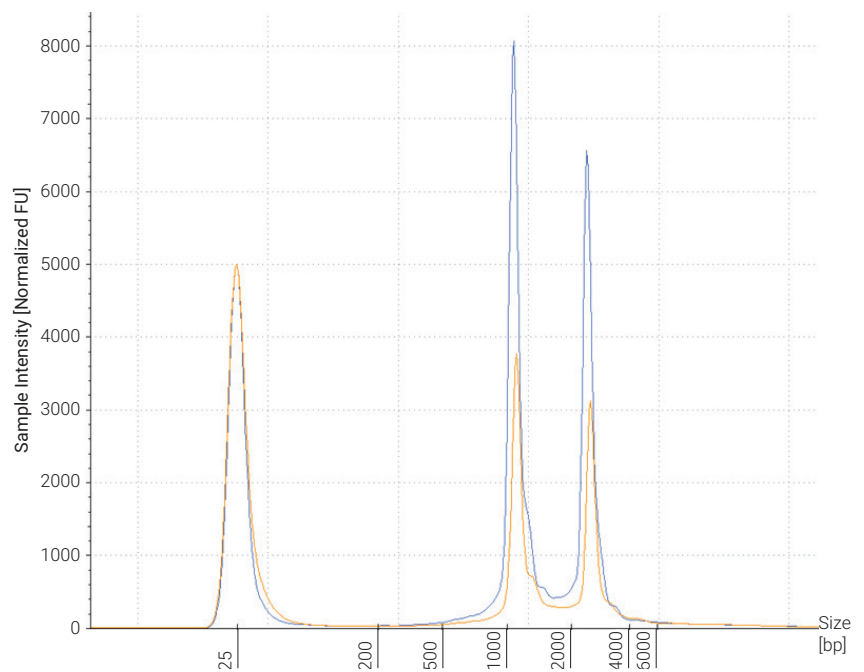


Figure 4. Overlay of the IVT RNA fragments analyzed on the Agilent 4200 TapeStation system with the Agilent RNA ScreenTape assay. IVT RNA fragments from sample 1, with expected sizes of 1,065 and 2,346 nt, were analyzed from dilutions of approximately 100 ng/μL (blue) and 50 ng/μL (yellow).

Summary

The Agilent 4200 TapeStation system with the Agilent D5000 ScreenTape and Agilent RNA ScreenTape assays provides accurate and precise sizing for PCR-amplified DNA templates and final IVT RNA products. The TapeStation software automatically provides peak size, which assists the user in ensuring the accuracy of both the DNA templates and final IVT RNA products. QC of the DNA template ensures appropriate templates are used in the IVT reaction, saving time and money. The TapeStation system and ScreenTape assays assist researchers in verifying that the final IVT RNA is suitable for the intended downstream applications.

References

1. Benefits of Quality Control in the IVT RNA workflow using the Agilent 5200 Fragment Analyzer System. *Agilent Technologies application note*, publication number 5994-0512EN, **2019**.

www.agilent.com/genomics/tapestation

For Research Use Only. Not for use in diagnostic procedures.
PR7000-8706

This information is subject to change without notice.

© Agilent Technologies, Inc. 2022
Published in the USA, July 10, 2022
5994-4882EN

Rapid Analysis of mRNA 5' Capping with High Resolution LC/MS

Author

Brian Liau
Agilent Technologies, Inc.

Introduction

Industrial-scale production of mRNA has received growing attention due to the ongoing SARS-CoV-2 pandemic. mRNA vaccines have proven to be one of the most effective tools against the virus and depend on high-quality mRNA synthesized by *in vitro* transcription.¹ Efficient translation of mRNA to protein depends critically on a 5'-terminal dinucleotide modification called capping which is appended to mRNA during² or after³ the transcription process. Importantly, the percentage of successfully capped material and the type of capping structure appended is influenced by factors such as the quality of input materials, the reaction conditions, and the mRNA sequence. mRNA 5' capping is therefore a critical quality attribute that should be thoroughly characterized and monitored.

This work uses an Agilent 6545XT AdvanceBio LC/Q-TOF for rapid mRNA capping analysis with a combined sample preparation and analysis time of only 75 minutes. Sample preparation is accelerated using a thermostable enzyme to liberate 5' terminal oligonucleotides containing capping structures at an elevated reaction temperature (Figure 1). Capped oligonucleotides are then separated from the sample matrix using an AdvanceBio Oligonucleotide column using only simple cleanup procedures.

To demonstrate the utility of this method, we optimize a Vaccinia enzyme capping reaction for a challenging mRNA sequence. Our results show the value of high-resolution LC/MS as a sensitive and efficient method for process optimization and quality control of nucleic acid therapies.

Abbreviations used in this work

- DNA: Deoxyribose nucleic acid
- PCR: Polymerase chain reaction
- mRNA: Messenger ribonucleic acid
- ARCA: Anti-reverse cap analogue
- UTR: Untranslated region
- GTP: Guanosine triphosphate
- NTP: Nucleoside triphosphate
- SAM: S-adenosylmethionine

Experimental

All PCR primers and synthetic RNA/DNA chimeric probes were synthesized by Integrated DNA Technologies.

In vitro transcription and mRNA capping

A plasmid encoding a model ~3,800 nt sequence downstream of a T7 promoter was purchased from Sino Biological. The sequence included 5' and 3' UTRs as well as a coding region. The T7 promoter and sequence of interest were PCR-amplified using a Herculase II Fusion DNA Polymerase kit (Agilent part number 600677) and cleaned up using a StrataPrep PCR purification kit (Agilent part number 400771). The specificity of the PCR reaction and concentration of the product were measured on an Agilent 2100 Bioanalyzer Instrument with DNA 7500 kit (part number 5067-1506).

The PCR product was then transcribed to mRNA using T7 RNA polymerase (New England Biolabs M0251) using the manufacturer's recommended protocol. 100 µL *in vitro* transcription reactions were diluted with 100 µL nuclease-free water prior to DNase-I (New England Biolabs M0303) digestion to eliminate DNA template and residual PCR primers. mRNA was then precipitated by adding 70 µL of 8 M LiCl, chilling overnight at -20 °C, then centrifuging at 12,000x g for 15 minutes at 4 °C. mRNA pellets were washed twice in 70% ethanol, air-dried, then dissolved in nuclease-free water and quantitated using an Agilent 2100 Bioanalyzer Instrument with RNA 6,000 Nano kit (part number 5064-1511). The mRNA was then made into 5 µg aliquots and frozen at -80 °C.

Two methods of mRNA capping were used:

- 1) Co-transcriptional capping with ARCA
- 2) Enzymatic capping with Vaccinia capping enzyme

For ARCA capping, mRNA samples were transcribed with an NTP mix containing a 4:1 ratio of ARCA to GTP. For enzymatic capping, 5 to 10 µg of purified uncapped mRNA was capped using a Vaccinia Capping System kit (New England Biolabs M2080), then purified using a Monarch RNA cleanup kit (New England Biolabs T2040) and eluted in nuclease-free water prior to analysis.

Site-directed RNase-H cleavage

In-solution RNase-H site-directed cleavage was implemented as described by Lapham, J. *et al.*⁴ 15 nt chimeric 2'-O-methyl RNA/DNA probes were designed complementary to the mRNA sample (Figure 1) and used to direct RNase-H cleavage under two conditions: (1) 1-hour thermal annealing

program followed by 30-minute cleavage with RNase-H at 37 °C, or (2) 30-minute cleavage with thermostable RNase-H at 50 °C. After cleavage, oligonucleotides of length 40 nt or 50 nt containing the 5' cap were liberated and digested samples were purified using a Monarch RNA cleanup kit (New England Biolabs T2040) prior to visualization on an Agilent 2100 Bioanalyzer Instrument with Small RNA kit (part number 5067-1548).

LC-DAD/MS of 5' capped oligonucleotides Instrumentation

- 1290 Infinity II LC with diode array detector (part number G7117B)
- 6545XT AdvanceBio LC/Q-TOF

Care was taken to eliminate glass from the flow path to reduce alkaline metal adduction. Agilent Nalgene bottles (part number 9301-6460) were used as mobile phase containers, and each solvent line was equipped with a steel frit. Agilent polypropylene sample vials were used (part number 5190-2242). Before the start of each day's experiments, the LC system and column were flushed with a 50% MeOH + 0.1% formic acid solution for 30 mins to further reduce alkaline metal adducts.

Digested mRNA samples were separated on an AdvanceBio Oligonucleotide column (2.1 × 50 mm, 2.7 µm, 120 Å, part number 659750-702). The mobile phase and LC gradients are shown in Table 1, mass spectrometer settings in Table 2, and data analysis was performed in MassHunter BioConfirm 10.0 with deconvolution settings shown in Table 3.

Table 1. Mobile phase and LC gradient.

Agilent 1290 Infinity II LC System	
Column	AdvanceBio Oligonucleotide, 2.7 µm, 2.1 × 50 mm, 120 Å
Solvent A	15 mM dibutylamine + 25 mM HFIP in DI water
Solvent B	15 mM dibutylamine + 25 mM HFIP in methanol
Gradient	Time (min) % B
	0 10
	4 30
	25 51
	25 to 28 90
Column Temperature	50 °C
Flow Rate	0.4 mL/min
Injection Volume	20 µL
mRNA Per Injection	2 µg

Table 2. Mass spectrometer settings.

Agilent 6545XT AdvanceBio LC/Q-TOF	
Acquisition Mode	Negative, standard (3,200 <i>m/z</i>) mass range, High Sensitivity (2 GHz)
Gas Temperature	350 °C
Gas Flow	12 L/min
Nebulizer	25 psig
Sheath Gas Temperature	275 °C
Sheath Gas Flow	10 L/min
V _{cap}	4,500 V
Nozzle Voltage	2,000 V
Fragmentor	250 V
Skimmer	65 V
MS1 Range	400 to 3,200 <i>m/z</i>
MS1 Scan Rate	2 Hz
Reference Mass	1,033.9881

Table 3. Deconvolution settings.

MassHunter BioConfirm 10.0 Settings	
Extract Chromatogram (MS)	Diode Array Detector
MS1 Delay Time	0.06 seconds
Decon. Algorithm	Maximum Entropy
Subtract Baseline	1
Adduct	Proton Loss
Mass Range	10,000 to 30,000 Da
Mass Step	0.5 Da
Use Limited <i>m/z</i> Range	1,040 to 3,200

Results and discussion

As full-length mRNA is typically too large for standard LC/MS analysis, we first optimized RNase-H site-directed cleavage. Two RNA/DNA chimeric probes were designed complementary to different sequences within the 5' UTR, directing RNase-H cleavage⁴ to either nucleotide 40 or 50 (Figure 1A) so that oligonucleotides of 40 nt or 50 nt in length, bearing the 5' capping structure, would be liberated upon successful cleavage. These smaller 5' capped oligonucleotides are amenable to LC/MS analysis.

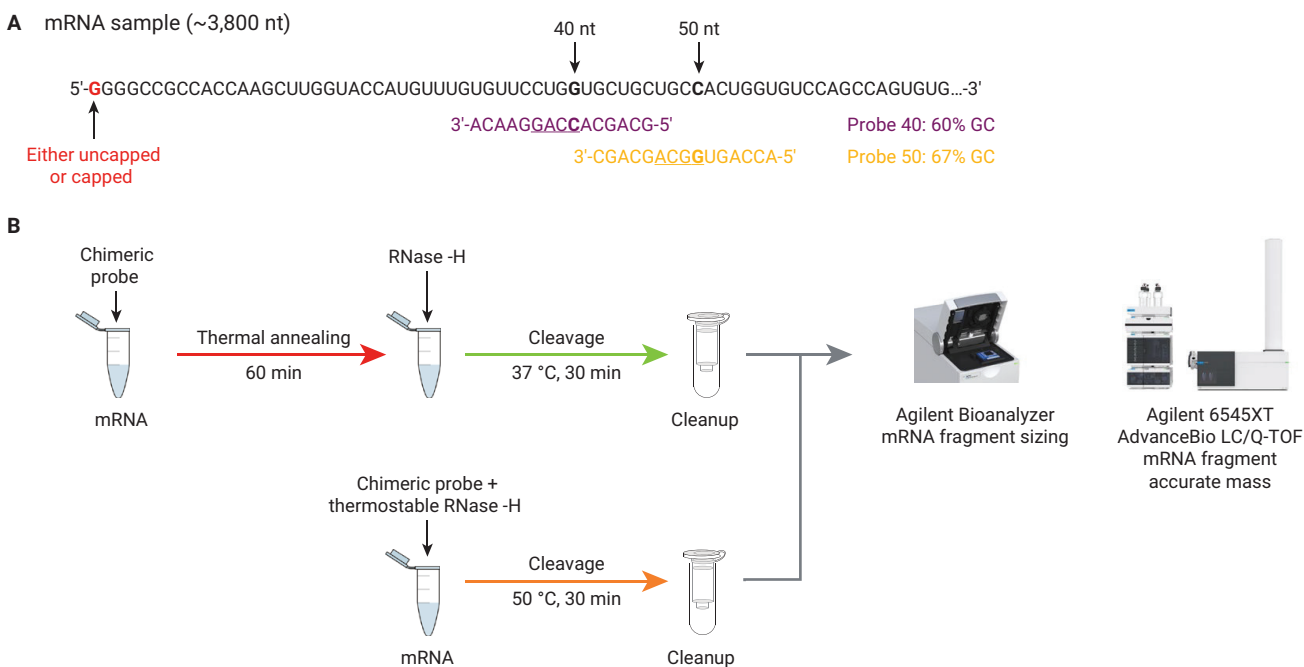


Figure 1. mRNA sample preparation and analysis. (A) Chimeric probes complementary to the mRNA sample were designed to direct RNase-H cleavage at 40 nt (purple) and 50 nt (gold). Underlined probe nucleotides were composed of DNA and were otherwise composed of 2'-O-methyl RNA. (B) Sample preparation scheme using non-thermostable (top scheme) or thermostable RNase-H (bottom scheme). Total analysis time using bottom scheme: cleavage (30 minutes) + cleanup (10 minutes) + LC/MS (25 minutes) + data analysis (10 minutes) = 75 minutes.

As published elsewhere⁵, the typical workflow for such an experiment entails a separate one-hour thermal annealing step prior to the addition of non-thermostable RNase-H enzyme, followed by sample cleavage at 37 °C (Figure 1B, top scheme). Separate steps are necessary because the high temperature (~95 °C) used during thermal annealing would otherwise: (1) denature non-thermostable RNase-H, and (2) promote mRNA hydrolysis due to divalent cations present in the reaction buffer.⁶

We hypothesized that the cleavage reaction could be expedited by performing it at a moderately raised temperature of 50 °C with thermostable RNase-H (Figure 1B, bottom scheme) provided chimeric probes of sufficiently high GC content were used. In principle, the elevated temperature would be expected to unwind mRNA secondary structure, permitting high GC content chimeric probes to bind to their complementary mRNA regions and direct cleavage by thermostable RNase-H.

As shown in Figure 2, site-directed cleavage was performed using two different high GC content probes (Probe 40 and Probe 50, each >60% GC) with either non-thermostable or thermostable RNase-H. The resulting digests were separated using an Agilent 2100 Bioanalyzer automated electrophoresis tool with Small RNA kit (part number 5067-1548) and qualitatively assessed using a virtual gel image representation.

Both Probe 40 and Probe 50 successfully directed cleavage of the mRNA sample under all conditions. However, Probe 50 exhibited off-target binding when using non-thermostable RNase-H, resulting in undesirable products (Figure 2, red arrows). When thermostable RNase-H was used, Probe 50 directed specific cleavage, allowing a cleaner sample to be obtained in a shorter time frame.

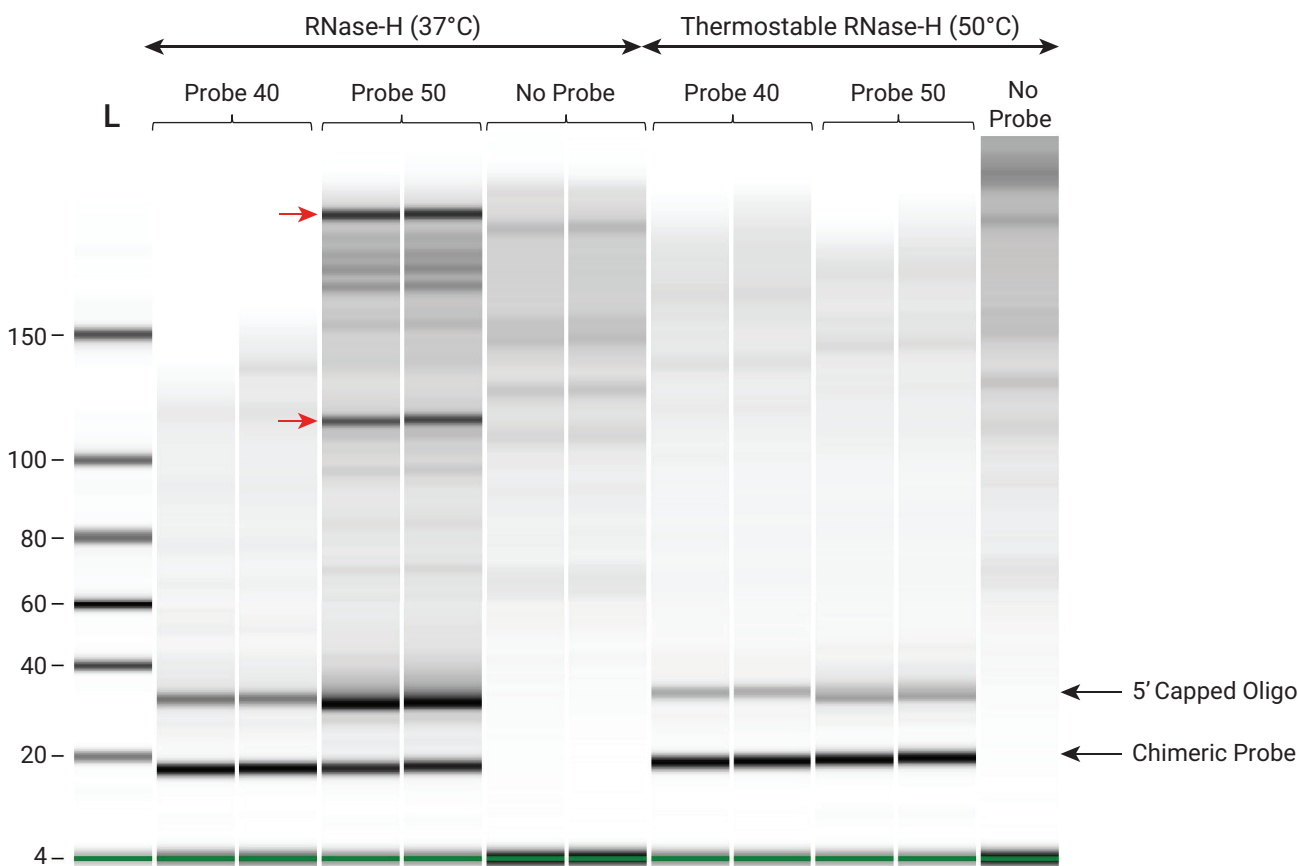


Figure 2. Assessment of site-directed cleavage using thermostable and non-thermostable RNase-H. Probe 40 and Probe 50 direct enzymatic cleavage at nucleotides 40 and 50 respectively. Red arrows indicate off-target cleavage products. L: ladder.

Next, uncapped mRNA digested using Probe 50 + thermostable RNase-H was analyzed by IP-RP LC/MS. Figure 3 shows the separation of uncapped 5' oligonucleotides from Probe 50 and the remaining mRNA on an Agilent AdvanceBio Oligonucleotide column (2.1 × 50 mm, 2.7 μm, 120 Å, part number 659750-702). Using automated data analysis workflows built into MassHunter BioConfirm 10.0, mass spectra were extracted from peaks identified in the UV chromatogram, then automatically deconvoluted using the settings shown in Table 3. Table 4 shows the expected uncapped, capping intermediate and fully capped species that may be present in each reaction.

As uncapped mRNA consists of a labile 5' terminal triphosphate group, some amount of hydrolyzed di- or monophosphate species³ might be observed depending on the reaction conditions. Figure 4 shows the extracted mass spectra and deconvoluted masses from triphosphate and

diphosphate peaks. The optimized thermostable RNase-H cleavage protocol yielded only a small quantity (4.2%) of diphosphate and no detectable monophosphate species, suggesting that reaction conditions were suitably mild.

About 15% of triphosphate oligonucleotides in the uncapped sample were found to be sequence variants containing an additional non-templated +G nucleotide (Figure 4D). This presumably occurs due to T7 transcriptional slippage, which is commonly seen when repeating G nucleotides are present at the start of a transcribed sequence.⁷ As seen in Figure 5, slippage sequence variants were also evident in mRNA samples co-transcriptionally capped with ARCA, both before and after a subsequent methylation reaction to Cap 1. Slippage sequence variants could be identified as distinct chromatographic peaks but were not baseline separated. All capped oligonucleotides were well-separated from uncapped oligonucleotides.

Table 4. Uncapped, capping intermediate, and capped species. Red letters indicate the 5' terminal nucleotide with phosphates marked by 'p', which may be elaborated or substituted by enzymatic reactions into capping structures.

Uncapped		Capping Intermediates		Capped Species	
Name	Sequence	Name	Sequence	Name	Sequence
Triphosphate	pppGGGGCC...	Diphosphate	ppGGGGCC...	ARCA Cap 0	3'-O-Me-m7GpppGGGGCC...
		G-Cap	GpppGGGGCC...	ARCA Cap 1	3'-O-Me-m7GpppmGGGGCC...
				Cap 0	m7GpppGGGGCC...

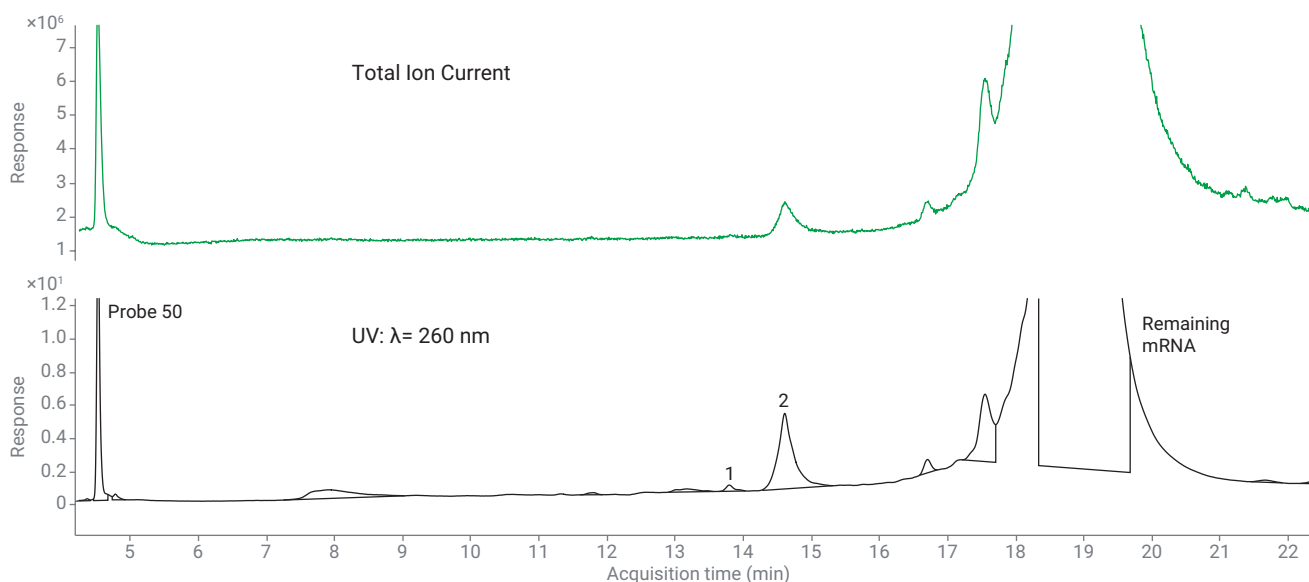


Figure 3. Chromatographic separation of 5' uncapped oligonucleotides from chimeric probe and sample matrix. Peak 1: 5' diphosphate, Peak 2: 5' triphosphate oligonucleotides.

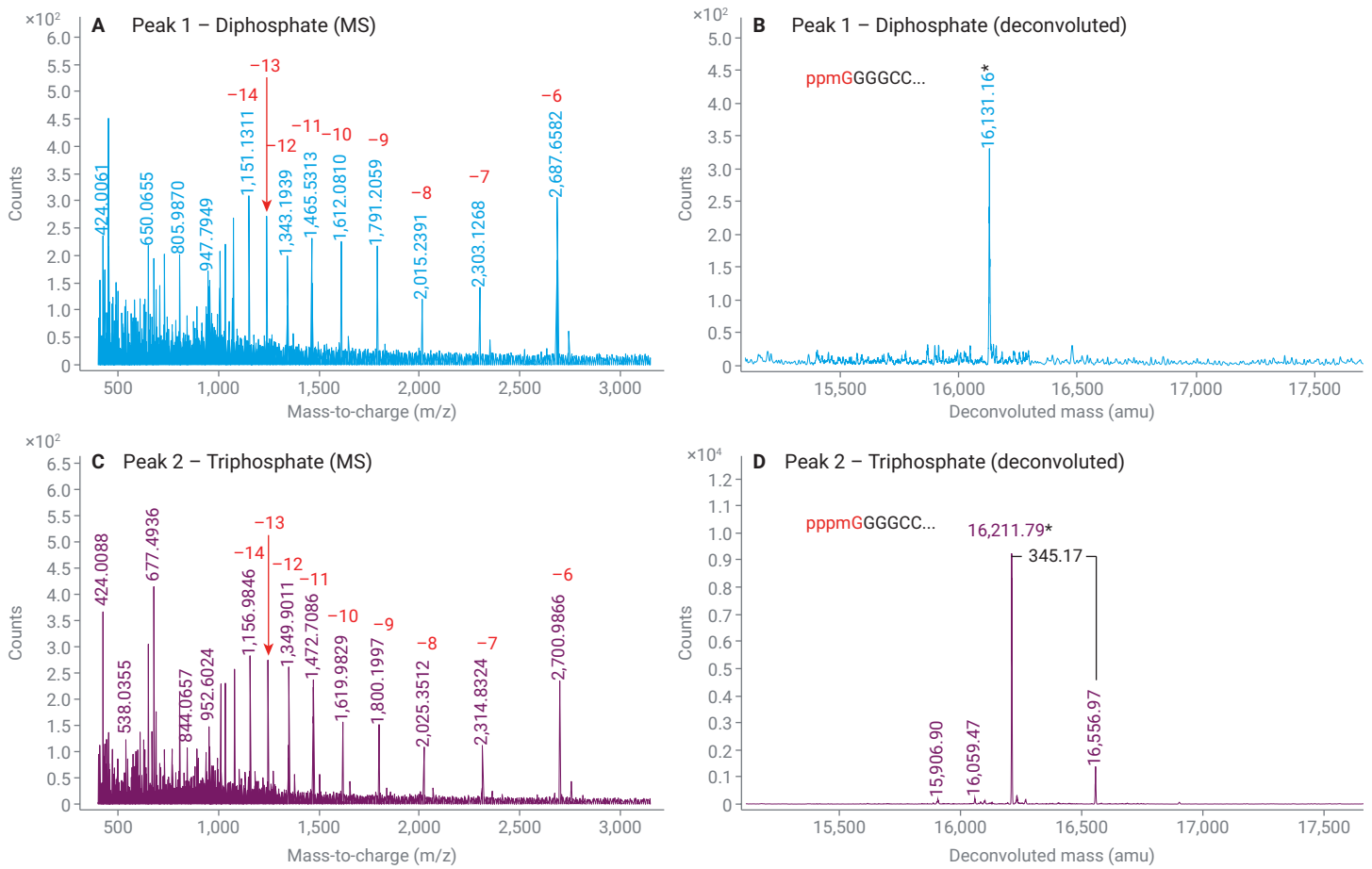


Figure 4. Mass spectra of 5' uncapped mRNA oligonucleotides. (A) Extracted and (B) deconvoluted mass spectra from Peak 1 of Figure 3. (C) Extracted and (D) deconvoluted mass spectra from Peak 2 of Figure 3. Numbers in red indicate the charge state of each peak in the extracted mass spectra arising from the diphosphate and triphosphate oligonucleotides. Mass peaks marked with asterisks (16131.16 Da and 16211.79 Da) were matched to their putative diphosphate and triphosphate identities (sequences inset) with <10 ppm mass error (Table 5). In panel D, triphosphate + G sequence variant (+345.17 Da) was observed co-eluting with triphosphate uncapped oligonucleotides.

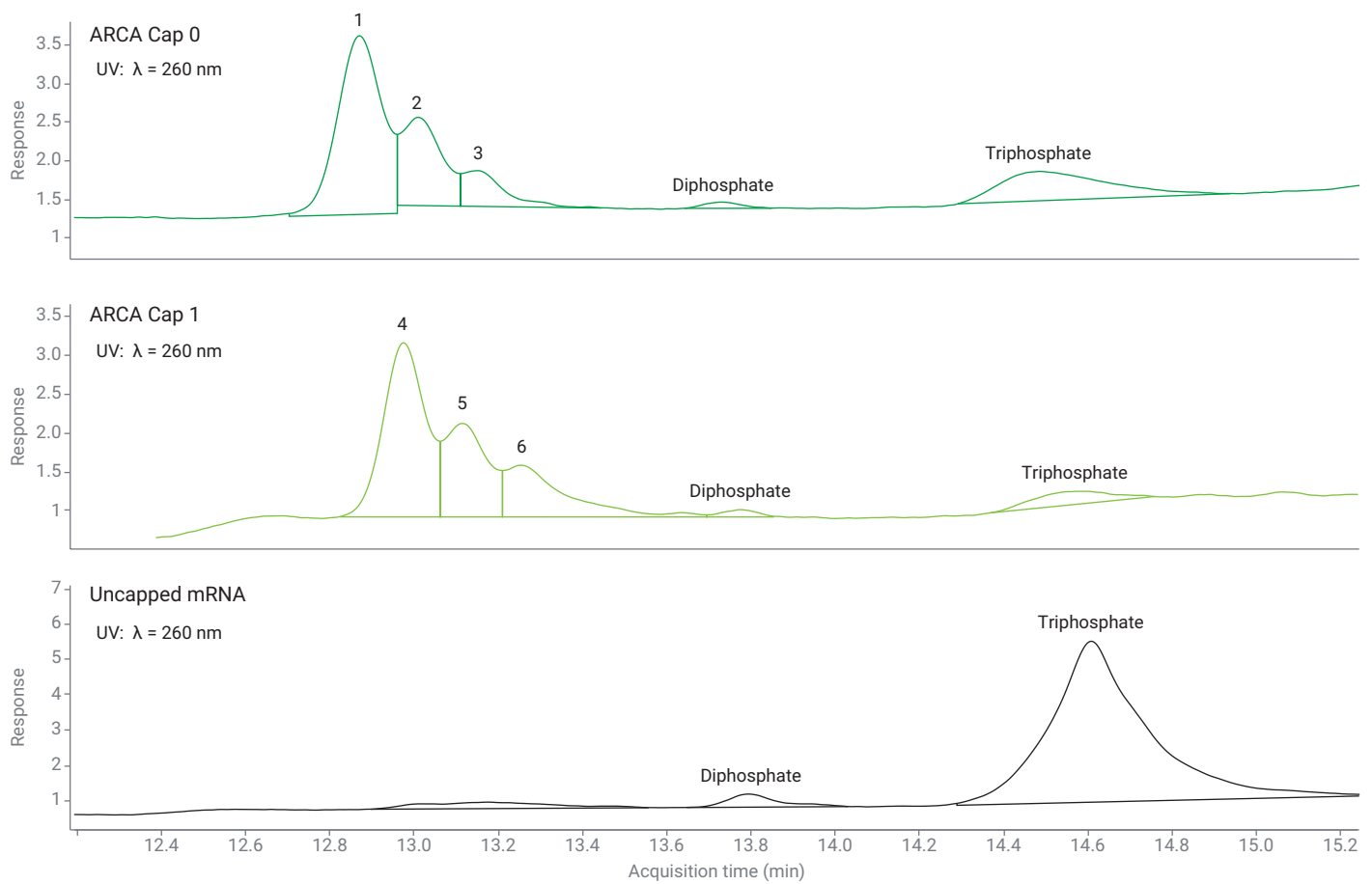


Figure 5. Separation of capped from uncapped oligonucleotides. Peaks 1 to 3: ARCA Cap 0, Peaks 4 to 6: ARCA Cap 1. Capped species contain 0 to 2 non-templated G nucleotides as slippage sequence variants.

Figure 6 shows the extracted mass spectra and deconvoluted masses from ARCA Cap 0 and ARCA Cap 1 peaks. Consistent with published literature², we found the ARCA Cap 0 co-transcriptional capping efficiency to be high ($91.3 \pm 1.76\%$), but not complete. In samples subsequently methylated to ARCA Cap 1, the capping efficiency was not significantly different ($90.6 \pm 1.53\%$) from ARCA Cap 0, indicating an essentially complete conversion of all Cap 0 structures to Cap 1.

Finally, the LC/MS method was used to assess the efficiency of Vaccinia enzymatic capping. Although this reaction has been claimed³ to be more efficient than ARCA co-transcriptional capping and relatively independent of sample sequence, in our hands it proved to be otherwise. Using the manufacturer's recommended reaction conditions, Vaccinia enzymatic capping resulted in a mixture of uncapped material, capping intermediates, and fully capped sample (Figure 7 and Table 6). As shown in Figure 8, most of the sample ($90.9 \pm 0.6\%$) remained uncapped with 5' terminal di- or triphosphate, and $6.5 \pm 0.7\%$ was capped but unmethylated i.e. G-Cap. Only $2.6 \pm 0.5\%$ of the sample was capped and methylated to Cap 0.

Table 5. Mass accuracy of ARCA-capped and capping intermediate oligonucleotides.

ARCA Co-Transcriptional Capping			
Identity	Theoretical Mass	Observed Mass	Accuracy (ppm)
ARCA Cap 0	16504.59	16504.62	2.01
ARCA Cap 0 + G	16849.80	16849.69	6.37
ARCA Cap 0 + 2G	17195.01	17195.03	1.50
ARCA Cap 1	16518.59	16518.85	15.77
ARCA Cap 1 + G	16863.80	16864.11	18.47
ARCA Cap 1 + 2G	17209.01	17208.73	16.13
Di-phosphate	16131.52	16131.37	9.21
Tri-phosphate	16211.51	16211.50	0.38
Tri-phosphate + G	16556.55	-	-

Table 6. Mass accuracy of enzymatically capped and capping intermediate oligonucleotides.

Enzymatic Capping			
Identity	Theoretical Mass	Observed Mass	Accuracy (ppm)
Cap 0	16490.59	16490.65	3.55
Cap 0 + G	16835.80	16836.00	11.97
G-Cap	16476.57	16476.65	4.85
Di-phosphate	16131.52	16131.49	1.95
Tri-phosphate	16211.51	16211.61	6.24
Tri-phosphate + G	16556.72	16556.97	15.33

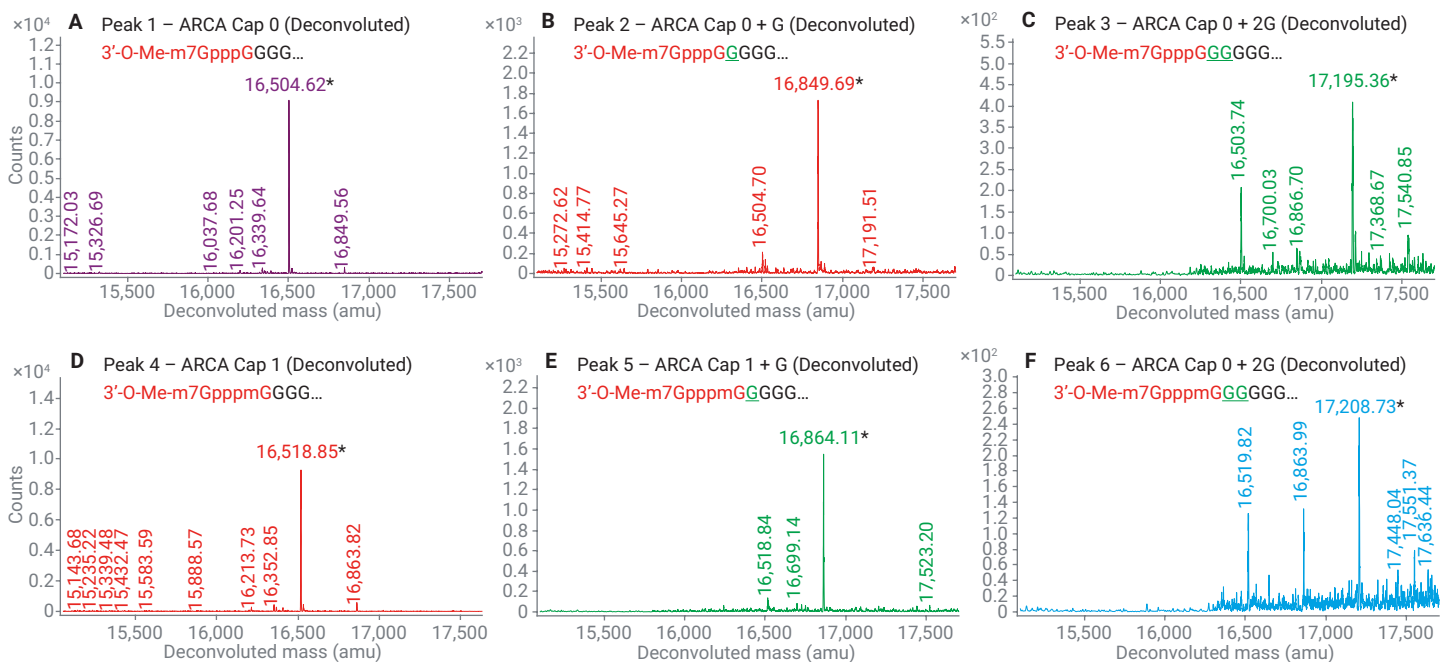


Figure 6. Mass spectra of ARCA Cap 0 mRNA oligonucleotides. (A – C) Deconvoluted mass spectra from Peaks 1 – 3 of Figure 5. (D – F) Deconvoluted mass spectra from Peaks 4 – 6 of Figure 5. Mass peaks marked with asterisks (16504.62 Da, 16849.69 Da, 17195.36 Da, 16518.85 Da, 16864.11 Da and 17208.73 Da) were matched to their putative identities (sequences inset) with < 20 ppm mass error (Table 5). Underlined letters in green indicate non-templated nucleotides likely due to T7 transcriptional slippage.

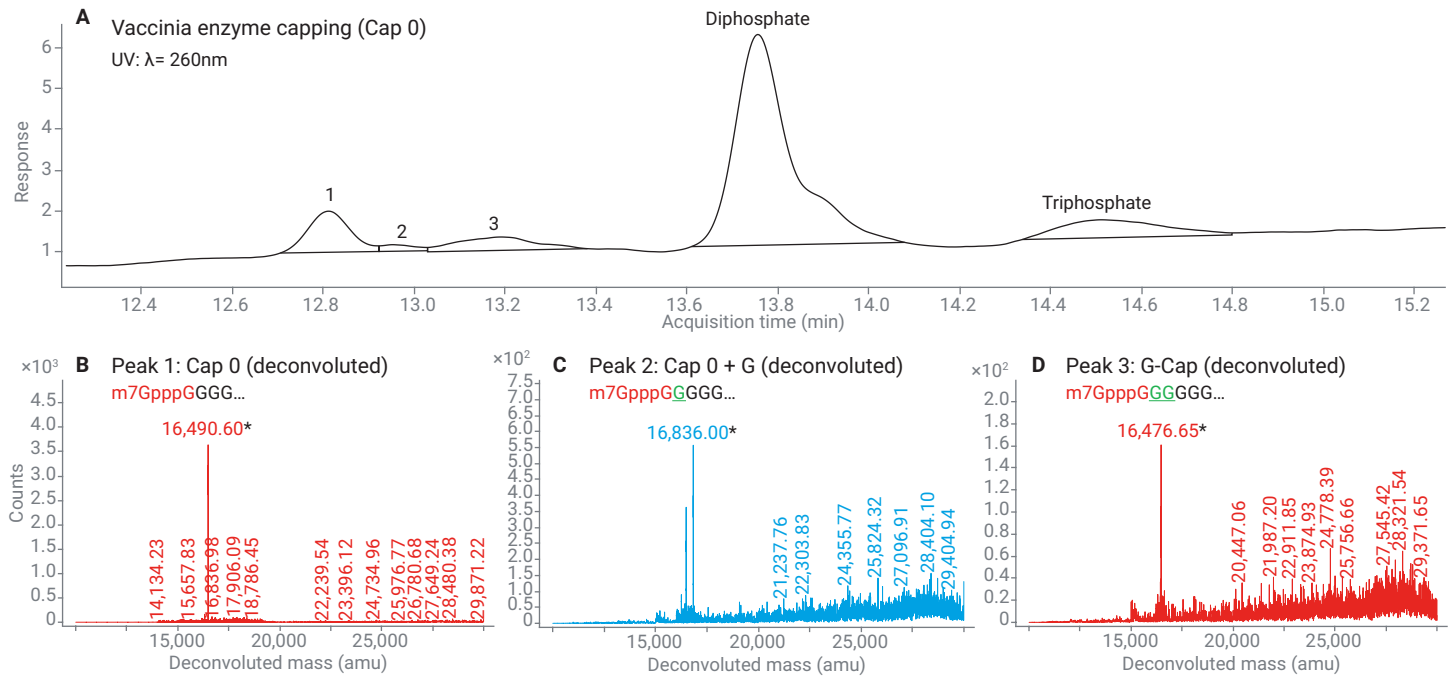


Figure 7. LC/MS of Vaccinia enzyme capped oligonucleotides and capping intermediates. (A) Peaks 1 to 2: Cap 0 and +G sequence variant, Peak 3: G-capped oligonucleotide, (B to D) Deconvoluted mass spectra of capped oligonucleotides. All mass peaks marked with asterisks (16,490.60, 16,836.00, and 16,476.65 Da) were matched to their putative identities (sequences inset) with <12 ppm (Table 6). Underlined letters in green indicate non-templated nucleotides likely due to T7 transcriptional slippage.

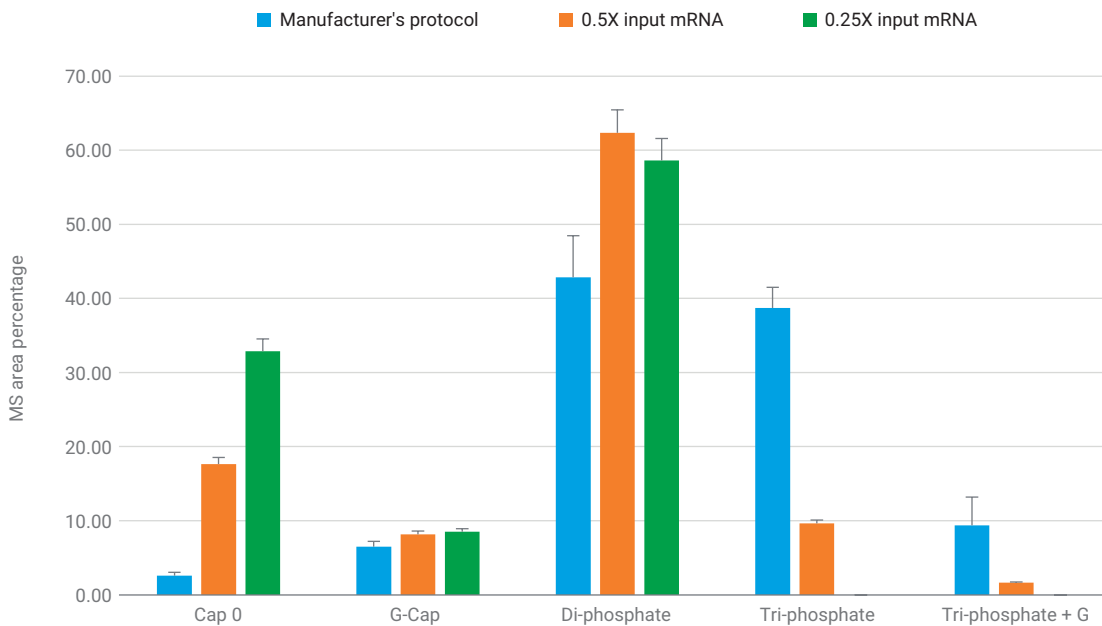


Figure 8. Optimization of Vaccinia enzymatic capping guided by LC/MS.

To increase capping efficiency, we reduced the quantity of input mRNA by 0.5x and 0.25x, thus raising the molar ratio of SAM, GTP and Vaccinia capping enzyme relative to mRNA. This strategy was moderately successful, resulting in a decrease in uncapped material (0.5x = 73.6 ±1.3% uncapped, 0.25x = 58.6 ±0.8% uncapped) and a corresponding increase in capped material (0.5x = 17.7 ±1.8% Cap 0, 0.25x = 32.9 ±0.4% Cap 0). Increasing the concentration of individual reactants in isolation did not increase capping efficiency (data not shown), suggesting that no individual component was faulty.

Conclusion

In this study we have developed a faster LC/MS method for quantifying mRNA 5' capping. One of the key enhancements in this workflow has been the use of thermostable RNase-H in conjunction with chimeric RNA/DNA oligonucleotide probes of sufficiently high GC content to expedite mRNA cleavage without a separate thermal annealing step. Probes with excessively high GC content may be unsuitable due to the increased likelihood of off-target binding or the formation of secondary structures. Indeed, we observed off-target cleavage with Probe 50 (67% GC content, Figure 2) when performing cleavage at 37 °C. As off-target binding is favored at lower reaction temperatures, performing cleavage at elevated temperatures resulted in cleaner samples in addition to hastening the reaction. In separate experiments, we found that probes with low GC content (40%) were unsuccessful at directing thermostable RNase-H cutting (data not shown).

We have demonstrated this workflow using two different capping methodologies: (1) co-transcriptional capping with ARCA, (2) enzymatic capping with Vaccinia capping enzyme. Although ARCA capping results agreed well with the literature, our experience with Vaccinia enzymatic capping was disappointing. Analysis of the sample sequence highlights a possible cause: the first 12 nucleotides have a very high GC content of over 90%, increasing the likelihood of secondary structure formation which may have interfered with Vaccinia enzymatic capping. As homopolymeric G repeats can also lead to inclusion of non-templated G nucleotides as sequence variants (Figure 5), these results indicate that redesigning the 5' UTR of this sequence could improve ease of processing and product quality.

www.agilent.com/chem

For Research Use Only. Not for use in diagnostic procedures.

This information is subject to change without notice.

We note that a similar analytical approach was published recently by M. Beverly *et al.*⁵, where chimeric probes were covalently conjugated to magnetic beads to enable simultaneous site-directed cutting by RNase-H and affinity enrichment of cleaved oligonucleotides. In our hands, this approach failed to direct specific cleavage of our sample despite numerous optimizations (data not shown). This could have been because the chimeric probes complementary to the sample's 5' terminus possessed very high GC content, thereby causing widespread nonspecific binding. We found our workflow to be more flexible as chimeric probes could be designed to avoid challenging regions in the sample. Moreover, sample cleanup using silica-based spin columns is likely to be less sequence-dependent than affinity-based approaches, and will probably lead to greater sample recovery.

In conclusion, this application note highlights the utility of the Agilent 6545XT AdvanceBio LC/Q-TOF for high-resolution, rapid analysis of mRNA 5' capping. We anticipate this workflow to be useful in both drug development and quality control laboratories.

References

1. Hassett, K. J. *et al.* Optimization of Lipid Nanoparticles for Intramuscular Administration of mRNA Vaccines. *Mol. Thera. Nucleic Acids* **2019**, *15*, 1–11.
2. Stepinski, J. *et al.* Synthesis and Properties of mRNAs Containing the Novel "Anti-Reverse" Cap Analogues 7-methyl(3'-O-methyl)GpppG and 7-methyl(3'-deoxy)GpppG. *RNA* **2001**, *7*, 1486–1495.
3. Fuchs, A. L. *et al.* A General Method for Rapid and Cost-Efficient Large-Scale Production of 5' Capped RNA. *RNA* **2016**, *22*, 1454–1466.
4. Lapham, J. *et al.* Site-Specific Cleavage of Transcript RNA. *Methods in Enzymology* **2000**, *317*, 132–139.
5. Beverly, M. *et al.* Label-Free Analysis of mRNA Capping Efficiency using RNase H Probes and LC-MS. *Anal. Bioanal. Chem.* **2016**, *408*, 5021–5030.
6. AbouHaidar, M. G. *et al.* Non-Enzymatic RNA Hydrolysis Promoted by the Combined Catalytic Activity of Buffers and Magnesium Ions. *Z Naturforsch C J Biosci* **1999**, *54*, 542–548.
7. T. Conrad *et al.* Maximizing Transcription of Nucleic Acids with Efficient T7 Promoters. *Nat. Comm. Biol.* **2020**, *3*, 1–8.

Determining mRNA Capping with HILIC-MS on a Low-Adsorption Flow Path

Limiting interfering interactions with iron surfaces using the Agilent 1290 Infinity II Bio LC System

Authors

Gerd Vanhoenacker,
Kris Morreel,
Stefanie Jonckheere,
Pat Sandra, and Koen Sandra
RIC group
President Kennedypark 6,
8500 Kortrijk, Belgium

Sonja Schneider and
Udo Huber
Agilent Technologies, Inc.

Abstract

The scientific leap taken in the development of therapeutic and prophylactic messenger ribonucleic acids (mRNA), and the increased public acceptance of the more recently available mRNA-related biopharmaceuticals, have propelled the search for new analytical methodologies for their characterization. Among these techniques are the determination of the incorporation efficiency of the cap structure onto the 5'-terminus of the mRNA. The measurement of this critical quality attribute (CQA) involves liquid chromatography/mass spectrometry (LC/MS) yet is hampered by the tendency of nucleic acids to adsorb to the iron surfaces of columns and instruments, especially when using hydrophilic interaction chromatography (HILIC) instead of ion pair reversed-phase (IP-RP) LC. As demonstrated in this application note, this phenomenon can be counteracted by opting for low-adsorption LC flow paths using a polyether ether ketone (PEEK)-lined HILIC column and an Agilent 1290 Infinity II Bio LC System.

Introduction

Worldwide successes in confining the COVID pandemic can largely be ascribed to the development of vaccines based on mRNA.¹ The approval of these landmark mRNA vaccines has paved the way for the full exploration of this technology both for prophylactic and therapeutic purposes. As a result, this evolution has urged the development of analytical methods to study various mRNA properties such as, among others, the 5'-cap structure and the proportion of capped mRNA.²⁻⁷

The mRNA cap is present at the 5'-end of the mRNA and consists of a 7N-methylguanosine that is 5'-5'-linked to the mRNA via a triphosphate ester (m7Gppp). However, small modifications might provide alternative cap structures, such as the Cap-1 structure resulting from an additional 2'-O-methylation of the first mRNA nucleotide being an adenosine (m7GpppAm), as shown in Figure 1.⁸

By preventing degradation, aiding cellular trafficking, and promoting the translation initiation and efficiency in eukaryotes, the cap is essential in yielding functional mRNA and so is considered a CQA.^{9,10} Within the production process, capping occurs during in vitro transcription of the mRNA (cotranscriptional capping) or, less commonly, is performed post-transcriptionally using a combination of enzymatic reactions. Whatever method is used, a small fraction of the mRNA pool will remain uncapped, displaying a 5'-terminus comprising 0 to 3 ester-linked phosphate groups.

Given the massive size of mRNA, determining the capping efficiency is typically performed by digesting the mRNA with ribonuclease (RNase) prior to analyzing the 5'-terminal fragments (Figure 1). Digestion might occur either on the single-stranded mRNA using RNase A or T1, or on an mRNA/DNA hybrid using the double-strand specific RNase H.

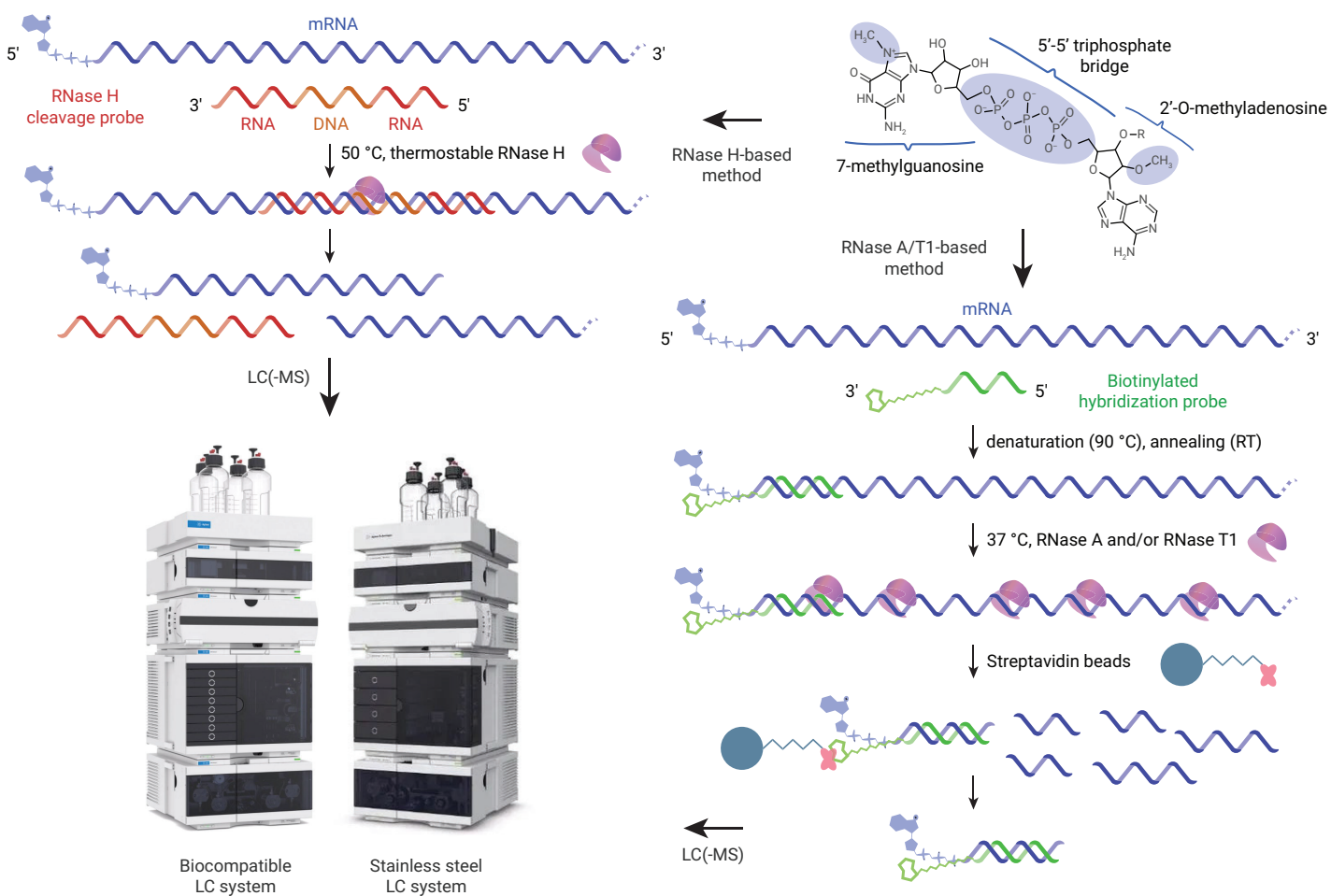


Figure 1. Capping efficiency analysis workflow. Most of the 5'-termini of eukaryotic mRNA bear a cap structure consisting of a 7-methylguanosine (m7G) that is 5'-5'-linked to a 2'-O-methyladenosine (Am) via a triphosphate ester (m7GpppAm, which can be abbreviated to Cap-1; upper right). Variations on this cap structure, especially with respect to the methylation sites, also occur. The mRNA cap can be isolated using either the DNA/RNA duplex-dependent RNase H (left) or via RNA single-strand-dependent RNase A and/or T1 (right) prior to LC/MS analysis. RT: room temperature. See the Experimental section for further explanation.

While fragmentation of the phosphodiester bond by RNase A or T1 yields a 5'-terminal fragment retaining the phosphate group at its 3'-end, the latter position is not phosphorylated when RNase H is employed. Both strategies involve a hybridization probe. When using RNase A or T1, this probe protects the mRNA 5'-terminus against digestion.⁵ Alternatively, the probe directs RNase H cleavage towards its hybridization site near the 5'-terminus.^{2,3} Regardless of the method used, the resulting 5'-terminal mRNA fragments are analyzed via LC coupled to MS.

The many negatively charged phosphate moieties of nucleic acids offer at least two challenges when being analyzed via LC/MS: iron surface adsorption and iron complexation. Whereas the former problem (adsorption to the stainless-steel surfaces present in the LC flow path) will induce peak broadening and loss, the latter issue is especially detrimental to the detection sensitivity when using MS. Noticeably, as numerous metal ions, especially sodium and potassium ions, are electrostatically attracted by nucleic acids, the MS signal is distributed across many charge states and adducts.⁴ By thorough cleaning of the LC/MS flow path and avoiding glassware and glass surfaces during the analysis and handling of nucleic acids, the contribution of adducts to the MS signal can be partially circumvented. Furthermore, analyzing nucleic acids via IPRP-LC/MS affords less metal surface adsorption owing to the neutralization of the nucleic acids by the N-alkyl amine ion-pairing reagent (IPR). This ion-pairing effect drives the retention mechanism in IPRP as the IPR bears a hydrophobic moiety that will be retained by the apolar stationary phase.⁴ However, while metal adsorption is seemingly solved by IP-RP LC/MS, other hurdles come into play, such as the high concentrations of IPR and counterions that contaminate and affect the LC/MS instrument. As a cleaner and more sustainable alternative, HILIC is increasingly preferred for the LC/MS analysis of nucleic acids.¹¹⁻¹³ As HILIC separation involves the partitioning of the "naked" nucleic acids between an apolar mobile phase and a water-layered polar stationary phase, stainless-steel flow paths will readily interfere with the separation. To deal with this metal surface adsorption, LC instruments and columns from which iron is eliminated, or metal surfaces deactivated or covered with, for example, PEEK, have been developed.

This application note describes the determination of mRNA capping following probe-guided RNase digestion and LC/MS analysis of the resulting 5'-containing mRNA oligonucleotides using a PEEK-lined diol HILIC column installed on a 1290 Infinity II Bio LC System and hyphenated with an Agilent 6545 LC/Q-TOF. The benefit of using low-adsorption flow paths is described and illustrated.

Experimental

Critical materials

Ammonium acetate (LC/MS grade) was acquired from Merck. Water (ULC/MS CC/SFC grade) and acetonitrile (HPLC-S grade) were supplied by Biosolve. Thermostable RNase H was purchased from New England Biolabs and RNase A from Thermo Fisher Scientific. Hybridization probes were ordered from Integrated DNA Technologies. Dynabeads MyOne Streptavidin C1 were purchased from Invitrogen. RNA Resolution Standard was received from Agilent Technologies and CleanCap Firefly Luciferase (Fluc) mRNA from TriLink BioTechnologies. The 1.2 kilobase (kb) mRNA was synthesized in-house by in vitro transcription from linearized plasmid DNA.

Sample preparation

The RNA resolution standard was dissolved in 1 mL of water/acetonitrile 50/50 (v/v). Further 10 and 50-fold dilutions were done in water/acetonitrile 50/50 (v/v).

Two procedures were employed for mRNA cap isolation (Figure 1). The first procedure was performed as described by Liao³ and starts with the hybridization of the probe to an mRNA region near the 5'-terminus followed by thermostable RNase H-targeted cleavage of the mRNA in this RNA/probe duplex region at 50 °C for 45 minutes. A second procedure was based on the methods described by Nwokeji *et al.*⁵ and Wolf *et al.*⁶, in which hybridization of the probe protects the mRNA 5'-terminus from degradation by RNase A, which proceeded for 1 hour at 37 °C. Because the different mRNA fragments resulting from RNase A digestion (covering a mass range from monomers up to oligomers) would readily mask any eluting 5'-terminal mRNA fragment, a prior isolation of the latter fragments is necessary. For this purpose, the hybridization probe contained a biotin label that enabled purification of the probe/5'-terminus duplexes through the use of streptavidin-loaded magnetic beads according to the manufacturer's protocol.

Instrumentation and method

Two Agilent LC systems were used: the 1290 Infinity II LC (stainless steel - SST) and the 1290 Infinity II Bio LC (biocompatible - BIO). Details of both configurations can be found in Table 1 and method parameters are summarized in Table 2. Data were acquired and processed in Agilent OpenLab CDS version 2.6, Agilent MassHunter for Data Acquisition B 10.0, and Agilent MassHunter Qualitative Analysis B.07.00.

Table 1. Details of the LC and MS systems used.

	SST LC System	BIO LC System
Pump	Agilent 1290 Infinity II High-Speed Pump (G7120A)	Agilent 1290 Infinity II Bio High-Speed Pump (G7132A)
Autosampler	Agilent 1290 Infinity II Multisampler (G7167B) with integrated sample thermostat	Agilent 1290 Infinity II Bio Multisampler (G7137A) with integrated sample thermostat
Column Compartment	Agilent 1290 Infinity II Multicolumn Thermostat (G7116B) with Agilent InfinityLab Quick Connect heat exchanger, standard flow (G7116-60015)	Agilent 1290 Infinity II Multicolumn Thermostat (G7116B) with Agilent InfinityLab Quick Connect Bio heat exchanger, standard flow (G7116-60071)
Detector	Agilent 1290 Infinity II DAD (G7117B)	Agilent 1290 Infinity II DAD (G7117B)
Flow Cell	Agilent InfinityLab Max-Light Cartridge Cell, standard, 10 mm (G4212-60008)	Agilent InfinityLab Max-Light Cartridge Cell, LSS, 10 mm (G7117-60020)
Q-TOF MS	Agilent 6545 LC/Q-TOF (G6545A)	Agilent 6545 LC/Q-TOF (G6545A)

Table 2. LC method parameters.

Parameter	Value						
Columns	Diol-HILIC column, 2.1 × 100 mm, 1.9 μm Stainless-steel version and PEEK-lined version						
Flow Rate	0.35 mL/min						
Mobile Phase	A) 20 mM ammonium acetate in water/acetonitrile 20/80 (v/v) B) 20 mM ammonium acetate in water/acetonitrile 80/20 (v/v)						
Gradient 1	<table border="1"> <thead> <tr> <th>Time (min)</th> <th>%B</th> </tr> </thead> <tbody> <tr> <td>0</td> <td>10</td> </tr> <tr> <td>17</td> <td>55</td> </tr> </tbody> </table>	Time (min)	%B	0	10	17	55
Time (min)	%B						
0	10						
17	55						
Gradient 2	<table border="1"> <thead> <tr> <th>Time (min)</th> <th>%B</th> </tr> </thead> <tbody> <tr> <td>0</td> <td>0</td> </tr> <tr> <td>21</td> <td>55</td> </tr> </tbody> </table>	Time (min)	%B	0	0	21	55
Time (min)	%B						
0	0						
21	55						
Injection	2 μL						
Needle Wash	Flush port, 3 s, water/acetonitrile 75/25 (v/v)						
Autosampler Temperature	8 °C						
Column Temperature	40 °C						
Detection DAD	260/4 nm, reference 360/40 nm, peak width > 0.013 min (20 Hz), collect all spectra						

Table 3. LC method parameters, for detection MS.

Parameter	Value
Detection MS	ESI, negative ionization, diverter valve bypassed*
Source	
Drying Gas Temperature	300 °C
Drying Gas Flow	8 L/min
Sheath Gas Temperature	350 °C
Sheath Gas Flow	10 L/min
Nebulizer Pressure	35 psi
Capillary Voltage	4,500 V
Nozzle Voltage	1,800 V
Fragmentor	200 V
Skimmer	65 V
Acquisition	
Acquisition Mode	Extended dynamic range (2 GHz)
Mass Range	<i>m/z</i> 400 to 3,200
Scan Rate	3 Spectra/s
Reference Mass	Disabled

*Diverter valve was bypassed to prevent potential non-specific interactions with stainless-steel components of the valve hardware.

Results and discussion

Prior to mRNA capping analysis, an RNA resolution standard composed of a 14, 17, 20, and 21-mer was subjected to the diol HILIC phase present in a stainless-steel or PEEK-lined housing installed on a 1290 Infinity II Bio LC system (Figure 2). On the stainless-steel column, the initial response for the oligonucleotides is disappointingly low, and increases gradually with subsequent injections to reach a steady state after five injections. However, even after conditioning, the peak height and area are much lower compared to that obtained on a PEEK-lined column, where maximum peak intensity is obtained with the first injection. These observations are in line with the findings recently noted by Lardeux *et al.*¹⁴ Next to the optimal intensity, peak shape and resolution are also dramatically better on the PEEK-lined column. The recovery for diluted solutions is furthermore greatly enhanced using this column. As shown in Figure 2, upon 50-fold dilution, all oligonucleotides are clearly detected, with the excellent peak shape maintained. On the stainless-steel column, however, this level can no longer be detected. Even a 10-fold dilution of the RNA resolution standard is problematic with this hardware.

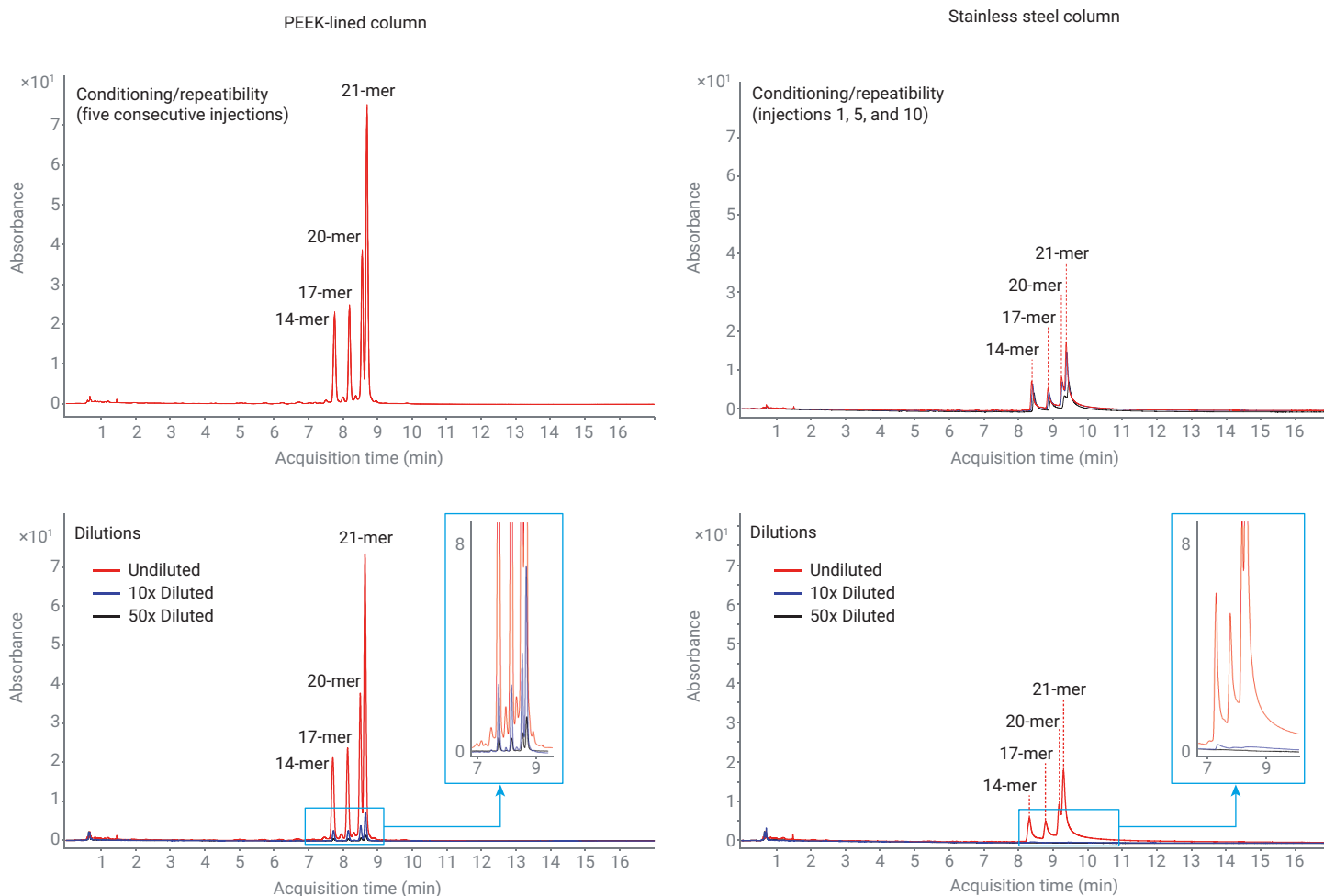


Figure 2. HILIC-DAD analysis (UV 260 nm) of the RNA resolution standard on a PEEK-lined column (left) and stainless-steel column (right) installed on an Agilent 1290 Infinity II Bio LC System. Gradient 1 (Table 2) was applied. Upper pane shows multiple injections of the same solution on brand new columns; lower pane shows the undiluted, 10, and 50-fold diluted RNA resolution standards.

Beyond column hardware, the impact of the LC instrument (stainless steel versus biocompatible) was evaluated using the RNA resolution standard. Figure 3 plots the peak area and tailing factor obtained for all instrument/column combinations and reveals that the effect of column hardware is greater than the system hardware. This is in accordance with earlier findings¹⁴⁻¹⁸ and can be explained by the fact that the column (tube and frits) represents 70% of the accessible

surface and that analyte residence time in the column largely exceeds the time in the LC instrument. Nevertheless, the impact of the system, although less obvious, cannot be neglected. To maximize chromatographic performance, it is therefore recommended to choose a configuration devoid of iron components in the sample flow path (i.e., a PEEK-lined column and a 1290 Infinity II Bio LC).

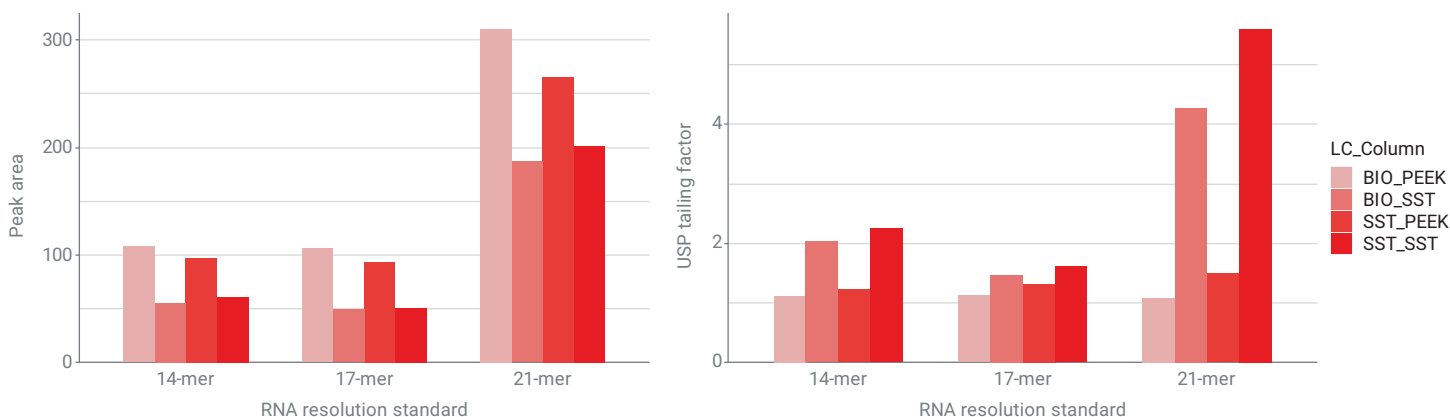


Figure 3. Peak area and USP tailing factor retrieved from the analysis of the RNA resolution standard on HILIC-DAD (UV 260 nm) using various instrument (BIO and SST) and column combinations (PEEK and SST). The 20-mer is excluded from the graphs as the marginal resolution (on SST configurations) disturbs the accurate calculation of peak area and tailing.

The disturbed peak shapes and intensities during HILIC analysis of nucleic acids in the presence of stainless-steel surfaces are due to the electrostatic interactions of the negatively charged phosphate ester moieties and the iron surfaces. Such interactions might especially affect the analysis of the 5'-termini of in vitro transcribed mRNA, where a high number and diverse set of phosphate moieties are encountered.

Procedures for the isolation of the mRNA 5'-termini are based on the use of hybridization probes, either to direct the cleavage to the mRNA site that is hybridized to the probe (e.g., by way of RNase H) or to protect the 5'-terminal regions from mRNA digestion by single-strand cutters such as RNase A or T1 (Figure 1). Whereas RNase H cleavage yields single-stranded 5'-terminal fragments with a non-phosphorylated 3'-end, RNase A and T1 provide fragments having either a 3'-phosphate ester or cyclic 2',3'-phosphodiester moiety. Furthermore, the RNase A/T1 procedure results in 5'-terminal fragments that are still annealed to the hybridization probe. The 5'-termini isolated via both approaches were subjected to HILIC-MS using either a stainless-steel or iron-free LC flow path (column and system). A 1.9-kb-long (Fluc mRNA) and a 1.2-kb-long mRNA were employed for the RNase H- and RNase A-dependent methods, respectively.

In the case of the RNase H-derived 5'-terminal mRNA fragments, the benefit of using an iron-free rather than a stainless-steel LC flow path is immediately clear when comparing the HILIC-MS base peak chromatograms (Figure 4). While readily measurable by way of the low-adsorption flow path, the capped 5'-terminus, referred to as m7GpppAm (N)_{25'}, is not observed using a stainless-steel configuration. As displayed in Figure 4, the full MS spectrum of this capped peak is rather complex, showing two skewed distributions of *m/z* peaks, each distribution representing a particular charge state (−5 and −6) and containing *m/z* peaks for various isotopes and adducts. This spreading of the detection signal across many *m/z* peaks turns MS into a precarious detection technique. A complex mass spectrum is also recorded for the hybridization probe which, being shorter and lacking 2'-hydroxy ribosyl moieties, elutes earlier than the capped fragment m7GpppAm (N)_{25'}. Due to the absence of the 5'-5' triphosphate motif, the hybridization probe is observed on both the stainless-steel and low-adsorption flow path.

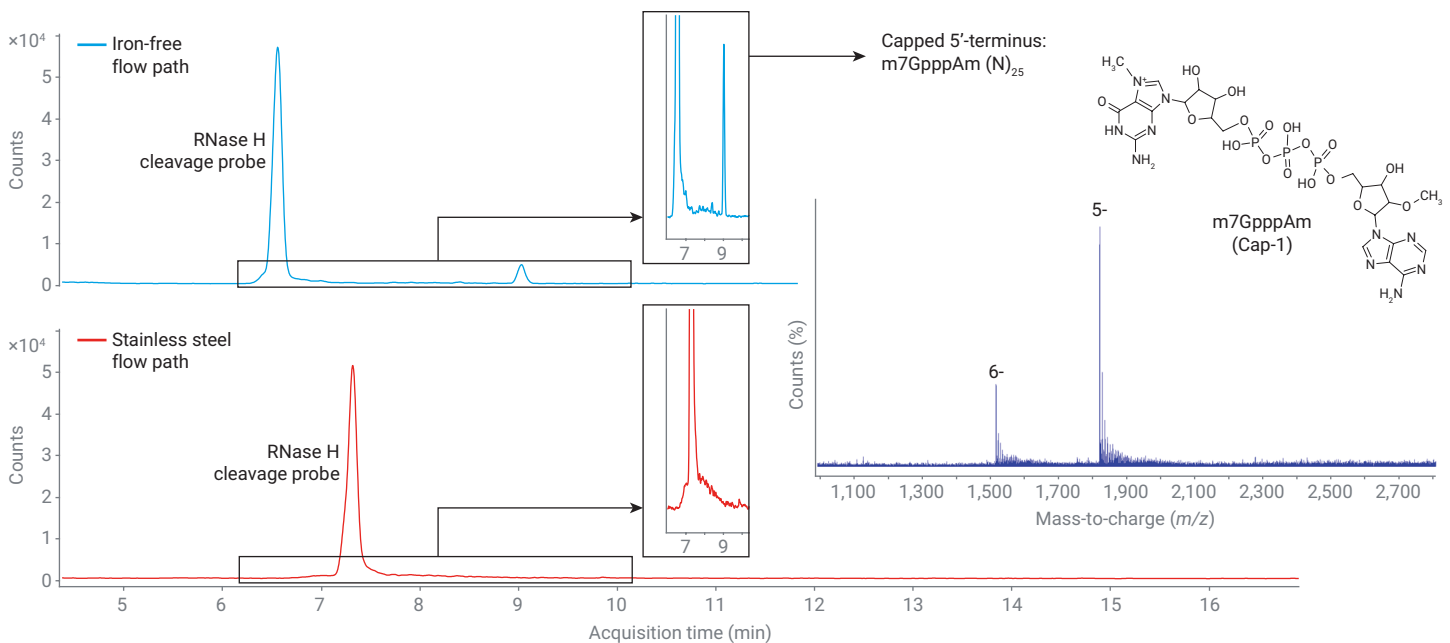


Figure 4. HILIC-MS base peak chromatograms of 5'-terminal Fluc mRNA fragments generated by the RNase H-based method obtained on a iron-free (blue) and stainless-steel configuration (red). The MS spectrum shown in the insert corresponds to the capped 5'-terminus. Gradient 1 (Table 2) was applied.

The RNase A-dependent procedure applied to the 1.2 kb proprietary mRNA, returns both capped ($m7GpppAm (N)_6 Cp$) and uncapped ($A (N)_6 Cp$) 5'-terminal fragments as displayed by the HILIC-MS base peak chromatograms (Figure 5). These species, carrying 3' terminal phosphate on top of the internal phosphodiester as a result of RNase A digestion, appear much less intense on the stainless-steel than on the iron-free configuration. Unlike the RNase H procedure, the RNase

A method yields double-stranded molecules in which the hybridization probe remains annealed to the 5'-terminal RNA fragment. HILIC separation at modest temperatures (40 °C here) conserves this RNA/probe double-helical conformation, yet in-source melting might explain their MS spectra, which display m/z peaks for both the single-stranded probe and the 5'-terminal fragment next to those for the RNA/probe double helix (Figure 5).

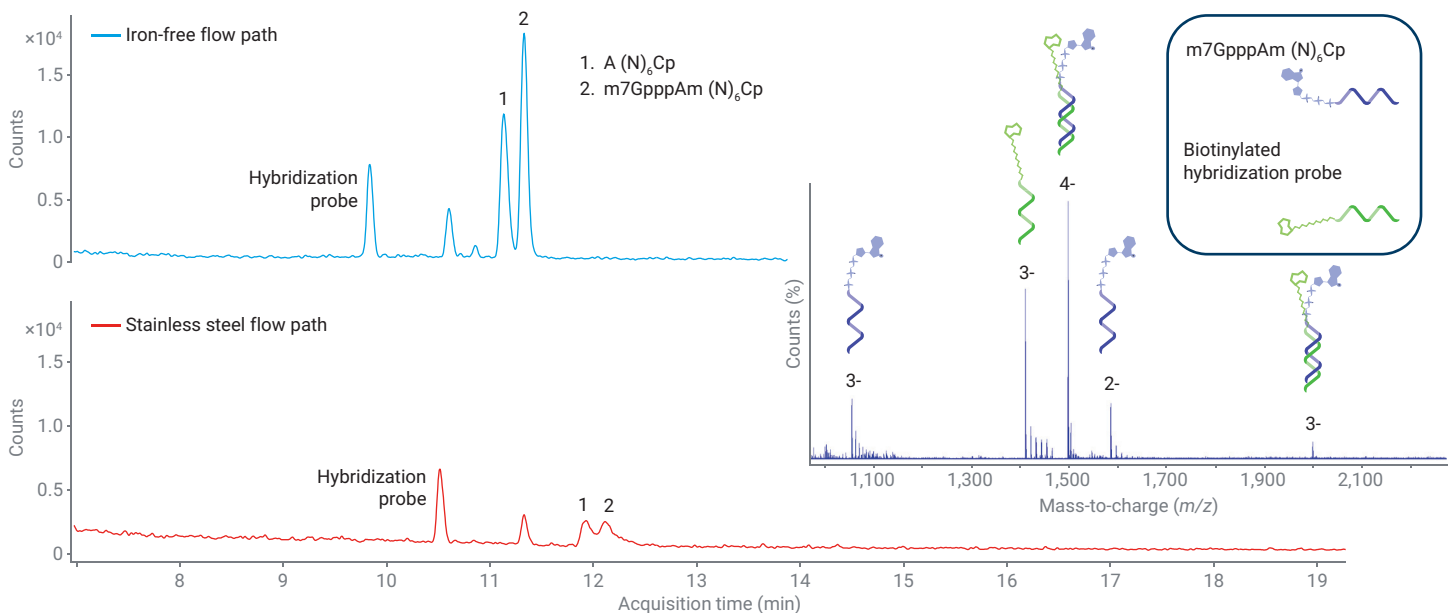


Figure 5. HILIC-MS profiling of 5'-terminal 1.2 kb proprietary mRNA fragments generated by the RNase A-based method. Due to the smaller oligonucleotides encountered, adapted gradient 2 (Table 2) was applied.

Conclusion

The recent tendency to analyze oligonucleotides using LC/MS via HILIC rather than less sustainable IPRP unveils the effect of the iron surfaces in classical stainless-steel columns and systems. Next to a lowered detection sensitivity, peak tailing biases the separation. This peak tailing arises from the internal phosphodiester and, especially, the triphosphates and terminal phosphates of the 5' mRNA fragments. All these phosphate moieties are fully negatively charged above pH 3 and, thus, electrostatically attracted to the iron parts present in both the LC and the column. By employing an Agilent 1290 Infinity II Bio LC and PEEK-lined column, such peak shape distortions and sensitivity losses can be circumvented, paving the way for the unprecedented characterization of IVT mRNA.

References

1. Callaway, E.; Naddaf, M. Pioneers of mRNA COVID Vaccines Win Medicine Nobel. *Nature* **2023**, 622, 228–229.
2. Beverly, M.; Dell, A.; Parmar, P.; Houghton, L. Label-Free Analysis of mRNA Capping Efficiency Using RNase H Probes and LC-MS. *Anal. Bioanal. Chem.* **2016**, 408, 5021–5030.
3. Liao, B. Rapid Analysis of mRNA 5' Capping with High Resolution LC/MS. *Agilent Technologies application note*, publication number 5994-3984EN, **2021**.
4. Morreel, K.; t'Kindt, R.; Debyser, G.; Jonckheere, S.; Sandra, P.; Sandra, K. Diving into the Structural Details of In Vitro Transcribed mRNA Using Liquid Chromatography-Mass Spectrometry-Based Oligonucleotide Profiling. *LCGC Europe* **2022**, 35, 220–236.
5. Nwokeoji, A. O.; Chou, T.; Nwokeoji, E. A. Low Resource Integrated Platform for Production and Analysis of Capped mRNA. *ACS Synth. Biol.* **2023**, 12, 329–339.
6. Wolf, E. J.; Dai, N.; Chan, S. H.; Corrêa, I. R. Selective Characterization of mRNA 5' End-Capping by DNA-Probe Directed Enrichment with Site-Specific Endoribonucleases. *ACS Pharmacol. Transl. Sci.* **2023**, 6, 1692–1702.
7. Guimaraes, G. J.; Kim, J.; Bartlett, M. G. Characterization of mRNA Therapeutics. *Mass Spectrom. Rev.* **2023**, doi: 10.1002/mas.21856.
8. Ramanathan, A.; Robb, G. B.; Chan, S. H. mRNA Capping: Biological Functions and Applications. *Nucleic Acids Res.* **2016**, 44, 7511–7526.
9. Daniel, S.; Kis, Z.; Kontoravdi, C.; Shah, N. Quality by Design for Enabling RNA Platform Production Processes. *Trends Biotechnol.* **2022**, 40, 1213–1228.
10. USP. Analytical Procedures for mRNA Vaccine Quality. USP guideline EA966W_ 2023-04, draft guidelines, second edition. [vaccine-mrna-guidelines-2.pdf \(usp.org\)](#).
11. Huang, M.; Xu, X.; Qiu, H.; Li, N. Analytical Characterization of DNA and RNA Oligonucleotides by Hydrophilic Interaction Liquid Chromatography-Tandem Mass Spectrometry. *J. Chromatogr. A.* **2021**, 1648, 462184.
12. Goyon, A.; Nguyen, D.; Boulanouar, S.; Yehl, P.; Zhang, K. Characterization of Impurities in Therapeutic RNAs at the Single Nucleotide Level. *Anal. Chem.* **2022**, 94, 16960–16966.
13. Li, G.; Rye, P. MS/MS Oligonucleotide Sequencing Using LC/Q-TOF with HILIC Chromatography. *Agilent Technologies application note*, publication number 5994-5632EN, **2023**.
14. Lardeux, H.; Goyon, A.; Zhang, K.; Nguyen, J. M.; Lauber, M. A.; Guillaume, G.; D'Atri, V. The Impact of Low Adsorption Surfaces for the Analysis of DNA and RNA Oligonucleotides. *J. Chromatogr. A.* **2022**, 1677, 463324.
15. Schneider, S. Analysis of Phosphate Compounds with the Agilent 1260 Infinity Bio-Inert Quaternary LC System. *Agilent Technologies application note*, publication number 5991-0025EN, 2012.
16. Sandra K.; Vandenbussche, J.; Vanhoenacker, G.; t'Kindt, R.; Sandra, P.; Krieger, S.; Schneider, S.; Huber, U. Analysis of Nucleotides Using a Fully Inert Flowpath. *Agilent Technologies application note*, publication number 5994-0680EN, **2019**.
17. Schneider, S. Comparability Studies for the Analysis of Nucleotides on Four Different LC Systems. *Agilent Technologies application note*, publication number 5994-4392EN, **2021**.
18. Vanhoenacker, G.; Sandra, P.; Sandra, K.; Schneider, S.; Huber, U. Improving Peak Shape and Recovery in LC Studies of Phosphated Vitamin B2. *Agilent Technologies application note*, publication number 5994-5830EN, **2023**.

www.agilent.com

DE95186582

This information is subject to change without notice.

© Agilent Technologies, Inc. 2024
Printed in the USA, February 14, 2024
5994-7118EN

Analysis of mRNA Poly-A Sequence Variants by High-Resolution LC/MS

Author

Brian Liao
Agilent Technologies, Inc.

Introduction

The urgency engendered by the SARS-CoV-2 pandemic of 2020 has prompted policy makers and pharmaceutical firms alike to develop and deploy mRNA vaccines with unprecedented speed. mRNA vaccines have shown impressive safety and efficacy in clinical trials¹⁻⁴, outperforming vaccines based on alternative technologies. As mRNA vaccines are considered gene therapies⁵, FDA guidance requires extensive characterization of product-related impurities. These may include populations of mRNA molecules with slight errors in their sequence, known as sequence variants. In addition, mRNA vaccines require lengthy, repetitive sections of A nucleotides (poly-A) at the 3' terminus for optimal stability and biological activity.⁶ Both the length and the composition of poly-A sequences are therefore critical quality attributes.

This work uses an Agilent AdvanceBio 6545XT LC/Q-TOF to analyze poly-A tail sequences formed by *E. coli* Poly-A Polymerase (PAP), which is a common component of *in vitro* transcription systems. Findings show that PAP is not fully selective for ATP, and can act on both CTP and UTP precursors to incorporate significant quantities of undesirable C and U nucleotides under standard *in vitro* transcription conditions. As these sequence variants can be regarded as product-related impurities, the results caution against the use of PAP and show the value of LC/MS as a sensitive and efficient method for process optimization and quality control of nucleic acid therapies.

Abbreviations used in this work:

- ATP – adenosine triphosphate
- CTP – cytidine triphosphate
- UTP – uridine triphosphate
- GTP – guanosine triphosphate
- A, C, U, and G nucleotides – adenosine, cytidine, uridine, and guanosine monophosphate
- Poly-A – polyadenosine
- PAP – *E. coli* Poly-A Polymerase
- RNA-seq – RNA sequencing

Experimental

In-vitro transcription of mRNA

A pCMV3 plasmid encoding a 3822 nt gene flanked by an upstream T7 promoter and a downstream BGH terminator sequence was purchased from Sino Biological. The DNA sequence was PCR amplified for 35 cycles using T7 and BGH terminator primers (Agilent Herculase II Fusion DNA Polymerase, part number 600677). After cleanup (Agilent StrataPrep PCR Purification kit, part number 400771), the amplified dsDNA was analyzed on an Agilent 2100 Bioanalyzer with a DNA 7500 kit (part number 5067-1506) to measure its concentration and to assess the uniformity of amplification. The amplified dsDNA (~13 nM) was then transcribed *in vitro* using a HiScribe T7 ARCA mRNA Kit (New England Biolabs, part number E2060S) and tailed with the included PAP enzyme using the manufacturer's recommended protocol, then precipitated with LiCl. Aliquots of transcribed mRNA before and after PAP tailing were analyzed on a 2100 Bioanalyzer with an RNA 6000

Nano kit (part number 5064-1511) to monitor the reaction.

For PAP selectivity studies, a synthetic 10-mer poly-A sequence with 5' and 3'-OH (Integrated DNA Technologies) was extended with PAP enzyme using only one precursor nucleoside triphosphate per reaction (1 mM of either ATP, CTP, UTP, or GTP) for 30 minutes at 37 °C, as illustrated in Figure 1A.

Sample preparation

Approximately twenty picomoles of poly-A tailed mRNA was digested with 1,000 U of RNase T1 for 3 hours at 37 °C to liberate poly-A sequences. Each sample was subjected to five rounds of purification using 200 µL of oligo-dT magnetic beads to pull down poly-A sequences.⁷ Each pull-down was eluted in 50 µL of 1x IDTE buffer (Integrated DNA Technologies, part number 11-05-01-05) and pooled into a final volume of 250 µL. Prior to LC/MS analysis, the pooled eluate was desalted into 60 µL of deionized water using Vivaspin 500 cartridges with 10 kDa MWCO (Sartorius, part number VS0102).

Poly-A tailing experiments

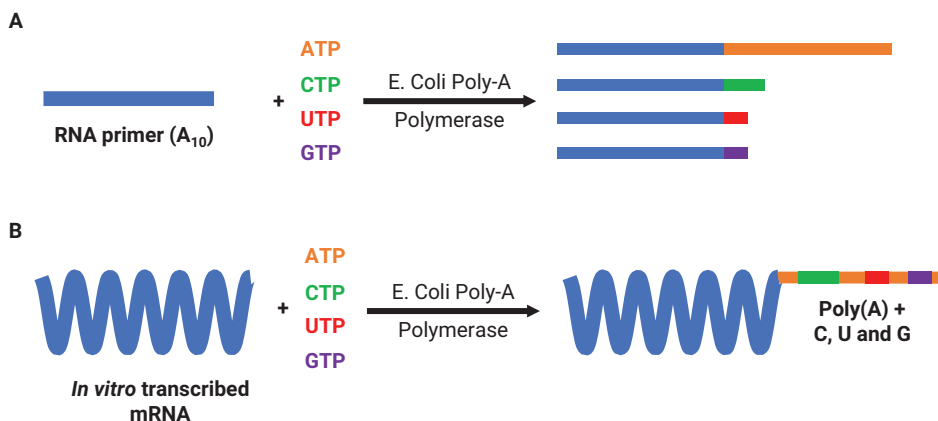


Figure 1. Schematic of tailing reactions performed in this application note. (A) Reactions on RNA primer carried out with only one precursor per reaction. (B) Reactions carried out on *in vitro* transcribed mRNA under standard conditions (all precursors).

LC-DAD/MS of poly-A sequences

Instrumentation consisted of:

- 1290 Infinity II LC with diode array detector (P/N G7117B)
- 6545XT AdvanceBio LC/Q-TOF

Care was taken to eliminate glass from the flow path to reduce alkaline metal adduction. Agilent Nalgene bottles (part number 9301-6460) were used as mobile phase containers, and each solvent line was equipped with a steel frit. Agilent polypropylene sample vials were used (part number 5190-2242). Before first use, the LC system and column were flushed with a 50% MeOH + 0.1% formic acid solution overnight to further reduce alkaline metal adducts. If required, a 30-minute flush with 50% MeOH + 0.1% formic acid was usually enough to clean the system between experiments.⁸

Poly-A sequences were separated on a PLRP-S column (2.1 × 50 mm, 5 μm, 1,000 Å, part number PL1912-1502). To achieve higher chromatographic resolution, an Infinity Poroshell 120 HPH-C18 column (2.1 × 50 mm, 1.9 μm, 120 Å, part number 699675-702) was used in PAP selectivity experiments. The mobile phase and LC gradients are shown in Table 1. The mass spectrometer was operated in negative ion mode with settings in Table 2, and data analysis was performed in BioConfirm 10.0 with deconvolution settings in Table 3.

Table 1. Mobile phase and LC gradients.

Agilent 1290 Infinity II LC System		
Column	InfinityLab Poroshell 120 HPH-C18, 1.9 μm, 2.1 × 50 mm, 120 Å	Agilent PLRP-S, 5 μm, 2.1 × 50 mm, 1,000 Å
Solvent A	15 mM dibutylamine + 25 mM HFIP in DI water	
Solvent B	15 mM dibutylamine + 25 mM HFIP in methanol	
Gradient	0 to 2 min, 15% B 12 min, 30% B 12.1 to 13 min, 90% B	0 to 1 min, 15% B 10.5 min, 45% B 10.6 to 11.5 min, 90% B
Column Temperature	50 °C	80 °C
Flow Rate	0.4 mL/min	
Injection Volume	10 to 20 μL	

Table 2. Mass spectrometer settings.

Agilent 6545XT AdvanceBio LC/Q-TOF		
	LC/MS	LC/MS/MS
Acquisition Mode	Negative, standard (3,200 <i>m/z</i>) mass range, high sensitivity (2 Ghz)	
Gas Temperature	350 °C	
Gas Flow	12 L/min	
Nebulizer	55 psig	
Sheath Gas Temperature	275 °C	
Sheath Gas Flow	10 L/min	
Vcap	4,500 V	
Nozzle Voltage	2,000 V	
Fragmentor	250 V	
Skimmer	65 V	
MS1 Range	400 to 3,200 <i>m/z</i>	
MS1 Scan Rate	2 Hz	5 Hz
MS2 Range	N/A	50 to 3,200 <i>m/z</i>
MS2 Scan Rate		3 Hz
MS2 Isolation Width		Medium (~4 amu)
Collision Energy		0, 40, 60 V
Threshold for MS2		On; 3 repeat then exclude for 0.2 min
Precursor Abundance Based Scan Speed		Yes
Target (Counts/Spectrum)		25,000
Use MS2 Accumulation Time Limit		Yes
Purity		100% stringency, 30% cutoff
Sort Precursors		By abundance only; +3, +2, +1
Reference Mass		1,033.9881

Table 3. Deconvolution settings.

Agilent MassHunter BioConfirm B10.0 Settings		
Oligonucleotide Length	≤30 nt	≥90 nt
Deconvolution Algorithm	Maximum Entropy	
Subtract Baseline	1	
Adduct	Proton loss	
Mass Range	3,000 to 10,000 Da	30,000 to 60,000 Da
Mass Step	0.05 Da	0.05 Da
Use Limited <i>m/z</i> Range	1,040 to 3,200	800 to 2,500

Results and discussion

This first test analyzed poly-A sequences extended by PAP on a synthetic RNA primer consisting of 10 repeated A nucleotides (A_{10}) in the presence of 1 mM ATP. As shown in Figure 2 this resulted in a bimodal distribution of poly-A sequences, with one population consisting of shorter oligonucleotides eluting from 2.5 to 6 minutes, and

another consisting of longer nucleotides eluting in a broad peak at ~10.6 minutes. Mass spectrometric analysis indicated the shorter population ranged in size from 11 to 22 nt (Figure 3D), whereas the longer population ranged from 108 to 149 nt in length (35,492.89 to 48,990.17 Da, Figure 4C).

Extracted and deconvoluted mass spectra from three selected peaks from the shorter oligonucleotide

population are shown in Figure 3. Mass spectra consisted primarily of doubly and triply charged ions generated through proton loss, as well as minor populations of sodium adducts. Isotopically resolved deconvoluted mass spectra were assigned identities of A_{20} , A_{21} , and A_{22} (Figures 3B to 3D) with <5 ppm error based on the respective monoisotopic peaks.

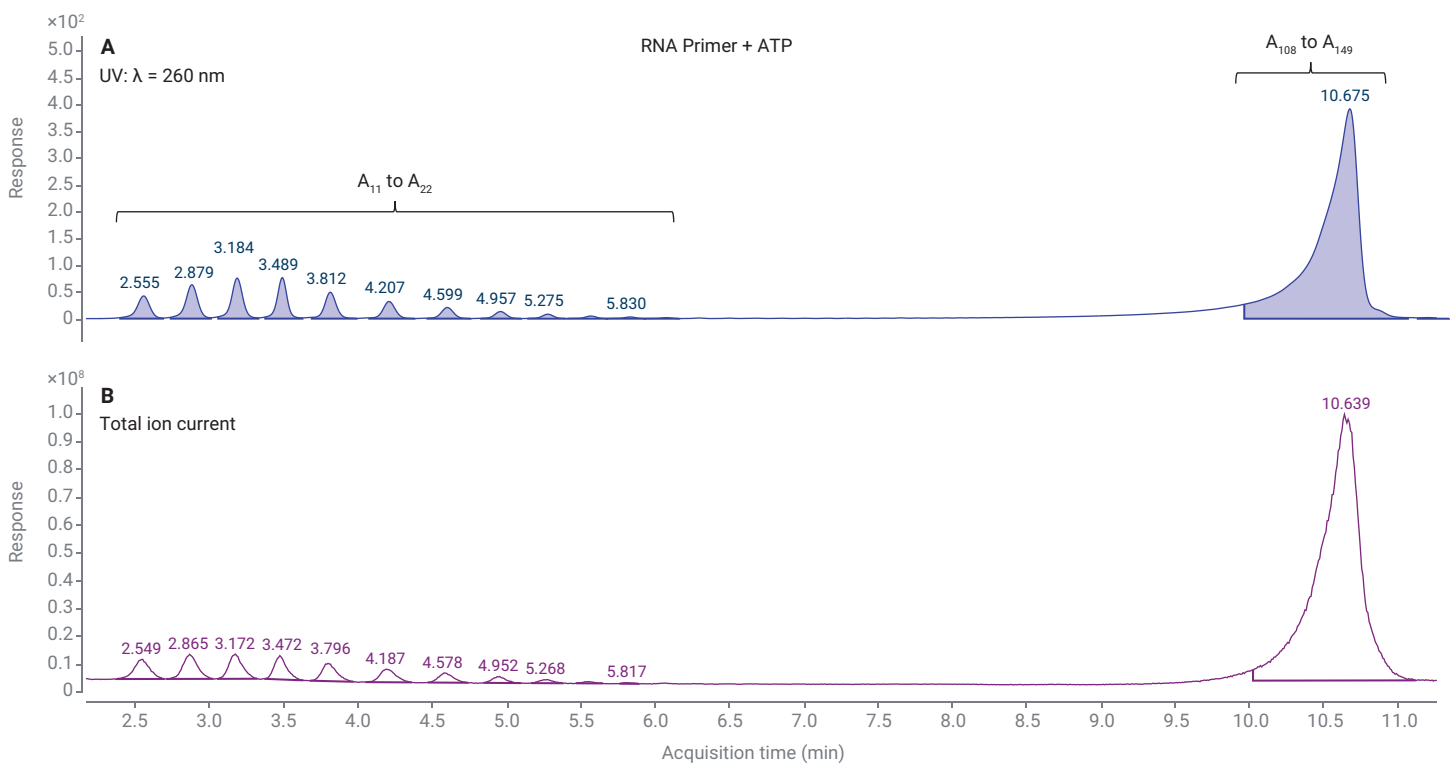


Figure 2. UV absorbance at 260 nm (A: reference = 360 nm) and total ion chromatogram (B) of RNA primers extended with PAP in the presence of only ATP. Separation was carried out on a PLRP-S column.

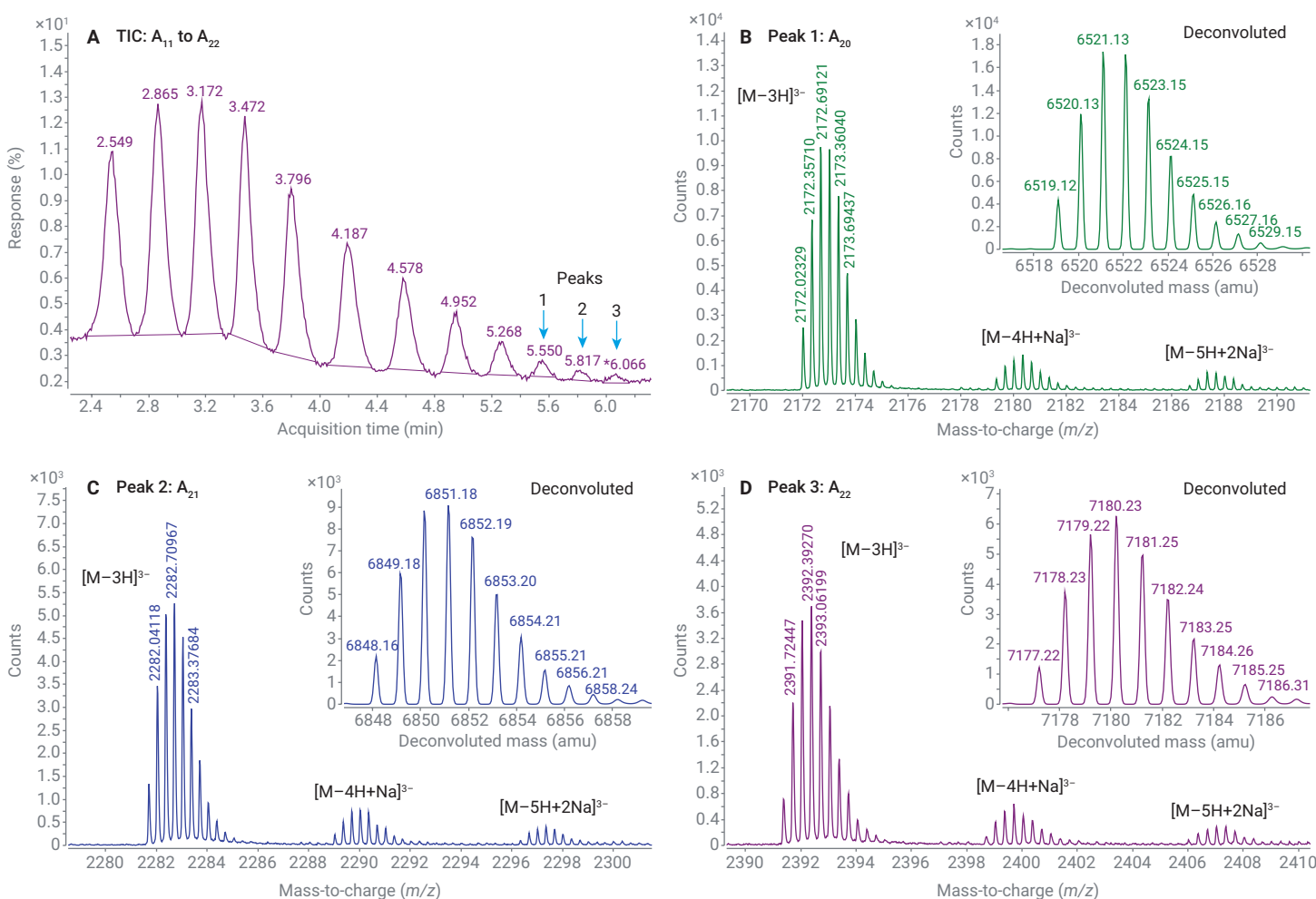


Figure 3. A₁₁ to A₂₂ oligonucleotides formed by PAP. (A) Total ion current chromatogram showing the three selected peaks with extracted mass spectra shown in (B to D). Deconvoluted mass spectra of A₂₀ ($M_{\text{obs}} = 6,519.12$ Da, $M_{\text{theo}} = 6,519.09$ Da), A₂₁ ($M_{\text{obs}} = 6,848.16$ Da, $M_{\text{theo}} = 6,848.15$ Da), and A₂₂ ($M_{\text{obs}} = 7,177.22$ Da, $M_{\text{theo}} = 7,177.20$ Da) are shown as insets. M_{obs} : observed monoisotopic mass; M_{theo} : theoretical monoisotopic mass.

A portion of the longer oligonucleotides was sampled for deconvolution (Figure 4A). The charge envelope in the extracted mass spectra from 10 to 10.3 minutes primarily fell between 800 to 2,500 m/z (Figure 4B) and was deconvoluted to a destination mass range of 30 to 60 kDa. The deconvoluted mass spectra (Figure 4C) clearly showed a heterogeneous population of sample peaks from 34 to 50 kDa, which were evenly separated by 329.2 ± 1 Da (Figure 4D). These mass increments were consistent with single additions of

A nucleotides, increasing the theoretical average mass by 329.209 Da. Table 4 shows that mass peaks in Figure 4D were confidently annotated as A₁₂₁ to A₁₃₈ with differences between theoretical and observed masses ≤ 1.16 Da.

To assess the selectivity of PAP for ATP, duplicate experiments were conducted where PAP was added to the RNA primer in the presence of only 1mM CTP, UTP, or GTP. Although the extension of long polymeric chains were not observed, chromatographically resolved

additions of up to two monomers of C nucleotides (Figure 5A) or one U nucleotide (Figure 5B) to the RNA primer, indicating that PAP was not wholly selective for ATP. The addition of guanosine monophosphate was not observed in this experiment (Figure 5C) but could not rule out the possibility that appreciable quantities might be added with longer reaction times or higher GTP concentrations. Overall, PAP showed the highest activity with ATP, followed by CTP, UTP, and GTP in descending order.

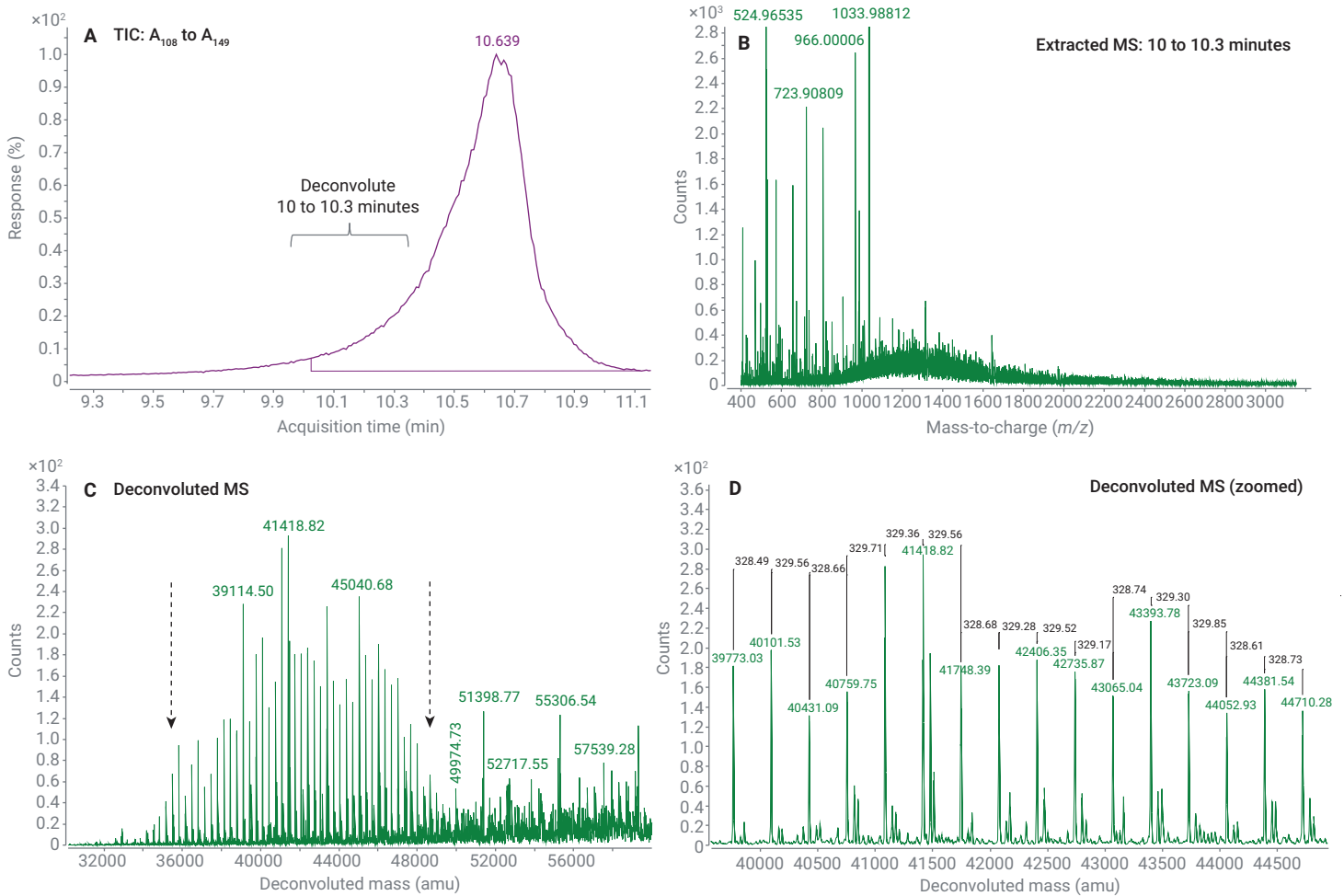


Figure 4. A_{108} to A_{149} oligonucleotides formed by PAP. (A) Total ion current chromatogram showing the region 10 to 10.3 minutes sampled for deconvolution. (B) Charge envelope and (C) Deconvoluted mass spectrum of sampled region. Dashed arrows (left = 35,492.89 Da, right = 48,990.17 Da) indicate the range of mass peaks that could be confidently assigned identities A_{108} to A_{149} . (D) Enlarged deconvoluted mass spectrum showing regular intervals between peaks from 39,773.03 to 44,710.28 Da.

Table 4. Annotated mass peaks from Figure 4D.

Oligonucleotide	Observed Mass (Da)	Theoretical Mass (Da)	Mass Difference (Da)
A_{121}	39,773.03	39,772.08	0.95
A_{122}	40,101.53	40,101.28	0.25
A_{123}	40,431.09	40,430.49	0.6
A_{124}	40,759.75	40,759.70	0.05
A_{125}	41,089.46	41,088.90	0.56
A_{126}	41,418.82	41,418.11	0.71
A_{127}	41,748.39	41,747.32	1.07
A_{128}	42,077.06	42,076.52	0.54
A_{129}	42,406.35	42,405.73	0.62
A_{130}	42,735.87	42,734.94	0.93
A_{131}	43,065.04	43,064.15	0.89
A_{132}	43,393.78	43,393.35	0.43
A_{133}	43,723.09	43,722.56	0.53
A_{134}	44,052.93	44,051.77	1.16
A_{135}	44,381.54	44,380.97	0.57
A_{136}	44,710.28	44,710.18	0.1

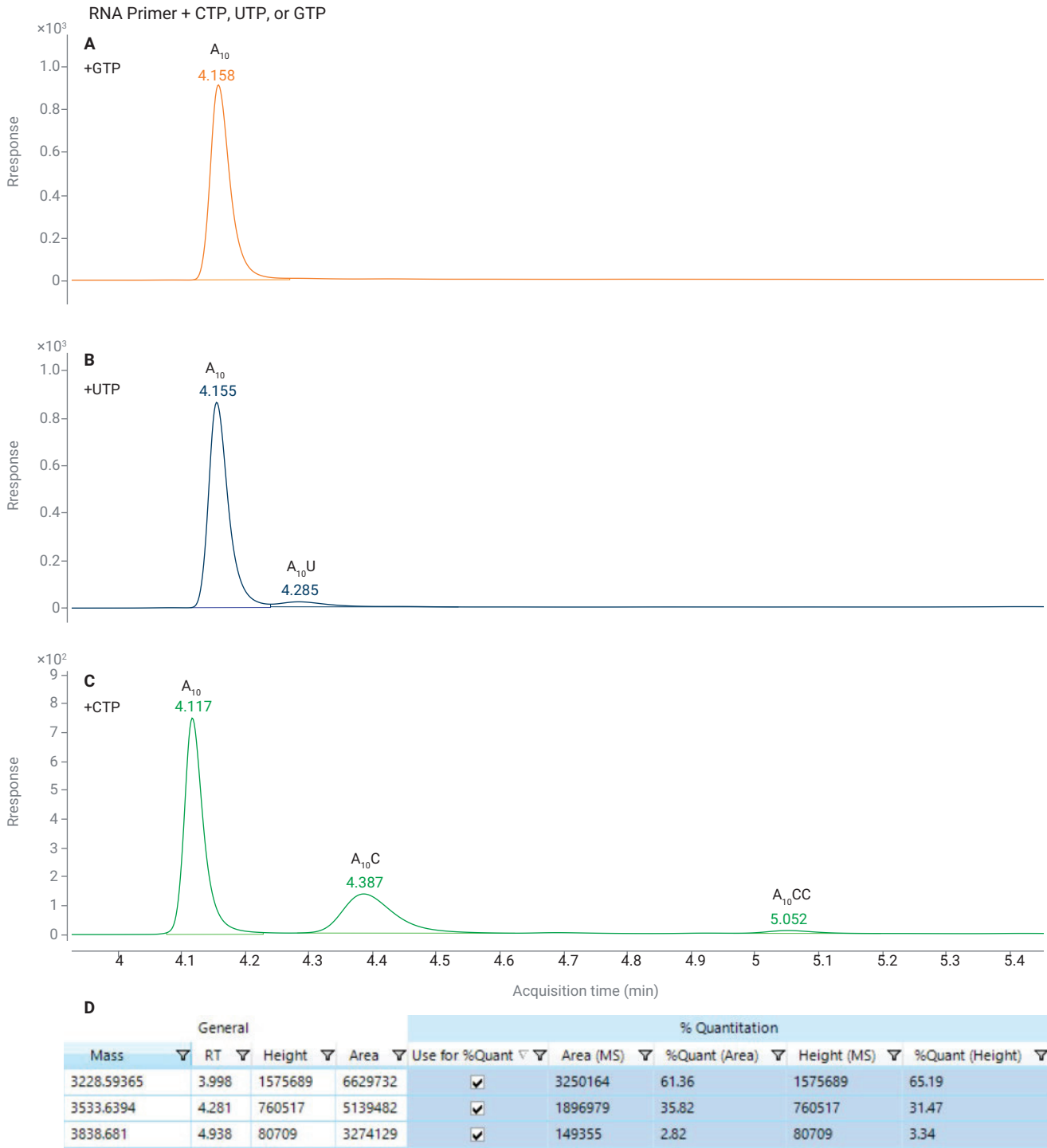


Figure 5. UV absorbance (Abs = 260 nm, Ref = 360 nm) chromatograms showing promiscuous activity of PAP towards (A) GTP, (B) UTP, and (C) CTP. No addition of guanosine monophosphate was detected. (D) Relative quantitation of A_{10} , $A_{10}C$, and $A_{10}CC$ as shown in panel (C). Separation was carried out on an Agilent Poroshell 120 HPH-C18 column.

The deconvoluted mass spectra of the unmodified RNA primer and those extended with C or U nucleotides are shown in Figure 6. Isotopically resolved deconvoluted mass spectra were assigned identities of A_{10} , $A_{10}C$, $A_{10}CC$ and $A_{10}U$ with <13 ppm error based on the respective monoisotopic peaks. MS/MS experiments showed that C

and U nucleotides were indeed added to the 3' terminus of the RNA primer (Figure 7), resulting in the formation of characteristic doubly charged y -ions 1601.271 m/z and 1601.758 m/z . In contrast, the unmodified RNA primer was terminated with a 3' A nucleotide, yielding a doubly charged y -ion 1448.749 m/z upon fragmentation.

Next, full-length, *in vitro* transcribed mRNA were analyzed on a Bioanalyzer equipped with RNA 6000 Nano kit and by LC/MS. Before tailing, transcribed mRNA showed the expected length of ~3,800 nt which increased to ~4,200 nt after reaction with PAP (Figure 8A), indicating that successful poly-A tailing had been achieved.

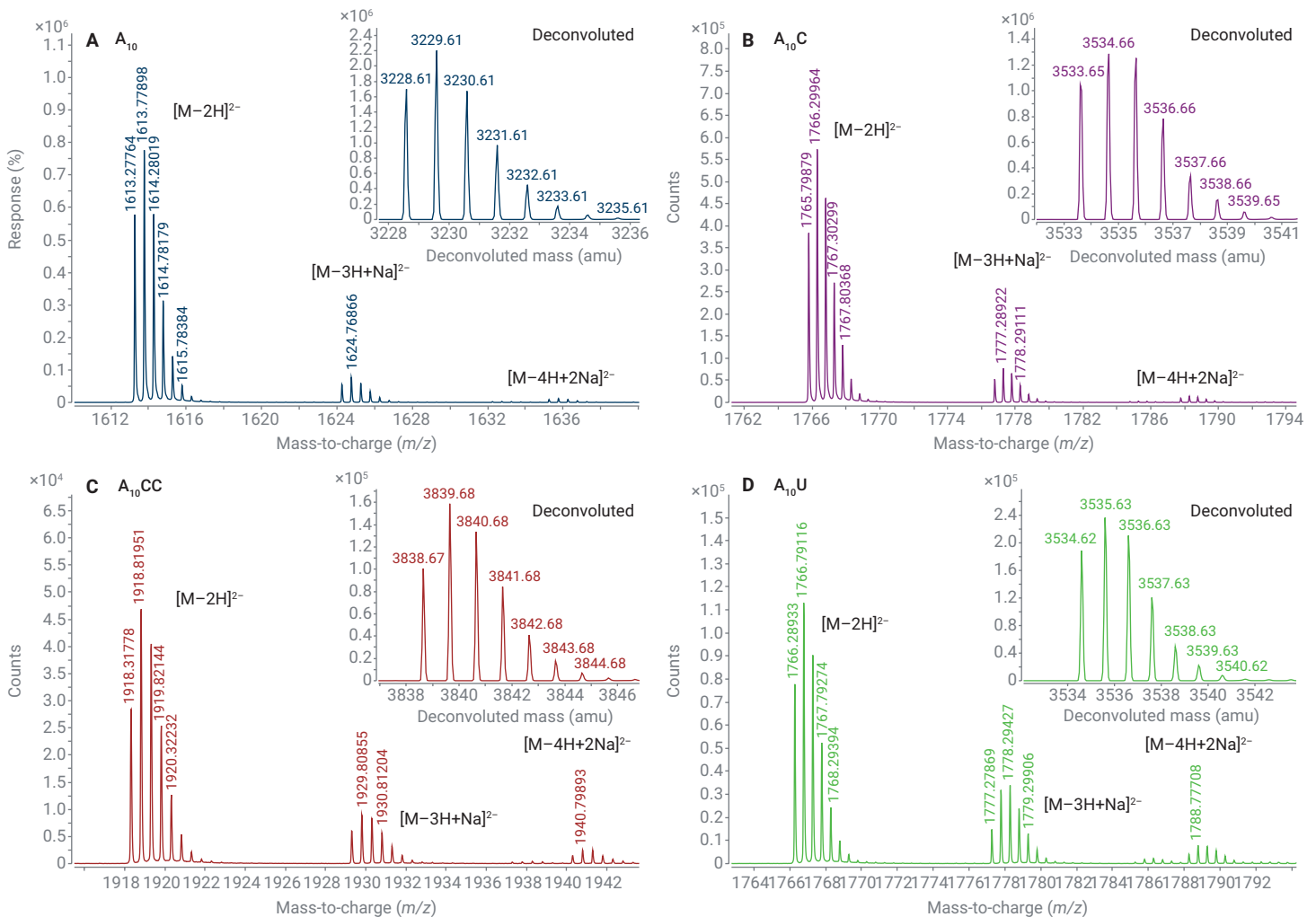


Figure 6. Extracted and deconvoluted mass spectra of (A) Unmodified A_{10} RNA primer ($M_{obs} = 3,228.61$ Da, $M_{theo} = 3,228.57$ Da), (B) Extended with one C nucleotide ($M_{obs} = 3,533.65$ Da, $M_{theo} = 3,533.61$ Da), (C) Extended with two C nucleotides ($M_{obs} = 3,838.67$ Da, $M_{theo} = 3,838.65$ Da), (D) Extended with one U nucleotide ($M_{obs} = 3,534.62$ Da, $M_{theo} = 3,534.59$ Da). M_{obs} : observed monoisotopic mass; M_{theo} : theoretical monoisotopic mass.

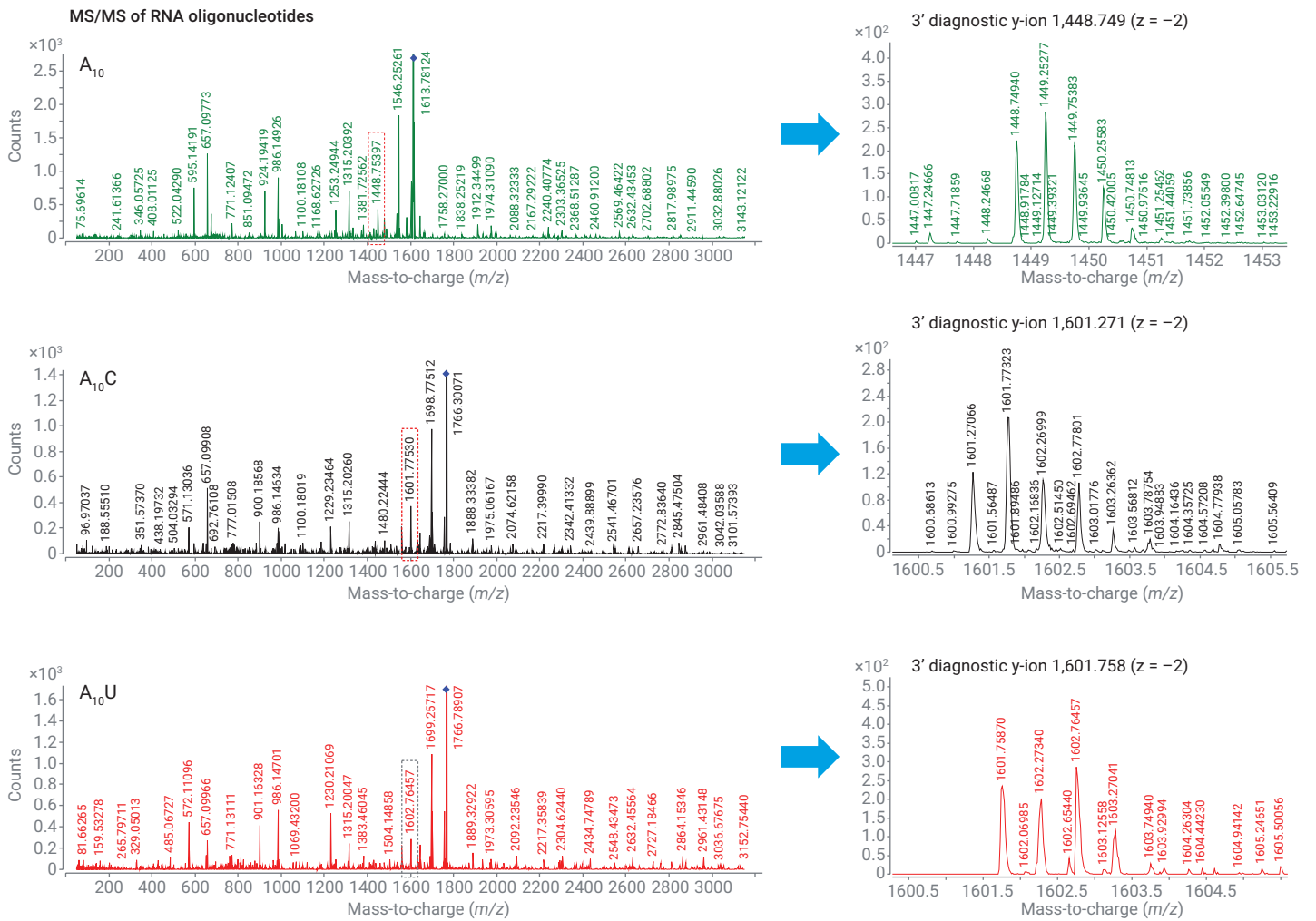


Figure 7. MS/MS of selected oligonucleotides showing diagnostic ions characteristic of their different 3' termini.

Full length mRNA samples were digested with RNase T1, followed by repeated pull-downs with oligo dT magnetic beads to yield purified tail sequences. As with PAP-extended RNA primers, tail sequences derived from *in vitro* transcribed mRNA consisted of both a shorter population of oligonucleotides eluting between 3.7 to 7.5 minutes and a longer population eluting ~10.6 minutes (Figure 8B). Extracted and deconvoluted

mass spectra from selected peaks in the shorter population revealed poly-A sequences ranging in length from 16 to 27 nt, with each containing a single misincorporated U nucleotide (Figure 9). Although not seen in this dataset, misincorporated C nucleotides were also observed in other experiments.

As noted by M. Beverly *et al.*⁷, tail sequences formed by PAP are considerably more heterogenous in

length as compared to genetically templated poly-A sequences. The results indicate that this heterogeneity is compounded by the misincorporation of differing numbers of C and U nucleotides when the tailing reaction takes place under standard conditions with all four precursor nucleoside triphosphates present, making the mass spectra of longer tail sequences very challenging to deconvolute.

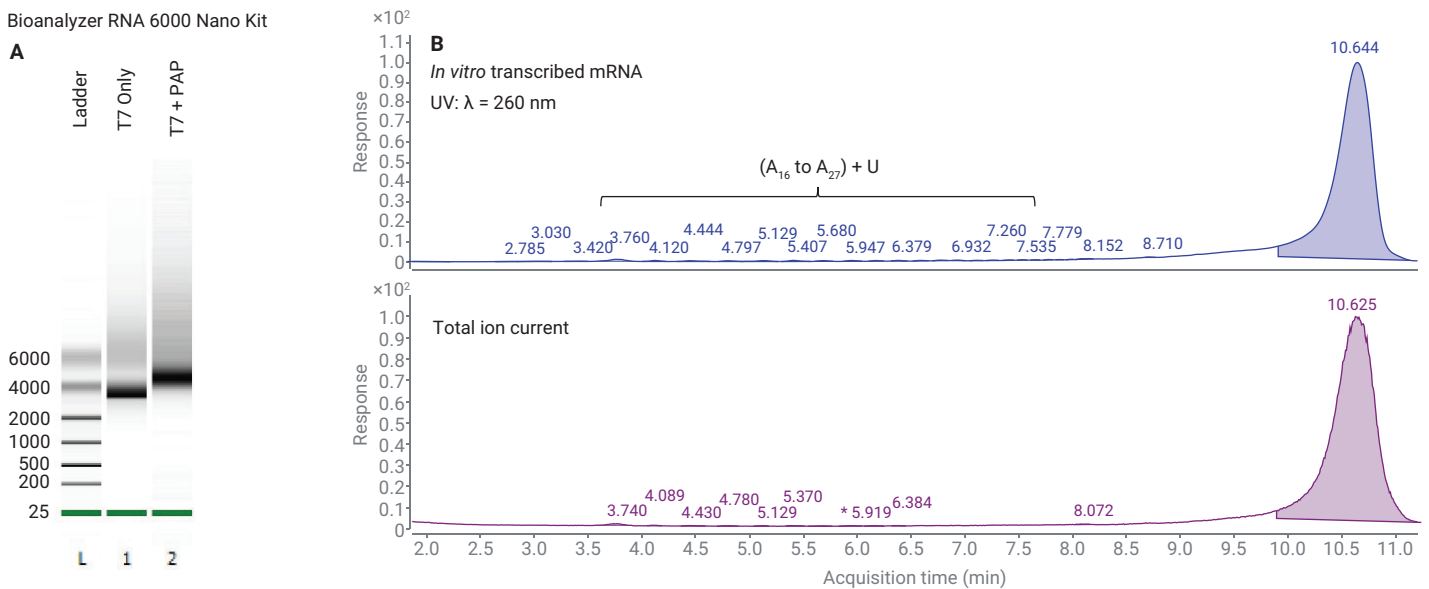


Figure 8. (A) Bioanalyzer analysis of *in vitro* transcribed mRNA before (lane 1) and after (lane 2) tailing with PAP. (B) UV absorbance at 260 nm (top panel) and total ion chromatogram (bottom panel) of poly-A sequences appended to *in vitro* transcribed mRNA in the presence of all four nucleoside phosphate precursors. Separation was carried out on a PLRP-S column.

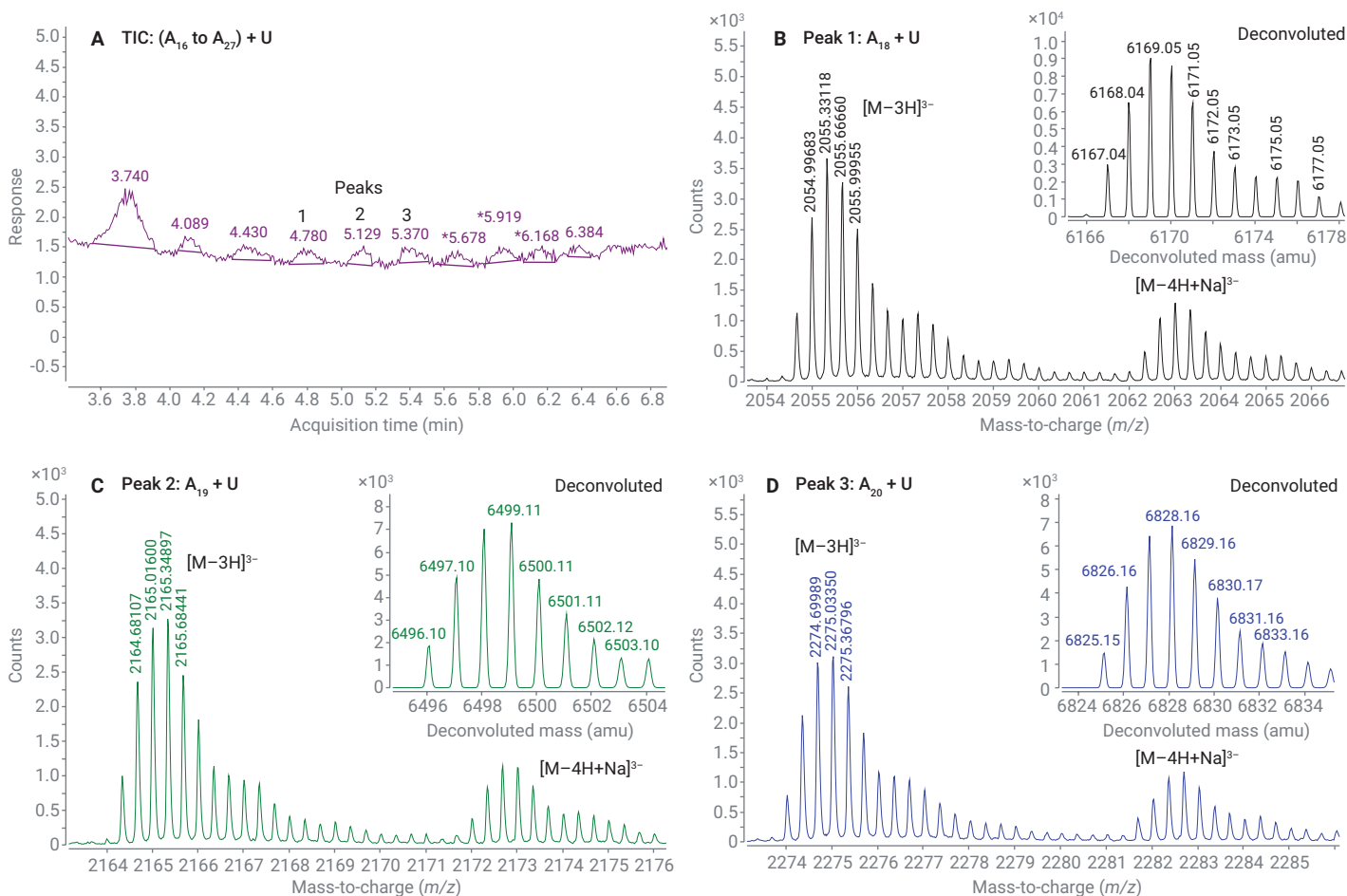


Figure 9. A_{16} to A_{27} oligonucleotides with misincorporated U nucleotide. (A) Total ion current chromatogram showing three selected peaks with extracted mass spectra shown in (B to D). Deconvoluted mass spectra of A_{18} + U ($M_{\text{obs}} = 6,167.04$ Da, $M_{\text{theo}} = 6,167.01$ Da), A_{19} + U ($M_{\text{obs}} = 6,496.10$ Da, $M_{\text{theo}} = 6,496.07$ Da), and A_{20} + U ($M_{\text{obs}} = 6,825.15$ Da, $M_{\text{theo}} = 6,825.12$ Da) are shown as insets. M_{obs} : observed monoisotopic mass; M_{theo} : theoretical monoisotopic mass.

Conclusion

This study shows that: (1) the intact masses of long (121 to 136 nt), heterogenous poly-A sequences can be accurately measured by deconvolution of their ensemble mass spectra, and (2) PAP is not fully selective for ATP under standard *in vitro* transcription conditions, causing both C and U nucleotides to be added to poly-A tail sequences.

Although these sequence variants may be inconsequential for *in vitro* studies, they are highly significant from a regulatory standpoint. Notably, other *in vitro* transcription enzymes such as T7 polymerase may also produce sequence variants through mechanisms such as slippage or transcriptional arrest⁹, underscoring the need for highly sensitive and selective methods for detecting these impurities.

To achieve such sensitivity and selectivity, one prior study demonstrated PAP's off-target activity by using radiolabeled nucleotides.¹⁰ Such techniques can be hazardous and are ill-suited for production environments. LC/MS can achieve single-nucleotide selectivity without the need for such reagents. Moreover, LC/MS can detect and quantify sequence variants without the lengthy reverse transcription, ligation and amplification steps characteristic of RNA-seq, which are known to introduce biases and artifacts.

References

1. Jackson, L. A. *et al.* An mRNA Vaccine against SARS-CoV-2 — Preliminary Report. *N. Engl. J. Med.* **2020**, 383, 1920–1931.
2. Mulligan, M. J. *et al.* Phase I/II Study of COVID-19 RNA Vaccine BNT162b1 in Adults. *Nature* **2020**, 586, 589–593.
3. Pfizer and BioNTech Announce Vaccine Candidate Against COVID-19 Achieved Success in First Interim Analysis from Phase 3 Study.
4. Promising Interim Results from Clinical Trial of NIH-Moderna COVID-19 Vaccine.
5. Wadhwa, A. *et al.* Opportunities and Challenges in the Delivery of mRNA-Based Vaccines. *Pharmaceutics* **2020**, 12, 102.
6. Kahvejian, A. *et al.* Mammalian Poly (A)-Binding Protein Is a Eukaryotic Translation Initiation Factor, Which Acts via Multiple Mechanisms. *Genes Dev.* **2005**, 19, 104–113.
7. Beverly, M.; Hagen, C.; Slack, O. Poly A Tail Length Analysis of *In Vitro* Transcribed mRNA by LC/MS. *Anal. Bioanal. Chem.* **2018**, 410, 1667–1677.
8. Birdsall, R. E. *et al.* Reduction of Metal Adducts in Oligonucleotide Mass Spectra in Ion-Pair Reversed-Phase Chromatography/Mass Spectrometry Analysis. *Rapid Commun. Mass Spectrom.* **2016**, 30, 1667–1679.
9. Tateishi-Karimata, H.; Isono, N.; Sugimoto, N. New Insights into Transcription Fidelity: Thermal Stability of Non-Canonical Structures in Template DNA Regulates Transcriptional Arrest, Pause, and Slippage. *PLOS ONE* **2014**, 9.
10. Yehudai-Resheff, S.; Schuster, G. Characterization of the E.Coli Poly(A) Polymerase: Nucleotide Specificity, RNA-Binding Affinities and RNA Structure Dependence. *Nucleic Acids Res.* **2000**, 28, 1139–1144.

www.agilent.com/chem

For Research Use Only. Not for use in diagnostic procedures.

RA44231.5456365741

This information is subject to change without notice.

© Agilent Technologies, Inc. 2021
Printed in the USA, March 8, 2021
5994-3005EN

Analyzing Poly(A) Tails of In Vitro Transcribed RNA with the Agilent Fragment Analyzer System

Authors

Lisa Houston and
Whitney Pike,
Agilent Technologies, Inc.

Abstract

Poly(A) tails are important for the process of mRNA translation. The length of a poly(A) tail has been shown to affect translation efficiency and the rate of mRNA degradation. Therefore, confirming the expected or optimal length of the poly(A) tail is important for research including in vitro transcribed (IVT) RNA. Agilent Fragment Analyzer systems provide efficient, cost-effective, and consistent analysis of nucleic acids. This application note describes the procedures necessary to obtain reliable sizing for poly(A) tails using the Fragment Analyzer.

Introduction

An important component of mRNA is the poly(A) tail. Poly(A) tails are composed of multiple adenine nucleotides added to the 3' end of mRNA. Research has shown that the length of the poly(A) tails helps minimize mRNA degradation and plays a key role in translation¹. Poly(A) tails are found in various lengths from 20 nt to over 200 nt². The length of the poly(A) tail contributes to mRNA stability and protein expression^{1,2}.

Poly(A) tails can be added to in vitro transcribed (IVT) RNA and are critical for IVT RNA used in therapeutics. There are two ways to add poly(A) tails to IVT RNA, either as part of the IVT RNA template or enzymatically, with a recombinant poly(A) polymerase. Poly(A) tails added as part of the IVT RNA template produce poly(A) tails of specific, known lengths. However, tails greater than 30 nt in length are difficult to synthesize since long poly(A) sequences cause polymerases to slip. Poly(A) enzymes can quickly add a poly(A) tail longer than 100 nucleotides. The length of a poly(A) generated with poly(A) enzyme is varied and undefined. Changing the amount of enzyme, ATP, reaction time, or concentration of RNA can alter the length of the final poly(A) tail.

Analyzing the size and quality of a poly(A) tail is a critical part of the IVT RNA workflow since the length of a poly(A) tail affects mRNA stability and influences translation efficiency. There are several techniques for poly(A) quality control (QC), including next-generation sequencing (NGS), chromatography, mass spectrometry (MS), and gel electrophoresis methods^{1,2}. However, even with these techniques it is challenging to accurately analyze the length of poly(A) tails. Most of these methods are labor intensive, require large amounts of RNA, are time consuming, or expensive². Additionally, each technique varies in accuracy².

An alternative method to accurately assess poly(A) tails is the Agilent 5200 Fragment Analyzer system. In this application note, template and enzymatically added poly(A) tails were analyzed on the Fragment Analyzer system with the Agilent Small RNA kit. This application note demonstrates that the Fragment Analyzer system can quickly, cost-effectively, and reliably analyze the size and quality of poly(A) sequences.

Experimental

The experiments in this study were performed using the Agilent 5200 Fragment Analyzer system and can be replicated on the Agilent 5300 and 5400 Fragment Analyzer systems.

Poly(A) tail samples

Three poly(A) tail samples were analyzed in this experiment (Table 1). Sample 1, generated from IVT RNA, synthesized from a plasmid borne DNA template, has a 30 nt poly(A) tail. Cleaving the IVT RNA with T1 RNase (described below) at the G nucleotide, just before the poly(A) sequence, generates a 31 nt fragment. Figure 1A illustrates the workflow to generate sample 1.

Sample 2 was generated by enzymatically adding a poly(A) tail to IVT RNA, derived from a 2,055 bp PCR amplified DNA template. Cleaving the IVT RNA with T1 RNase produces a nonuniform poly(A) fragment, expected to be smaller than 200 nt. Figure 1B illustrates the workflow to generate sample 2. Additionally, an RNA oligo control, which consists of a single G followed by a 30 nt poly(A) sequence, was analyzed as a known standard for sample 1.

Table 1. Description of the samples used in this application note.

Sample	Size (nt)	DNA Template	Poly(A) Source
1	31	Plasmid	Template
2	Smear	PCR Amplified	Enzymatic
Control	31	NA	Oligo

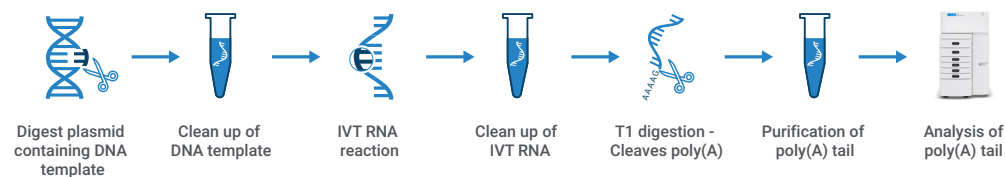
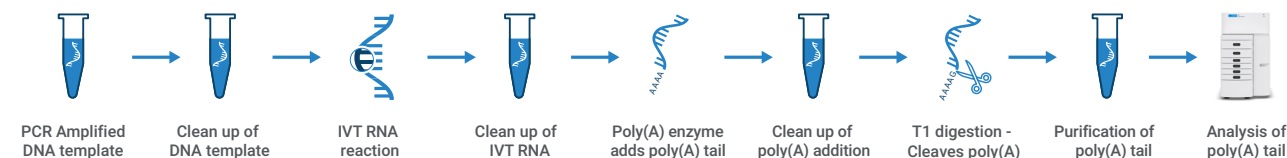
A) Sample 1 workflow**B) Sample 2 workflow**

Figure 1. Schematic of the workflows used to generate IVT RNA with poly(A) tails from A) a DNA plasmid template (sample 1) or B) enzymatically added (sample 2).

DNA templates

A pT7CFE1-NHis-GST-CHA vector (Thermo Fisher Scientific p/n 88871) was digested with *SpeI* (NEB p/n R3133S) to prepare a DNA template with a 30 nt poly(A) sequence for sample 1. For sample 2, a 2,055 bp DNA template lacking a poly(A) sequence was prepared from PCR amplification of Lambda DNA (Thermo Fisher Scientific p/n SD0021), with Phusion High-Fidelity DNA polymerase (Thermo Fisher Scientific p/n F530S) and appropriate primers (IDT). Both the *SpeI* digested vector and PCR amplified templates were isolated with NucleoSpin Gel and PCR Clean up (Takara Bio p/n 740609.50) following standard protocols³.

IVT RNA

IVT RNA was generated from the DNA templates using T7 RiboMAX express

(Promega p/n P1320) following the manufacturer's instructions⁴. DNA templates were removed using the provided RQ1 RNase-Free DNase, followed by purification with the Zymo RNA Clean & Concentrator-5 kit (p/n R1013) using standard procedures⁵.

Poly(A) tail synthesis

Poly(A) tails were added to IVT RNA generated from the 2,055 bp PCR amplified DNA template (sample 2) with *E. coli* Poly(A) polymerase (NEB p/n M0276S) following the manufacturer's instructions⁶. The poly(A) IVT RNA was purified with the Zymo RNA Clean & Concentrator-5 kit and standard procedures⁵.

T1 RNase digestion

IVT RNA containing poly(A) sequences were digested with RNase T1 (Thermo Fisher Scientific p/n EN0541), which cleaves RNA at G nucleotides. Each reaction contained 200 U of RNase T1

for each ug of RNA in 1x RNase H reaction buffer (NEB p/n M0297S). The reactions were incubated at 37 °C for 3 hours.

Poly(A) purification and analysis

Immediately following T1 digestion, the poly(A) tails for both sample 1 and sample 2, as well as a 31 nt RNA oligo control were purified using Invitrogen Dynabeads mRNA purification kit (Thermo Fisher Scientific p/n 61-006), following standard protocols⁷. The poly(A) sequences were eluted with 10 mM Tris-HCl at 80 °C for 2 minutes following the kit protocol. The eluates were diluted with nuclease-free water and immediately analyzed on the Agilent 5200 Fragment Analyzer system with the Agilent Small RNA kit (p/n DNF-470-0275).

Results and discussion

The Fragment Analyzer is an automated capillary electrophoresis instrument used for quality control of nucleic acids, including IVT RNA. The Fragment Analyzer generates an electropherogram and digital gel image. Electropherograms can display either a single peak or a smear. A single peak indicates that the sample is uniform in size. A smear is likely the result of several differently sized fragments being displayed together, generating an elongated image and indicating that the sample is not of uniform size. Since fragments and smears yield different separation profiles during electrophoresis, poly(A) tail samples were generated both from a DNA template to yield a poly(A) fragment (sample 1), and with poly(A) enzyme to yield a smear (sample 2). Both samples were analyzed on the 5200 Fragment Analyzer system with the Small RNA kit to demonstrate the difference between the two sample types.

Sample 1, a 31 nt poly(A) tail, produced a single peak (Figure 2A). Sample 1 measured slightly larger than the expected size of 31 nt. Moreover, the sample had little variation between replicates, with approximately 2.0% CV (n=3).

Sample 2, an enzymatically added poly(A) tail, displayed a smear less than 200 nt in length (Figure 2B). A smear analysis was generated using the Agilent Fragment Analyzer ProSize data analysis software. A smear size range was set from 25 to 130 nt to encompass the entire smear. As shown in Figure 2B, the smear is widespread, spanning from approximately 25 to 130 nt, with a larger peak at 59 nt, and a large portion of the smear sloping downwards from the peak towards the right. Triplicate analysis of the sample resulted in an average smear size of 76 nt (n=3).

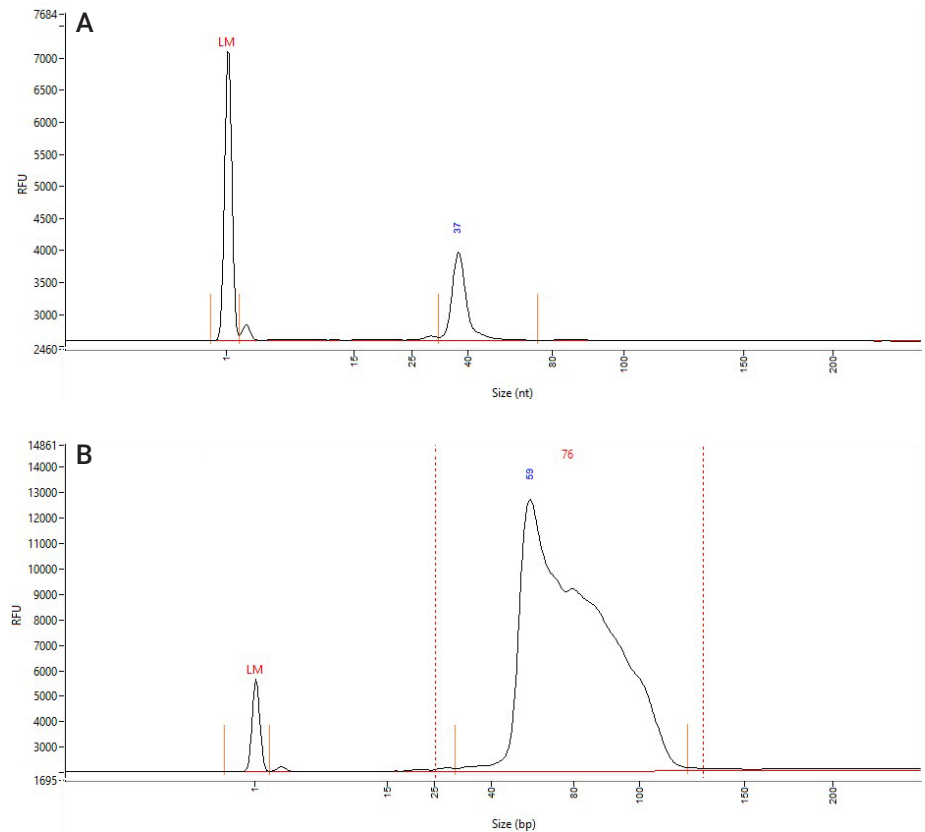


Figure 2. The Agilent Fragment Analyzer system was used to analyze IVT RNA poly(A) tails. Shown are the electropherograms of (A) sample 1, a template derived 31 nt poly(A) tail which is displayed as a fragment, and (B) sample 2, an enzymatically added poly(A) tail which appears as more of a smear. Red dotted lines indicate smear region.

Size analysis using a standard

An established method for determining if the length of a given sample represents the expected size is to compare the sample poly(A) tail length to the observed length of a standard poly(A) tail of a known size. An RNA oligo was designed with a G nucleotide followed by 30 A nucleotides to use as a standard, which the poly(A) fragment (sample 1) could be compared to. The poly(A) fragment displayed an average size of approximately 38 nt and the control displayed an average size of 37 nt (Table 2 and Figure 3), indicating that sample 1 is the same size as the control, as expected.

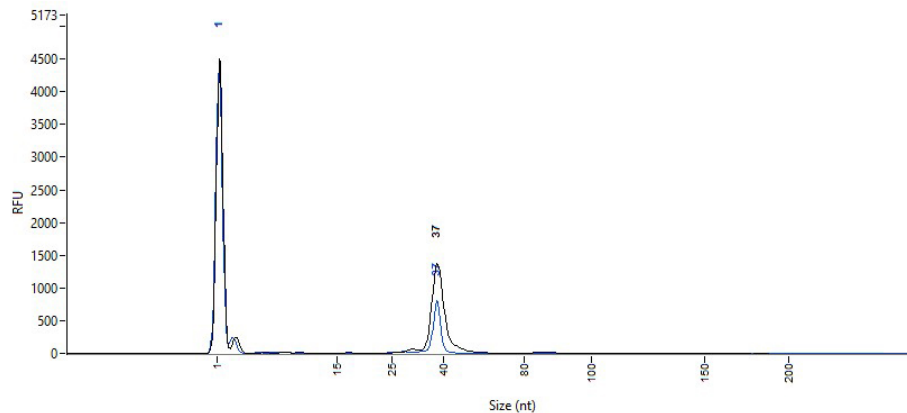


Figure 3. Comparison of representative electropherograms from sample 1, the 31 nt poly(A) tail (black), and a 31 nt poly(A) oligo control (blue) were analyzed on the Agilent Fragment Analyzer system. An overlay of the electropherograms indicates that the samples are the same size (37.7 and 37 nt, respectively) (n=3).

Table 2. Size comparison of sample 1, a 31 nt poly(A) tail, and a 31 nt oligo standard (n=3).

Sample	Average Size (nt)	%CV
1	37.7	1.25%
Control	37	0.00%

Sample salt concentration

In gel electrophoresis, the accuracy of sizing can be affected by the salt concentration of the samples⁹. The standard protocol for eluting mRNA from the Dynabeads mRNA purification kit uses 10 mM Tris-HCl⁷. To evaluate the effects of salt concentration on the poly(A) tail sizing, the oligo standard was eluted with different concentrations of Tris-HCl: 10 mM, 1 mM, 0.1 mM and no Tris-HCl (nuclease-free water). Each elution was diluted to a ratio of 1 μ L of sample to 3 μ L of nuclease-free water before analysis on the Fragment Analyzer. Regardless of the elution type, the poly(A) oligo displayed sizes between 35 and 39 nt (Figure 4).

The concentration of Tris-HCl in the elution buffer affected the observed size of the poly(A) fragment (Table 3). The 1 mM and 0.1 mM Tris-HCl samples yielded sizes of 35 and 36 nt, respectively. The 10 mM Tris-HCl and nuclease-free water samples yielded sizes of 37 and 38 nt, respectively. These results indicate that minimal amounts of Tris-HCl are required to achieve the most accurate sizing when analyzing poly(A) tails on the Fragment Analyzer.

Table 3. Aliquots of the control sample were purified with 10 mM, 1 mM, and 0.1 mM Tris-HCl elution buffer, and nuclease-free water. The samples were analyzed on the Agilent 5200 Fragment Analyzer system with the Small RNA kit. The 1 mM Tris-HCl elution displayed a size within 15% of the expected size.

	10 mM Tris-HCl	1 mM Tris-HCl	0.1 mM Tris-HCl	Nuclease-Free Water
Size (nt)	37	35	36	38
%CV	0.0	0.01	0.0	0.01
%Error	19.4%	13.8%	16.1%	23.7%

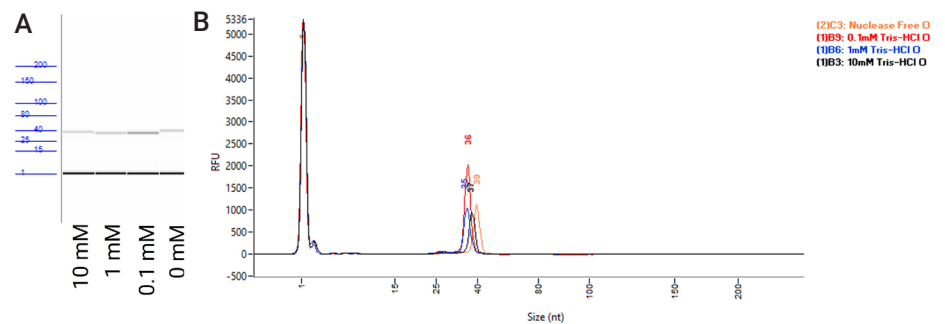


Figure 4. Analysis of Tris-HCl elution buffer dilution series. The oligo standard was eluted in various dilutions of Tris-HCl (10 mM (black), 1 mM (blue), 0.1 mM (red)) and nuclease-free water (orange) and analyzed with the Agilent Fragment Analyzer systems. A) The digital gel image of the representative samples for each dilution and B) the electropherogram overlay of the representative samples of each dilution. Examination of the results indicates that the samples eluted with the 1 mM and 0.1 mM Tris-HCl display more accurate sizing than those eluted with 10 mM Tris-HCl or nuclease-free water.

Conclusions

Analyzing the length of poly(A) tails is an important part of IVT RNA workflows where efficient gene expression is required. Typical methods of poly(A) analysis, such as qPCR and MS, are time consuming and expensive. The Fragment Analyzer system with the Small RNA kit is a cost-effective, efficient, and reliable way to determine the length of poly(A) sequences. This application note demonstrates that the Agilent Fragment Analyzer systems can accurately and reliably separate and analyze poly(A) tails from IVT RNA fragments.

Reference

1. Jalkanen, A.; Coleman, S.; Wilusz, J. Determinants and implications of mRNA poly(A) tail size – Does this protein make my tail look big? *Semin Cell Dev Biol.* **2014**, *34*, 24-32.
2. Beverly, M.; Hagen, C.; Slack, O. Poly A tail length analysis of in vitro transcribed mRNA by LC-MS. *Analytical and Bioanalytical Chemistry.* **2018**, *410*, 1667-1677.
3. NucleoSpin Gel and PCR Clean-Up, *Takara Bio user manual*, product number A019950/0797.5, **2017**.
4. T7 Ribomax Express Large Scale RNA Production System. *Promega technical bulletin*, product number TB298, **2019**.
5. RNA Clean & Concentrator-5, *Zymo instruction manual*, version 2.2.1.
6. Poly(A) tailing of RNA using E. coli poly(a) polymerase (NEB# M0276). <https://www.neb.com/protocols/2014/08/13/poly-a-tailing-of-rna-using-e-coli-poly-a-polymerase-neb-m0276> (accessed May 1, 2022).
7. Dynabeads mRNA Purification Kit, *Invitrogen user manual*, product number MAN0015808, **2016**.
8. Shihabi, Z. Effect of sample composition on electrophoretic migration: Application to hemoglobin analysis by capillary electrophoresis and agarose electrophoresis. *J. Chromatog A.* **2004**, *1027*, 179-184.

www.agilent.com

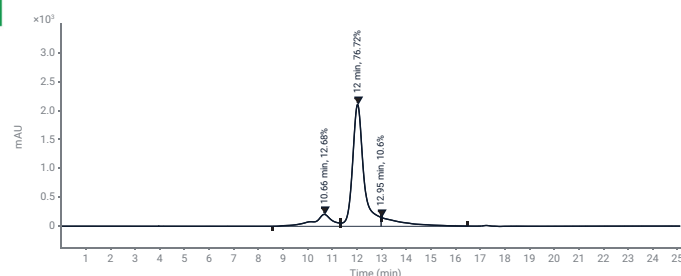
For Research Use Only. Not for use in diagnostic procedures.
PR7000-9015

This information is subject to change without notice.

© Agilent Technologies, Inc. 2022
Published in the USA, September 13, 2022
5994-5325EN

Aggregate Analysis of mRNA Using the Agilent Infinity II Bio LC System and Bio-SEC Columns

mRNA aggregation by SEC-HPLC – USP analytical procedures for mRNA vaccine quality



Author

Chae-Young Ryu
Agilent Technologies, Inc.

Abstract

The United States Pharmacopeia (USP) has proposed quality evaluation methods for managing key quality attributes of mRNA production processes through the Analytical Procedures for mRNA Vaccine Quality Draft guidelines, second edition.¹ The guidelines introduce methods for analyzing mRNA aggregates and provide respective test methods for mRNA drug substances and mRNA drug products. This application note investigates the impact of column and mobile phase selection on the analysis of mRNA aggregates to assess their cohesiveness.

Introduction

mRNA can form secondary structures based on complementary binding between nucleotides, or exist in the form of aggregates. These secondary structures and aggregates not only act as interfering factors that can disrupt the translation of RNA into proteins^{2,3}, but may also impact the efficiency of formulation into lipid nanoparticles⁴. Therefore, the management of mRNA aggregates is considered a crucial quality assessment criterion from both formulation and efficacy perspectives.

Under low-pH environments, especially below pH 7, nucleic acids can undergo hydrolysis. Thus, for mRNA vaccine production, an appropriate buffering system must be chosen to maintain stability. While phosphate buffers are commonly used in the manufacturing of biopharmaceuticals, concerns arise about potential pH changes at lower temperatures. This is a particular consideration for the typical storage conditions of mRNA vaccines, which involve freezing. Moreover, magnesium (Mg^{2+}) or calcium (Ca^{2+}) ions participate in enzyme-mediated cleavage of mRNA, and the inclusion of EDTA in the mobile phase aids in stabilizing mRNA.⁴

The analytical method for mRNA drug substances, as suggested by USP guidelines, employs a mobile phase with a 150 mM phosphate buffer. In contrast, the method for analyzing mRNA drug products suggests a mobile phase with a 100 mM Tris acetate/2.5 mM EDTA buffer. Under these conditions, considering the influence of salt concentrations in the mobile phase and nucleotide – stainless steel interactions, the evaluation of aggregates requires the use of HPLC with biocompatible materials. Therefore, in this study, the Agilent 1290 Infinity II Bio LC System was used to assess the impact of mobile phase and column selection on the analysis of mRNA aggregates.

Methods

Standards and reagents

The sodium phosphate monobasic, sodium phosphate dibasic, and 10x TAE buffer used in the experiment were purchased from Sigma-Aldrich.

The 100 bp DNA ladder and 1 kbp DNA ladder were purchased from Thermo Fisher. Poly(A) (average length 4,831 nucleotides) was purchased from Sigma-Aldrich, CleanCap FLuc mRNA (ORF 1,929 nucleotides, UTR 261 nucleotides) and CleanCap β -galactosidase mRNA (ORF 3420) were purchased from TriLink, and mRNA samples 1 and 2 were provided by the customer.

Instruments

- Agilent 1290 Infinity II Bio High-Speed Pump (G7132A)
- Agilent 1290 Infinity II Bio Multisampler (G7137A) with sample thermostat
- Agilent 1290 Infinity II Multicolumn Thermostat (G7116B) with Agilent InfinityLab Bio-Inert Quick Connect heat exchanger (G7116-60071)
- Agilent 1290 Infinity II Diode Array Detector (G7117B) with Bio-Inert Max-Light cartridge cell, 60 mm (G5615-60017)

Columns

- Agilent Bio SEC-5 500Å, 7.8 × 300 mm, 5 μ m (part number 5190-2531)
- Agilent Bio SEC-5 1000Å, 7.8 × 300 mm, 5 μ m (part number 5190-2536)
- Agilent Bio SEC-5 2000Å, 7.8 × 300 mm, 5 μ m (part number 5190-2541)

Software

Agilent OpenLab CDS, version 2.7

Mobile phases

150 mM phosphate buffer (pH 7.0) was prepared by dissolving 6.32 grams of sodium phosphate monobasic and 13.8 grams of sodium hydrogen phosphate dibasic in water, and adjusting the volume to 1 L. Additionally, 100 mM Tris acetate/2.5 mM EDTA buffer was prepared by mixing 250 mL of 10x TAE buffer with 750 mL of water and adjusting the volume to 1 L.

Methods

Table 1. Phosphate buffer HPLC analytical conditions.

Parameter	Value
Flow Rate	0.6 mL/min
Column Temperature	25 °C
Injection Volume	5 µL
Sampler Temperature	4 °C
Detector	UV 260 nm
Mobile Phase	150 mM Phosphate buffer
Analysis Time	25 min

Table 2. 100 mM Tris acetate/2.5mM EDTA HPLC analytical conditions.

Parameter	Value
Flow Rate	0.6 mL/min
Column Temperature	40 °C
Injection Volume	5 µL
Sampler Temperature	4 °C
Detector	UV 260 nm
Mobile Phase	100 mM Tris acetate/2.5 mM EDTA
Analysis Time	25 min

Results and discussion

Using the 150 mM phosphate buffer suggested as an aggregate analysis method (Table 1) for mRNA drug substances in the USP mRNA guidelines, the 100 bp DNA ladder and poly(A) (1 mg/mL) were analyzed under SEC-5 500Å, 1000Å, and 2000Å column conditions, respectively. Variations in the resolution of peaks derived from the DNA ladder were observed, depending on the pore size of the column. Additionally, by performing the test on the peak distribution of poly(A), the effective retention time range for SEC was inferred. For mRNA corresponding to DNA sizes less than 300 bp, the 500Å condition was found to be suitable, while mRNA with sizes less than 1,000 bp required the 1000Å condition, and relatively large mRNA corresponding to 2,000 bp was well-suited for the 2000Å column (Figure 1).

On the other hand, using the same standard solution and column with 100 mM Tris acetate/2.5 mM EDTA as the mobile phase (Table 2), the chromatogram obtained appears as follows: compared to the 150 mM phosphate buffer, there was no significant difference in chromatogram patterns, but it was observed that the elution time was slightly shortened and the average molecular weight of each peak was larger (Figure 2).

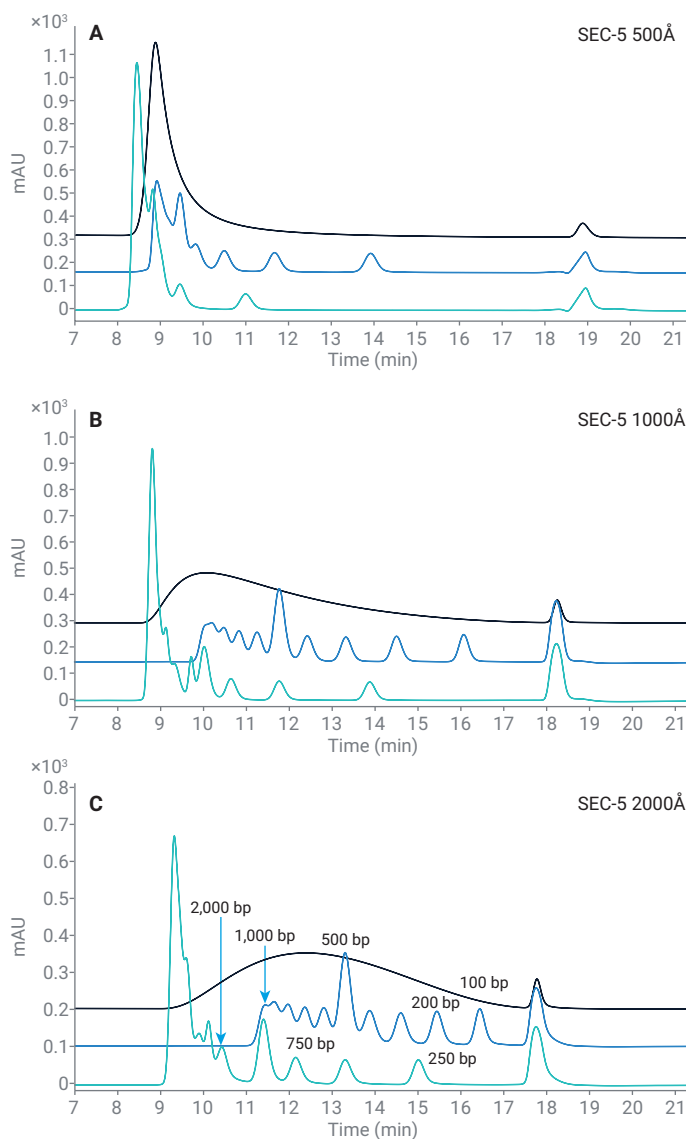


Figure 1. Chromatograms of (A) poly(A), (B) 100 bp DNA ladder, and (C) 1 kbp DNA ladder by column dimension under 150 mM phosphate buffer conditions (poly(A) (black), 100 bp DNA ladder (blue), and 1 kbp DNA ladder (green) from the top down in each chromatogram).

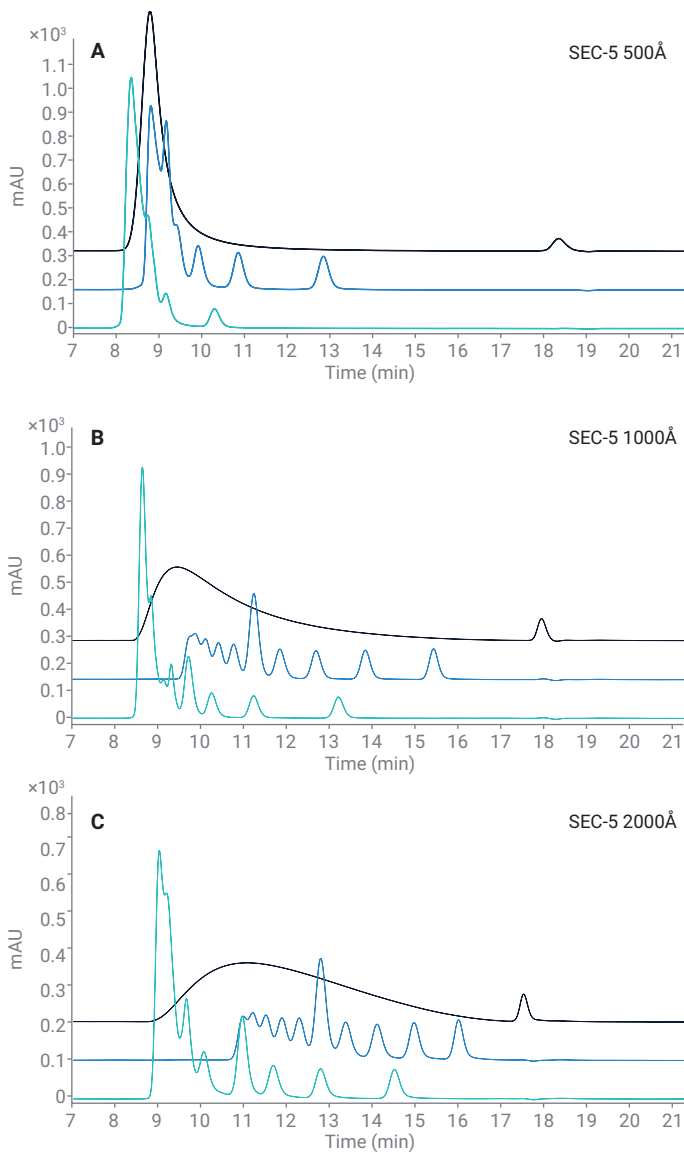


Figure 2. Chromatograms of (A) poly(A), (B) 100 bp DNA ladder, and (C) 1 kbp DNA ladder under 100 mM Tris acetate/2.5 mM EDTA conditions and various column pore sizes (poly(A) (black), 100 bp DNA ladder (blue), and 1 kbp DNA ladder (green) from the top down in each chromatogram).

However, for the evaluation of mRNA aggregates, column selection must also consider the size of the aggregates. Approximately 2,000 nt of CleanCap FLuc mRNA was analyzed under each condition, and the results were compared. The column calibration information from the OpenLab CDS 2.7 GPC add-on was used to estimate the size of mRNA by converting it based on the number of base pairs in the DNA ladder. When comparing the size using the 100 bp DNA ladder and 1 kbp DNA ladder as references, the peak value corresponded to a size of 422 bp (Figures 3 and 4). It was observed that not only the target mRNA, but also the peak fronting corresponding to aggregates were all encompassed within the range of the column.

Double-stranded DNA has a relatively simple three-dimensional structure, forming a long linear structure through complementary binding, while single-stranded RNA, representing a complex three-dimensional structure, exhibits secondary structures through localized complementary binding. The retention time based on molecular size in size exclusion chromatography is directly influenced by the hydrodynamic radius (Rh), and the branching structure of RNA due to complementary binding affects Rh. Therefore, the elution time of single-stranded RNA may vary based on the structure of RNA compared to dsDNA. Furthermore, the diversity of secondary structures and the length distribution of poly(A) contribute to the characteristic of having a broad peak width.

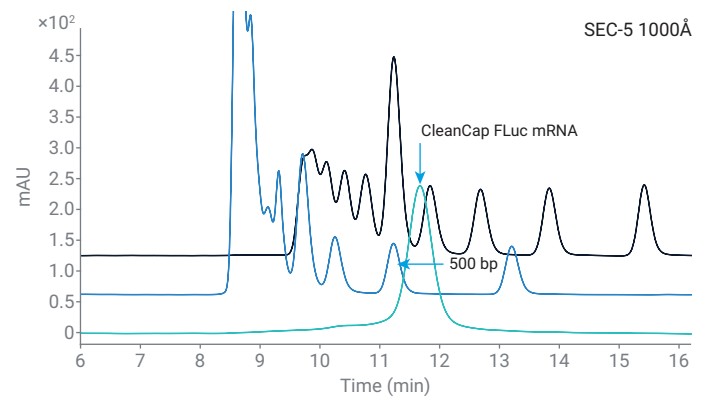
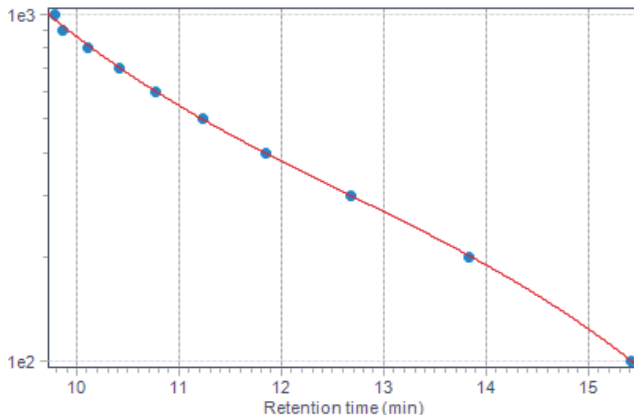


Figure 3. Chromatogram of CleanCap FLuc mRNA under 100 mM Tris acetate/2.5 mM EDTA + SEC-5 1000Å condition (100 bp DNA ladder (black), 1 kbp DNA ladder (blue), and CleanCap FLuc mRNA (green) from the top).



Curve fit	
Order of curve fit	3
Curve fit equation	$y = -0.00380656x^3 + 0.144361x^2 - 1.96903x + 11.9933$
Curve fit statistics	
Residual sum of squares	0.000448
Coefficient of determination	0.999509
Linear correlation coefficient	-0.998317
Corrected sum of squares	0.912110
Standard Y error estimate	0.008641

Figure 4. Example of length conversion of retention time using the Agilent OpenLab CDS GPC add-on based on 100 bp DNA ladder results (calibration curve horizontal axis: retention time, vertical axis: length (bp)).

When analyzing RNA aggregates, it is essential to choose a column that considers both the measurable size range of the column and the distribution range of the aggregates. Analyzing samples that cover the full exclusion and full permeation ranges of the column, such as poly(A) with a broad distribution or a 1 kbp DNA ladder, allows for the assessment of the column's measurable range.

Additionally, it is crucial to identify analysis conditions that facilitate the easy confirmation of aggregates. In the case of CleanCap FLuc mRNA, when analyzed under SEC-5 1000Å conditions with 100 mM Tris acetate/2.5 mM EDTA (Table 2), approximately 8.5% of aggregates were observed (Figure 5). However, obtaining satisfactory resolution between the target mRNA and aggregates proved to be challenging under SEC-5 2000Å conditions (Figure 5).

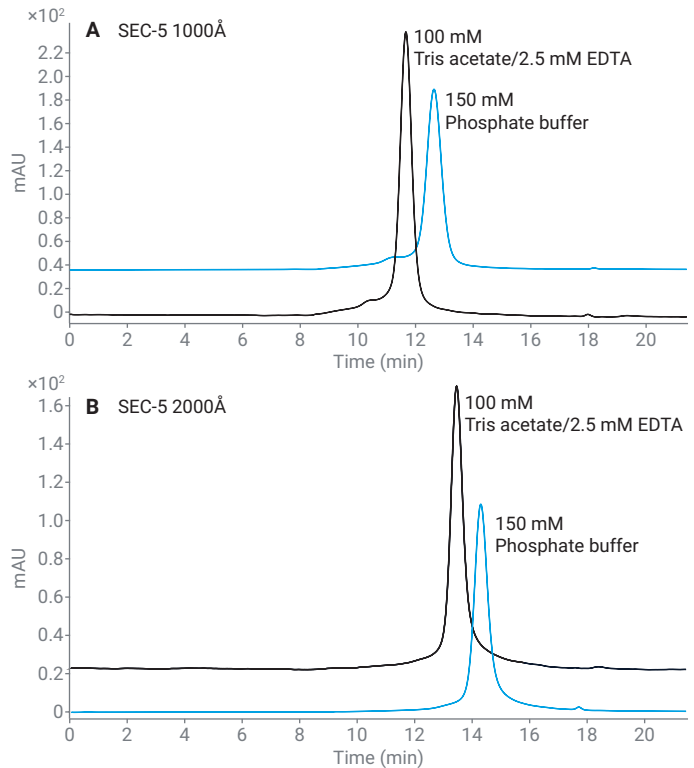


Figure 5. Chromatograms of CleanCap FLuc mRNA under various conditions.

When approximately 3,500 nt of CleanCap β -galactosidase mRNA was analyzed using 100 mM Tris acetate/2.5 mM EDTA conditions (Table 2), the SEC-5 1000Å column showed good results, with an aggregate ratio of approximately 24.9% (Figure 6).

Similar-sized mRNA of samples 1 and 2 exhibited optimal test results in the previous condition, screening under the SEC-5 2000Å column and the mobile phase condition of 100 mM Tris acetate/2.5 mM EDTA (Figure 7). The evaluation of the target mRNA was also suitable for the SEC-5 1000Å column; however, considering the range at which aggregates are eluted and the column's range, the SEC-5 2000 Å column was more appropriate. In this setup, approximately 12.7% of aggregates were observed for sample 1, and about 9.6% for sample 2.

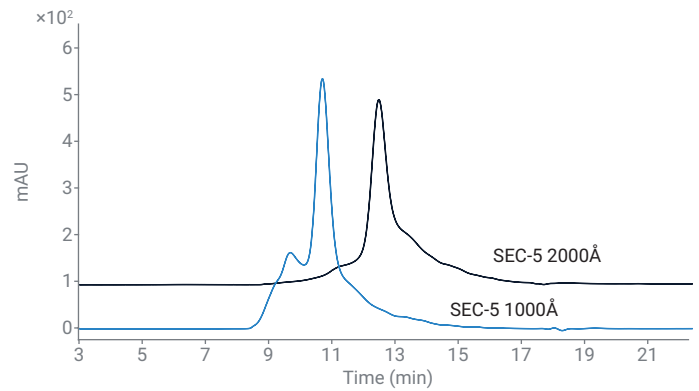


Figure 6. Chromatogram of CleanCap β -galactosidase mRNA under the different pore size column conditions.

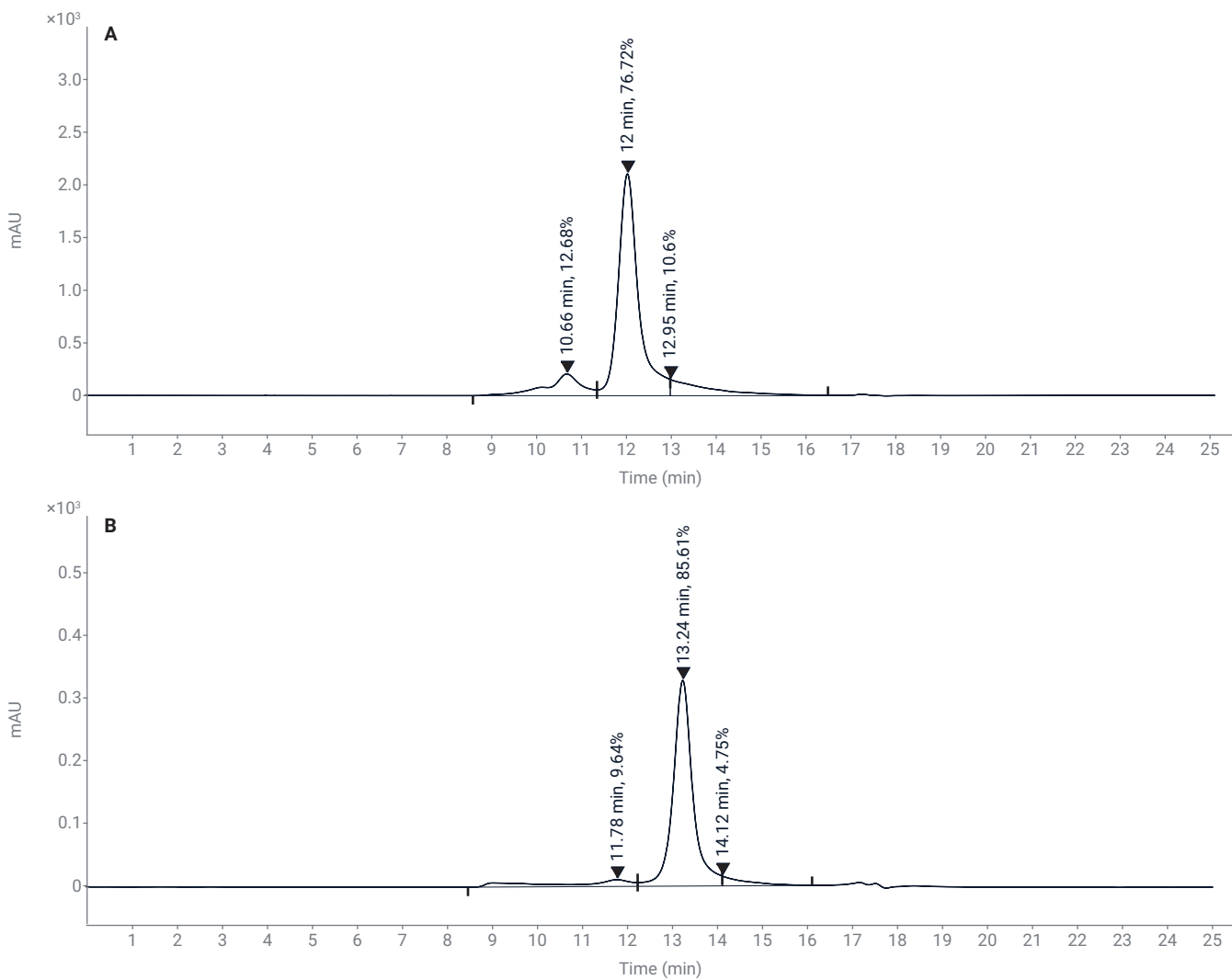


Figure 7. Aggregate analysis results of mRNA, (A) sample 1 and (B) sample 2.

Conclusion

The analysis of mRNA aggregates was performed using the Agilent 1290 Infinity II Bio LC, guided by the USP Analytical Procedures for mRNA Vaccine Quality Draft guidelines, second edition. The selection of an appropriate mobile phase and column was crucial based on the size and characteristics of mRNA. The measurable range of the column was verified using ladder standards. mRNA, with its diverse structural isoforms and poly(A) distribution, exhibited a broader peak width compared to the DNA ladder. Therefore, optimal separation conditions induced by the mobile phase and column were essential for clear differentiation from aggregates. Additionally, column selection should consider the range that covers the distribution of aggregates.

The tests indicated that for the evaluation of mRNA aggregates, a 1000Å column is suitable for mRNA of approximately 2,000 nt, while a 2000Å column is suitable for mRNA below 4,000 nt. However, considering exceptional cases like CleanCap β-galactosidase mRNA, it is necessary to establish optimal conditions through column screening.

The Agilent 1290 Infinity II Bio LC System, with its completely iron-free flow path, is optimally suited for the conditions used in size exclusion chromatography – avoiding potential corrosive damage to the system.

References

1. USP. Analytical Procedures for mRNA Vaccine Quality Draft Guidelines: 2nd Edition. **2023**.
2. Park, C.; Chen, X.; Yang, J. R.; Zhang, J. Differential Requirements for mRNA Folding Partially Explain Why Highly Expressed Proteins Evolve Slowly. *PNAS*, **2013**, *110*(8), E678–E686.
3. Borodavka, A.; Singaram, S. W.; Stockley, P. G.; Gelbart, W. M.; Ben-Shaul, A.; Tuma, R. Sizes of Long RNA Molecules are Determined by the Branching Patterns of Their Secondary Structures. *Biophys. J.* **2016**, *111*(10), 2077–2085.
4. Cheng, F.; Wang, Y.; Bai, Y.; Liang, Z.; Mao, Q.; Liu, D.; Wu, X.; Xu, M. Research Advances on the Stability of mRNA Vaccines. *Viruses* **2023**, *15*(3), 668.

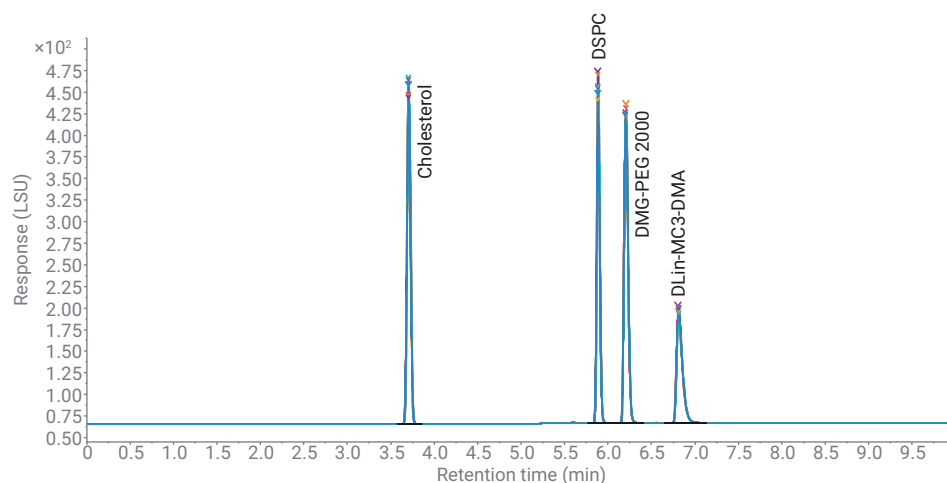


Final: IVT mRNA drug product

Lipid identity and content, RNA concentration and RNA encapsulation efficiency, RNA size and integrity, Product related impurities: aggregate quantification

Analysis of Lipid Nanoparticle Composition

Quaternary method development for highest resolution with evaporative light scattering detection



Author

Sonja Schneider
Agilent Technologies, Inc.

Abstract

Lipid nanoparticles (LNPs) have emerged as promising delivery vehicles for nucleic acids in the pharmaceutical industry. To ensure safety and efficacy of the final drug product, the lipid components need analytical characterization of composition, ratio, and degradation. In this application note, liquid chromatographic method development for the analysis of the lipid components of patisaran (trade name Onpattro) is shown in a quaternary setup. A method-combining methanol (MeOH) and acetonitrile (ACN) resulted in optimal separation of the four LNP components with excellent peak shapes, precision, and sensitivity. The Agilent 1260 Infinity II Prime Bio LC with Agilent 1290 Infinity II ELSD enables universal detection of the lipid components lacking a UV chromophore. In addition, the high dynamic range of the Agilent 1290 Infinity II ELSD allows the detection of all four lipids in the patisaran-like sample.

Introduction

In recent years, promising opportunities for RNA-based therapy and gene-editing technology have raised interest in LNP research.

LNPs act as safe and efficient delivery vehicles, and combinations of lipids with oligonucleotides have especially shown great success in the pharmaceutical industry. The LNP system enables stable drug loading and enhanced delivery efficiency to the targeted sites of action. In formulated drugs, oligonucleotides such as small interfering RNA (siRNA) or messenger RNA (mRNA) are encapsulated in LNPs to facilitate cellular uptake via endocytosis and delivery into the cytosol.

LNPs are spherical vesicles, and are typically composed of four main components (Figure 1):^{1,2}

- Cholesterol
- A neutral phospholipid (mostly DSPC)
- A polyethylene-glycol (PEG)-lipid
- An ionizable cationic lipid (often proprietary)

The primary purpose of the structural lipids DSPC, cholesterol, and the PEG-lipid is to control the particle size, provide particle stability and blood compatibility, and in addition, improve LNP circulation lifetime.³ The PEG-lipid, the least abundant lipid in the LNP formulation, also acts as a steric barrier to prevent aggregation during storage. Ionizable lipids, the second generation of cationic lipids, are pH-dependent. At low pH, their positively charged ionizable amine groups enable these lipids to interact (for example, with the anionic RNA used in the loading process of LNP-RNA formation). They are virtually uncharged at physiological pH in the bloodstream, minimizing toxicity.

The first LNP-encapsulated RNA drug approved by the FDA and the EMA is patisiran (trade name Onpattro), which is an LNP formulation of siRNA.⁴ It contains DLin-MC3-DMA as ionizable cationic lipid, DSPC, cholesterol, and

DMG-PEG-2000 (see Figure 2). The regulatory approval of Onpattro paved the way for the development of many nucleic acid-based therapies, enabled by nanoparticle delivery.

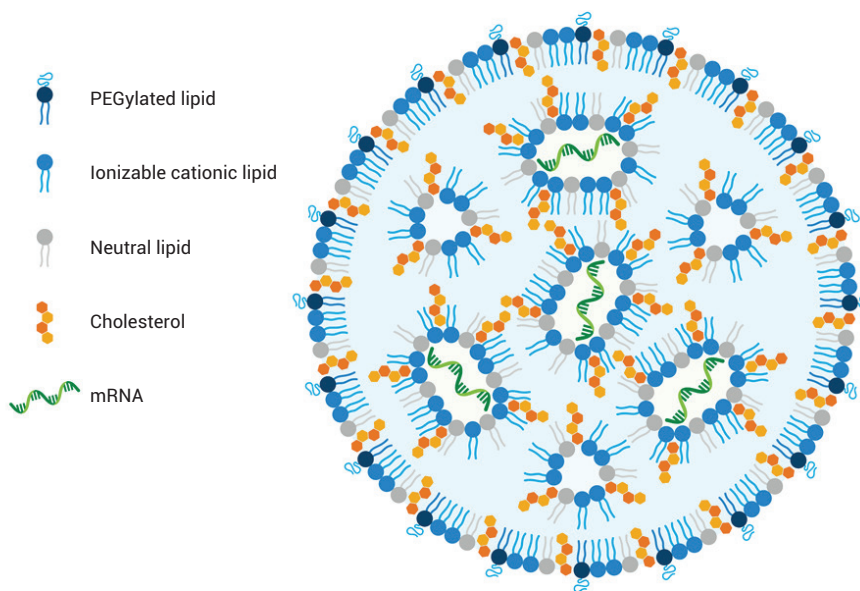


Figure 1. Schematic representation of mRNA or siRNA-LNP structure inspired by Schoenmakers *et al.*¹ and Evers *et al.*².

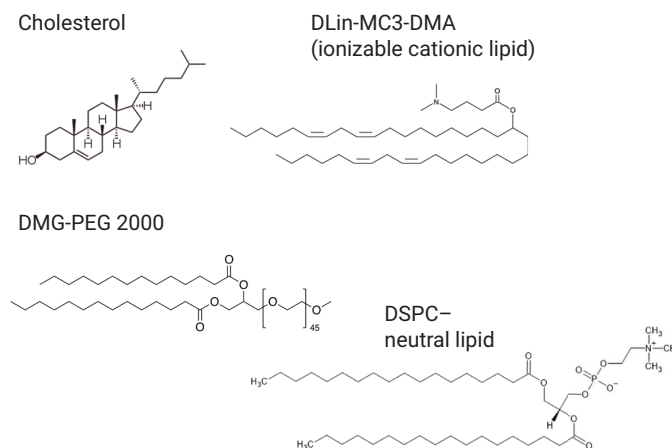


Figure 2. Main components of the Onpattro Patisiran LNP.

In addition to the analysis of the loaded RNA portion of the LNPs, the lipid components need analytical characterization to ensure safety and efficacy of the complete drug. In the process of drug and formulation design, extensive analysis is required for *in vivo* performance and quality control of the finished drug product.⁵ Regulatory specifications include tests for physical parameters such as siRNA encapsulation or particle size, as well as assays for the individual lipid components (e.g. composition, identity, and purity).⁵

Before analysis, liposomes and LNPs are usually disrupted by dilution with organic solvents such as methanol or isopropanol.

Typically, LNP analysis for composition or degradation is carried out by reverse-phase high performance liquid chromatography (RP-HPLC).⁶

Following chromatographic separation, evaporative light scattering detection (ELSD) is an ideal detection technique for molecules such as lipids, which lack a UV chromophore. The Agilent 1290 Infinity II ELSD is ideal for reproducible and sensitive detection of lipids.⁷ In addition to its universal detection capabilities, a huge advantage is the flexibility to allow the use of gradients (in contrast to refractive index detection (RID)).

This application note shows UHPLC method development for the analysis of the four components of the LNP composition of Onpattro. The different chemical nature of the four components (including the hydrophobic DSPC, the ionizable lipid, and the PEGylated lipid) makes it very challenging to achieve symmetrical and sharp peak shapes for all components within one stationary and mobile phase combination. The use of the Agilent 1260 Infinity II Prime Bio LC system provides the flexibility of a quaternary pump, and enables easy method development to test different solvent and buffer combinations.

Experimental

Equipment

The Agilent 1260 Infinity II Prime Bio LC System comprised the following modules:

- Agilent 1260 Infinity II Bio Flexible Pump (G7131C)
- Agilent 1290 Infinity II Bio Multisampler (G7137A) with Sample Thermostat (option #101)
- Agilent 1290 Infinity II Multicolumn Thermostat (G7116B) with standard flow biocompatible heat exchanger (G7116-60071)
- Agilent 1290 Infinity II ELSD (G7102A)

Software

Agilent OpenLab CDS Version 2.6 or later versions

Column

InfinityLab Poroshell 120 Phenyl-Hexyl, 2.1 × 50 mm, 1.9 μm (part number 699675-912)

Chemicals

Agilent InfinityLab ultrapure LC/MS methanol (5191-4497) and Agilent InfinityLab ultrapure LC/MS acetonitrile (5191-4496) was used for all ELSD analyses. Isopropanol was purchased from Merck (Darmstadt, Germany). Fresh ultrapure water was obtained from a Milli-Q Integral system equipped with a 0.22 μm membrane point-of-use cartridge (Millipak, Merck-Millipore, Billerica, MA, USA). Ammonium acetate was obtained from Sigma-Aldrich (Steinheim, Germany).

Samples

Cholesterol and 1,2-distearoyl-sn-glycero-3-phosphocholine (18:0 PC or DSPC) were obtained from Merck (Darmstadt, Germany). DLin-MC3-DMA (4-(dimethylamino)-butanoic acid, (10Z,13Z)-1-(9Z,12Z)-9,12-octadecadien-1-yl-10,13-nonadecadien-1-yl ester) was obtained from Cayman Chemical (MI, USA). 1,2-Dimyristoyl-rac-glycero-3-methoxypolyethylene glycol-2000 (DMG-PEG 2000) was obtained from Avanti Polar Lipids (AL, USA).

The samples were dissolved in two different concentrations. To enable complete dissolution, the tubes were warmed to 35 °C for 3 to 4 minutes before further use.

The mixed sample for method development was composed in 1,220 μL MeOH to enable approximately similar peak heights and areas for all components, as described in Table 1.

The components of the sample mimicking the Onpattro LNP component ratio were mixed as follows: The lipids were dissolved in MeOH to a concentration of 3.89 mM. Cholesterol, DLin-MC3-DMA, DMG-PEG, and DSPC were dissolved in a ratio of 38.5:50:1.5:10 from the 3.89 mM equimolar concentrations.

From this mix, a dilution series was prepared, ranging from 972.5 μM down to 0.44 μM for linearity analyses in 1:3 serial dilution steps (4.8625 nmol to 2.22 pmol for 5 μL injections).

Table 1. Sample composition for method development.

Lipid	Molecular Weight [Da]	Concentration [mM]	Mass [μg]
DMG-PEG 2000	2,509.20 (average molecular weight due to polydispersity of PEG)	0.0984	300
DLin-MC3-DMA	642.09	0.6380	500
Cholesterol	386.67	0.1060	50
DSPC	790.15	0.1670	150

Buffer preparation

500 mM ammonium acetate (~pH 7, no further pH adjustment) was prepared and filtered using a 0.2 µm membrane filter. For the binary method, the ammonium acetate stock solution was diluted to 100 mM with water, and 100 mL of this buffer was mixed with either 900 mL of methanol (Channel A) or 900 mL of acetonitrile (Channel B).

Results and discussion

An initial binary gradient setup using water + 10 mM ammonium acetate (Channel A) and MeOH + 10 mM ammonium acetate (Channel B)⁷ for the analysis of components (running a gradient from 82 to 100% B in 5 minutes with a 5-minute hold) showed the following result, as displayed in Figure 3. All other parameters were the same as described in the Experimental section. The first three neutral lipid peaks showed a good peak shape and resolution. The last ionizable lipid DLin-MC3-DMA eluted in a broad (and therefore shallow) peak. Method development options such as changing temperature or gradient slope did not improve the peak shape of the ionizable lipid. Therefore, changing the solvent combination was the central point of intervention. Further experiments using water and ACN (both with 0.1% formic acid) instead of water and MeOH, did not result in good resolution or peak shape (data not shown).

As a basis to enable solvent combination method development, the quaternary Agilent 1260 Infinity II Prime Bio LC system was used. With water, ACN, MeOH, and 500 mM ammonium acetate supplied separately in each of the four channels, different solvent combinations were tested with a continuous delivery of 2% ammonium acetate from channel D to enable a constant concentration of 10 mM buffered solution.

Method

Table 2. Chromatographic conditions.

Parameter	Value				
Solvent	A: Water B: ACN C: MeOH D: 500 mM Ammonium Acetate				
Flow Rate	0.4 mL/min				
Quaternary Gradient Final	Time	Channel A %	Channel B %	Channel C %	Channel D %
	0 minutes	16	0	82	2
	3 minutes	8	0	90	2
	5 minutes	8	90	0	2
	Stop time: 10 minutes Post-time: 5 minutes				
Quaternary Gradient Final Short	Time	Channel A %	Channel B %	Channel C %	Channel D %
	0 minutes	8	0	90	2
	3 minutes	8	90	0	2
	Stop time: 5 minutes Post-time: 5 minutes				
Gradient Binary	Time	Channel A %	Channel B %		
	0 minutes	90% Methanol, 10% H ₂ O, 10 mM ammonium acetate	0	90% Acetonitrile, 10% H ₂ O, 10 mM ammonium acetate	
	4 minutes	100	0	100	
	Stop time: 7 minutes Post-time: 5 minutes				
Column Temperature	30 °C				
Detection ELSD	Evaporator Temperature: 40 °C Nebulizer Temperature: 40 °C Gas Flow Rate: 1.6 SLM Data Rate: 80 Hz Smoothing: 10 (1.0 second)				
Injection	Injection volume: 2 and 5 µL Sample temperature: 25 °C Needle wash: 3 seconds with 50 % Isopropanol in H ₂ O				

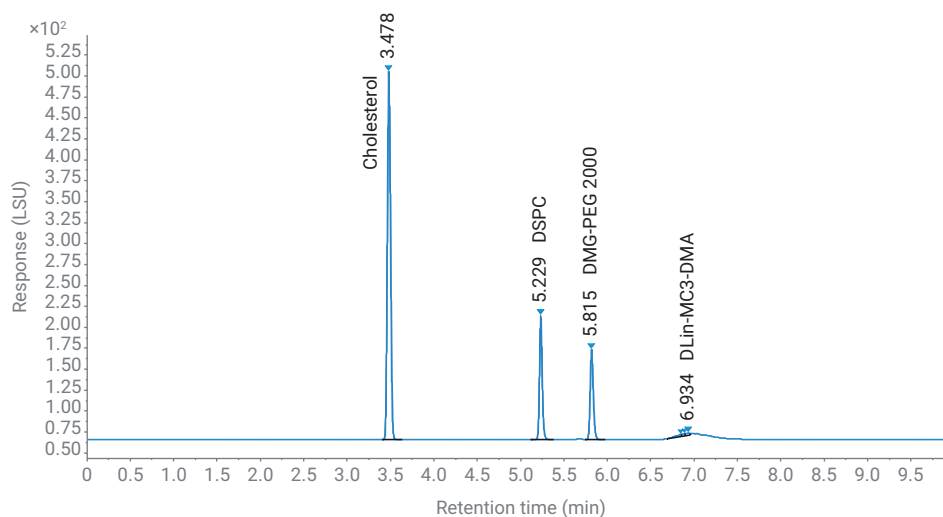


Figure 3. Binary gradient with water and MeOH, with 10 mM ammonium acetate for the analysis of the four LNP components.

Gradient using MeOH

Using MeOH in the quaternary setup, it was not possible to elute all four lipids (Figure 4), as presumably 100% of MeOH in a longer hold would be needed for complete elution. In the quaternary setup, a maximum of 90% MeOH was possible, while still including the buffer functionality of ammonium acetate and some water to prevent crystallization. Figure 4 shows the results for the ternary separation from 80 to 90% MeOH. Only two peaks were eluted from the column, even with a 5-minute 90% hold of MeOH. In the next experiments, ACN was used as a stronger eluent to test for complete elution of all four lipid components.

Gradient using ACN

Figure 5 shows the results of a ternary gradient using ACN as eluent. The gradient was set to 50 to 90% B in 5 minutes, with a 5-minute hold. With ACN, all four peaks could be completely eluted. However, the peak shapes of three lipids were suboptimal, with only cholesterol (first peak) showing a Gaussian peak shape.

Further method development to enable faster elution and enhanced resolution was started by using higher organic starting conditions and shallower gradients. Although faster elution was achieved, flatter gradients did not show an improvement in resolution of the first two peaks. See Figures 6A to 6C.

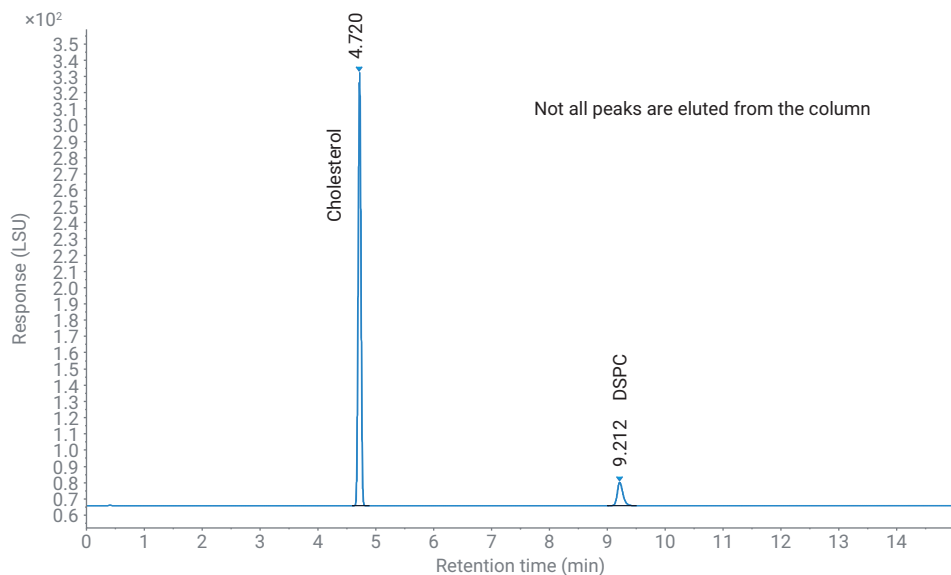


Figure 4. Ternary gradient from 80 to 90% MeOH in 5 minutes with a 5-minute hold.

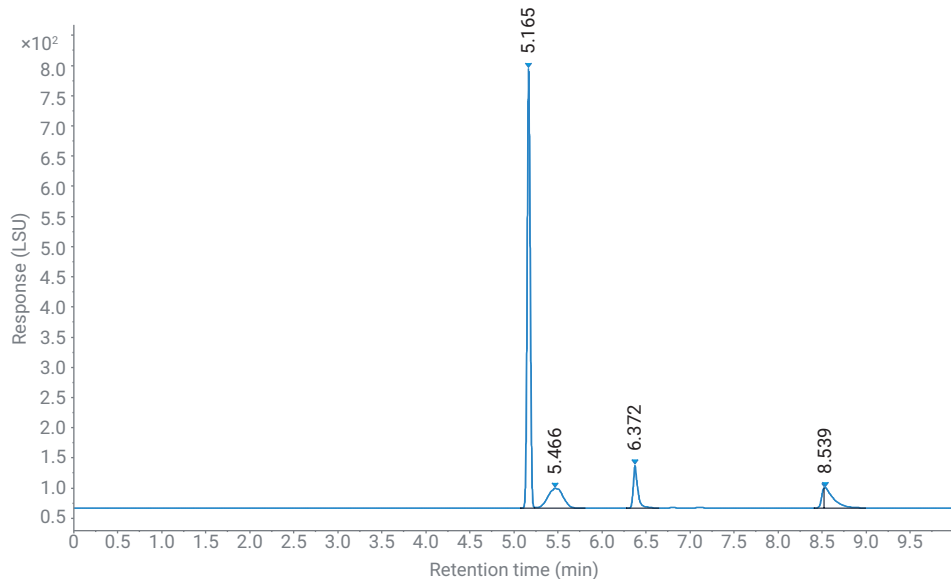


Figure 5. Ternary gradient from 50 to 90% B (ACN) in 5 minutes with a 5-minute hold.

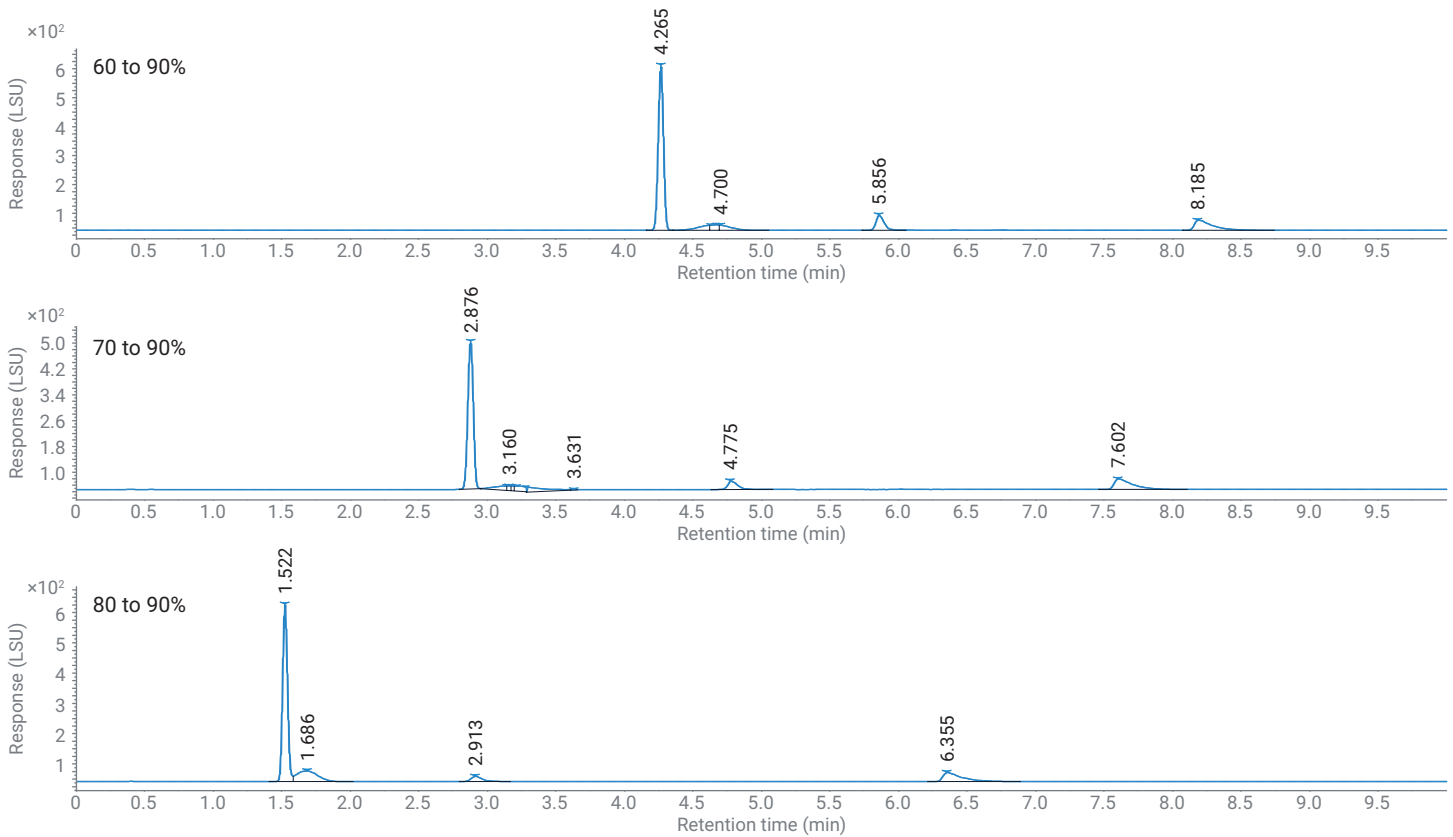


Figure 6. Different gradient slopes for the elution from the four LNP components using ACN.

Quaternary gradient combining MeOH and ACN

To enable complete elution with improved peak shapes, a quaternary gradient combining ACN with MeOH was evaluated, see Table 2 (experimental conditions). The quaternary gradient starting from 82% MeOH over 90% MeOH to 90% ACN resulted in baseline chromatographic separation with excellent peak shapes for all LNP components, even the ionizable lipid. An overlay of seven subsequent runs also showed excellent precision of retention time (RT) and good area precision (Figure 7 and Table 3).

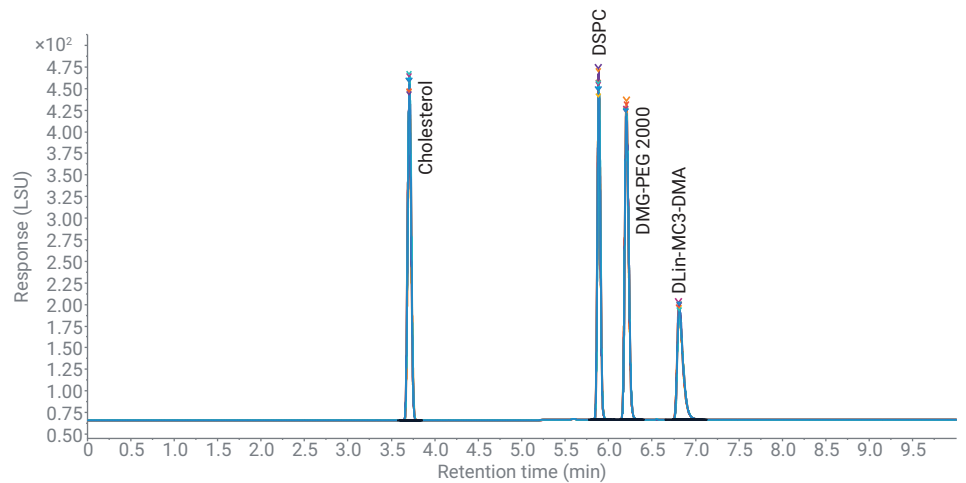


Figure 7. Quaternary gradient using MeOH as well as ACN – Overlay of seven subsequent runs.

Table 3. Figure 7 peak RSD information.

Peak	RSD RT (%)	RSD Area (%)
Cholesterol	0.1	1.875
DSPC	0.054	3.236
DMG-PEG 2000	0.055	1.172
DLin-MC3-DMA	0.061	0.998

Using this method, an equimolar mixture of all four lipids was analyzed on the column. These were diluted in series 1:3, ranging from 4.8625 nmol down to 2.22 pmol. Excellent limits of detection (LOD) were found between 0.46 and 8.1 pmol on column for a signal-to-noise (S/N) ratio of 3. Limits of quantification (LOQ) were found between 1.6 and 27 pmol on column for S/N = 10. The noise was calculated P2P for all peaks. All correlation curves showed excellent values for a quadratic curve model, with coefficients of determination (R^2) over 0.999, except for DSPC with 0.995 (Table 4).

Table 4. LOD, LOQ, and correlation for the LNP components.

Peak	Lipid	LOD [pmol]	LOQ [pmol]	R^2
1	Cholesterol	8.1	27	0.99913
2	DSPC	2.3	7.8	0.99524
3	DMG-PEG 2000	0.46	1.6	0.99988
4	DLin-MC3-DMA	5.31	17.7	0.99963

Further method development to achieve shorter methods, while maintaining excellent peak shapes and resolution, led to a second variation of the MeOH/ACN solvent combination. The linear MeOH gradient step from 82 to 90% MeOH was omitted, and a gradient from 90% MeOH to 90% ACN in 3 minutes with 2-minute hold (Table 2) was used. Figure 8 shows the separation of the four LNP components using the short gradient. Table 5 lists the RSD values for Figure 8 peaks. Excellent resolution, peak shapes, and reproducibility for all lipid components was obtained using this short method. The area precision could be improved by injecting 5 μ L instead of 2 μ L (long method). The short method has the further advantage of being feasible to run on a binary pump, which can be beneficial for LC/MS and other analyses.

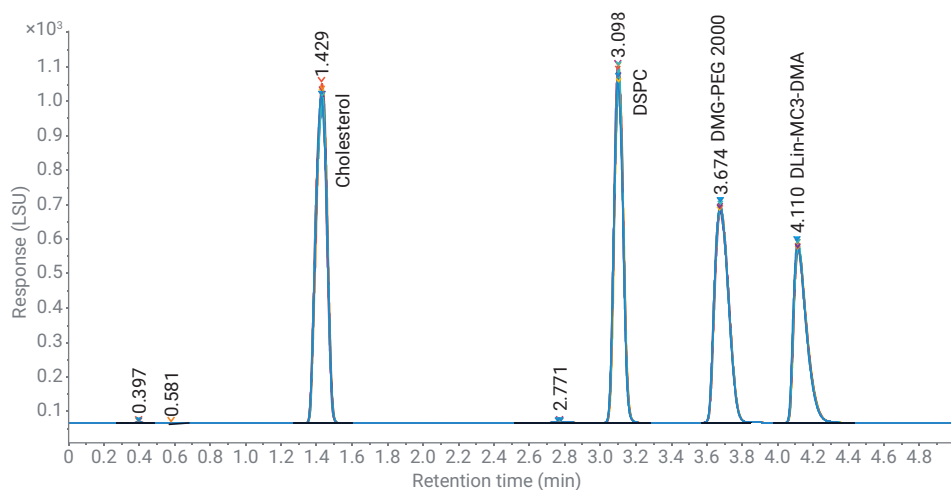


Figure 8. Short quaternary gradient from 90% MeOH to 90% ACN – Overlay of seven subsequent runs.

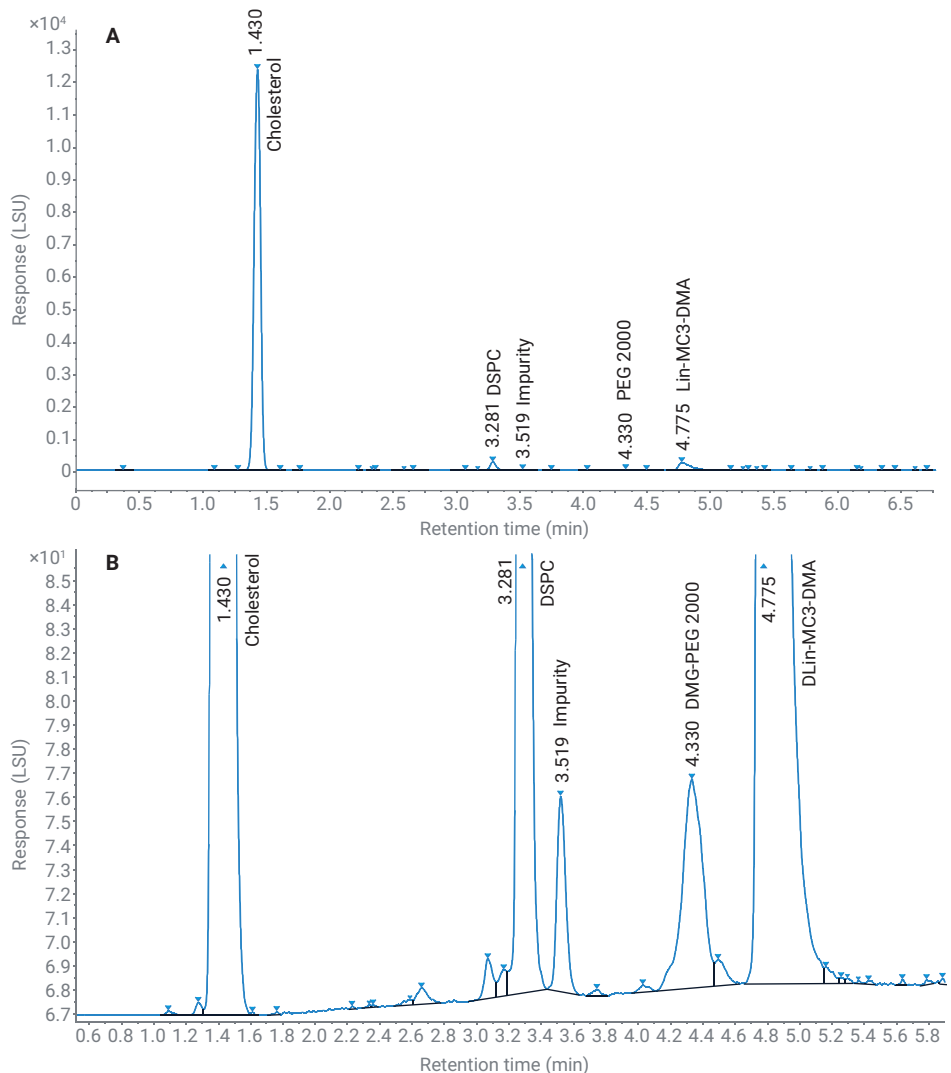


Figure 9. Analysis of the patisiran-like LNP sample (A), zoomed in version (B).

Table 5. Figure 8 peak RSD information.

Peak	RSD RT (%)	RSD Area (%)
Cholesterol	0.148	0.428
DSPC	0.090	1.807
DMG-PEG 2000	0.040	0.788
DLin-MC3-DMA	0.032	0.759

The quaternary method was transferred to a binary method, and applied to a sample mix of the four LNP components mimicking the LNP ratio of patisiran¹ with DMG-PEG 2,000, DLin-MC3-DMA, Cholesterol, and DSPC in a ratio of 1.5:50:38.5:10. This shows a need to achieve detection and quantification over a wide dynamic range, as shown in Figure 9.

Conclusion

The quaternary setup used with the 1260 Infinity II Prime Bio LC has been shown to be ideal for solvent method development. The InfinityLab Poroshell 120 Phenyl-Hexyl chemistry provides superior flow dynamics with its superficially porous base particle, and a slightly lower hydrophobicity from traditional C18 when interacting with the large hydrophobic lipids found in LNPs. Along with the column, the solvent combination has proven to be the most critical factor in influencing peak shape and resolution. Within one organic solvent setup using only MeOH or ACN as a strong mobile phase, either incomplete elution of the lipid components (MeOH) or suboptimal peak shape and resolution were observed for all four peaks (ACN). With the quaternary setup, a high-resolution method using both organic solvents MeOH and ACN was developed.

The developed methods enabled the complete elution of all four LNP components with excellent peak shape and high resolution in a highly precise method for RT and area. In addition to excellent quadratic correlation with high coefficients of determination, the high dynamic range of the 1290 Infinity II ELSD enabled the detection and quantification of all four lipid components in the original ratio of the patisiran sample. The 1260 Infinity II Prime Bio LC, in combination with the 1290 Infinity II ELSD can therefore be highly recommended for the analysis of LNP components.

References

1. Schoenmaker, L. *et al.* mRNA-lipid Nanoparticle COVID-19 Vaccines: Structure and Stability *Int. J. Pharm.* **2021**, 601.
2. Evers, M. *et al.* Small Methods **2018**, 2.
3. Kim, J. *et al.* Self-assembled mRNA Vaccines *Adv. Drug Deliv. Rev.* **2021**, 170, 83-112.
4. Akinc, A. *et al.* The Onpattro Story and the Clinical Translation of Nanomedicines Containing Nucleic Acid-Based Drugs *Nat. Nanotechnol.* **2019**, 12, 1084–1087.
5. NDA 210922 ONPATTRO (patisiran) Lipid Complex Injection Addendum to Drug Product Quality Review – Quality Assessment **2018**.
6. Fan, Y.; Marioli, M.; Zhang K.; Analytical Characterization of Liposomes and Other Lipid Nanoparticles for Drug Delivery. *J. Pharm. Biomed. Anal.* **2021**, 5.
7. A Sensitive Detection Technique for Analysis of Lipids in Liposomal Formulations Using an Agilent 1290 Infinity II ELSD. *Agilent Technologies application note*, publication number 5994-0965EN, **2019**.

www.agilent.com

For Research Use Only. Not for use in diagnostic procedures.

RA44620.0930902778

This information is subject to change without notice.

© Agilent Technologies, Inc. 2022
Printed in the USA, July 27, 2022
5994-4709EN

Analysis of Lipid Nanoparticle Components Using an Agilent 6545XT AdvanceBio LC/Q-TOF

Authors

Li Zhang and Yi Yan Yang
Bioprocessing Technology
Institute, Agency for Science,
Technology, and Research
(A*STAR)
Republic of Singapore
Suresh Babu C.V. and
Ravindra Gudhial
Agilent Technologies, Inc.

Abstract

The identity and quantity of lipid components are among the several critical quality attributes (CQAs) for lipid-based nanoparticle delivery systems. This application note proposes a liquid chromatography/mass spectrometry (LC/MS) method for the analysis of lipid components of mRNA encapsulated in lipid nanoparticles (mRNA LNPs). The method uses an Agilent 1290 Infinity II LC system and an Agilent 6545XT AdvanceBio LC/Q-TOF, and demonstrates high-resolution separation as well as lipid identification with high mass accuracy. The method performance was evaluated with mRNA LNPs to demonstrate simultaneous analysis of the lipid components.

Introduction

Drug development teams use lipid nanoparticles (LNPs)—a versatile formulation method—to deliver a range of therapeutics. Due to expanding research of LNP-encapsulated mRNA in the biopharmaceutical area¹, the need for analytical techniques to understand LNP properties has increased. Different physical aspects of LNPs, including size, morphology, zeta potential, polydispersity, composition, and stability, are part of the drug product CQAs. LNPs are composed of four different lipids: ionizable lipids, helper or neutral lipids, cholesterol, and polyethylene glycol (PEG) lipids. LNP composition is crucial to functionality and must be characterized in the formulation.^{2,3} The lipid quantity, ratio, and purity are CQAs for manufacturing, and are needed to enable process and formulation development.

In this application note, we outline a lipid analysis procedure using LC/MS for LNPs used in potential vaccines. The method uses the 1290 Infinity II LC system and 6545XT AdvanceBio LC/Q-TOF.

Experimental

Materials

Heptadecan-9-yl 8-((2-hydroxyethyl)(6-oxo-6-(undecyloxy)hexyl)amino)octanoate (SM-102), 6-((2-hexyldecanoyl)oxy)-N-(6-((2-hexyldecanoyl)oxy)hexyl)-N-(4-hydroxybutyl)hexan-1-aminium (ALC-0315), 1,2-distearoyl-sn-glycero-3-phosphocholine (DSPC), 1,2-dimyristoyl-rac-glycero-3-methoxypolyethylene glycol-2000 (DMG-PEG 2k), dioleoylphosphatidylethanolamine (DOPE), 1,2-dioleoyl-3-trimethylammonium propane (DOTAP), and cholesterol were supplied from MedChemExpress. Methanol (MeOH) was obtained from Agilent Technologies. Acetonitrile (ACN) and formic acid was obtained from Fisher Chemicals. Sodium acetate and Tris were obtained from Sigma. Monarch RNA cleanup kit spin columns were obtained from New England Biolabs.

Instrumentation

The 1290 Infinity II LC system, which was coupled to the 6545XT AdvanceBio LC/Q-TOF, comprised the following modules:

- Agilent 1290 Infinity II high-speed pump (G7120A)
- Agilent 1290 Infinity II multicolumn thermostat (G7116B)
- Agilent 1290 Infinity II multisampler (G7167B)
- Agilent 6545XT AdvanceBio LC/QTOF (G6549AA)

Software

The following software packages were used:

- Agilent MassHunter Workstation Data Acquisition software (version 11)
- Agilent MassHunter Qualitative Analysis software (version 10)

Standard and calibration curve

An 8 mM lipid standard was prepared in MeOH. Different working concentrations of each lipid standard or mixture of lipids were prepared in MeOH using the stock solutions. To generate calibration curves, a stock solution containing 2 mM SM-102, 2 mM DMG-PEG 2K, 2 mM DSPC, and 20 mM cholesterol was freshly prepared in MeOH. The calibration solution was then serially diluted in MeOH to the minimum concentration of 0.1 fmol SM-102, 0.1 fmol DMG-PEG 2K, 0.1 fmol DSPC, and 10 pmol cholesterol.

Liquid chromatography/mass spectrometry

LC/MS lipid separation was performed on an Agilent InfinityLab Poroshell 120 Phenyl-Hexyl column (2.1 × 50 mm, 1.9 μm) using a seven-minute gradient. LC/MS conditions are detailed in Table 1. The mRNA LNP samples were dissolved in water, and MeOH dilution aliquots were injected into the LC/MS system.

Table 1. LC/MS parameters. (Continued on next page).

Parameter	Value												
Agilent 1290 Infinity II LC System													
Column	Agilent InfinityLab Poroshell 120 Phenyl-Hexyl, 2.1 × 50 mm, 1.9 μm												
Sample Thermostat	25 °C												
Mobile Phase A	90% MeOH in 10 mM ammonium acetate												
Mobile Phase B	90% ACN in 10 mM ammonium acetate												
Gradient	<table border="1"> <thead> <tr> <th>Time (min)</th> <th>%A</th> <th>%B</th> </tr> </thead> <tbody> <tr> <td>0.00</td> <td>100</td> <td>0</td> </tr> <tr> <td>2.00</td> <td>100</td> <td>0</td> </tr> <tr> <td>7.00</td> <td>0</td> <td>100</td> </tr> </tbody> </table>	Time (min)	%A	%B	0.00	100	0	2.00	100	0	7.00	0	100
Time (min)	%A	%B											
0.00	100	0											
2.00	100	0											
7.00	0	100											
Stop Time	7 min												
Column Temperature	55 °C												
Flow Rate	0.4 mL/min												

Table 1. LC/MS parameters. (Continued).

Parameter	Value
Agilent 6545XT AdvanceBio LC/Q-TOF	
Ion Mode	Positive ion mode, dual AJS ESI
Drying Gas Temperature	250 °C
Drying Gas Flow	10 L/min
Sheath Gas Temperature	300 °C
Sheath Gas Flow	12 L/min
Nebulizer	35 psi
Capillary Voltage	3,500 V
Nozzle Voltage	500 V
Fragmentor Voltage	150 V
Skimmer Voltage	65 V
Octupole Ion Guide Voltage	750 V
Reference Mass	922.009798
Acquisition Mode	Data were acquired in Extended Dynamic Range (2 GHz)
MS Mass Range	110 to 1,700 <i>m/z</i>
Acquisition Rate	8 spectra/s
MS Range	350 to 3,200 <i>m/z</i>
MS Acquisition Rate	2 spectra/s

Preparation of mRNA LNPs

The mRNA LNPs were produced using the same composition as Spikevax—the COVID-19 vaccine pioneered by Moderna. The mRNA was in vitro transcribed from a PCR-amplified dsDNA template, purified using spin columns, then dissolved in 1 mM sodium acetate buffer (pH 4.7) to form the aqueous phase. For the Spikevax formulation⁴, SM-102, DMG-PEG 2K, DSPC, and cholesterol were dissolved in ethanol at the molar ratio of 50:1.5:10:38.5 to form the organic phase. The mRNA was dispersed in 25 mM sodium acetate to form the aqueous phase. These two phases were mixed using the benchtop microfluidic device (NanoAssemblr platform, Precision NanoSystems) at the volume ratio 3:1, and the total flow rate was 12 mL/min. The N:P ratio was 5.67:1. Then, the formed mRNA LNPs were buffer exchanged with 20 mM Tris (pH 7.4) and concentrated by ultracentrifuge tubes with a molecular weight cutoff of 30 kDa at 4 °C and 2,500 g for 60 minutes to a total lipid concentration of ~ 4 mg/mL. The formed mRNA LNPs were subjected to lyophilization.

Results and discussion

Lipid components in the formulation of nanoparticles have been separated and quantified using RP-HPLC. Since most lipids lack a chromophore, they must be detected by alternative detection methods. HPLC coupled with MS detection has emerged as one of the most effective methods for identifying lipids. During the nanoparticle development phase, various lipid classes can be investigated to obtain the most effective LNPs. Table 2 shows the lipids used in this study. Separation and identification of lipids were performed on a 1290 Infinity II LC coupled with a 6545XT AdvanceBio LC/Q-TOF. Figure 1A shows the extracted ion chromatograms (EICs) from the simultaneous analysis of seven lipids with high-resolution separation using an InfinityLab Poroshell 120 Phenyl-Hexyl column. All the peak assignments were based on accurate mass measurements from Q-TOF analysis. The lipids were eluted in the order of: cholesterol, DOPE, DOTAP, DSPC, SM-102, ALC-0315, and DMG-PEG 2K. The mass spectrum corresponding to individually resolved lipids is depicted in Figure 1B. The most abundant charge states observed in the mass spectrum are indicated, and all spectra matched theoretical masses to within 2.5 ppm.

Table 2. LNP components employed in this study.

Lipid Role	Lipids	Formula	Molecular Weight
Ionizable Lipids	ALC-0315	C ₄₈ H ₉₅ NO ₅	766.27
	SM-102	C ₄₄ H ₈₇ NO ₅	710.17
	DOTAP	C ₄₂ H ₈₀ ClNO ₄	698.54
Phospholipid	DSPC	C ₄₄ H ₈₈ NO ₈ P	790.15
Helper Lipid	Cholesterol	C ₂₇ H ₄₆ O	386.65
	DOPE	C ₄₁ H ₇₈ NO ₈ P	744.03
PEG-Lipid	DMG-PEG 2K	(C ₂ H ₄ O) _n C ₃₂ H ₆₂ O ₅	2,526.00

The reproducibility of the method was evaluated with three consecutive LC/MS runs. Figure 2 shows the overlay EIC of the standard lipid mixture. The result shows excellent lipid separation with no observable shift in the chromatographic profile between the replicate injections. The retention time (Rt) and peak area relative standard deviation (RSD) for the lipids were less than 0.5 and 1.5% respectively, demonstrating the excellent reproducibility and precision of the method.

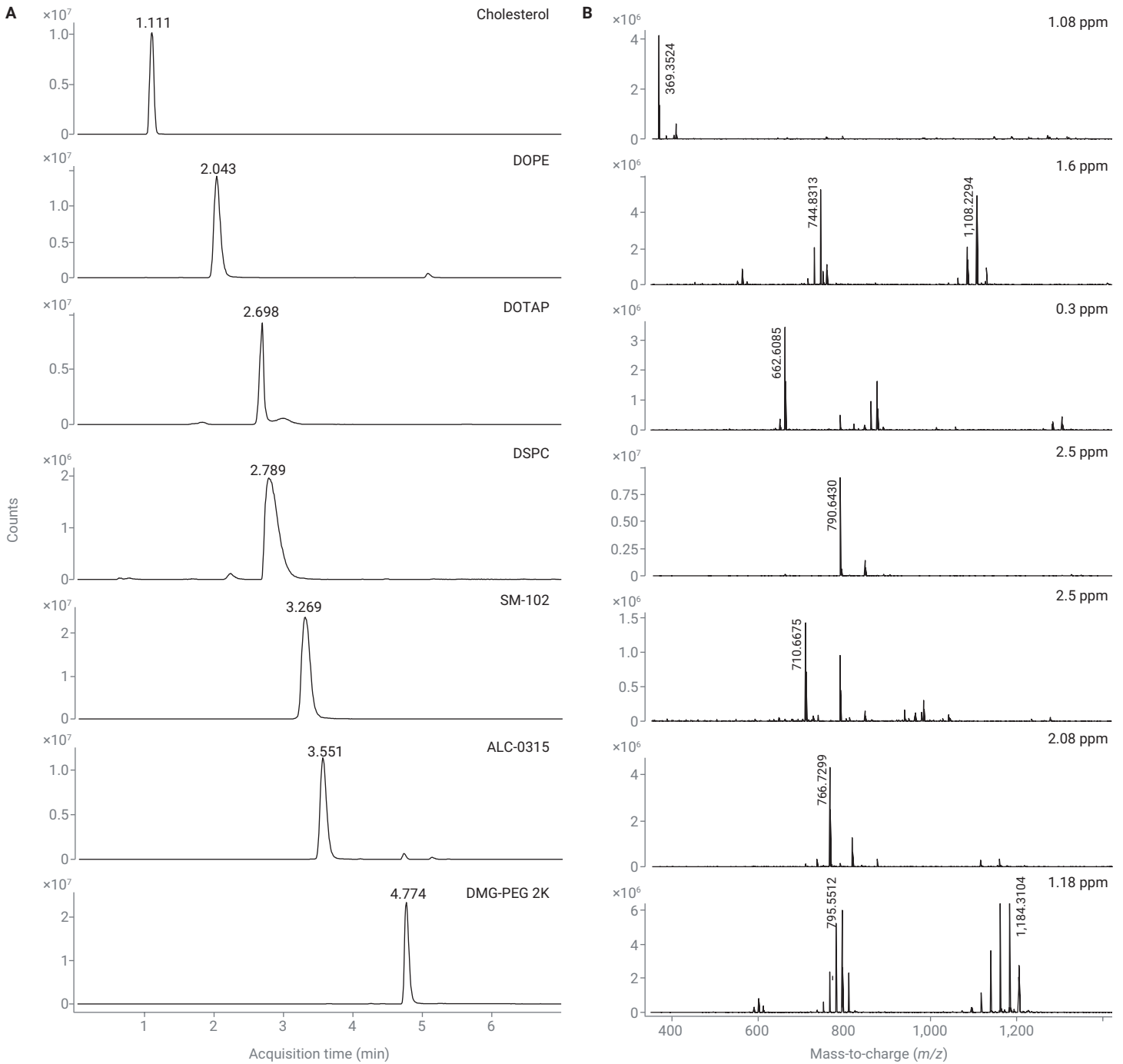


Figure 1. High-resolution and accurate mass identification of LNP components. (A) EICs and (B) mass spectra of the seven lipid components.

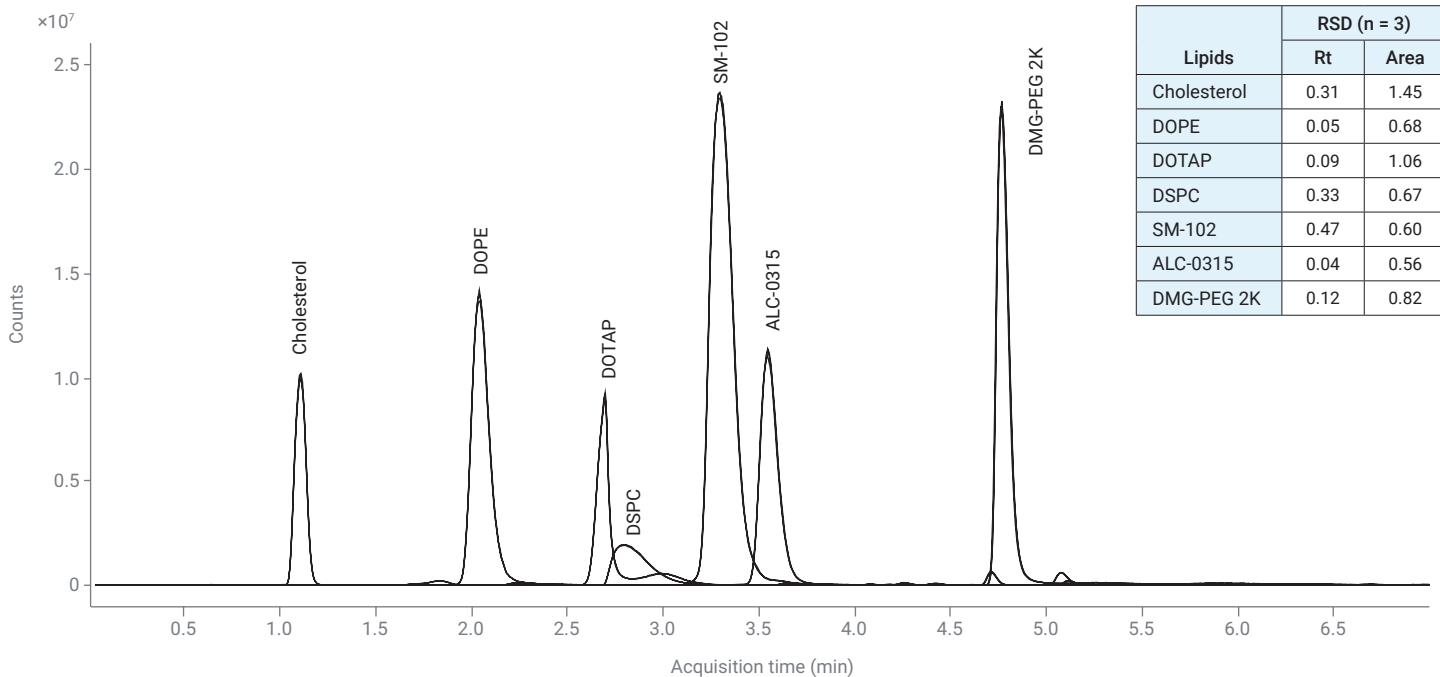


Figure 2. Overlay EIC of the lipid standards, demonstrating reproducibility.

The linearity of the method was assessed at a 0.1 to 1,000 pmol concentration range for four lipids: cholesterol, DMG, SM-102, and DSPC. Calibration curves (Figure 3) were established on a logarithmic scale by plotting log (peak area) versus log (lipid concentration) and fitted with a linear curve. The coefficient of determination $R^2 \geq 0.99$ demonstrated a strong linearity on the concentration ranges under study. The EIC overlay of the four lipids employed for the quantitative determination is displayed in Figure 4.

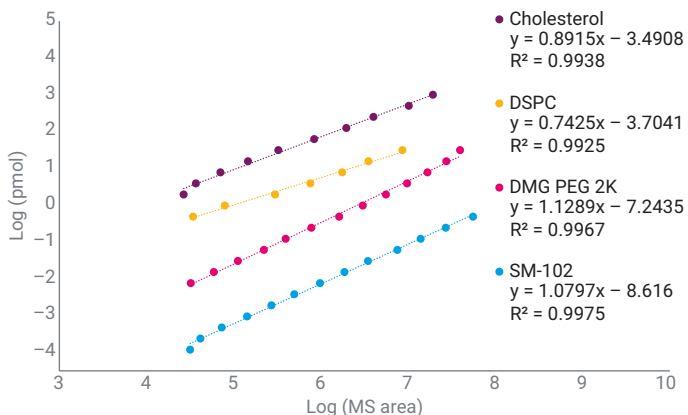


Figure 3. Calibration curve of lipid standards (n = 3).

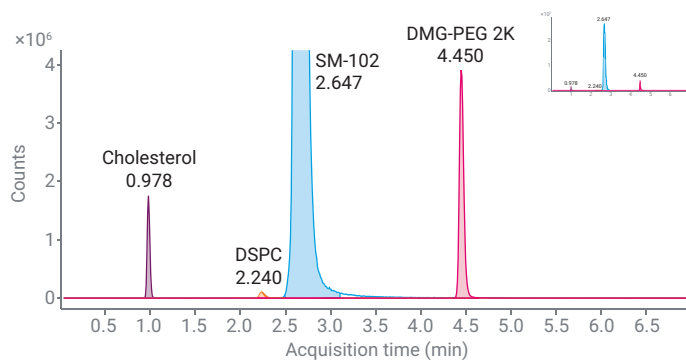


Figure 4. EIC of the four lipid standards used to prepare LNP.

Lipid stability observation is one of the important goals of mRNA LNP production. The applicability of the LC/MS method was evaluated as a quality control tool by examining the lipid content in different mRNA LNP formulation conditions. The mRNA LNP preparations (both with and without lyophilization storage conditions) are detailed in the "Experimental" section. The percent molar ratios of lipids under the two storage scenarios are displayed in Figure 5. The lipid content in lyophilized samples was consistent with the targeted mRNA LNP formulation (SM-102:DMG-PEG 2K:DSPC:cholesterol at 50:1.5:10:38.5), demonstrating the reliability of the LC/MS method. On the other hand, substantial changes in lipid concentration were noted in the nonlyophilized samples, suggesting inadequate lipid stability, which could be due to the chemical degradation of lipids. Overall, the LC/MS method highlighted the variations in lipid content over the various formulation conditions, which helps to improve the formulation process. Detailed LNP stability studies of different storage conditions (temperature and time) are currently under investigation.

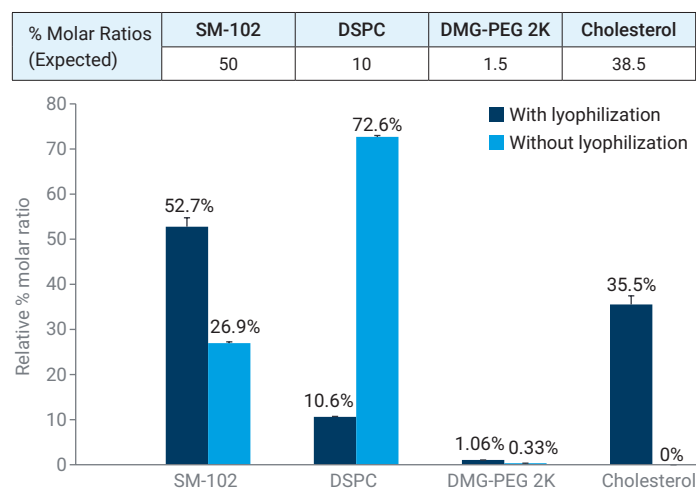


Figure 5. LC/MS analysis of lipid content of mRNA loaded in LNP samples stored at -20°C for one month ($n = 3$).

Conclusion

In this application note, an LC/MS method using an Agilent 1290 Infinity II LC system and an Agilent 6545XT AdvanceBio LC/Q-TOF was developed for the identification and quantification of lipid components. The developed method enabled the separation of all lipids with good linearity and repeatability. The LC/MS method was applied to assess the stability of lipid excipients in mRNA LNP formulation preparations.

References

- Verma, M.; Ozer, I.; Xie, W.; Gallagher, R.; Teixeira, A.; Choy, M. The Landscape for Lipid-Nanoparticle-Based Genomic Medicines. *Nature Reviews Drug Discovery* **2023**, *22*, 349–350.
- Cárdenas, M.; Campbell, R. A.; Arteta, M. Y.; Lawrence, M. J.; Sebastiani, F. Review of Structural Design Guiding the Development of Lipid Nanoparticles for Nucleic Acid Delivery. *Current Opinion in Colloid & Interface Science* **2023**, *66*, 101705.
- Albertsen, C. H.; Kulkarni, J. A.; Witzigmann, D.; Lind, M.; Petersson, K.; Simonsena, J. B. The Role of Lipid Components in Lipid Nanoparticles for Vaccines and Gene Therapy. *Adv. Drug Deliv. Rev.* **2022**, *188*, 114416.
- Hassett, K. J.; *et al.* Optimization of Lipid Nanoparticles for Intramuscular Administration of mRNA Vaccines. *Mol. Ther. Nucleic Acids.* **2012**, *15*, 1–11.

LC/MS Analysis of Lipid Composition in an mRNA LNP Formulation: A Stability Study

Authors

Li Zhang and Yi Yan Yang
Bioprocessing Technology
Institute

Suresh Babu C.V. and
Ravindra Gudhial
Agilent Technologies, Inc.

Abstract

Lipid-based nanocarriers, known as lipid nanoparticles (LNPs), can deliver a wide range of bioactive molecules, including nucleic acids. As a crucial quality aspect of LNPs, lipid identification and ratio composition must be precisely monitored. In this study, the lipid components in an LNP formulation were analyzed with a liquid chromatography/mass spectrometry (LC/MS) technique using the Agilent 1290 Infinity II LC system and Agilent 6545XT AdvanceBio LC/Q-TOF. The LC/MS method was applied to study the influence of storage conditions on mRNA LNPs.

Introduction

mRNA-based biopharmaceuticals have emerged as a new class of therapeutics. mRNA molecules must cross several extracellular and intracellular obstacles to function in vivo.¹ With recent advances in the nanomedicine field, LNPs are becoming well-known in vivo mRNA delivery systems. Encapsulating mRNA into the LNP system protects nucleic acids from degradation and aids in cellular absorption and expression.^{2,3}

The LNP formulation usually consists of an ionizable amino lipid, phospholipid, cholesterol, and polyethylene glycol (PEG)-lipid conjugate. The role of lipids includes ionizable lipids to facilitate nucleic acid encapsulation, PEG-lipids to prevent aggregation, cholesterol, and helper lipids to enhance nanoparticle stability during circulation.^{4,5} When aqueous (RNA) and organic (lipid) solutions are mixed, the positively charged amine groups on the lipid and the negative charge on the RNA phosphate backbone electrostatically interact to produce mRNA LNPs. This technique yields robust nanoparticles (with fixed lipid molar ratio) in shorter periods; however, it is uncertain how stable the nanoparticles will be under prolonged storage conditions. LNP stability is one of the key quality attributes since aggregation and degradation processes during storage could result in imbalance of the lipid ratio. The changes in the lipid content may affect the efficiency and safety of mRNA vaccines. Therefore, lipid identification and quantification are critical to the stability and functionality of LNPs and call for robust stability-indicating analytical methods.

Previously, LC and GC techniques coupled with aerosol, flame ionization, and MS detection have been used to analyze lipid components.⁶⁻⁹ Among these, LC/MS offers high-resolution and simultaneous analysis of lipid composition in LNPs.¹⁰ Although LC/MS was used for lipid identification, the technique was not applied in the investigation of LNP stability studies.

In this application note, the lipid composition of an mRNA LNP sample was analyzed with the previously developed LC/MS method.¹¹ The LC/MS method was applied to examine LNP stability under various formulation and storage conditions.

Experimental

Materials

Heptadecan-9-yl 8-((2-hydroxyethyl)(6-oxo-6-(undecyloxy)hexyl)amino)octanoate (SM-102), 6-((2-hexyldecanoyl)oxy)-N-(6-((2-hexyldecanoyl)oxy)hexyl)-N-(4-hydroxybutyl)hexan-1-ammonium (ALC-0315), 1,2-distearoyl-sn-glycero-3-phosphocholine (DSPC), 1,2-dimyristoyl-rac-glycero-3-methoxypolyethylene glycol-2000 (DMG-PEG 2K), dioleoylphosphatidylethanolamine (DOPE), 1,2-dioleoyl-3-trimethylammonium propane (DOTAP), and cholesterol were supplied from MedChemExpress. Methanol (MeOH) was obtained from Agilent Technologies. Formic acid and acetonitrile (ACN) were obtained from Fisher Chemical. Sodium acetate and Tris were obtained from Sigma. Monarch RNA cleanup kit spin columns were obtained from New England Biolabs.

Instrumentation

The 1290 Infinity II LC system, which was coupled to the 6545XT AdvanceBio LC/Q-TOF, comprised the following modules:

- Agilent 1290 Infinity II high-speed pump (G7120A)
- Agilent 1290 Infinity II multicolumn thermostat (G7116B)
- Agilent 1290 Infinity II multisampler (G7167B)
- Agilent 6545XT AdvanceBio LC/Q-TOF (G6549AA)

Column

The column used in this study was the Agilent InfinityLab Poroshell 120 Phenyl-Hexyl column (2.1 × 50 mm, 1.9 μm; part number 699675-912).

Software

The following software packages were used:

- Agilent MassHunter Workstation Data Acquisition software (version 11)
- Agilent MassHunter Qualitative Analysis software (version 10)

Standard and calibration curve

An 8 mM lipid standard was prepared in MeOH. Different working concentrations of each lipid standard or mixture of lipids were prepared in MeOH using the stock solutions. To generate calibration curves, a stock solution containing 2 mM SM-102, 2 mM DMG-PEG 2K, 2 mM DSPC, and 20 mM cholesterol was freshly prepared in MeOH. The calibration solution was then serially diluted in methanol to the minimum concentration of 0.1 fmol SM-102, 0.1 fmol DMG-PEG 2K, 0.1 fmol DSPC, and 10 pmol cholesterol.

Liquid chromatography/ mass spectrometry

LC/MS lipid separation was performed on an InfinityLab Poroshell 120 Phenyl-Hexyl column (2.1 × 50 mm, 1.9 μm) using a seven-minute gradient. LC/MS conditions are detailed in Table 1. mRNA-LNP samples were dissolved in water, and MeOH dilution aliquots were injected into the LC/MS system.

Preparation of mRNA LNPs

The LNPs produced and used in this application note were similar in composition to the Moderna COVID-19 vaccine LNP. mRNA was in vitro transcribed from a PCR-amplified dsDNA template, purified using spin columns, then dissolved in 1 mM sodium acetate buffer (pH 4.7) to form the aqueous phase.

For the Spikevax LNP formulation⁴, SM-102, DMG-PEG 2K, DSPC, and cholesterol were dissolved in ethanol at the molar ratio of 50:1.5:10:38.5 to form the organic phase. The mRNA was dispersed in 25 mM sodium acetate to form the aqueous phase. These two phases were mixed using the benchtop microfluidic device at the volume ratio 3:1, and the total flow rate was 12 mL/min. The N:P ratio was 5.67:1. Then, the formed mRNA LNPs were buffer exchanged with 20 mM Tris (pH 7.4) and concentrated by ultracentrifuge tubes with a molecular weight cutoff of 30 kDa at 4 °C × 2,500 g × 60 minutes to a total lipid concentration of approximately 4 mg/mL. The formed mRNA LNPs were subjected to lyophilization. The LNPs were mixed and diluted to reach a final concentration of 200 ng/μL mRNA and an 8% w/v lyoprotectant (trehalose, sucrose, and mannitol). Then, the lyophilization process was carried out using a chamber benchtop freeze dryer (FreeZone Triad, Labconco). The aliquoted samples were frozen at -40 °C for 24 hours. The primary drying cycle was conducted under vacuum at -55 °C for 24 hours. Then, the temperature was increased gradually, and the secondary drying cycle was conducted at 10 °C for 4 hours. After drying, the lyophilized samples were sealed immediately and stored at different conditions for the stability test.

Table 1. LC/MS parameters

Parameter	Value		
Agilent 1290 Infinity II LC System			
Column	InfinityLab Poroshell 120 Phenyl-Hexyl, 2.1 × 50 mm, 1.9 μm		
Sample Thermostat	25 °C		
Mobile Phase A	90% MeOH in 10 mM ammonium acetate		
Mobile Phase B	90% ACN in 10 mM ammonium acetate		
Gradient	Time	%A	%B
	0.00	100	0
	2.00	100	0
	7.00	0	100
Stop Time	7 min		
Column Temperature	55 °C		
Flow Rate	0.4 mL/min		
Agilent 6545XT AdvanceBio LC/Q-TOF			
Ion Mode	Positive ion mode, dual AJS ESI		
Drying Gas Temperature	250 °C		
Drying Gas Flow	10 L/min		
Sheath Gas Temperature	300 °C		
Sheath Gas Flow	12 L/min		
Nebulizer	35 psi		
Capillary Voltage	3,500 V		
Nozzle Voltage	500 V		
Fragmentor Voltage	150 V		
Skimmer Voltage	65 V		
Octupole Ion Guide Voltage	750 V		
Reference Mass	922.009798		
Acquisition Mode	Data were acquired in Extended Dynamic Range (2 GHz)		
MS Mass Range	<i>m/z</i> 110 to 1,700		
Acquisition Rate	8 spectra/s		
MS Range	<i>m/z</i> 350 to 3,200		
MS Acquisition Rate	2 spectra/s		

Results and discussion

Previously, an LC/MS method to separate and identify different lipid classes employed in LNPs preparation¹¹ was developed using an accurate mass LC/Q-TOF system. The method demonstrated high-resolution separation of lipids with high precision.

In this study, the LC/MS method was used to examine the different mRNA-LNP formation production samples.

To quantify the lipids, first the linearity of the LC/MS method was assessed at a 0.1 to 1,000 pmol concentration range for four lipids: cholesterol, DMG-PEG 2K, SM-102, and DSPC. Calibration curves (Figure 1) were established on a

logarithmic scale by plotting log peak area versus log lipid concentration and fitted with a linear curve. The coefficients of determination $R^2 \geq 0.99$ demonstrated a strong linearity on the concentration ranges under study. The extracted ion chromatogram (EIC) overlay of the lipids employed for the quantitative determination is displayed in Figure 2.

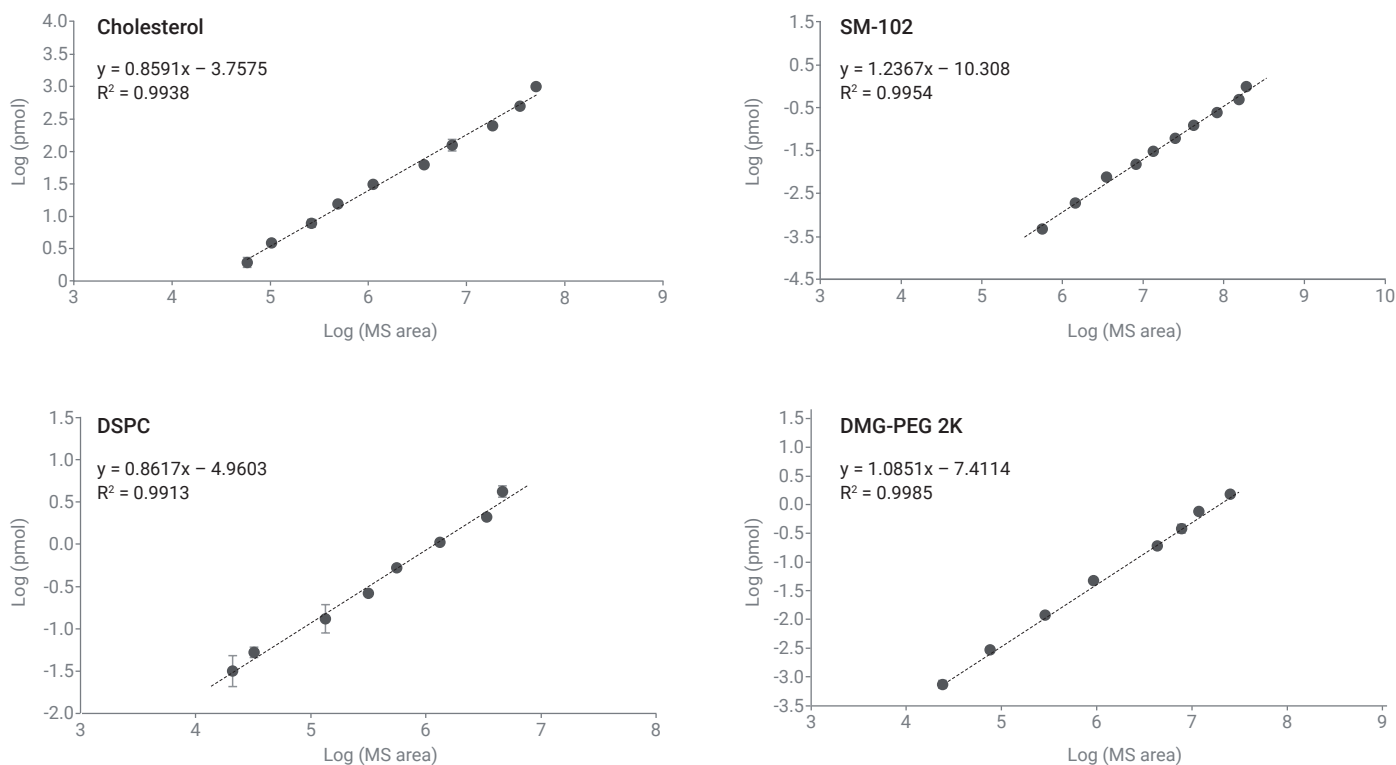


Figure 1. Calibration curve of lipid standards (n = 3).

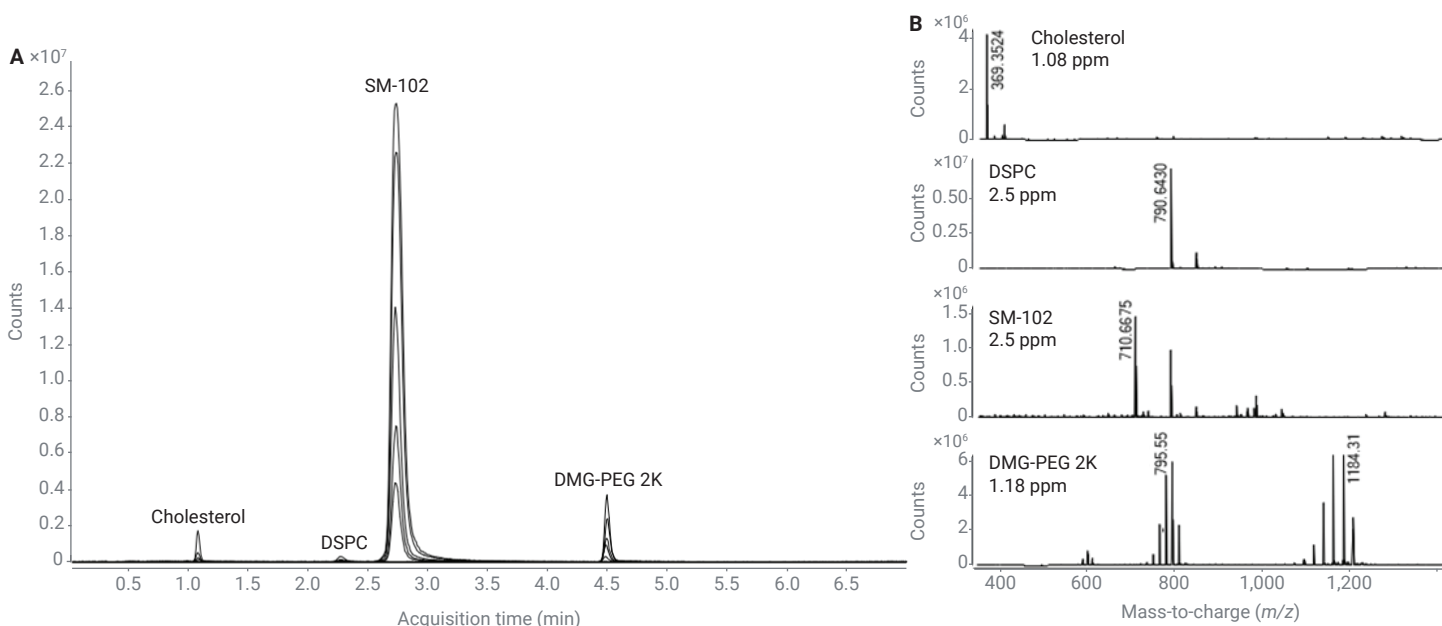


Figure 2. (A) Selected EIC overlay of lipid standards used to prepare LNPs. Cholesterol (20 to 625 pmol); DSPC, SM-102, DMG-PEG 2K (0.06 to 1 pmol). (B) Mass spectra of the lipid components.

The applicability of the LC/MS method was evaluated as a quality control tool by examining the lipid content in different mRNA LNP formulation conditions. The percent molar ratios of lipids determined by LC/MS under cryoprotectant conditions are displayed in Figure 3. The lipid content in all the samples was consistent with the targeted mRNA LNP formulation (SM-102:DMG-PEG 2K:DSPC:cholesterol at 50:1.5:10:38.5), demonstrating the reliability of the LC/MS method.

mRNA LNPs pose a significant challenge for transportation and long-term storage. To gain a deeper understanding of mRNA-loaded LNP stability and the impact of storage conditions, the stability of LNPs was evaluated with and without cryoprotectants (sucrose, trehalose, or mannitol) under the conditions of freezing and lyophilization processes at multiple time points over the course of four weeks.

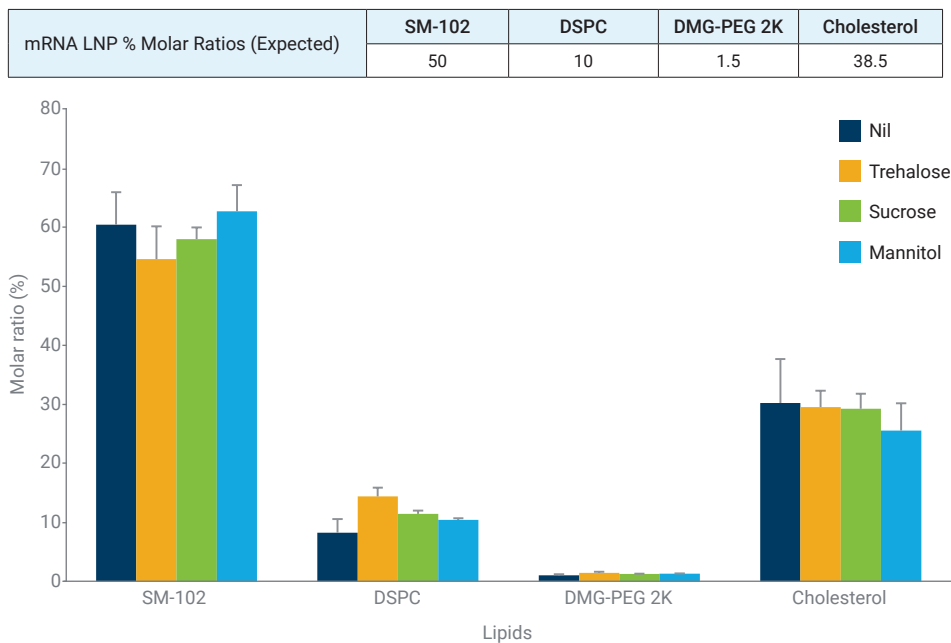


Figure 3. LC/MS analysis of lipid composition of mRNA-LNP lyophilized samples (stored at -70 °C). LNP encapsulating firefly luciferase mRNA (n = 3 measurements).

Both lyophilized and nonlyophilized mRNA LNPs with cryoprotectants were stored at 4, -20, and -70 °C. The samples were reconstituted with double distilled water and further diluted in MeOH for LC/MS analysis. At different time intervals—0 (control), 1, and 4 weeks—the stability of LNPs was evaluated by measuring the molar ratio of lipids.

Figure 4 depicts the percent molar ratio changes of the lipid composition of nonlyophilized mRNA LNPs under different formulation and storage conditions. At -70 °C, freshly prepared (control) LNPs maintained their lipid percent molar ratio, and there were no changes in lipid composition under the conditions of different cryoprotectants.

Regardless of cryoprotectants, however, significant lipid composition alterations occurred during different storage conditions (both 1 and 4 weeks at -20 and -70 °C). These results demonstrated that it is not advisable to store mRNA LNPs for extended periods of time in nonlyophilized conditions.

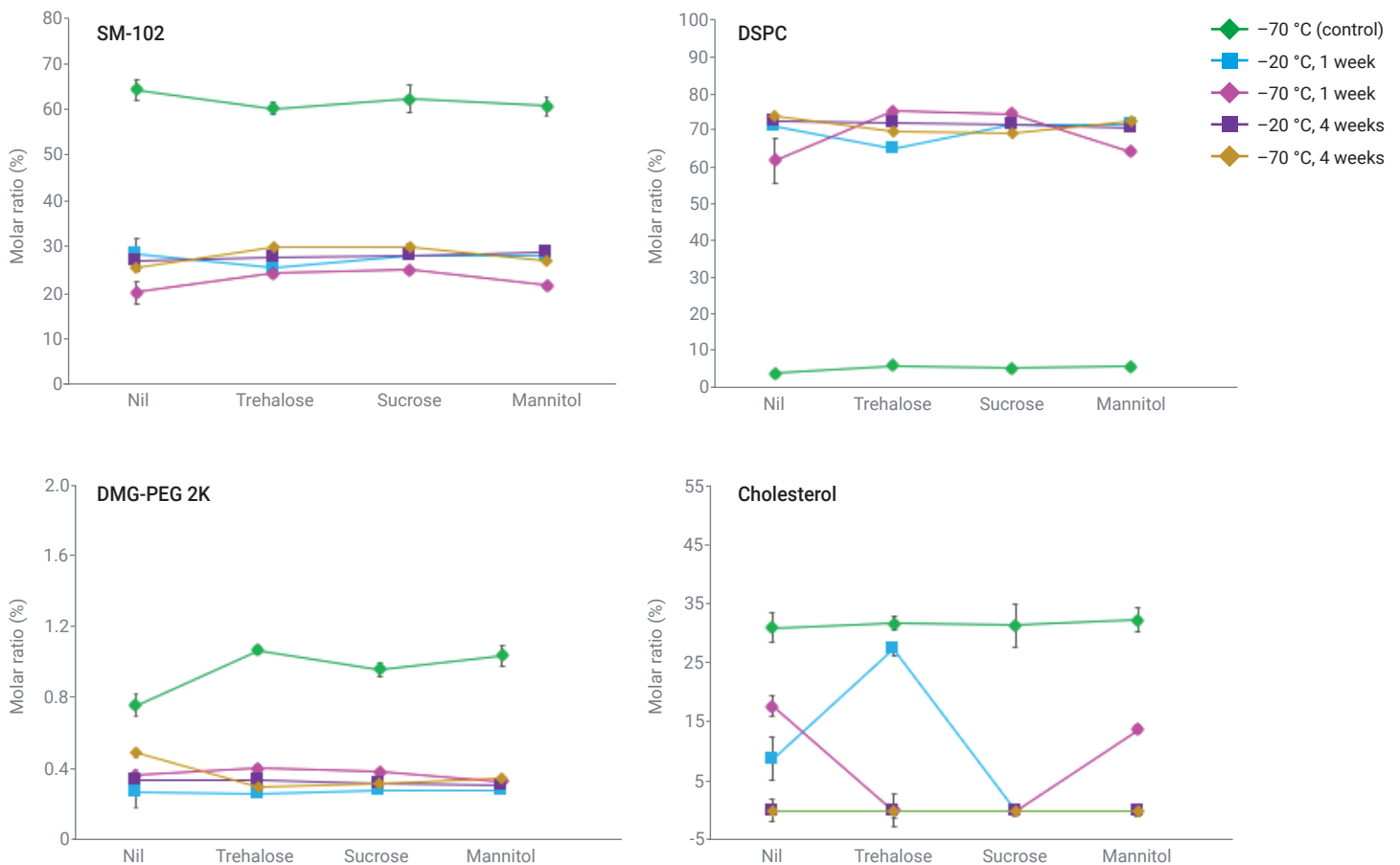


Figure 4. LC/MS analysis of nonlyophilized mRNA LNPs stored at -70 and -20 °C, for 0 (control), 1, and 4 weeks.

Since mRNA LNPs cannot be kept in aqueous conditions for an extended period, their stability under lyophilized conditions was examined. Figure 5 depicts the percent molar ratio changes of the lipid composition of postlyophilized mRNA LNPs under different formulation and storage conditions.

Again, the percent molar ratios of the lipid components of lyophilized mRNA LNPs were consistent with the target molar ratio used for the preparation of LNPs at $-70\text{ }^{\circ}\text{C}$. Lipid composition was maintained in sucrose and mannitol conditions at all the storage conditions, except for DMG-PEG 2K at 4 weeks at $4\text{ }^{\circ}\text{C}$, which showed decreased levels.

Storage of lyophilized LNPs for the 12 weeks tested did not result in any changes in the lipid composition, demonstrating the stability and integrity of lyophilized LNPs. In general, lyophilized conditions provided improved stability over nonlyophilized samples.

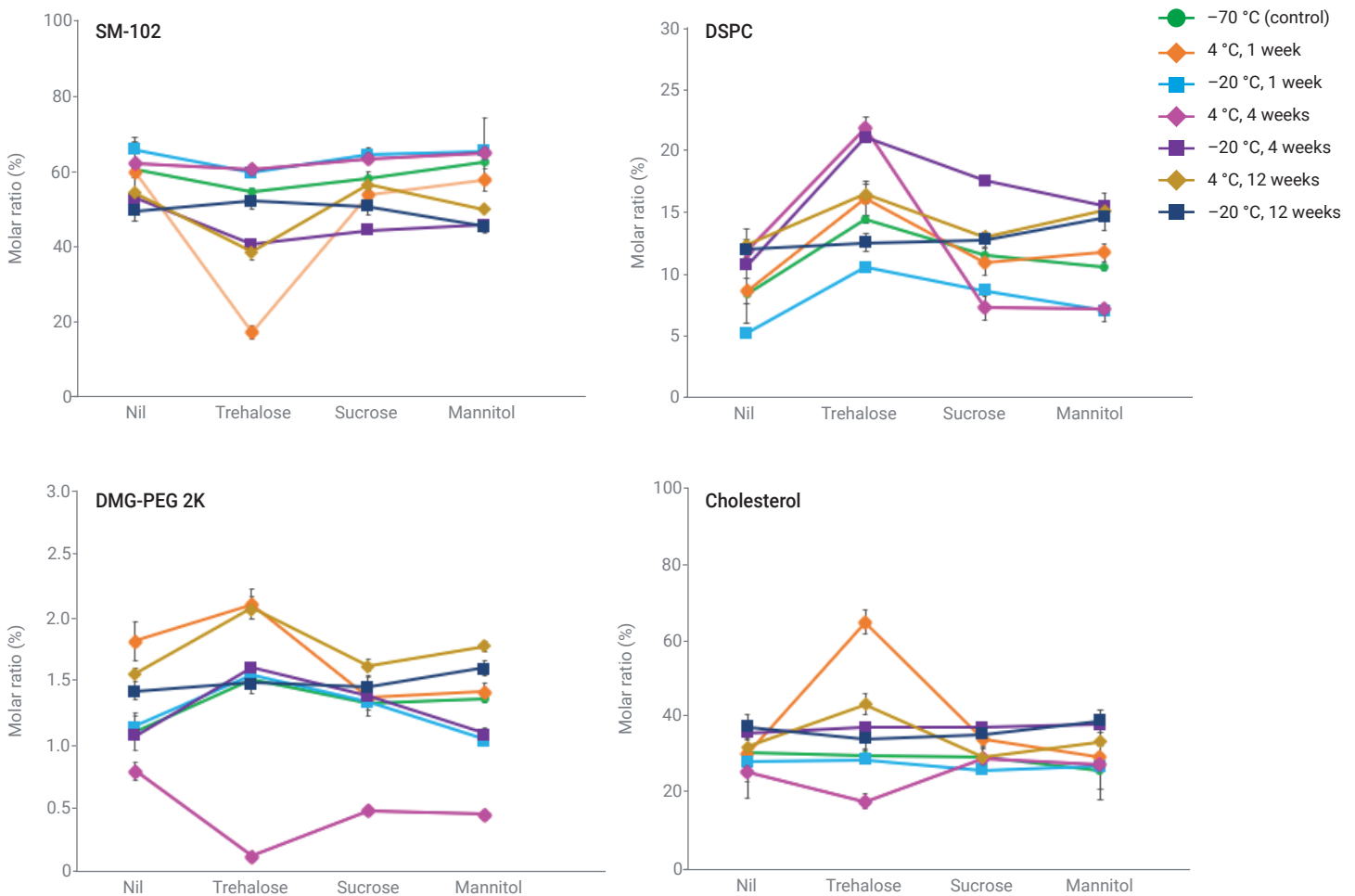


Figure 5. LC/MS analysis of postreconstitution of lyophilized mRNA LNPs stored at -70 , -20 , and $4\text{ }^{\circ}\text{C}$, for 0 (control), 1, 4, and 12 weeks.

Conclusion

In this application note, an LC/MS method using the Agilent 1290 Infinity II LC system and 6545XT AdvanceBio LC/Q-TOF was employed to analyze the lipid composition of LNPs. Further, the mRNA LNP stability was investigated under various formulation and storage conditions. The results demonstrate that lyophilized conditions exhibit greater stability compared to nonlyophilized samples. The described LC/MS method is ideal for determining the lipid content and identity, and monitoring the stability of LNP formulations, and can be applied to LNP development and the quality control process.

References

1. Hou, X.; Zaks, T.; Langer, R.; Dong, Y. Lipid Nanoparticles for mRNA Delivery. *Nature Reviews Materials* **2021**, *6*, 1078–1094. DOI: 10.1038/s41578-021-00358-0.
2. Gilleron, J.; Querbes, W.; Zeigerer, A.; Borodovsky, A.; Marsico, G.; Schubert, U.; Manygoats, K.; Seifert, S.; Andree, C.; Stöter, M. Image-Based Analysis of Lipid Nanoparticle-Mediated siRNA Delivery, Intracellular Trafficking and Endosomal Escape. *Nat. Biotechnol.* **2021**, *31*(7), 638–646. DOI: 10.1038/nbt.2612.
3. Reichmuth, A. M.; Oberli, M. A.; Jaklenec, A.; Langer, R.; Blankschtein, D. mRNA Vaccine Delivery Using Lipid Nanoparticles. *Ther. Deliv.* **2016**, *7*(5), 319–334. DOI: 10.4155/tde-2016-0006.
4. Albertsen, C. H.; Kulkarni, J. A.; Witzigmann, D.; Lind, M.; Petersson, K.; Simonsen, J. B. The Role of Lipid Components in Lipid Nanoparticles for Vaccines and Gene Therapy. *Adv. Drug Deliv. Rev.* **2022**, *188*, 114416. DOI: [10.1016/j.addr.2022.114416](#).
5. Jung, H. N.; Lee, S.; Lee, S.; Youn, H.; Im, H. Lipid Nanoparticles For Delivery of RNA Therapeutics: Current Status and The Role of In Vivo Imaging. *Theranostics* **2022**, *12*(17), 7509–7531. DOI: [10.7150/thno.77259](#).
6. Radomska-Soukharev, A. Stability of Lipid Excipients in Solid Lipid Nanoparticles. *Adv. Drug Deliv. Rev.* **2007**, *59*(6), 411–418. DOI: 10.1016/j.addr.2007.04.004.
7. Sommer, U.; Herscovitz, H.; Welty, F. K.; Costello, C. E. LC-MS-Based Method for the Qualitative and Quantitative Analysis of Complex Lipid Mixtures. *J. Lipid Res.* **2006**, *47*(4), 804–814. DOI: [10.1194/jlr.M500506-JLR200](#).
8. Varache M.; Ciancone M.; Couffin A.-C. Development and Validation of a Novel UPLC-ELSD Method for the Assessment of Lipid Composition of Nanomedicine Formulation. *Int. J. Pharm.* **2019**, *566*, 11–23. DOI: [10.1016/j.ijpharm.2019.05.038](#).
9. Li, Z.; Schariter, J. A.; Zhang, J.; Davis, J. C.; Leone, A. M. Application of Ultra-high Performance Liquid Chromatography for Chemical Characterization of Liposome-based Therapeutic Small-interfering RNA. *Am. Pharm.* **2010**, Rev. 13, 102.
10. Fekete, S.; Doneanu, C.; Addepalli, B.; Gaye, M.; Nguyen, J.; Alden, B.; Birdsall, R.; Han, D.; Isaac, G.; Lauber, M. Challenges and Emerging Trends in Liquid Chromatography-Based Analyses of mRNA Pharmaceuticals. *J. Pharm. Biomed. Anal.* **2023**, *224*, 115174. DOI: 10.1016/j.jpba.2022.1151.
11. Zhang, L.; Yang, Y. Y. Analysis of Lipid Nanoparticle Components Using an Agilent 6545XT AdvanceBio LC/Q-TOF, *Agilent application note*, publication number 5994-7520EN, **2024**.

www.agilent.com

This information is subject to change without notice.

DE72821094

© Agilent Technologies, Inc. 2024
Printed in the USA, August 1, 2024
5994-7655EN

Determination of mRNA Encapsulation Efficiency with the Agilent 1290 Infinity II Bio LC System

Authors

Aveline Neo, Suresh Babu C.V.,
and Zhi Ting Teo
Agilent Technologies, Inc.

Li Zhang and Yi Yan Yang
Bioprocessing Technology
Institute, Agency for Science,
Technology and Research
(A*STAR), Republic of
Singapore

Abstract

Encapsulation is an effective way of delivering pharmacologically active compounds to a specific site of action in the body. This study demonstrates the determination of encapsulation efficiency of F-luciferase mRNA-loaded lipid nanoparticle (LNP) using an alternative HPLC method other than the usual RiboGreen assay method. An ion-pair reversed-phase high-performance liquid chromatography (IP-RP-HPLC) method was developed using the Agilent 1290 Infinity II bio LC system with a diode array detector (DAD). Extracted mRNA was separated on the Agilent PLRP-S column with triethylammonium acetate (TEAA) as the ion-pairing reagent. This enabled the determination of the encapsulation efficiency of mRNA LNPs using IP-RP-HPLC.

Introduction

The encapsulation of in vitro transcription (IVT) mRNA with LNPs is a promising therapeutic modality with potential to treat a variety of diseases. The development of mRNA LNP therapeutics requires the implementation of robust quality control methods throughout the development process. The Agilent Fragment Analyzer system has been widely adopted to measure purity and size to ensure success throughout the IVT mRNA development workflow.¹ LNPs are a nonviral delivery vector that protect and ensure the delivery of the delicate RNA therapeutic to the site of action. They are synthesized by co-assembly of five distinct components: ionizable lipid, helper phospholipids, polyethylene glycol (PEG)-lipid, sterol, and nucleic acid.² High-flow-rate microfluidic mixing involves the fast mixing of aqueous (containing nucleic acid cargo) and organic (containing lipid mixture) phases, which results in the formation of LNPs with low polydispersity and high encapsulation efficiency.³

The encapsulation of the mRNA into LNPs is routinely assessed using the RiboGreen assay⁴ early in development, in part because of the high-throughput functionality of this method using a detection platform such as the Agilent BioTek Synergy multimode reader or Agilent BioTek Cytation multimode microplate reader.⁵ One of the limitations of this method is that it cannot distinguish between intact and other RNA impurities.⁶ Characterization of nucleic acid encapsulation efficiency is one of the critical quality attributes to determine the success of an mRNA-LNP formation.² The ability to distinguish between full-length and fragment-encapsulated improves mRNA-LNP characterization. IP-RP-HPLC is a versatile analytical method that is used to separate and quantify RNA molecules^{7,8}, distinguishing RNA impurities from intact RNA. This method uses the separation principle based on the complex formation between the polyanionic nucleic acid and positively charged ion-pairing reagent.⁶ The neutral and relatively hydrophobic complexes were then separated using RP-HPLC.

In this study, the LNP-extracted F-luciferase mRNA by IP-RP-HPLC was analyzed using the 1290 Infinity II bio LC system with a DAD. The concentration of the extracted mRNA was estimated using the calibration curve of F-luciferase mRNA and subsequently, the encapsulation efficiency was determined.

Experimental

Equipment

Analysis of F-luciferase mRNA was performed using 1290 Infinity II bio LC system with the following components. The LC system was operated using Agilent OpenLab CDS version 2.7 or later versions.

- Agilent 1290 Infinity II bio high-speed pump (G7132A)
- Agilent 1290 Infinity II bio multisampler (G7137A)
- Agilent 1290 Infinity II multicolumn thermostat (G7116B)
- Agilent 1290 Infinity II diode array detector (with variable slit) (G7117B)
- Agilent Max-Light cartridge cell, 10 mm, 1.0 μ L, 60 bar (G4212-60008)

Reagents and materials

Chemicals: All solvents used were LC grade. Acetonitrile and isopropanol were purchased from JT Baker (Phillipsburg, NJ, U.S.), and methanol and TEAA were purchased from Sigma-Aldrich (St. Louis, MO, U.S.). Fresh ultrapure water was obtained from a Milli-Q Integral system (Millipak, Merck-Millipore, Billerica, MA, U.S.) equipped with a 0.22 μ m membrane point-of-use cartridge.

Preparation of mRNA-LNPs:

mRNA-LNPs were produced using the same lipid composition as Spikevax, the COVID-19 vaccine pioneered by Moderna. mRNA was in vitro transcribed from a PCR-amplified dsDNA template, purified using spin columns, and then dissolved in 1 mM sodium acetate buffer (pH 4.7) for the stock solution. For the Spikevax formulation, heptadecan-9-yl 8-((2-hydroxyethyl) (6-oxo-6-(undecyloxy)hexyl)amino) octanoate (SM-102), 1,2-distearoyl-sn-glycero[1]3-phosphocholine (DSPC), 1,2-dimyristoyl-rac-glycero[1]3-methoxypolyethylene glycol-2000 (DMG-PEG 2K), and cholesterol, which were supplied from MedChemExpress, were dissolved in ethanol at the molar ratio of 50:1.5:10:38.5 to form the organic phase. The mRNA was dispersed in 25 mM sodium acetate to form the aqueous phase. These two phases were mixed using the benchtop microfluidic device at the volume ratio 3:1, and the total flow rate was 12 mL/min. The N:P ratio was 5.67:1. The formed mRNA LNPs were then buffer exchanged with 20 mM Tris (pH 7.4) and concentrated in ultracentrifuge tubes with a molecular weight cutoff of 30 kDa at 4 °C × 2,500 g × 60 minutes to a total lipid concentration of approximately 4 mg/mL. The formed mRNA-LNPs were subjected to lyophilization with or without cryoprotectants such as mannitol and trehalose.

Preparation of F-luciferase mRNA:

F-luciferase mRNA was synthesized using the HiScribe T7 High Yield RNA synthesis kit for mRNA synthesis from New England BioLabs (Ipswich, Massachusetts, U.S.).

Concentration of F-luciferase mRNA:

The concentration of the synthesized F-luciferase mRNA was determined using the Agilent Cary 60 UV-Vis spectrophotometer (part number G6860A). The concentration of the mRNA was calculated using Beer-Lambert's law. The calibration curve for F-luciferase mRNA was prepared for concentrations of 4.35, 8.7, 13, 34.8, and 43.5 µg/mL.

Extraction of mRNA from mRNA LNP:

mRNA was extracted from mRNA LNP using the isopropanol precipitation method.⁹ For the nonlyophilized samples, 20 µL of the sample was diluted 10-fold in 180 µL ammonium acetate (60 mM) in isopropanol. For lyophilized samples, 30 µL of nuclease-free water was added before taking 20 µL of the dissolved samples and diluting 10-fold in 180 µL ammonium acetate (60 mM) in isopropanol. The samples were vortexed briefly and centrifuged at 14,000 × g for 15 minutes at 4 °C. The supernatant was discarded, and the pellet was washed with 1 mL isopropanol, vortexed, and centrifuged at 4 °C. The pellet was dried and resuspended in 100 µL nuclease-free water at room temperature.

LC analysis**Table 1.** IP-RP-HPLC method for analysis of mRNA.

Parameter	Value																				
Column	Agilent PLRP-S column, 4000Å, 2.1 × 150 mm, 8 µm (p/n PL1912-3803)																				
Mobile Phase	A) 100 mM TEAA, pH 7 B) 100 mM TEAA, pH 7 in acetonitrile																				
Gradient	<table border="1"> <thead> <tr> <th>Time (min)</th> <th>%B</th> </tr> </thead> <tbody> <tr><td>0.0</td><td>10</td></tr> <tr><td>1.5</td><td>10</td></tr> <tr><td>7.5</td><td>15</td></tr> <tr><td>9.5</td><td>15</td></tr> <tr><td>16</td><td>25</td></tr> <tr><td>20</td><td>25</td></tr> <tr><td>25</td><td>90</td></tr> <tr><td>27</td><td>90</td></tr> <tr><td>27.1</td><td>10</td></tr> </tbody> </table> Stop time: 30 min Post time: 3 min	Time (min)	%B	0.0	10	1.5	10	7.5	15	9.5	15	16	25	20	25	25	90	27	90	27.1	10
Time (min)	%B																				
0.0	10																				
1.5	10																				
7.5	15																				
9.5	15																				
16	25																				
20	25																				
25	90																				
27	90																				
27.1	10																				
Flow Rate	0.3 mL/min																				
Temperature	50 °C																				
Detection (DAD)	260 nm, 4 nm bandwidth, and reference wavelength 360 nm, 40 nm bandwidth																				
Peak Width	> 0.013 min (0.25 s response time) (20 Hz)																				
Injection	5 µL, use vial/well bottom sensing Draw speed 100 µL/min; Ejection speed 400 µL/min																				
Needle Wash	Flush port, 5 s 50% Methanol (50:50; v:v)																				

Calculation of encapsulation efficiency

The concentration of LNP-extracted mRNA was measured against the calibration curve generated with the F-luciferase mRNA. Using Equation 1, the encapsulation efficiency of the mRNA loaded LNP samples was calculated.⁴

$$\text{Encapsulation Efficiency} = \frac{\text{Concentration of LNP - extracted mRNA}}{\text{Concentration of mRNA used in encapsulation}} \times 100\%$$

Equation 1.

Results and discussion

An IP-RP-HPLC method was developed on the PLRP-S column. Gradient separation conditions were optimized for separation of the F-luciferase mRNA and minor impurity. Figure 1 shows the chromatogram of F-luciferase mRNA at 43.5 µg/mL. The chromatogram clearly indicates the successful elution of the F-luciferase mRNA peak at a retention time of 13.2 minutes. Additionally, the presence of a smaller peak, eluted at 10.6 minutes, suggests the possible presence of an mRNA fragment.

The calibration curve for F-luciferase mRNA described indicates a robust analytical method with high precision and accuracy. The concentration range of 4.35 to 43.5 µg/mL covers a suitable span for quantification, and the limit of quantification being less than 5 µg/mL is quite sensitive for most experimental needs. The precision of the analysis (n = 6) is excellent, with retention time %RSD being less than 1% and area %RSD less than 10%, ensuring reproducibility and reliability of the results. Moreover, the linearity of the calibration curve with an R² value greater than 0.997 demonstrates a strong direct relationship between the concentration of F-luciferase mRNA and the detector response. This level of linearity is essential for accurate quantification across the specified range. The calibration curve, as shown in Figure 2A, is a critical component for the validation of the analytical method and supports the integrity of the data. Figure 2B shows the overlaid chromatograms of F-luciferase mRNA at different calibration levels.

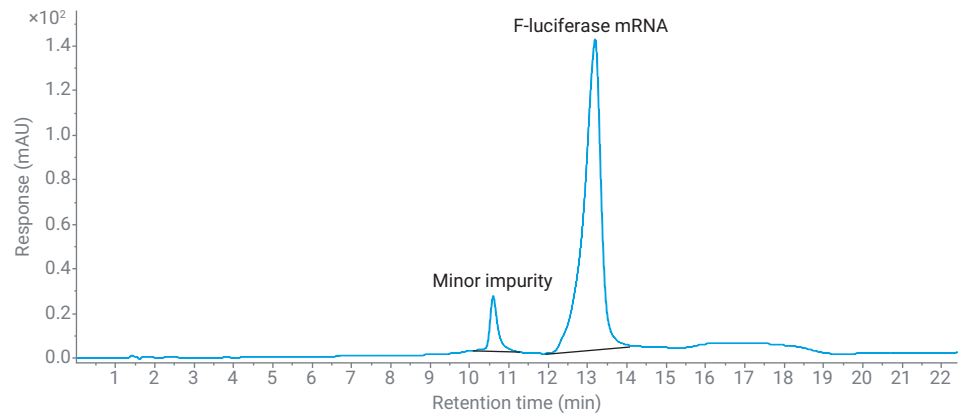


Figure 1. Representative HPLC chromatogram of F-luciferase mRNA (43.5 µg/mL) analyzed on the Agilent PLRP-S column at 50 °C.

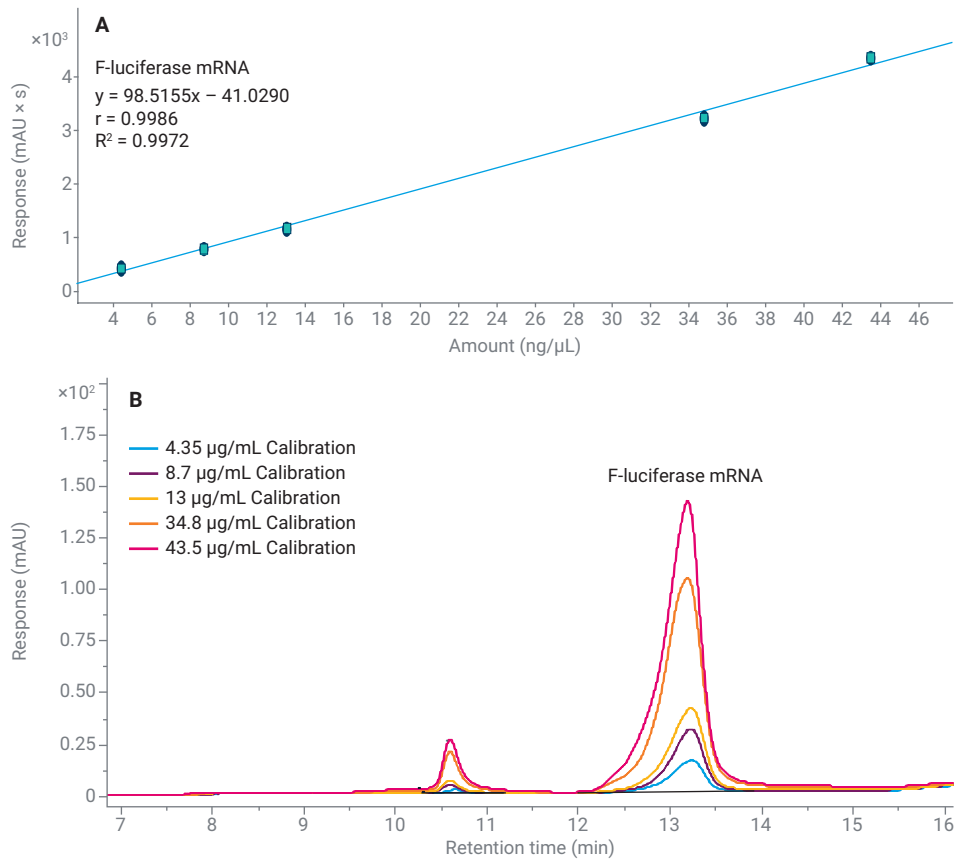


Figure 2. (A) Calibration curve of free F-luciferase mRNA from 4.35 to 43.5 µg/mL. (B) Overlaid chromatograms showing the peaks at different calibration levels.

Figure 3 shows the overlaid chromatograms of extracted mRNA from lyophilized mRNA LNP without cryoprotectant (NIL) and free F-luciferase mRNA. The LNP-extracted F-luciferase mRNA peak elutes at the same retention time as the free mRNA, confirming the size of F-luciferase mRNA and demonstrating the applicability of the method for measuring the concentration of mRNA.

To estimate the encapsulation efficiency for the F-luciferase mRNA-loaded LNP, the concentration of the LNP-extracted mRNA was required to be expressed as a percentage of concentration of mRNA used in the encapsulation. The concentration of the LNP-extracted mRNA was estimated from the calibration curve. The encapsulation efficiency for the LNP, with or without lyophilization, and with or without cryoprotectants, was calculated.

The encapsulation efficiency for the respective cryoprotectants, lyophilized or nonlyophilized, is plotted in a bar graph in Figure 4. Lyophilized LNPs show higher encapsulation efficiency than nonlyophilized LNPs. The encapsulation efficiency is also higher with cryoprotectant than without cryoprotectant. mRNA of lyophilized LNPs with cryoprotectant may be more stable during storage compared to nonlyophilized LNPs without cryoprotectant.

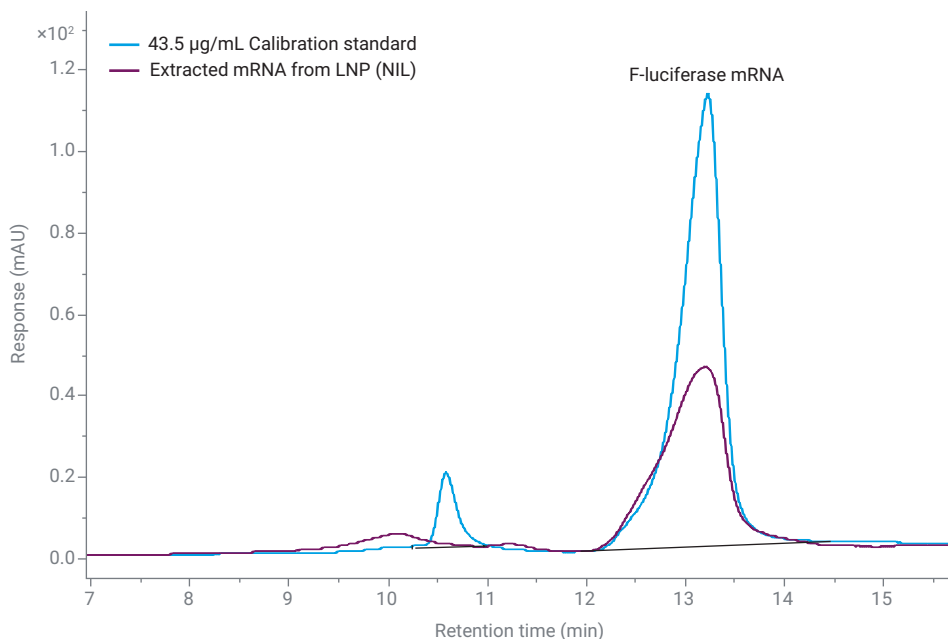


Figure 3. Overlaid chromatograms of 43.5 µg/mL calibration standard and extracted F-luciferase mRNA from lyophilized mRNA LNP without cryoprotectant (NIL).

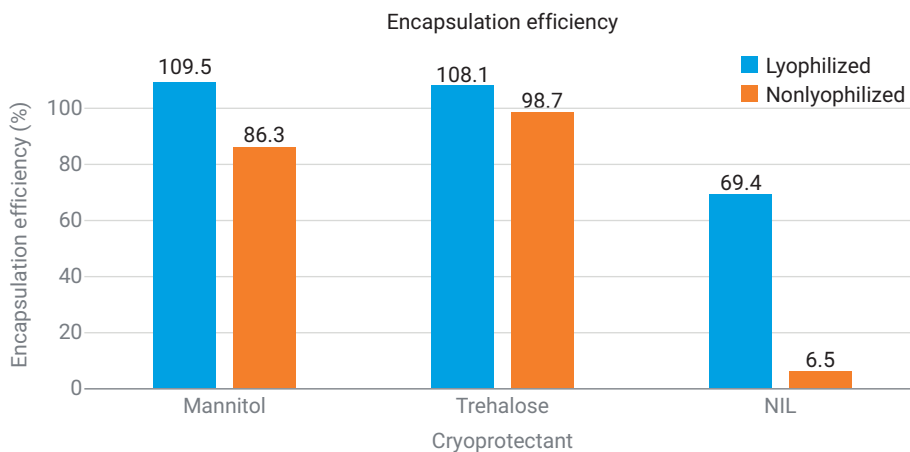


Figure 4. Encapsulation efficiency of lyophilized and nonlyophilized mRNA-LNPs with or without cryoprotectants.

Conclusion

This study presents an IP-RP-HPLC method for detecting F-luciferase mRNA and highlights the use of isopropanol extraction of lipid nanoparticles (LNPs) to analyze mRNA. This method represents an alternative approach to the standard RiboGreen assay to determine encapsulation efficiency, using the Agilent 1290 Infinity II bio LC system and the Agilent PLRP-S column. This method has added advantages for identifying impurities formed during mRNA-lipid reactions or mRNA synthesis. Such advancements in analytical techniques are crucial for progress in nanomedicine, particularly for the optimization of mRNA delivery systems in therapeutic applications.

References

1. Best Practices for Analysis of In Vitro Transcribed (IVT) mRNA Using the Agilent Fragment Analyzer Systems. *Agilent Technologies technical overview*, publication number 5994-5927EN, **2023**.
2. Schober, G. B.; Story, S.; Arya, D. P. A Careful Look at Lipid Nanoparticle Characterization: Analysis of Benchmark Formulations for Encapsulation of RNA Cargo Size Gradient. *Sci. Rep.* **2024**, *14*(1), 2403.
3. Maeki, M.; Uno, S.; Niwa, A.; Okada, Y.; Tokeshi, M. Microfluidic Technologies and Devices for Lipid Nanoparticle-Based RNA Delivery. *JCR.* **2022**, *344*, 80-96.
4. USP. Analytical Procedures for mRNA Vaccine Quality, **2022**. Accessed May 10, 2022. <https://www.usp.org/mrna>
5. Carrasco, M. J.; Alishetty, S.; Alameh, M. G.; Said, H.; Wright, L.; Paige, M.; Soliman, O.; Weissman, D.; Cleveland IV, T.E.; Grishaev, A.; *et al.* Ionization and Structural Properties of mRNA Lipid Nanoparticles Influence Expression in Intramuscular and Intravascular Administration. *Commun. Biol.* **2021**, *4*(1), 956.
6. Lokras, A.; Chakravarty, A.; Rades, T.; Christensen, D.; Franzyk, H.; Thakur, A.; Foged, C. Simultaneous Quantification of Multiple RNA Cargos Co-Loaded into Nanoparticle-Based Delivery Systems. *Int. J. Pharm.* **2022**, *626*, 122171.
7. Currie, J.; Dahlberg, J. R.; Lundberg, E.; Thunberg, L.; Eriksson, J.; Schweikart, F.; Nilsson, G. A.; Oernskov, E. Stability Indicating Ion-Pair Reversed-Phase Liquid Chromatography Method for Modified mRNA. *JPBA.* **2024**, *1*(245), 116144.
8. Azarani, A.; Hecker, K. H. RNA Analysis by Ion-Pair Reversed-Phase High Performance Liquid Chromatography. *Nucleic Acids Res.* **2001** Jan 15, *29*(2), e7-.
9. Packer, M.; Gyawali, D.; Yerabolu, R.; Schariter, J.; White, P. A Novel Mechanism for the Loss of mRNA Activity in Lipid Nanoparticle Delivery Systems. *Nat. Commun.* **2021**, Nov. 22, *12*(1), 6777.

Quality Assurance in In Vitro Transcribed (IVT) RNA Vaccine Development using Agilent Automated Electrophoresis Instruments

Author

Whitney Pike
and Lisa Houston,
Agilent Technologies

Abstract

Highly adaptable, efficient, and ideally suited for fast production, in vitro transcribed (IVT) RNA vaccines have emerged as a valuable tool against infectious diseases. The exceptionally successful IVT RNA vaccines against SARS-CoV-2 were built on years of research into mRNA. As infectious diseases rise in number and spread rapidly across the world, there is an urgent need for expeditious development and comprehensive distribution of vaccines against both known and previously unknown pathogens. Correspondingly, these vaccines drive a rising need for robust, reliable, rapid, and high-throughput quality control (QC) testing. The Agilent automated electrophoresis systems offer platforms for nucleic acid QC. Agilent instruments are used in QC during vaccine production and are ideally suited for in-process quality checks, and purity and integrity testing of the final vaccine.

Introduction

Pandemics

Pandemics such as COVID-19 are not new phenomena: since the first agricultural revolution 12,000 years ago during which humans settled into villages to cultivate crops and domesticate animals, societies became more sedentary and infectious diseases spread rapidly¹. Among the most lethal pandemics are the Justinian Plague (541 AD), which was responsible for at least 30 million deaths, and the Black Death (1347–1351 AD), which killed approximately 50 million people^{1,2}. About a century ago, the 1918-1919 influenza pandemic, known as the Spanish Flu, took a deadly toll¹. Still today, pandemics continue to present a risk. In the past two decades, several pandemics emerged: H1N1 “swine” influenza (2009), chikungunya (2014), and Zika (2015), as well as pandemic-like emergences of Ebola fever over large parts of Africa (2014 to present)¹. The timing and fatalities of these and other pandemics is shown in Figure 1.

Zoonotic diseases

About 60 percent of human infections are estimated to have an animal origin, including some with deadly consequences such as influenza, smallpox, measles, and bubonic/pneumonic plague³. One such infection, COVID-19, is caused by the novel coronavirus SARS-CoV-2. A variety of coronaviruses exist, which cause illnesses ranging from the common cold to more severe acute respiratory diseases. Of all new and emerging human infectious diseases, some 75 percent “jump species” from animals to people⁴.

History of vaccines, vaccine development

As early as 1000 AD, cowpox inoculations were performed in China to create immunity against smallpox. It was over 800 years after the first smallpox vaccine was used before the next vaccines, against rabies and cholera, were developed⁵. Additional vaccines were developed through the 1930s against many diseases, including diphtheria, tetanus, plague, and tuberculosis. In the mid-twentieth century, research and discovery led to the development of several vaccines against common childhood diseases such as measles, mumps, and rubella⁵. The use of vaccines has led to the successful eradication of diseases such as smallpox. While the earliest vaccines used trial-and-error approaches, current vaccines are based on increasing knowledge of microbiology, virology, mechanisms of infection and immunity, and the biology of the infecting organisms, including basic biochemical structures and genetic sequences⁵.

As the possibility of new diseases continue to arise and with worldwide spread of severe infections, which can occur rapidly, there is the potential urgent need for expeditious development and comprehensive distribution of new vaccines⁶. Recent advances in vaccine development, leading to the highly successful COVID-19 vaccines, were made possible by decades of research into mRNA, including its properties and immunogenicity. This research could easily be adapted to other pathogens, including those yet unknown, expanding future vaccine production.

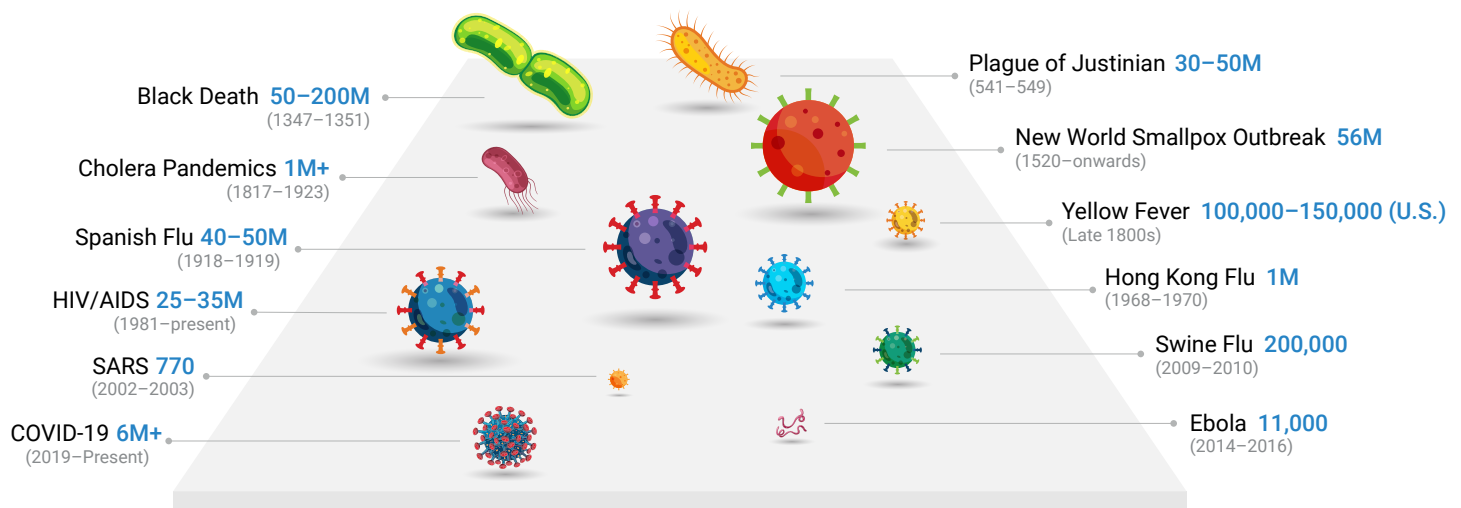


Figure 1. Infectious disease outbreaks over time. The approximate numbers of deaths are given (blue) along with the time of each pandemic. The COVID-19 pandemic is ongoing and has claimed over 6 million lives worldwide as of January 2022. Adapted from LePan, N. Visualizing the History of Pandemics. Visual Capitalist. 2020 Infographic: The History of Pandemics, by Death Toll (visualcapitalist.com).

mRNA: key discoveries

Research into RNA has been ongoing for decades. Notably, the development of synthetic genes led to the exploration of in vitro transcribed (IVT) RNA in therapeutic applications, including vaccination approaches for infectious disease. However, the therapeutic use of IVT RNA has been hampered by two major hurdles. First, IVT RNA activates the host immune response which can destroy foreign RNA prior to translation. Second, the large size and negative charge of mRNA impedes diffusion of mRNA across cell membranes. The research into mRNA over the past two decades has helped overcome these challenges and laid the foundation for IVT RNA therapies⁷ (Figure 2).

Two pioneering scientists in the advancement of mRNA vaccine technology are Dr. Katalin Karikó and Dr. Drew Weissman. Karikó et al. found that mRNAs containing pseudouridine (Ψ), a naturally occurring modified nucleoside, were translated more efficiently and showed less activation of the

host immune response^{8,9}. The authors, therefore, suggested that modification within the foreign RNA might allow the RNA to avoid host immune activation. Additionally, the large size and negative charge of mRNA makes it difficult to deliver mRNA into a cell, necessitating the use of a vehicle to transport IVT RNA. Years of research into the use of lipid nanoparticles (LNPs) as mRNA carriers led to their use as efficient and safe delivery vehicles for IVT RNA vaccines^{10,11,12}. Today, modified RNA and LNPs such as these are being used for the Pfizer-BioNTech and Moderna COVID-19 vaccines¹³.

Translational and clinical research on mRNA-based vaccines progressed steadily, from animal models in the 1990s onwards, to the first human cancer immunotherapy trial using direct injection of mRNA in 2009. The first successful demonstration of an infectious disease vaccine in humans was with a rabies vaccine in a clinical trial begun in 2013¹⁴. These and other key advancements in mRNA research are shown in Figure 2.

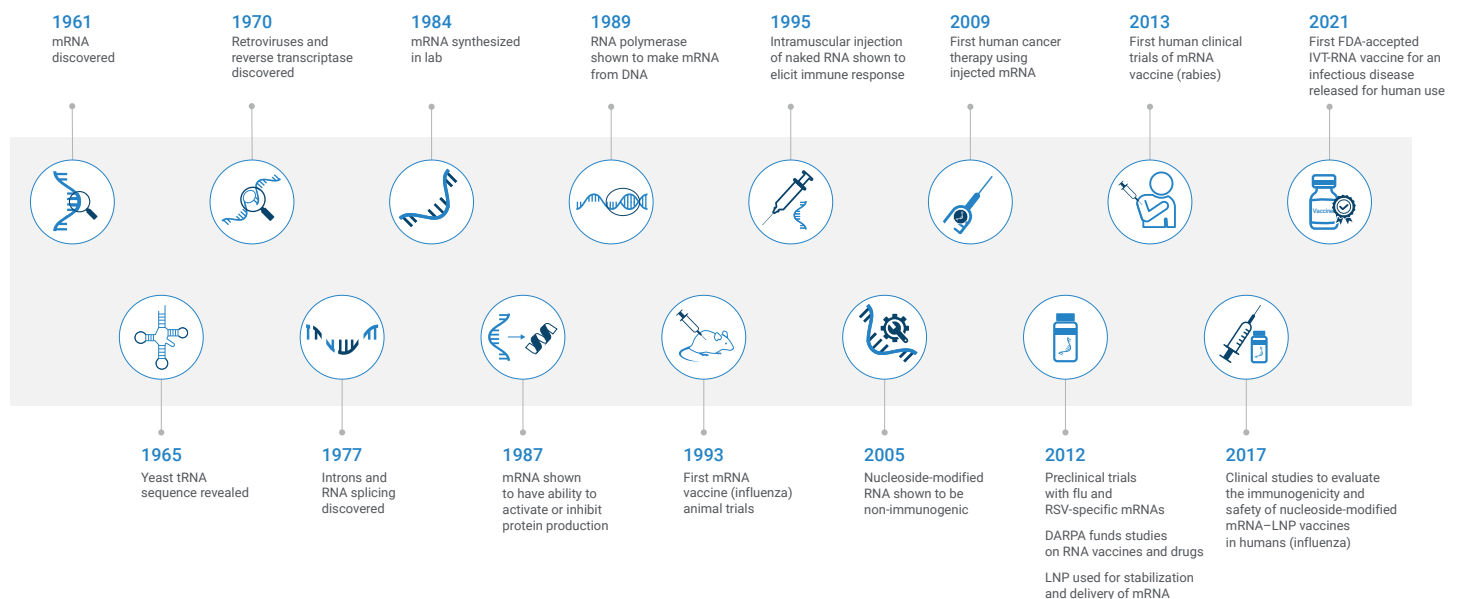


Figure 2. Important RNA research milestones. Timeline of some key achievements in RNA research which contributed to the development of IVT RNA vaccines against COVID-19.

Collectively, these findings laid the foundation for the design of therapeutic mRNAs. Currently, there are almost 2,000 clinical trials, worldwide, involving the use of therapeutic mRNAs¹⁵. These trials range from protein replacement therapies to vaccines against various viruses including SARS-CoV-2¹⁵. Figure 3 shows other potential therapeutic applications of IVT RNA, including cancer immunotherapies and infectious disease vaccines.

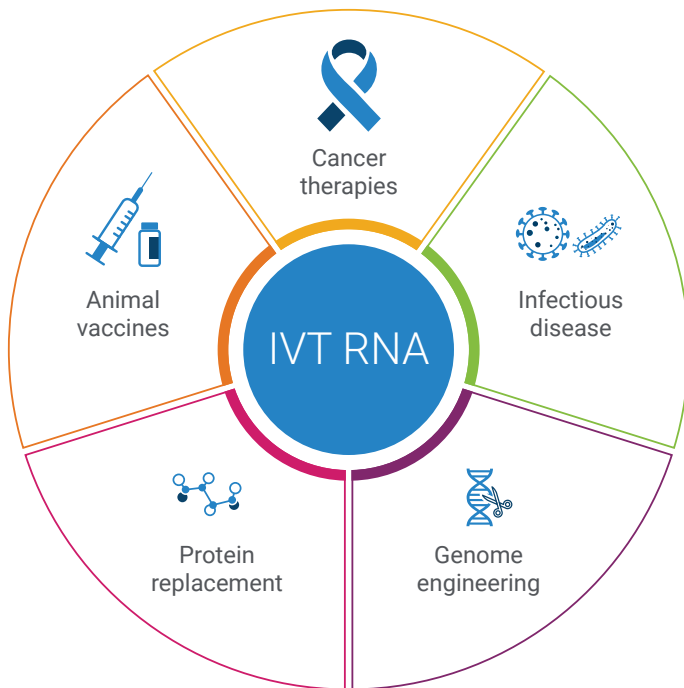


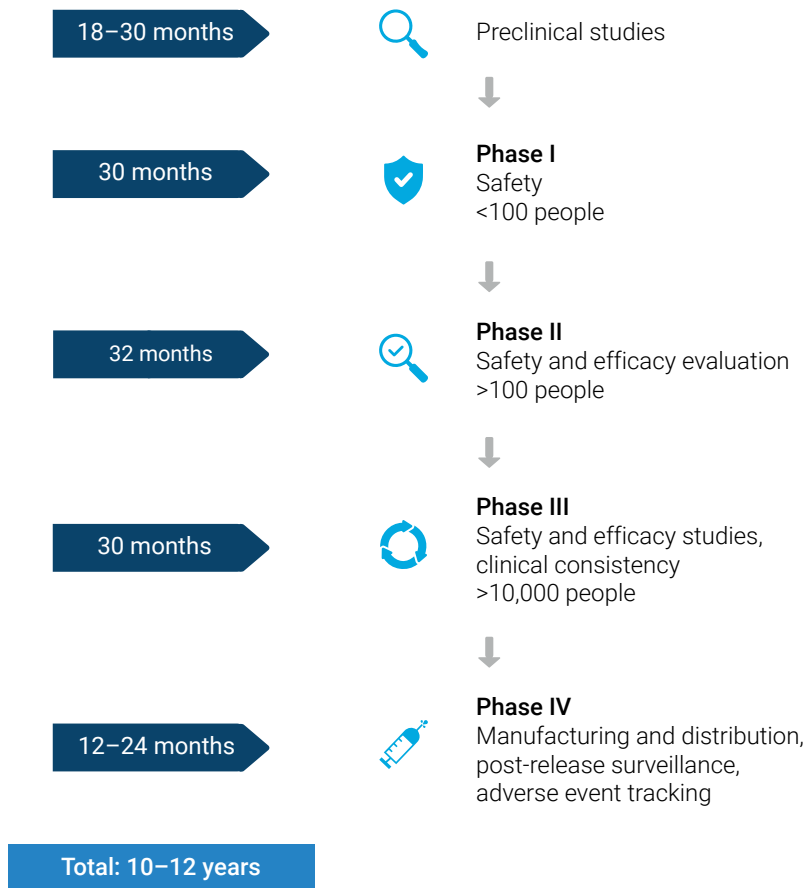
Figure 3. Potential therapeutic applications of IVT RNA. IVT RNA therapies involve introducing genetic material like mRNA, which is a template for a particular protein, into a cell where it can prevent or alter a disease⁷. Some potential therapeutic applications of IVT RNA are depicted.

Vaccine development: conventional vaccines vs. COVID-19 mRNA vaccines

Vaccine development is traditionally a complex and time-consuming process that typically takes 10 to 12 years¹⁶. As illustrated in Figure 4, vaccine development usually begins with an exploratory stage focusing on basic research and computational modeling to identify potential natural or synthetic antigens as vaccine candidates. Preclinical studies generally take about 18 to 30 months, and human clinical trials can take several years. After completion of these trials, the vaccine safety and efficacy data are reviewed for approval by regulatory bodies, such as the Food and Drug Administration (FDA) in the US or the European Medicines Agency in the EU¹⁷.

In COVID-19 vaccine development, the 10 to 12-year timeline was significantly reduced to 12 to 24 months¹⁶ (Figure 4). A large portion of this reduction in time was made possible by decades of research into RNA and using the data from the preclinical development of vaccine candidates for SARS-CoV-1 and MERS-CoV, thus omitting the initial exploratory phase¹⁶. Additionally, overlapping clinical trial phases and Emergency Use Authorization (EUA) contributed to the rapid development of the COVID-19 vaccine¹⁶.

Conventional vaccine development



COVID-19 IVT RNA vaccine development

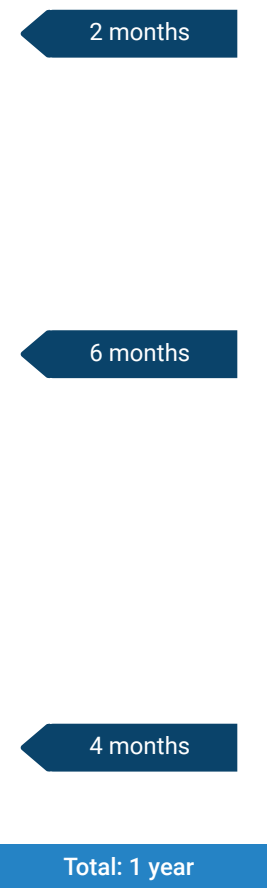


Figure 4. Timeline of traditional and COVID-19 IVT RNA vaccine development. Conventional vaccine development takes 10-12 years (left) compared to the COVID-19 IVT RNA vaccine, which was developed in one year (right). Data obtained from decades of research into RNA, and the preclinical development of vaccines against SARS-CoV-1 and MERS-CoV, along with overlapping clinical trials and Emergency Use Authorization (EUA) were key in the substantially reduced time needed to develop the COVID-19 IVT RNA vaccines.

mRNA vaccines and COVID-19

When the deadly SARS-CoV-2 virus emerged in late 2019 and the pandemic spread rapidly around the world, the culmination of decades-long research into mRNA led to the rapid development of the highly successful COVID-19 mRNA vaccines¹⁷. The development of these vaccines started once the viral genome sequence was available. A mere two months after sequence identification of SARS-CoV-2, Moderna started clinical testing of its novel mRNA-based vaccine mRNA-1273¹⁸. On 11 December 2020, less than a year after SARS-CoV-2 was identified, the first vaccine consisting of mRNA encoding the spike protein of the virus was granted EUA by the US FDA: BNT162b2, developed by Pfizer-BioNTech¹⁹. A week later, Moderna received an EUA for its vaccine²⁰.

As of January 2022, 59.6% of the world population has received at least one dose of a COVID-19 vaccine, including, viral vector, inactivated virus, live attenuated virus, DNA, and mRNA vaccines^{7,21}. Over 11 billion doses of the COVID-19 vaccines were distributed in 2021, approximately 27% of these being mRNA vaccines^{22,23}. There are still over three billion individuals worldwide yet to receive a single vaccine dose²². Additionally, most fully vaccinated individuals have yet to receive a booster shot²². It is likely that more vaccine will need to be produced in 2022 than was produced in 2021.

Vaccine production

The steps to produce IVT RNA used in mRNA vaccines are well established: the target pathogen is identified and sequenced, candidate antigen sequences are designed, and plasmid DNA vectors prepared. This is followed by synthesis of the target RNA from DNA templates, generated by linearization of the purified plasmid. This established procedure, shown in Figure 5, is easily adapted to novel sequences. For example, both Pfizer-BioNTech and Moderna are expecting to release Omicron-specific vaccines in March of 2022^{25, 26}.

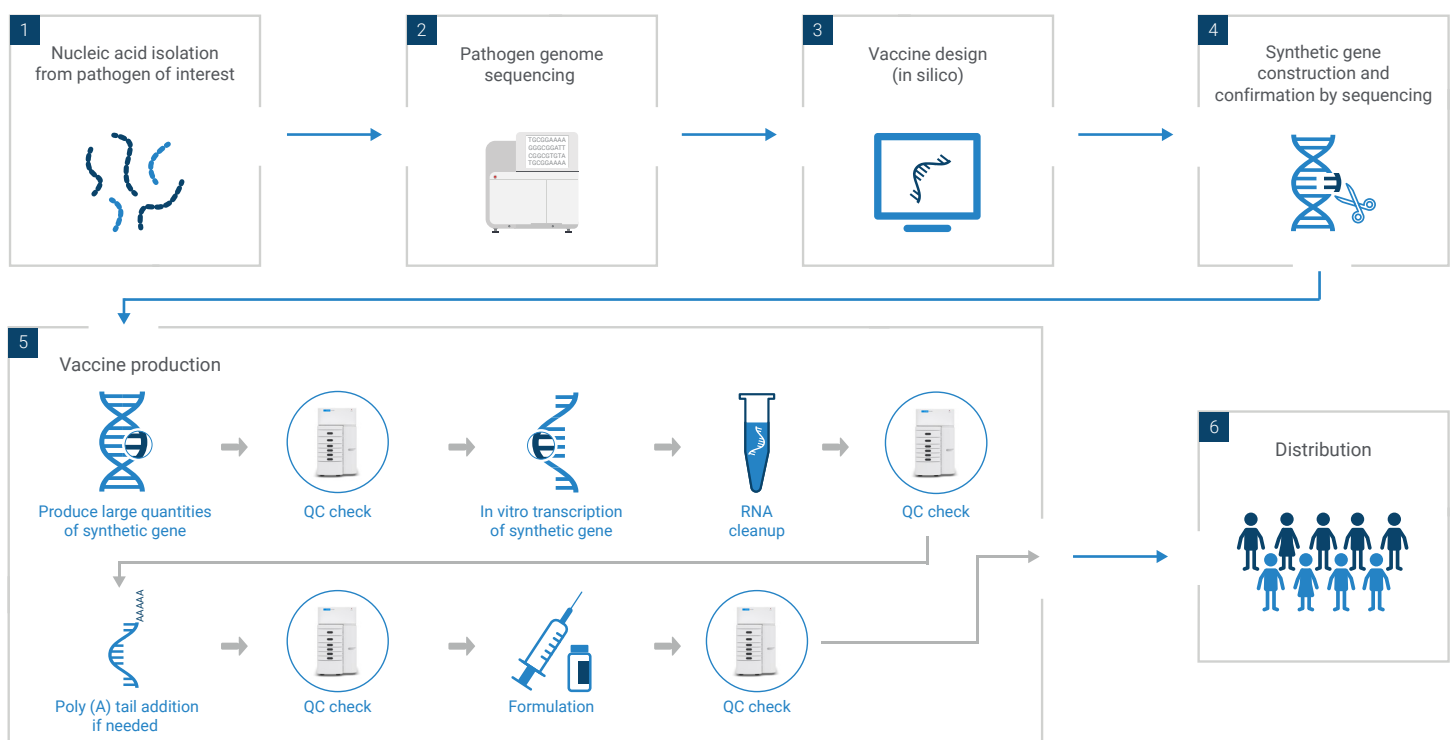


Figure 5. Schematic of IVT RNA vaccine development. The steps of COVID-19 IVT RNA vaccine development are shown, from the initial isolation of the pathogen to vaccine distribution. Included in this workflow are potential QC steps where the Agilent Fragment Analyzer and Agilent TapeStation systems can be used to help ensure the quality of the sample before moving to the next step, and helping to ensure that the final vaccine is suitable for distribution.

For the manufacture and control of mRNA vaccines using good manufacturing practices (GMP), the World Health Organization (WHO) requires the establishment of quality control systems²⁷. They state "...adequate control of the starting raw materials and manufacturing process is as important as that of the final product. Regulatory considerations therefore place considerable emphasis on the control strategy of the manufacturing process of the vaccine as well as on comprehensive characterization and release testing of the bulk substance and the vaccine itself."²⁷

The WHO further recommends that throughout the process, several in-process control tests should be established to allow quality to be monitored for each batch or lot from the beginning to the end of production. The purity of final RNA is especially vital for the potency of mRNA vaccines²⁴. During IVT RNA vaccine production, typical analyses of the linearized plasmid, as well as of the final product address identity, appearance, content, integrity, residual DNA, endotoxin contamination, and sterility⁸. Figure 5 shows the in-process QC steps, which include quality and size of the linearized plasmid, purity of the IVT product, quality and size following addition of the

poly(A) tail, and the purity of the final product. The Agilent automated electrophoresis instruments are ideally suited for several in-process quality checks as well as for testing the vaccine in its final form, as evidenced by their use in quality control by the manufacturers of the COVID-19 mRNA vaccines.

While the highly successful SARS-CoV-2 vaccines are currently the most prominent example of mRNA vaccines, several other applications are being actively investigated, and therapeutic uses of mRNA will continue to proliferate. Over 200 mRNA vaccines, including several for influenza, are in or are soon to enter clinical trials¹⁵. Thus, mRNA vaccine technology shows great promise in meeting the challenge for rapid development and large-scale production of new vaccines. With the increasing number of vaccine targets, coupled with high production goals, there is a rising need for robust, reliable, rapid, and high-throughput quality control testing during vaccine production.

Agilent automated electrophoresis systems in mRNA vaccine production

The Agilent automated electrophoresis instruments, including the Bioanalyzer, Fragment Analyzer, and TapeStation systems, have played an important role in quality assurance of the SARS-CoV-2 vaccines currently being administered. The instruments are each capable of quantitative and qualitative analysis of DNA and RNA with a broad reagent portfolio, ideal for many applications.

While the details of vaccine manufacturing are kept highly confidential by companies, Pfizer revealed some key aspects of its COVID-19 vaccine manufacturing process to USA Today. The article states, "More than half of the production time for Pfizer's COVID-19 vaccine is devoted to testing and quality assurance – making sure the resulting product, at each stage is safe, pure and exactly the same as the tested vaccine that proved effective."²⁸ The entire vaccine production process is split among three sites for maximal efficiency: purification of the plasmid which encodes the mRNA of the spike protein at the first site, production and purification of mRNA at the second, and finally, encapsulation of mRNA into lipid nanoparticles, followed by distribution into vials at the third. Figure 6 summarizes the reported timeline and depicts where the Agilent Fragment Analyzer can be used at different steps in the Pfizer vaccine manufacturing process, to assure purity and integrity of the intermediates, as well as the final product.

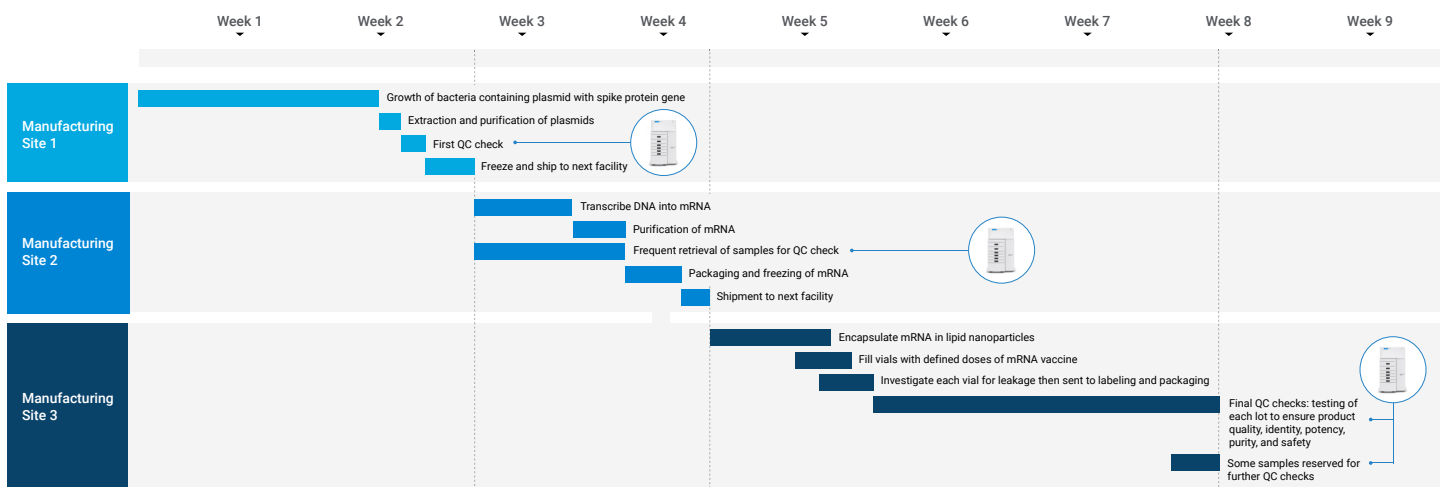


Figure 6. Steps in Pfizer-BioNTech COVID-19 vaccine production, QC steps, and role for Agilent Technologies. The production of the Pfizer-BioNTech COVID-19 vaccine, split between three different production sites, takes just over eight weeks. Among the many different QC steps, the Agilent automated electrophoresis systems can be used to ensure the size and quality of the samples at various steps in the workflow, as indicated by the inset images of the Agilent Fragment Analyzer system. By using the Fragment Analyzer at each site, quality can be ensured across the manufacturing locations. Timeline adapted from Weise and Weintraub²⁸.

Some recent published examples which use Agilent instruments for quality control during vaccine production are discussed below.

Example 1: Pfizer–BioNTech BNT162b vaccine production, and quality assessment using the Agilent Fragment Analyzer¹³

The preclinical development of two Pfizer-BioNTech mRNA vaccine candidates (BNT162b1 and BNT162b2) encoding immunogens derived from the spike glycoprotein (S) of SARS-CoV-2, formulated in lipid nanoparticles, was reported in September 2020¹³. While both candidate vaccines induced strong antigen-specific immune responses in mice and macaques, BNT162b2 was selected over BNT162b1 for further clinical testing due to its greater tolerability with comparable immunogenicity. RNA integrity was assessed by capillary electrophoresis, with the Fragment Analyzer.

Example 2: Assessment of stability of the Moderna and Pfizer–BioNTech BNT162b vaccines using the Agilent Bioanalyzer²⁹

Once vaccines were available, there was an urgent need for vaccine deployment to sites around the world without compromising the integrity of the vaccines. Initially it was thought that reconstituted vaccines would not be stable. Grau et. al. demonstrated that both the Pfizer-BioNTech and Moderna vaccines retain their integrity at ambient temperature under movement conditions consistent with agitation that would occur during three hours of driving on roads with good condition. This implied that vaccines could be more widely distributed after reconstitution, thus improving the efficiency of vaccine distribution, particularly via ground transportation in rural areas²⁹. While the Bioanalyzer was used to analyze mRNA integrity, the Fragment Analyzer and the TapeStation are also well-suited for such analysis and could handle a higher throughput of samples.

Example 3. Quality assessment of a self-replicating RNA vaccine against SARS-CoV-2 using the Agilent Fragment Analyzer³⁰

A self-replicating RNA vaccine was developed by Arcturus Therapeutics with the goal of a single low-dose administration, using proprietary self-transcribing and replicating RNA (STARR technology) against SARS-CoV-2³⁰. In assessing the immunogenicity and host response in a mouse model, the authors found that self-replication amplified the immunogenicity of the RNA vaccine, showing potential for an effective single-shot vaccination against COVID-19. Quality and integrity of the purified RNA, as well as the final vaccine lipid nanoparticle, was assessed using the Fragment Analyzer.

Example 4: Quality assurance of neoantigen-encoding messenger RNA manufactured under GMP for early-phase cancer vaccine clinical trials using the Agilent Fragment Analyzer³¹

Neoantigens are mutated peptides expressed in a tumor, which are rarely shared between patients. Hence, including these antigens in a vaccine requires the production of individual batches of patient-tailored mRNA. A dendritic cell vaccine targeting tumor neoantigens was developed for evaluation in lung cancer patients, and in their GMP facility, the authors demonstrated that the process delivers consistently high-quality patient-tailored neoantigen mRNA³¹. mRNA identity and integrity were analyzed by capillary gel electrophoresis (CGE) using the Fragment Analyzer. The authors also established the storage stability of the neoantigen mRNA by analyzing the integrity of the mRNA using CGE. The quality assessment approach they described was approved by the competent regulatory authority in Belgium (Federal Agency for Medicines and Health Products) as part of the investigational medicinal product dossier of their vaccine candidate.

Agilent automated electrophoresis systems

The Agilent Fragment Analyzer systems and the Agilent TapeStation systems, shown in Figure 7, enable nucleic acid analysis with flexible throughput options. Both the Fragment Analyzer and the TapeStation require a minimal amount of sample (1-2 μL). The Fragment Analyzer systems offer reliable DNA and RNA QC analyses, including accurate sizing of IVT RNA through 9,000 nt, to confirm transcription efficiency and perform smear analysis to assess minute amounts of degradation^{32,33}. The systems are available in a range of throughputs, holding up to three 96-well plates, and their benefits include unattended operation, reduced sample handling, and decreased preparation time³⁴. The TapeStation systems, based on ScreenTape technology, offer ease-of use in combination with a fast analysis time of 1-2 minutes per RNA and DNA samples. Ready-to-use consumables ensure straightforward operation with minimal hands-on time³⁵.



Figure 7. Automated Electrophoresis Solutions for IVT RNA QC. The Agilent Fragment Analyzer systems and the Agilent TapeStation systems offer reliable nucleic acid quality control for a variety of applications, including accurate sizing of IVT RNA.

Conclusion

Vaccines produced using IVT RNA technology are highly adaptable, efficiently made, and ideally suited for fast production. IVT RNA vaccines are a valuable tool against COVID-19 and are in trials for other applications, including vaccines for various infectious diseases and cancer immunotherapy. The Agilent automated electrophoresis systems are well-suited to serve QC needs in current production markets, and are primed to play a continuing vital role in assuring in-process quality as well as quality of the final product. As the number of vaccine targets and production goals increase, so does the need for robust, reliable, and rapid quality control methods.

References

- Morens, D.; Fauci, A. Emerging Pandemic Diseases: How We Got to COVID-19. *Cell*. **2020**, *182*, 1077-1092.
- LePan, N.; Schell, H. *Infographic: The History of Pandemics, by Death Toll*. <https://www.visualcapitalist.com/history-of-pandemics-deadliest/>. (Accessed December 2021).
- Woolhouse, M.; Gowtage-Sequeria, S. Host range and emerging and reemerging pathogens. *Emerg Infect Dis*. **2005**, *11*, 1842-7.
- Taylor, L.; Latham, S.; Woolhouse, M. Risk factors for human disease emergence. *Philos Trans R Soc Lond B Biol Sci*. **2001**, *356*, 983-9.
- National Research Council (US) Division of Health Promotion and Disease Prevention. *Vaccine Supply and Innovation*. Washington (DC): National Academies Press (US); 1985. 2, *Vaccines: Past, Present, and Future*. Available from: <https://www.ncbi.nlm.nih.gov/books/NBK216821/>
- Rauch, S; Jasny, E; Schmidt, K; Petsch B. New Vaccine Technologies to Combat Outbreak Situations. *Front Immunol*. **2018**, *9*, 1963.
- Sahin, U.; Karikó, K.; Türeci, Ö. mRNA-based therapeutics—developing a new class of drugs. *Nat Rev Drug Discov*. **2014**, *13*, 759-80.
- Karikó, K.; Buckstein, M.; Ni, H.; Weissman, D. Suppression of RNA recognition by Toll-like receptors: the impact of nucleoside modification and the evolutionary origin of RNA. *Immunity*. **2005**, *23*, 165-75.
- Karikó, K.; Muramatsu, H.; Welsh, F.; Ludwig, J.; Kato, H.; Akira, S.; Weissman, D. Incorporation of pseudouridine into mRNA yields superior nonimmunogenic vector with increased translational capacity and biological stability. *Mol Ther*. **2008**, *16*, 1833-40.
- Let's talk about lipid nanoparticles. *Nat Rev Mater*. **2021**, *6*, 99. <https://doi.org/10.1038/s41578-021-00281-4>. (Accessed December 2021).
- Papahadjopoulos, D.; Vail, W.; Jacobson, K.; Poste, G. Cochleate lipid cylinders: formation by fusion of unilamellar lipid vesicles. *Biochim. Biophys. Acta* **1975**, *394*, 483–491.
- Dimitriadis, G. Translation of rabbit globin mRNA introduced by liposomes into mouse lymphocytes. *Nature* **1978**, *274*, 923–924.
- Vogel, A.; Kanevsky, I.; Che, Y.; Swanson, K.; Muik, A. Vormehr, M.; Kranz, L.; Walzer, K.; Hein, S.; Güler, A.; Loschko, J.; Maddur, M.; Ota-Setlik, A.; Tompkins, K.; Cole, J.; Lui, B.; Ziegenhals, T.; Plaschke, A.; Eisel, D.; Dany, S.; Fesser, S.; Erbar, S.; Bates, F.; Schneider, D.; Jesionek, B.; Sängler, B.; Wallisch, A.; Feuchter, Y.; Junginger, H.; Krumm, S.; Heinen, A.; Adams-Quack, P.; Schlereth, J.; Schille, S.; Kröner, C.; de la Caridad Güimil Garcia, R.; Hiller, T.; Fischer, L.; Sellers, R.; Choudhary, S.; Gonzalez, O.; Vascotto, F.; Gutman, M.; Fontenot, J.; Hall-Ursone, S.; Brasky, K.; Griffor, M.; Han, S.; Su, A.; Lees, J.; Nedoma, N.; Mashalidis, E.; Sahasrabudhe, P.; Tan, C.; Pavliakova, D.; Singh, G.; Fontes-Garfias, C.; Pride, M.; Scully, I.; Ciolino, T.; Obregon, J.; Gazi, M.; Carrion, R. Jr.; Alfson, K.; Kalina, W.; Kaushal, D.; Shi, P.; Klamp, T.; Rosenbaum, C.; Kuhn, A.; Türeci, Ö.; Dormitzer, P.; Jansen, K.; Sahin, U. BNT162b vaccines protect rhesus macaques from SARS-CoV-2. *Nature*. **2021**, *592*, 283-289.
- Alberer, M.; Gnad-Vogt, U.; Hong, H.; Mehr, K.; Backert, L.; Finak, G.; Gottardo, R.; Bica, M.; Garofano, A.; Koch, S.; Fotin-Mlecsek, M.; Ingmar, H.; Clemens, R.; von Sonnenburg, F. Safety and immunogenicity of a mRNA rabies vaccine in healthy adults: an open-label, non-randomised, prospective, first-in-human phase 1 clinical trial. *Lancet*. **2017**, *390*, 1511–1520.
- National Institutes of Health U. S. National Library of Medicine. ClinicalTrials.gov NIH, <https://clinicaltrials.gov/> (Accessed December 2021).
- Kashte, S.; Gulbake, A.; El-Amin Iii S.; Gupta, A. COVID-19 vaccines: rapid development, implications, challenges and future prospects. *Hum Cell*. **2021**, *34*, 711-733.
- U.S. Government Accountability Office Science & Tech Spotlight: COVID-19 Vaccine Development, GAO-20-583SP, <https://www.gao.gov/products/gao-20-583sp>. (accessed December 2021).
- Le, T.; Cramer, J.; Chen, R.; Mayhew, S. Evolution of the COVID-19 vaccine development landscape. *Nat Rev Drug Discov*. **2020**, *19*, 667-668.
- U. S. Food and Drug Administration. FDA takes key action in fight against COVID-19 by issuing emergency use authorization for first COVID-19 vaccine. U.S. Food and Drug Administration (FDA) **2021**.

20. U.S. Department of Health and Human Services, National Institutes of Health. Statement from NIH and BARDA on the FDA Emergency Use Authorization of the Moderna COVID-19 Vaccine. *National Institutes of Health (NIH)*, **2021**. <https://www.nih.gov/news-events/news-releases/statement-nih-barda-fda-emergency-use-authorization-moderna-covid-19-vaccine>. (Accessed December 2021).
21. Centers for Disease Control and Prevention. COVID Data Tracker. *CDC*. <https://covid.cdc.gov/covid-data-tracker/#datatracker-home> (Accessed January 2022).
22. Our World in Data. Statistics and Research Coronavirus (COVID-19) Vaccinations *Oxford Martin School, University of Oxford*, <https://ourworldindata.org/covid-vaccinations>. (Accessed January 2022).
23. Krellenstein, J.; Wilkinson, G.; Osmundson, J.; Keshavjee, S.; Rasmussen, A.; and El-Sadr, W. 22 billion in the hole: Omicron's implications for global mRNA vaccine needs in 2022. *PrEP4ALL*, (accessed January 2022).
24. Maruggi, G.; Zhang, C.; Li, J.; Ulmer, J.; Yu, D. mRNA as a Transformative Technology for Vaccine Development to Control Infectious Diseases. *Mol Ther.* **2019**, *27*, 757-772.
25. Cerullo, M. Pfizer says its vaccine targeting Omicron will be ready in March. *cbsnews.com*, (Accessed January 2022).
26. Langmaid, V. Moderna should have data on Omicron-specific vaccine in March, company CEO says. *cnn.com* (Accessed January 2022).
27. World Health Organization. Evaluation of the quality, safety and efficacy of RNA-based 5 prophylactic vaccines for infectious diseases: regulatory considerations. *WHO*, **2020**, https://www.who.int/docs/default-source/biologicals/ecbs/reg-considerations-on-rna-vaccines_1st-draft_pc_tz_22122020.pdf?sfvrsn=c13e1e20_3 (accessed January 2022).
28. Weise, E.; Weintraub, K. A COVID vaccine life cycle: from DNA to doses. *usatoday.com* (Accessed December 2021).
29. Grau, S.; Ferrández, O.; Martín-García, E.; Maldonado, R. Reconstituted mRNA COVID-19 vaccines may maintain stability after continuous movement. *Clin Microbiol Infect.* **2021**, *27*, 1698.
30. de Alwis, R.; Gan, E.; Chen, S.; Leong, Y.; Tan, H.; Zhang, S.; Yau, C.; Low, J.; Kalimuddin, S.; Matsuda, D.; Allen, E.; Hartman, P.; Park, K.; Alayyoubi, M.; Bhaskaran, H.; Dukanovic, A.; Bao, Y.; Clemente, B.; Vega, J.; Roberts, S.; Gonzalez, J.; Sablad, M.; Yelin, R.; Taylor, W.; Tachikawa, K.; Parker, S.; Karmali, P.; Davis, J.; Sullivan, B.; Sullivan, S.; Hughes, S.; Chivukula, P.; Ooi, E. A single dose of self-transcribing and replicating RNA-based SARS-CoV-2 vaccine produces protective adaptive immunity in mice. *Mol Ther.* **2021**, *29*, 1970-1983.
31. Ingels, J.; De Cock, L.; Mayer, R.; Devreker, P.; Weening, K.; Heyns, K.; Lootens, N.; De Smet, S.; Brusseel, M.; De Munter, S.; Pille, M.; Billiet, L.; Goetgeluk, G.; Bonte, S.; Jansen, H.; Van Lint, S.; Leclercq, G.; Taghon, T.; Menten, B.; Vermaelen, K.; Impens, F.; Vandekerckhove, B. Small-scale manufacturing of neoantigen-encoding messenger RNA for early-phase clinical trials. *Cytotherapy.* **2021**, *S1465-3249*, 00778-7.
32. Benefits of Quality Control in the IVT RNA workflow using the Agilent 5200 Fragment Analyzer System. *Agilent Technologies application note*, publication number 5994-0512EN, **2019**.
33. Assessment of Long IVT mRNA Fragments with the Agilent Fragment Analyzer Systems. *Agilent Technologies application note*, publication number 5994-0878EN, **2019**.
34. Reliable Results for Nucleic Acid Analysis. *Agilent Technologies brochure*, publication number 5994-0414EN, **2021**.
35. Complete Success Begins with Sample Quality Control. *Agilent Technologies brochure*, publication number 5994-0060EN, **2020**.

www.agilent.com/genomics/automated-electrophoresis

For Research Use Only. Not for use in diagnostic procedures.

PR7000-8561

This information is subject to change without notice.

© Agilent Technologies, Inc. 2022
Published in the USA, March 30, 2022
5994-4760EN

SEC-MALS for mRNA Characterization with the Agilent 1260 Infinity II Multi-Angle Light Scattering Detector



Authors

Sonja Schneider and
Florian Rieck
Agilent Technologies, Inc.

Abstract

The characterization of messenger ribonucleic acid (mRNA) with mass spectrometry can be particularly challenging due to the complex and large structure of RNA molecules. The combination of multiangle light scattering (MALS) detection with size exclusion chromatography (SEC) can successfully be applied to the analysis of mRNA, delivering biophysical and structural information.

The Agilent 1260 Infinity II Multi-Angle Light Scattering Detector coupled to the Agilent 1290 Infinity II Bio LC System enables the determination of molecular weight (MW) in addition to aggregate percentage information from the concentration detector. The 1290 Infinity II Bio LC is specifically designed for conditions used in biochromatography, with a completely iron-free flow path and high tolerance to the salt-based buffers typically used in SEC.

Introduction

mRNA-based biopharmaceuticals have been in development as a new class of drugs for over three decades.¹ They came into focus during the COVID pandemic with the development of mRNA-based vaccines. This evolution has led to the need for analytical methods to evaluate the critical quality attributes of mRNA.^{2,3}

mRNA is produced by in vitro transcription from a linear DNA template and is chemically modified at the regulatory elements present at the mRNA ends (5' cap and poly(A) tail) to improve efficiency and stability during translation.

High-performance liquid chromatography (HPLC) is especially advised for mRNA purity analysis by the USP guidelines.² Beyond the analysis of purity, capping efficiency, and poly(A) tail mostly with ion pairing reversed-phase (IP-RP) HPLC, an important characteristic of mRNA is the analysis of aggregates. Aggregates are considered product-related impurities, and their quantification and identification are important quality attributes.

In addition to quantitative information from the concentration detector (ultraviolet, or refractive index (RI)) as aggregation percentage, the addition of MALS detection to SEC enables the determination of MW for the identification of the large-sized mRNA monomer molecules and aggregates. These details cannot be revealed by conventional SEC due to the difference in conformation of the used globular protein standards versus the mRNA structure in solution.

Experimental

Equipment

Agilent 1290 Infinity II Bio LC System:

- Agilent 1290 Infinity II Bio Flexible Pump (G7131A)
- Agilent 1290 Infinity II Bio Multisampler (G7137A) with Sample Thermostat (option #101)
- Agilent 1290 Infinity II Multicolumn Thermostat (G7116B) with InfinityLab Quick Connect Heat Exchanger 1290 Bio Standard Flow (part number G7116-60071)
- Agilent 1290 Infinity II Refractive Index Detector (G7162B)
- Agilent 1290 Infinity II Variable Wavelength Detector (G7114B) with Bio Micro Flow Cell VWD, 3 mm, 2 μ L, RFID (part number G1314-60189)
- Agilent 1260 Infinity II Multi-Angle Light Scattering Detector (G7885A)

Note: All measurements shown in this application note can also be performed on other Agilent Bio LC systems such as the Agilent 1260 Infinity II Bio-Inert LC System or the Agilent 1260 Infinity II Prime Bio LC System.

Column

Agilent AdvanceBio SEC 1000Å, 7.8 × 300 mm, 2.7 μ m (part number PL1180-5302)

Software

The software used in this study was Agilent WinGPC software, version 1.0. Later versions also apply.

Chemicals, solvents and samples

Fresh ultrapure water was obtained from a Milli-Q Integral system equipped with a 0.22 μ m membrane point-of-use cartridge (Millipak, Merck-Millipore, Billerica, MA, U.S.). Sodium dihydrogen phosphate, di-sodium hydrogen phosphate heptahydrate, sodium hydroxide, and bovine serum albumin (BSA) were obtained from Sigma-Aldrich (Steinheim, Germany). MabThera (rituximab) was purchased from Medizone Germany GmbH, Munich, Germany. An mRNA sample was kindly provided from the Research Institute of Chromatography, Kortrijk, Belgium.

Solvent and sample preparation

Two liters of 150 mM phosphate buffer were prepared using 15.22 g of sodium dihydrogen phosphate and 46.41 g of di-sodium hydrogen phosphate heptahydrate. The pH was adjusted to 7 using sodium hydroxide solution. The prepared phosphate buffer was triple-filtered using a 0.2 μ m membrane filter. Samples were filtered using an Agilent Captiva Premium Syringe Filter with a regenerated 4 mm cellulose membrane, 0.2 μ m pore size (part number 5190-5106). BSA was dissolved in the prepared phosphate buffer to a concentration of 20 mg/mL. MabThera is formulized at a concentration of 10 mg/mL.

Note: Phosphate-buffered solvents at physiological pH are highly prone to bacteria and algae growth and should be replaced at least every few days. In between buffer changes, the LC needs to be flushed with water/organic mixtures to prevent contamination. To avoid buffer salt crystallization, the flow should be set to a low flow rate instead of stopping the flow after analysis.

Table 1. Method parameters.

Parameter	Value
Flow Rate	0.6 mL/min
Mobile Phase	150 mM Phosphate buffer, pH 7, triple-filtered
Injection Volume	5 to 20 μ L
Stop Time	30 min
Needle Wash	Flush port, 3 s, water:isopropanol 80:20 (v:v)
Autosampler Temperature	8 °C
Column Temperature	30 °C
Detection RID	30 °C, Peak width > 0.05 min (9.25 Hz)
Detection UV	260 nm, Peak width > 0.05 min (10 Hz)
Detection MALS	Cell temperature 30 °C, 20 angles recorded

For the MW calculation, a dn/dc value of 0.186 mL/g was used for proteins, and 0.172 mL/g was used for mRNA.

Unlike in conventional SEC, the MW analysis using an SEC light scattering detector requires knowledge of the sample concentration. There are different options to determine the concentration. If the extinction coefficient of the sample is known, using a calibrated UV detector and the extinction coefficient (ϵ or dA/dc) is a reliable way to determine the concentration of the analyzed molecule. This calculation method is often applied in protein analysis. If the extinction coefficient is not known, the sample concentration can also be determined using the RI increment (dn/dc) and a calibrated RI detector. RI detection is an alternative and more general detection method, and can also be applied to molecules without UV chromophores. If the dn/dc is also not known, it can be determined with RI detection using a dilution series of the molecules with known concentration, as described in the literature.^{4,5} In the case of the used mRNA sample, the extinction coefficient was not known, so RI detection was used for concentration calculation with a dn/dc of 0.172 mL/g. This value was also used for MW calculation.

The LC configuration consisted of two concentration detectors, UV and RI detection, in combination with MALS detection. Due to pressure restrictions and to minimize peak dispersion, the detectors were installed in the following order: UV-MALS-RI. The UV signal at 260 nm detects mRNA with high sensitivity, enabling the exact determination of aggregation percentage.

Results and discussion

mRNA are large RNA molecules exhibiting high MWs, so SEC columns with large pore size are required. The wide-pore Agilent AdvanceBio SEC columns meet the needs for robust, high-resolution separations with the ideal combination of small particles and large pore volumes. Static light scattering requires a single measurement with a monodisperse, baseline-resolved peak for interdetector delay calibration and light scattering detector constant determination. For SEC-MALS analysis of proteins, the BSA monomer is often used as a calibrant. With the Agilent AdvanceBio SEC 300Å, 7.8 × 300 mm, 2.7 μ m column, excellent resolution is achieved between the BSA monomer and dimer as shown in previous publications.⁶ With the wide-pore column of 1,000 Å pore size required for mRNA analysis, equal resolution for BSA cannot be achieved. Instead, the monoclonal antibody rituximab with a MW of 145,000 Da was used for calibration, showing a clear monomeric peak with negligible amounts of aggregates (Figure 1).

Figure 2 shows the separation of the analyzed mRNA monomer and its aggregates. Good separation of monomer and dimer was achieved on the AdvanceBio SEC 1000Å, 7.8 × 300 mm column. Based on the UV signal at 260 nm, the aggregation percentage was calculated to be 74% for the monomer, 20% for the dimer, and 6% for the higher aggregates. The MALS MW determination was calculated as bulk MW based on a dn/dc of 0.172 mL/g. For a length of 4,546 nucleotides for the monomer, an MW of 1,453,000 Da was calculated. This value is in near-perfect agreement with the theoretical value of the mRNA nucleotide sequence. The precision was also very high, with an RSD of ~2% for the MW values. With the determination of the MW by MALS, the dimer peak could be identified with a MW of 3,205,000 Da. In addition, higher MW species eluting in front of the dimer peak were detected.

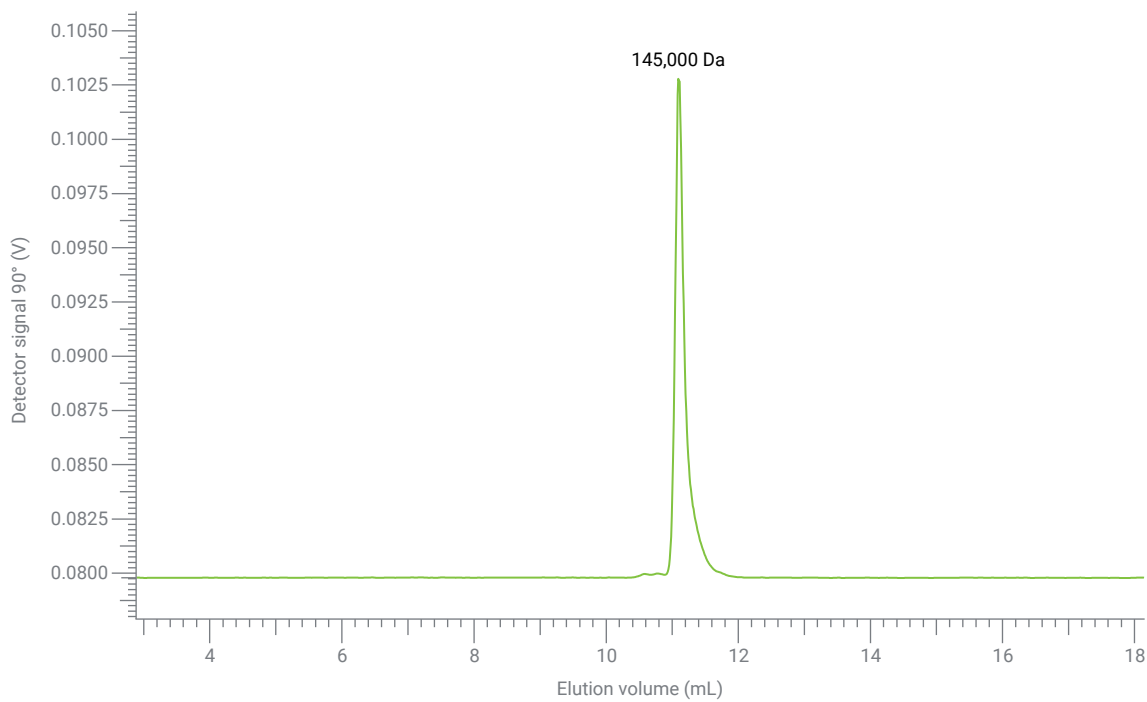


Figure 1. SEC-MALS analysis of rituximab at 90°. A monomeric peak is observed with only minimal amounts of aggregates, making it an excellent option for calibration purposes.

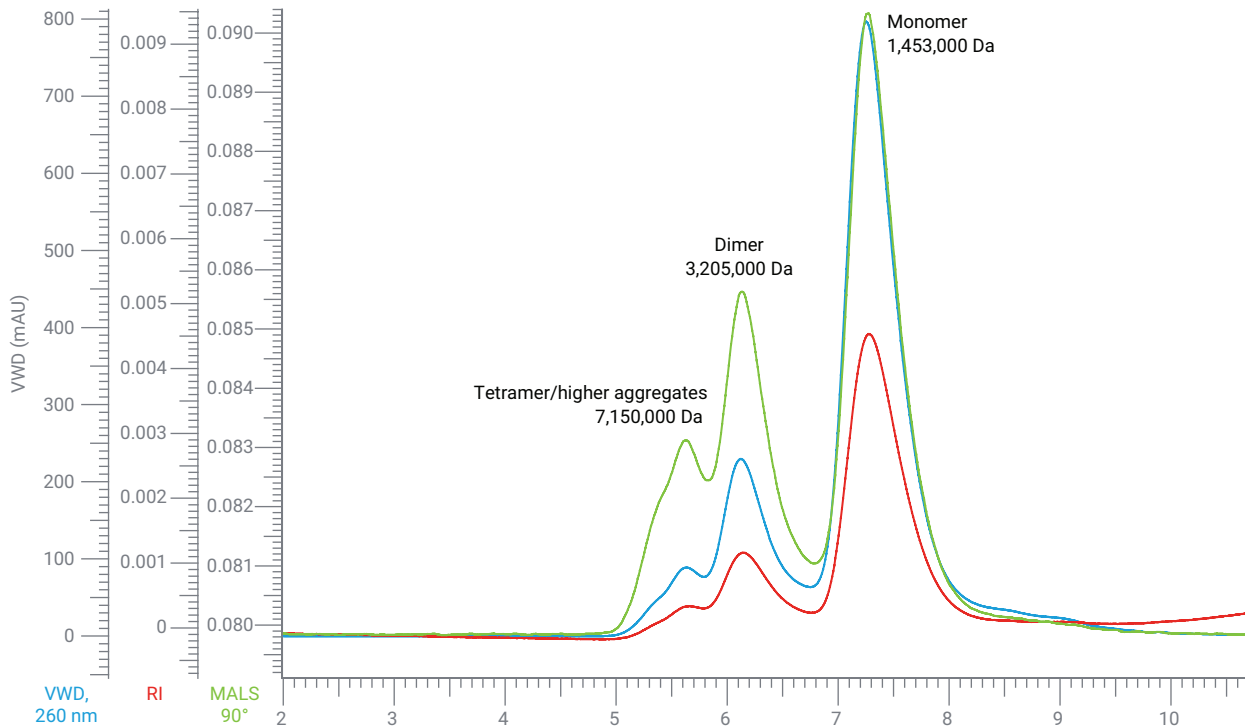


Figure 2. SEC-MALS analysis of an mRNA sample with 4,546 nucleotide length. The resulting concentration signals (UV: blue, RI: red) are displayed together with the 90° MALS signal (green).

Conclusion

An Agilent 1260 Infinity II Multi-Angle Light Scattering Detector coupled to an Agilent 1290 Infinity II Bio LC System provided biophysical information for the analysis of large mRNA molecules. The precise determination of the molecular weight was in near-perfect agreement with the theoretical value of the mRNA sequence. Good resolution was found between monomer and dimer of mRNA with an Agilent AdvanceBio SEC 1000Å column, leading to unique MW determination for the separated peaks.

The combination of the 1290 Infinity II Bio LC System and the 1260 Infinity II Multi-Angle Light Scattering Detector provides a complete biocompatible flow path to ensure trusted results for challenging solvent conditions or iron-reactive samples.

References

1. Sahin, U.; Karikó, K.; Tuereci, Ö. mRNA-Based Therapeutics—Developing a New Class of Drugs. *Nat. Rev. Drug Discov.* **2014**, *13*(10), 759–780.
2. USP-NF. Analytical Procedures for mRNA Vaccine Quality (Draft Guidelines)- 2nd Edition, **2023**.
3. De Vos, J.; Morreel, K.; Alvarez, P.; Vanluchene, H.; Vankeirsbilck, R.; Sandra, P.; Sandra, K. Evaluation of Size-Exclusion Chromatography, Multi-Angle Light Scattering Detection and Mass Photometry for the Characterization of mRNA. *J. Chromatogr. A* **2024**, *1719*, 464756.
4. Held, D. Tips & Tricks GPC/SEC: How to Determine dn/dc Values. *The Column* **2015**, *10*(7), 10–15.
5. Radke, W. Tips & Tricks: New and Old Approaches to Handle Unknown dn/dc in GPC/SEC-LS. *The Column* **2017**, *13*(14), 19–23.
6. Advanced SEC-MALS Analysis of Monoclonal Antibodies with the Agilent 1260 Infinity II Multi-Angle Light Scattering Detector. *Agilent Technologies application note*, publication number 5994-7664EN, **2024**.

Learn more:

www.agilent.com/genomics/vaccine-qc

www.agilent.com/en/solutions/biopharma-pharma/vaccines

U.S. and Canada

1-800-227-9770

agilent_inquiries@agilent.com

Europe

info_agilent@agilent.com

Asia Pacific

inquiry_lsca@agilent.com

For Research Use Only. Not for use in diagnostic procedures.
PR7001-3521

This information is subject to change without notice.

© Agilent Technologies, Inc. 2024
Published in the USA, November 1, 2024
5994-7961EN

